Population divergence between European lake and stream threespine stickleback

Inauguraldissertation

zur

Erlangung der Würde eines Doktors der Philosophie
vorgelegt der
Philosophisch–Naturwissenschaftlichen Fakultät der
Universität Basel

von

Dario Moser

aus Appenzell, Schweiz

Basel, 2017

Genehmigt von der Philosophisch–Naturwissenschaftlichen
Fakultät auf Antrag von Prof. Dr. Walter Salzburger, Dr. Josh
Van Buskirk

Basel, den 23.02.2016

Prof. Dr. Jörg Schibler

Dekan

Contents

1

OUTREACH CHAPTERS

Acknowledgements

First of all I want to thank everybody from the Salzburger Group, which let me be part of it and experience great mutual moments. Besides working in the field, in the lab or in front of a computer, it was possible to embed some free time. I often decided to spend it with people from the lab, who over the years, became friends. In particular I want to thank Astrid, Fabrizia, Beni, Marco and Marius. I cannot tell you how grateful I am for the numerous adventures in or at the water, exciting 4×4 rides through South Africas outback, charming bus rides, thrilling conversations, delicious cooking, rather unconventional shopping trips, outrageous parties, mutual living or just fooling around, which we did a lot. Guys you are great, thanks a lot, I hope you will continue to be part of my life!

Many thanks go to all co-authors and all people who contributed to this work. This thesis would not have been possible without them.

I also want to thank my supervisors Walter and Dani. Walter, thank you again, for accepting me how I am, and always making everything possible. I am very grateful for that! Dani, you are the best. In many ways you became a role model to me, although out of reach. Your fast, efficient, pragmatic and meticulous way to work is fascinating. Besides this, I loved our 'outreach' activities to some cliffs, where you taught me how to do a decent backflip.

Finally I want to thank my friends and family, which always supported me, whenever I was struggling. You made everything possible. Thank you so much!

General introduction

The fundamental question in evolutionary biology is to understand the diversity of life, how new species are formed and the processes which are involved therein. Charles Darwin called this the 'mystery of mysteries'. In 1859 Darwin ignited the still ongoing research on scientific theory of evolution with the publication of 'On the Origin of Species' (Darwin 1859). In his most famous piece of work he introduced the terms natural selection and, to a limited extend, sexual selection as the main forces in speciation. Natural selection means that certain phenotypes in a specific ecological surrounding have a higher probability of survival and reproduction. In other words, there is variation in fitness. As a direct consequence, phenotypes with higher fitness become more frequent over time. The same holds true for sexual selection. Here not ecology but the interaction between individuals of the same or the opposite sex influence the individual–specific probability of reproduction, depended on certain phenotypes. Again, favorable phenotypes become more frequent over time. Therefore, groups of individuals of a certain species, living in selectively divergent environments, become phenotypically divergent over time. In other words, these populations become locally adapted to their respective environments. As a consequence, migrating individuals or hybrids will have lower fitness compared to locally adapted ones.

The available tools and techniques researchers are able to work with changed a lot in the past 150 years. While Darwin was limited to a phenotype–based observational and/or morphometric approach to measure divergence between organisms, we nowadays know that most phenotypic traits have a genetic basis and developed numerous genetic tools to explore genetic divergence between populations (Coyne and Orr 2004). Empirical studies have shown that local adaptation is negatively correlated with gene flow, the transfer of genes or alleles between populations. The amount of gene flow on the other hand determines where comparing two populations on the speciation continuum are found (Slatkin 1987). This continuum ranges from interbreeding populations with no reproductive isolation and pronounced gene flow on one end and 'true' species with complete reproductive isolation and no gene

flow on the other end (Schluter 2000; Nosil 2012).

Something did not change since Darwin though. To answer empirical questions in evolutionary biology all researchers need a good model organism. Unfortunately a 'perfect' model organism does not exist. One has to choose a model system depending on the questions raised. I decided to do research with threespine stickleback (*Gasterosteus aculeatus* L. 1758), a small teleost fish from the Gasterosteidae family (Östlund–Nilsson et al. 2006), which is very popular in evolutionary biology related research. Five key features make this organism a great model in evolutionary biology:

1. Stickleback are, keeping in mind that we are talking about a vertebrate, very easy to handle in the laboratory. They can be kept in swarms, occupy little space, are tolerant to a vast array of rearing conditions such as salinity, temperature and abiotic chemicals, have a minimal generation time of one year, are easy to cross and show a full blown behavioral repertoire under laboratory conditions. Unsurprisingly, stickleback have a long history particularly in behavioral research because of their complex breeding behavior (Östlund–Nilsson et al. 2006).

2. Probably most important from an evolutionary perspective is that stickleback show a high degree of intra–specific variation in freshwater populations (McKinnon and Rundle 2002; Bell and Foster 1994). After the retreat of the ice sheets of the Pleistocene 10'000 years ago, newly formed freshwater bodies around the Northern Hemisphere got colonized by oceanic stickleback. Due to a high degree of standing genetic variation in marine ancestors, freshwater populations were able to locally adapt to a vast array of divergent selection pressures and are nowadays displaying an extraordinary adaptive radiation (Bell and Foster 1994; Schluter 2000). Examples for variation in freshwater stickleback are found in the two trait classes foraging (Reimchen et al. 1985; Berner et al. 2008, 2009; Kaeuffer et al. 2012) and anti–predation (Leinonen et al. 2011a), which are highly fitness related and therefore crucial in the process of speciation.

3. Another feature of stickleback research is the huge progress in molecular analysis which has been done in the last 15 years. Two important milestones were reached by publishing a genome–wide linkage map in 2001 (Peichel et al. 2001) and five years later by sequencing the full genome (Jones et al. 2012). QTL–mapping studies, candidate gene approaches, genome scans and analyses based on full genome data sets have become frequent and facilitated the understanding of speciation.

4. Out of a statistical perspective, stickleback are key. The countless independent colonizations of freshwater bodies make a high replication of any research project possible.

5. Divergence time in freshwater stickleback population pairs, occupying contrasting environments, is generally young. Assuming a generation time of 1–2 years we are talking about 5'000–10'000 generations, or even younger in recently colonized water bodies. This is crucial for an organism used for speciation related questions, since the probability of past but dramatic long–term shifts in ecology is reduced. Therefore the probability that the genetic signatures and described phenotypes in stickleback populations are not artifacts from the past, but really have fitness consequences in the present is increased.

During my PhD, I focused on lake and stream threespine stickleback. The two contrasting environments are geographically separated, allow gene flow and challenge with differential selection pressures. The most obvious differences between the lake and stream environment are found in the available food resources (zooplankton versus macroinvertebrates), predation (big fish predators versus insect larvae) and habitat structure (steady and open water versus current and complex habitat matrix). Clinal analyses in Canadian lake and stream systems based on neutral genetic markers exposed barriers to gene flow (Berner et al. 2009). Although replicated and predictable morphological divergence was described (Lavin et al. 2007), no reproductive barrier was found between these ecotypes so far (Hendry et al. 2009; Hanson et al. 2015). My studies aimed to find an answer to this open question with lake and stream populations from the Lake Constance basin in Central Europe.

My main chapters are structured as follow:

Chapter 1– I began my studies with a quantitative approach, which tested for life history divergence and barriers to gene flow. In particular, I used a landmark– and otholith–based approach to measure the two life history traits size and age at reproduction in four lake and five stream populations. Stream fish showed reduced size and younger age at reproduction and an annual life cycle compared to lake fish, which reproduced at age two. Based on F_{ST} comparisons (microsatellites) and a haploytype network (D–loop), I exposed the population structure in this watershed. The lake is harboring one panmictic population with existing barriers to gene flow between the lake and the streams.

Chapter 2 – In the second chapter, I answered two questions about the basis of this life history shift: i) is it plastic or genetically based and ii) what is the underlying mechanistic basis? Two alternative ways may lead

to the described shift: Assuming similar growth rates in lake and stream populations, higher maturation size thresholds in lake fish, which could only be attained in two years would lead to bigger and older fish in the lake when compared to the stream. Alternatively, maturation size thresholds may be the same with reduced growth rates in the lake, precluding them from overcoming minimal size for reproduction within one year. In this scenario, lake fish would have to invest into somatic growth for another year and become larger than stream fish at reproduction. I answered these questions using a combination of two lab experiments, testing for genetic differences in growth rates and unequal maturation size thresholds and a field experiment, testing for phenotypic plasticity in transplanted lake fish. I found evidence for a high degree of plasticity likely induced by differential feeding regimes, leading to drastically reduced growth rates in lake fish.

Chapter 3 – A high–resolution single nucleotide polymorphism (SNP) marker dataset (Outreach chapter 6) supported the low overall genetic differentiation between the lake and the stream populations, which I found in chapter 1. However, it also contained SNP markers with moderate to high differentiation. Hence, in the last experiment of my PhD, I wanted to test for local adaptation, despite weak genome wide differentiation. I used a long term field experiment to let lab reared stream, lake and F_1 lake–stream hybrids compete against each other. By measuring survival over time, I found strong evidence for selection against migrants and hybrids and hence gave an answer to the long standing question of the whereabouts of the barriers to gene flow in lake–stream stickleback populations.

Finally, my thesis is concluded by five outreach chapters, which involved different research approaches and gave me the opportunity to dive into completely different areas of biological research, while concentrating on the main chapters. The chapters 4–6 focused on the genetics and genomics in lake and stream stickleback. In particular, we quantified recombination rate and its implications on genome evolution in chapter 4, performed a QTL (quantitative trail locus)–mapping, investigating the genetic basis of feeding– motility– and defense–related traits in chapter 5 and demonstrated an ecological vicariance scenario on the basis of demographic and population genomic analyses in chapter 6. The last two outreach chapters explored the physiology in camelids and ruminants. Chapter 7 compared methane emission, whereas chapter 8 focused on digesta retention patterns.

Chapter 1

Repeated lake–stream divergence in stickleback life history within a Central European lake basin

Authors: DARIO MOSER, Marius Roesti & Daniel Berner

Preface: This chapter introduced me to evolutionary biology and stickleback science. I was able to do some field trips, learned basic laboratory techniques, such as DNA extraction and PCR, got familiar with a series of different softwares to analyze genetic data and made first contact with statistics. The data for the first chapter was collected during my master thesis. Nevertheless, I decided to include it here, since the publication process was the first task after I finished my Master studies. Additionally, the results of this chapter and the questions they raised, led to my main work in chapters 2 & 3.

1.1 Abstract

Life history divergence between populations inhabiting ecologically distinct habitats might be a potent source of reproductive isolation, but has received little attention in the context of speciation. We here test for life history divergence between threespine stickleback inhabiting Lake Constance (Central Europe) and multiple tributary streams. Otolith analysis shows that lake fish generally reproduce at two years of age, while their conspecifics in all streams have shifted to a primarily annual life cycle. This divergence is paralleled by a striking and consistent reduction in body size and fecundity in stream fish relative to lake fish. Stomach content analysis suggests that life history divergence might reflect a genetic or plastic response to pelagic *versus* benthic foraging modes in the lake and the streams. Microsatellite and mitochondrial markers further reveal that life history shifts in the different streams have occurred independently following the colonization by Lake Constance stickleback, and indicate the presence of strong barriers to gene flow across at least some of the lake–stream habitat transitions. Given that body size is known to strongly influence stickleback mating behavior, these barriers might well be related to life history divergence.

1.2 Introduction

Speciation is often initiated by adaptation to ecologically distinct habitats in the face of gene flow (Endler 1977; Gavrilets et al. 2000; Wu 2001; Sobel et al. 2010). This process is typically inferred from concurrent divergence in phenotypes and genetic marker frequencies across habitat transitions in the absence of physical dispersal barriers (e.g., Smith et al. 1997; Lu and Bernatchez 1999; Ogden and Thorpe 2002; Barluenga et al. 2006; Grahame et al. 2006; Foster et al. 2007; Seehausen et al. 2008; Berner et al. 2009; Rosenblum and Harmon 2011). Patterns aside, the actual mechanisms constraining gene flow in the early stages of ecological divergence generally remain poorly understood (Coyne and Orr 2004; Rundle and Nosil 2005; Sobel et al. 2010; but see Ramsey et al. 2003; Nosil 2007). At least partial reproductive isolation is often assumed to result directly from performance trade–offs associated with adaptive divergence. That is, divergence in ecologically important traits causes selection against maladapted migrants and hybrids between habitats (Schluter 2000; Coyne and Orr 2004; Hendry 2004; Nosil 2005). Further reductions in gene flow between populations can arise readily as indirect (correlated) consequences of adaptive divergence (Rice and Hostert 1993; Coyne and Orr 2004; Gavrilets 2004; Sobel et al. 2010), for

13

instance when traits under ecological divergence also influence reproductive behavior (Ritchie 2007; Bonduriansky 2011; Maan and Seehausen 2011). Understanding speciation thus benefits greatly from a thorough understanding of adaptive divergence.

In animals, the traits receiving greatest attention in the context of ecological divergence and reproductive isolation are typically those related to resource acquisition and predator avoidance (Schluter 2000; Coyne and Orr 2004). By contrast, divergence in life history is less frequently considered as a driver of speciation, despite its potential to contribute to reproductive isolation at multiple levels simultaneously: first, adaptive divergence in life history traits in response to ecologically distinct habitats (Stearns 1992; Roff 2002) might directly reduce gene flow between populations through reduced performance of migrants and hybrids between the habitats. Second, life history divergence often involves shifts in reproductive timing, thereby potentially causing phenological assortative mating as a correlated response. Evidence of this mechanism exists but is mostly limited to insects (e.g., Feder et al. 1997; Abbot and Withgott 2004; Santos et al. 2011; but see Friesen et al. 2007). Third, life history divergence commonly involves body size shifts (Stearns 1992; Roff 2002). Because body size is also frequently involved in sexual selection (Andersson 1994), life history divergence might drive sexual assortative mating as an additional correlated response. Finally, life history traits generally display higher levels of phenotypic plasticity than morphological, physiological, and behavioural traits, because the former represent greater targets for environmental perturbation (Price and Schluter 1991; Houle 1992). Life history shifts might thus follow rapidly upon the colonization of new habitats, and hence contribute to reproductive isolation well before genetically–based divergence in less plastic traits has occurred (West–Eberhard 2003; Thibert–Plante and Hendry 2011).

The objective of this study is to initiate an investigation of life history divergence in a natural model system for studying speciation with gene flow – lake and stream populations of threespine stickleback fish (*Gasterosteus aculeatus* Linnaeus, 1758). Marine (ancestral) stickleback have colonized freshwater environments all across the Northern Hemisphere after the last glacial retreat, thereby establishing numerous evolutionarily independent population pairs residing in adjacent lake and stream habitats (Hagen and Gilbertson 1972; Reimchen et al. 1985; Lavin and McPhail 1993; Thompson et al. 1997; Reusch 2001; Hendry and Taylor 2004; Berner et al. 2008; Aguirre 2009; Deagle et al. 2012). Lake and stream populations typically display predictable and at least partly genetically–based (Lavin and McPhail 1993; Sharpe et al. 2008; Berner et al. 2011) divergence in morphological traits, presumably reflecting adaptation to distinct foraging environments. This phenotypic di-

vergence often coincides with striking divergence in genetic markers on a small spatial scale (Berner et al. 2009; Deagle et al. 2012; Kaeuffer et al. 2012; Roesti et al. 2012a), indicating the presence of strong reproductive barriers associated with lake–stream transitions. The nature of these barriers, however, remains poorly understood (reviewed in Hendry et al. 2009).

A contribution of life history divergence to reproductive isolation in lake-stream stickleback, through one or several of the mechanisms described above, is plausible because life history evolution is reported from other stickleback systems. This includes divergence in age at reproduction and reproductive investment within and among lake populations (Reimchen 1992; Baker et al. 1998, 2005, 2011; Gambling and Reimchen 2012), and divergence in body size within and among lake populations (Moodie and Reimchen 1976; McPhail 1977; Reimchen 1992; Baker et al. 1998; Nagel and Schluter 1998; Gambling and Reimchen 2012) and between freshwater and marine stickleback (McKinnon et al. 2004, 2012). At least some of this divergence is partly genetically based (McPhail 1977; Snyder 1991). Furthermore, body size divergence is generally a strong contributor to mating isolation in the species (Dufresne et al. 1990; Nagel and Schluter 1998; Ishikawa and Mori 2000; McKinnon et al. 2004, 2012; Albert 2005; Boughman et al. 2005; but see Raeymaekers et al. 2010). Nevertheless, investigations of life history divergence in lake–stream stickleback are lacking.

Our study focuses on stickleback inhabiting contiguous lake and stream habitats within a single lake basin in Central Europe. We focus on multiple replicate lake–stream sample pairs to assess whether life history divergence has occurred repeatedly in a similar direction. Finally, we include nuclear and mitochondrial genetic marker data to search for signatures of habitat–associated barriers to gene flow, and to gain insight into the origin of lake and stream stickleback populations within the lake basin.

1.3   Materials and methods

1.3.1   Stickleback samples

The main focus of this life history investigation lies on stickleback in Lake Constance (LC) and its tributaries in Central Europe (Fig. 1.1, Table 1.1). The geographic distance between the different lake–stream pairs ('systems') was maximized to reduce the opportunity for gene flow among systems, and to provide phenotypic and genetic information representative of the entire lake basin. The systems include two lake–stream pairs subjected previously to an analysis of foraging morphology and population genetics ('Constance

South', COS, and 'Constance West', COW; Berner et al. 2010a; see also Roesti et al. 2012b). The majority of the study sites, however, have not been investigated before. The new systems include 'Constance North' (CON) and 'Constance East' (COE). In the latter, the stream site was sampled at two different locations (Grasbeuren, 7.6 km from the lake, and Mühlhofen, 4 km from the lake). These samples proved very similar phenotypically and genetically (e.g., $F_{ST} = 0.002$, $P = 0.40$; further details not presented), so that they were pooled to represent a single stream site (COE stream). Further, we sampled an additional stream for the COS system ('COS1 stream'). Because this stream drains into LC at almost the same location as COS2 stream, these two systems share their lake counterpart.

The origin of stickleback in the LC basin is unknown, but commonly attributed to human introduction (e.g., Berner et al. 2010b; Lucek et al. 2010). The first report of the species' widespread occurrence within the basin dates back to the mid 19th century (Heller 1871, p. 320). To obtain new genetic insights into the populations' possible origin, we complemented our paired lake–stream samples by samples from two solitary (allopatric) stream–resident populations. The first solitary population was sampled from a small creek draining into the River Rhine (the outlet stream of LC, draining into the Atlantic) near Basel, Switzerland (Fig. 1.1, Table 1.1). This sample is hereafter called the Rhine (RHI) sample. A recent study indicates strong differentiation in neutral markers between stickleback occurring in the Rhine catchment downstream of LC and the lake itself (Lucek et al. 2010), suggesting that the latter was not colonized via the Rhine. Our Rhine sample allowed an independent evaluation of this hypothesis. The second solitary stream population (DAN) was sampled in the headwaters of the Danube River drainage near Kirchbierlingen, Germany. This sample was included because of the close proximity of the Danube drainage to the LC basin, and because the LC region drained into the Danube (and eventually into the present–day black sea region) in postglacial times (Behrmann–Godel et al. 2004).

All new samples were collected in the spring 2011 (late April, May; i.e., during the stickleback breeding season). The samples taken in previous years, and a few specimens collected in 2012 exclusively for the analysis of fecundity and egg size (see below), were also collected within that seasonal time frame. All samples were taken with permission from the corresponding fisheries authorities (Austria: Landesfischereizentrum Vorarlberg, A. Lunardon; Germany: Fischereiforschungsstelle Baden–Württemberg, S. Blank, M. Bopp, C. Wenzel; Switzerland: Jagd– und Fischereiverwaltung Thurgau, R. Kistler; Amt für Umwelt und Energie Basel–Stadt, H.–P. Jermann). Sampling occurred on breeding grounds using unbaited minnow traps. All individuals
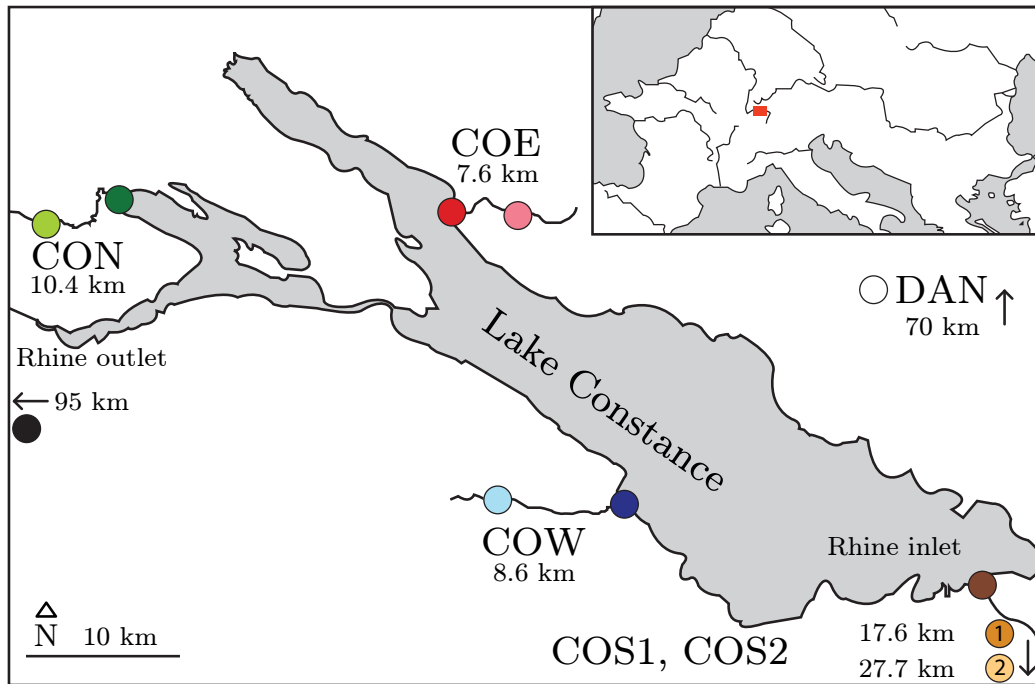
Figure 1.1: Geographical situation of the stickleback study sites. Shown are the five lake–stream stickleback pairs ('systems') in the Lake Constance basin (CON, COE, COS1, COS2, COW; colored circles, stream sites lighter), and the two solitary sample sites outside the basin (RHI, DAN; black and white circle). The black rectangle in the inset map locates the study area in Central Europe. Distances indicate the approximate water distance between the lake and stream site within each system, and the approximate map distance between Lake Constance and the solitary sample sites. Note that the COS1 and COS2 stream samples were not collected from the Rhine (the major inlet to Lake Constance), but from two small streams draining separately into Lake Constance. Further details on the samples and locations are given in Table 1.1.

used for this study were in reproductive stage because the males consistently displayed breeding coloration, and gravid females were frequent at every site. The specimens were euthanized with an overdose of MS–222, taking all efforts to minimize suffering, and immediately weighed, photographed with a reference scale as described in (Berner et al. 2009), and stored in absolute ethanol. For most sites, a minimum sample of 12 individuals per sex could be achieved (Table 1.1). Unless noted otherwise, all analyses are based on the full sample from a given site. All work in this study was approved by the Veterinary Office of the Canton of Basel–Stadt (permit number: 2383).

Table 1.1: Localities, geographical coordinates, sampling year, and sample size for the five lake–stream stickleback systems in the Lake Constance basin (CON, COE, COS1, COS2, COW), and the two solitary stream populations (RHI, DAN).

Locality	System or site code	Habitat	Latitude (North)	Longitude (East)	Sampling year	Sample size
Iznang (DE)	CON	lake	47°43'03.36"	8°57'42.48"	2011	22 (10/12)
Bohlingen (DE)	CON	stream	47°43'18.84"	8°53'01.68"	2011	23 (15/7)
Unteruhldingen (DE)	COE	lake	47°43'25.32"	9°13'37.56"	2011	33 (18/15)
Grasbeuren (DE)	COE	steam	47°43'39.72"	9°18'23.4"	2011	13 (9/4)
Mühlhofen (DE)	COE	steam	47°44'11.76"	9°15'49.68"	2011	12 (7/5)
Fussach(AT)	COS1&COS2	lake	47°29'29.7"	9°39'40.37"	2008	24 (3/21)
Hohenems (AT)	COS1	stream	47°21'18.55"	9°40'10.22"	2008	25 (11/14)
Rankweil (AT)	COS2	stream	47°16'19.28"	9°35'32.72"	2008	24 (12/12)
Romanshorn (CH)	COW	lake	47°33'22.5"	9°22'48.25"	2008/2009	24 (12/12)
Niederaach (CH)	COW	stream	47°33'29.25"	9°16'42.38"	2008/2009	25 (11/14)
Basel (CH)	RHI	stream	47°32'44.34"	7°33'51.84"	2011	24 (12/12)
Kirchbierlingen (DE)	DAN	stream	48°14'04.03"	9°43'30.86"	2011	34 (15/19)

The localities are situated in Germany (DE), Austria (AT), and Switzerland (CH). Sample sizes are total, and males and females in parentheses. Note that the same lake sample was used for both the COS1 and COS2 system, and that the COE stream site combines two samples (for details see text).

1.3.2 Analysis of lake–stream divergence in life history

Our prime interest was to investigate lake–stream divergence in age and size at reproduction. To quantify age at reproduction, we retrieved the left and right sagittal otolith from all specimens in each lake–stream pair. The otoliths were cleaned mechanically using fine forceps, dried, mounted in 20 ml Euparal on a microscope slide, and inspected under a stereomicroscope at 50× magnification by a single person (DM) blind to the specimens' origin. Illumination was from above on a black background to optimally visualize the opaque and transparent ring zones used for age determination following (Jones and Hynes 1950) (representative otoliths from different age classes are shown in Fig. S1 (Supplementary material)). Left and right otoliths always produced consistent results. A total of 4 specimens ($< 2\%$ of all specimens investigated) displayed unclear otolith ring patterns and could thus not be aged unambiguously. Excluding these specimens from analysis did not affect any conclusions; hence we present results based on the full data set. Differences in age composition between lake and stream fish were tested separately for each system through non–parametric permutation tests randomizing the response variable (age) 9999 times over the predictor (habitat) (Manly 2007), and using the lake–stream difference in average age as test statistic. All statistical inference in this study is based on analogous permutation tests.

To quantify body size at reproduction, we digitized 16 homologous landmarks (Berner et al. 2010a) on the photograph of each specimen by using TpsDig (Rohlf 2001). TpsRelw (Rohlf 2001) was then used to calculate centroid size from the landmark configurations. This size metric, hereafter referred to as 'body size', was considered more robust to variation in overall body shape and feeding or reproductive status than size metrics such

as standard length or linearized body mass (Using the latter as body size metric, however, produced very similar results in all analyses.). To test for lake–stream divergence in body size, we used the difference in average size between the habitats as test statistic.

In addition to age and size at reproduction, we investigated divergence in fecundity and egg size. For this, clutches of gravid females ready for spawning were collected in the field by gently squeezing the females' abdomen, and preserved in ethanol. We then counted the total number of eggs (fecundity) under a stereomicroscope, dried all eggs at 50 °C for 48 h, and determined their total dry mass. Egg size was then expressed as the total clutch dry mass divided by total egg number (i.e., the average dry mass of a single egg). This investigation used mainly females collected in 2012 for this specific purpose only (and hence not included in Table 1.1; lake: COE, COW, N = 11 each; stream: COW, CON, COE, N = 9, 1, 1), but additionally involved a few females also used for the other analyses. Testing for lake–stream divergence in fecundity and egg size was then performed in a single analysis for each trait by pooling data across the two lake sites and the three stream sites (Restricting the analysis to the COW system with sufficient data from each habitat produced similar results.). As above, the difference in trait means between the habitats was used as test statistic.

1.3.3 Comparison of body size among global populations

To interpret the body size patterns revealed in our lake–stream and solitary stickleback populations from Central Europe in a broader geographic and ecological context, we performed a comparison of reproductive body size by including a total of 21 additional stickleback populations from different geographic regions and habitats. We hereafter call this the 'global' data set, acknowledging that these samples do not represent the species' full body size diversity (e.g., Reimchen 1992). These additional samples comprised lake populations from Beaver, Boot, Joe's, Misty, Morton, Pye, and Robert's Lake (sites described in Berner et al. 2008), and from Hope Lake (coordinates: 50° 34' 0" N, 127° 20' 30" W), on Vancouver Island (British Columbia, Canada). Additional stream–resident populations were from the Beaver, Boot, Joe's, McCreight, Pye, and Robert's systems (Berner et. al 2008), and from the inlet stream to Misty Lake (Hendry et al. 2002; Lavin and McPhail 1993), on Vancouver Island. These freshwater samples were complemented by collections of marine stickleback from two estuaries on the east coast of Vancouver Island (Cluxewe: 50° 36' 51" N, 127° 11' 10" W; Sayward (Berner et al.

2010b)), from the Japan Sea and Pacific (Kitano et al. 2009), from the Atlantic Coast in Norway (Leinonen et al. 2011b), and from the coast of the White Sea in Russia (Mäkinen 2006). All these additional samples were also collected during the reproductive season on breeding grounds. Body size was quantified from available photographs as described above. Sample size was 20–36 individuals per site, with both sexes well represented.

For the global comparison of body size at reproduction, we first pooled all samples from the LC basin within each habitat type. This was done to avoid pseudo–replication, and because body size within each habitat type was highly consistent (see below). Interestingly, visual inspection of the data from the global samples suggested differences among the three habitat types (lake, stream, marine) in the *variability* of average body size across populations. This was tested formally through separate lake–stream and marine–stream tests using the variance in population means as test statistic.

1.3.4 Additional phenotypic analyses

The above analyses were complemented by investigating two additional variables potentially relevant to life history evolution. First, as life history divergence might be driven by differential food resources, we analyzed prey items in stomachs of stickleback from one system (COW lake and stream; N = 20 and 7). Because lake stickleback might exploit different prey resources during the reproductive period spent in littoral (near–shore) breeding habitat than during non–reproductive life stages (e.g., Bentzen et al. 1984), we additionally acquired a small sample (N = 5) of stickleback caught by LC fishermen in offshore drift nets targeting pelagic whitefish. This sample was taken off the COS lake site in April 2011. To ensure adequate quality of stomach content for analysis, all specimens (lake offshore, lake littoral, and stream) were preserved within 5 h upon setting the capturing device (minnow trap, drift net). Prey items were identified to order, family, or genus, and assigned to broad taxonomic groups (e.g., pelagic cladocera, vermiform insect larvae; see Table 1.2). For every stickleback, we determined the relative proportion of the total prey items accounted for by each taxonomic group, calculated summary statistics for each of the three habitat types, and interpreted these statistics qualitatively. This approach was preferred to a formal analysis because of the relatively small sample sizes.

The second additional variable was the lateral plate phenotype. Ancestral marine stickleback are protected from vertebrate predators in their pelagic environment by bony lateral plates along their entire body (Bell and Foster 1994). This phenotype is disfavoured in most freshwater environments, as stickleback in lakes and streams generally display an adaptive,

Table 1.2: Stomach content of stickleback from the Lake Constance offshore site, and from the lake and stream site in the COW system.

	Pelagic	Pelagic/Benthic	Benthic				
	Cladocera[1]	Copepods	Cladocera[2]	Other crustacea[3]	Vermiform insect larvae[4]	Other insect larvae[5]	Stickleback eggs
Lake offshore	0.34(0.21)	0.66(0.21)	-	-	-	-	-
COW lake	0.01(0.02)	0.07(0.1)	0.33(0.29)	0.03(0.08)	0.42(0.37)	0.15(0.24)	0.03(0.11)
COW stream	-	0.17(0.18)	0.2(0.25)	-	0.57(0.27)	0.06(0.08)	0.09(0.2)

1 Daphnia, Ceriodaphnia, Bosmina.
2 Chydoridae.
3 mainly Ostracoda
4 Chironomidae, Ceratopogonidae.
5 mainly Ephemeroptera and Plecoptera.
The values represent the proportion of the total prey items accounted for by each prey class, averaged across individuals within each site (standard deviation in parentheses). The copepods category subsumes pelagic, benthic, and/or generalist taxa difficult to distinguish; strictly pelagic calanoid copepods, however, were found in the offshore lake specimens only. Sample size is 5, 20, and 7 for offshore, COW lake, and COW stream.

genetically–based reduction in the number of lateral plates (Bell and Foster 1994). We considered this trait here because the major genetic factor determining plate phenotype (the ectodysplasin gene, *EDA*; Colosimo et al. 2005) might pleiotropically influence growth rate (Barrett et al. 2009), and because stickleback in the LC basin are polymorphic for both plate phenotype and the underlying *EDA* alleles (Berner et al. 2010a). Following this latter study, we assigned all individuals to one of three lateral plate phenotype morphs (full, partial and low). We then tested for lake–stream divergence in plate morph frequency within each system by using the Chi–square ratio as test statistic (extending similar tests already performed for the COW and one of the COS systems; Berner et al. 2010a). Next, sufficiently polymorphic samples (i.e., the stream samples of CON, COE, and COW) were used to test for an association between plate morph and body size by using the F ratio from analysis of variance as test statistic (Manly 2007). All statistical analyses and plotting were performed in R (R Development Core Team 2012).

1.3.5 Genetics

The major goal of our genetic investigation based on nuclear and mitochondrial markers was to quantify population structure within and among the replicate lake–stream systems in the LC basin. Of particular interest was the detection of strong genetic divergence within lake–stream systems, suggesting effective habitat–related barriers to gene flow. An additional goal was to explore the relationship between stickleback in the LC basin and fish from nearby water bodies. The present work greatly extends a previous population genetic study partly involving fish from the LC basin (Berner et al. 2010a) in that new lake–stream pairs are analyzed, samples from the Rhine

and Danube are included, and a greater number of genetic markers are used.

We first extracted DNA from pectoral and caudal fin tissue on a MagNA Pure LC extraction robot (Roche) by using the Isolation Kit II (tissue). Next, we amplified eight microsatellites with labelled primers in two separate multiplex PCRs by using the QIAGEN multiplex kit and following the manufacturer's protocol. All PCRs included a negative control to check for contamination. The microsatellite markers were chosen to be far from known quantitative trait loci in stickleback, and to lie on different chromosomes. They included the markers Stn67, Stn159, Stn171, and Stn195 used previously (Berner et al. 2009, 2010a), and additionally Stn28, Stn99, Stn119, and Stn200 (Peichel et al. 2001). For the latter, we designed our own primer pairs. PCR products were run on an ABI3130xl sequencer (Applied Biosystems), and alleles scored manually in PeakScanner v1.0. Input files for the different population genetic programs were prepared by using CREATE (Coombs et al. 2008).

The microsatellite data were first used to estimate differentiation among all 11 samples by Weir & Cockerham's F_{ST} (Weir and Cockerham 1984) calculated with GENETIX v4.0.5.2 (Belkhir et al. 2004) (P–values based on 999 permutations). To account for variation in heterozygosity within populations (Hedrick 2005), we also calculated *standardized* F_{ST} after data transformation with RECODEDATA v0.1 (Meirmans 2006). Next, we tested whether neighboring lake and stream samples qualified as genetically distinct populations by performing a genetic clustering analysis using STRUCTURE (v2.3.1; Hubisz et al. 2009; Pritchard et al. 2000) separately in each lake–stream pair (note that the COS system represents two pairs, both involving the same lake sample). The assumed number of populations (K) ranged from one to three, with each level replicated five times under the admixture and independent allele model with 100'000 iterations (20'000 iterations burnin). An additional analysis examined population structure among the 11 pooled samples, using K = 1–12. STRUCTURE results were combined using Structure Harvester v.0.6.92 (Earl and vonHoldt 2011), and interpreted following (Pritchard and Wen 2004; Evanno et al. 2005).

The above analyses using rapidly evolving microsatellites were complemented by a more coarse–grained investigation of genetic relationships based on single nucleotide polymorphisms (SNPs) within a 305 bp segment of the mitochondrial D–loop. Sample size was 18–32 individuals per site, 256 in total. Primers and PCR amplification conditions were as in (Berner et al. 2010a). Products were sequenced on an ABI3130xl sequencer (Applied Biosystems). We used jModelTest v0.1.1 (Posada 2008) to determine the most appropriate model of sequence evolution ('F81'; Felsenstein 1981), identified the most probable genealogical relationship by the maximum–likelihood

method implemented in PAUP* v4.0 (Swofford 2003), and generated a haplotype genealogy for visualization following (Salzburger et al. 2011). All D–loop sequences are deposited in GenBank (accession numbers JX436521–JX436776).

1.4 Results

1.4.1 Phenotypic analyses

The otolith analysis revealed strong and highly consistent lake–stream divergence in age at reproduction in all replicate systems in the LC basin (all P < 0.0015). Generally, stickleback on breeding grounds in the lake were in their third calendar year (i.e., approximately two years old), with a few individuals breeding in their second or fourth calendar year (Fig. 1.2). By contrast, stream stickleback essentially displayed an annual life cycle; individuals in their third calendar year were rare, and no single fish was found to breed in its fourth calendar year.

Lake–stream shifts in age at reproduction were paralleled by strong divergence in body size, with lake fish on average exhibiting 27% greater size than stream fish (lake mean centroid size across all systems: 80.4 mm; stream: 63.2 mm; P = 0.0001 in all systems) (Fig. 1.2). Translated to fresh body mass, the average size difference was more than twofold (lake: 2.53 g; stream 1.19 g; a photograph of a representative lake and stream individual is shown in Fig. S1 (Supplementary material)). Body size divergence was further associated with dramatic divergence in fecundity (Fig. 1.3): on average, the (larger) lake females displayed a threefold higher number of eggs than the stream females (284 *versus* 94; P = 0.0001). Egg size, however, did not differ between the habitats (P = 0.51).

Our comparison of body size across global stickleback samples from lakes, streams, and the sea indicated a clear difference in the variance in population average size among the habitats. Strikingly, all stream populations investigated displayed relatively similar average size, whereas the lake samples were much more variable (lake–stream difference in variance: P = 0.002; Fig. 1.4). The latter included very small–bodied populations (Morton, Pye, and Robert's) as well as large–bodied populations (Boot, Joe's). Body size among marine stickleback also tended to be more variable than among stream populations (marine–stream difference in variance: P = 0.065; note the small sample size for marine fish, and hence low statistical power in this test).

In addition to the above life history patterns, our analysis of stomach content revealed a very clear difference in prey utilization by lake and stream
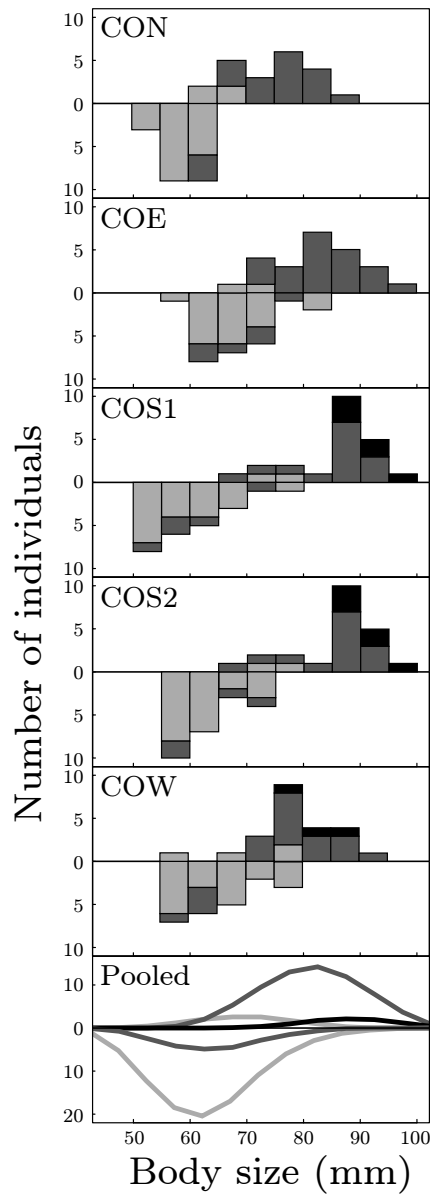
Figure 1.2: Age and body size at reproduction in lake and stream stickleback from the Lake Constance basin. The top panels show body size (quantified as landmark–based centroid size) histograms for each lake–stream system separately, with the lake data pointing upward and the stream data pointing downward. Proportions are shaded according to age class; individuals in their second, third, and fourth calendar year are drawn in light gray, dark gray, and black. The bottom panel follows the same drawing conventions, except that here the data are pooled across all systems within each habitat type, and smoothed by LOESS (locally weighted scatterplot smoothing) for each age class separately. Note the striking shift toward greater age and size at reproduction in lake stickleback as compared to their conspecifics from streams.
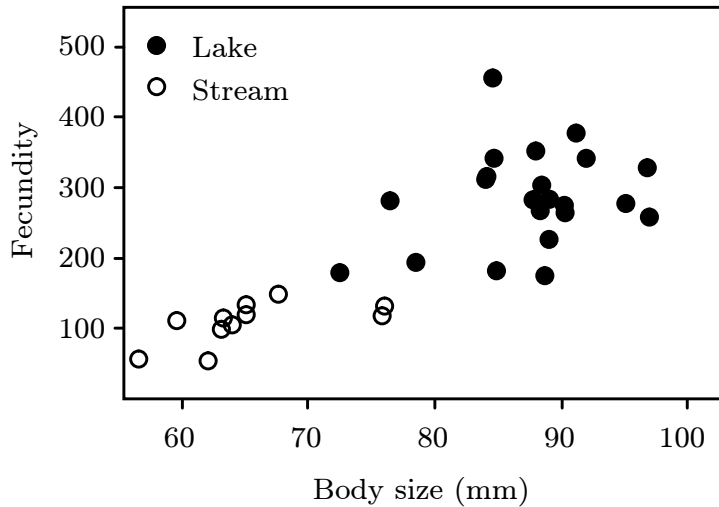
Figure 1.3: Fecundity in relation to body size in female stickleback from Lake Constance and its tributary streams. Fecundity is expressed as number of eggs per clutch. Within each habitat class, samples were pooled across different locations (lake: N = 22; stream: N = 11).

stickleback, despite the modest sample sizes. In particular, our pelagic sample showed clearly that LC stickleback forage on zooplankton outside the breeding grounds; the stomachs of these specimens contained exclusively small pelagic crustacea (Table 1.2). By contrast, the stomachs of the stream fish contained exclusively benthic prey (predominantly chironomid larvae and benthic cladocera), highly consistent with data from streams on Vancouver Island (Berner et al. 2008). Similar benthic prey was also found in the lake fish collected on (littoral) breeding grounds, indicating a reproductive shift in foraging mode in stickleback residing within LC.

In all three new lake–stream systems subjected to lateral plate morph analysis (CON, COE, COS1), we found a trend toward plate reduction in the stream as compared to the lake where fully plated fish predominated clearly. The shift in plate morph frequency was particularly striking in the COE system (P = 0.0001), paralleling a similar pattern found previously in the COW system (Berner et al. 2010a). However, we found no relationship between plate morph and body size at reproduction in any of the three investigated stream samples (CON, COE, COW; all P ≥ 0.35).

1.4.2 Genetics

A striking pattern revealed by our eight microsatellite markers was the absence of population structure among the four geographically distant LC sam-
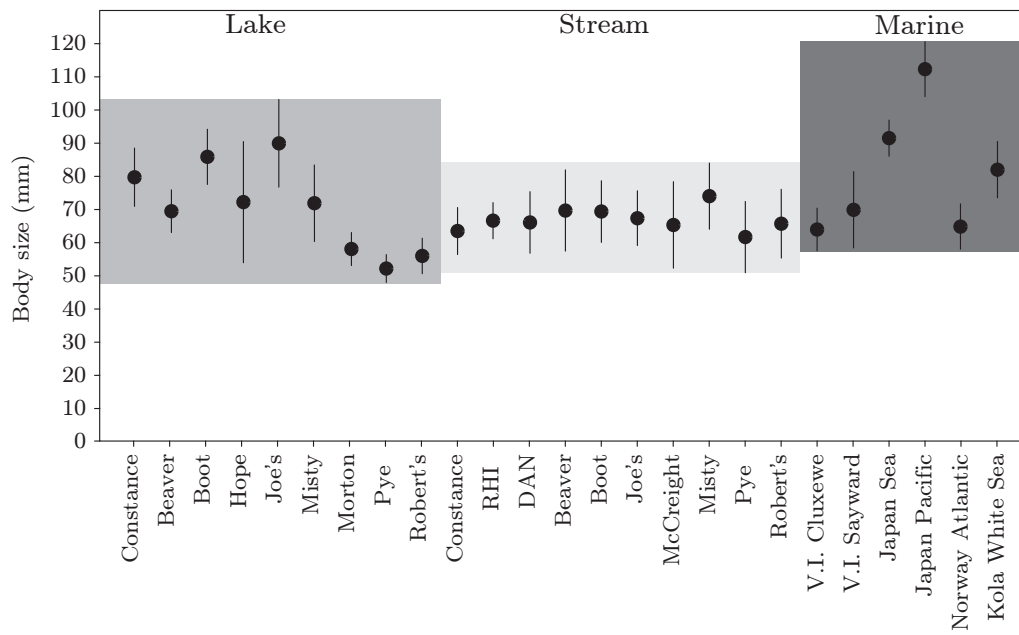
Figure 1.4: Body size at reproduction in the global stickleback populations from lake, stream, and marine habitats. Samples from the Lake Constance basin are pooled for each habitat type (further details on the samples are given in the text). Error bars are one standard deviation in each direction. The shaded boxes behind the symbols indicate the body size range spanned by the standard deviations in each habitat. Note the low variance in population mean size among the stream populations as compared to lake and marine fish.

ples. None of the six total pairwise F_{ST} values among these lake samples exceeded 0.01 (all P $\geq$ 0.07) (Table 1.3). Genetic differentiation *within* the lake–stream pairs was mostly modest as well, but sometimes reached substantial values despite a much shorter geographic distance between the paired lake and stream sites than among the lake sites (COE: F_{ST} = 0.18, P = 0.001; COS2: F_{ST} = 0.08, P = 0.001). Microsatellite differentiation among the stream samples was generally substantial, with F_{ST} averaging 0.10 (all P < 0.004 except CON–COS1, P = 0.13). Furthermore, our Rhine sample (RHI) displayed strong differentiation from all samples in the LC basin (F_{ST} = 0.16–0.29), whereas differentiation between the Danube sample (DAN) and stickleback from the LC basin was rather low. For instance, all five comparisons between DAN and LC samples produced $F_{ST} \leq 0.04$ (P = 0.001–0.023).

The results from the STRUCTURE analysis agreed well with the F_{ST}–based patterns. First, analyzing each system separately, STRUCTURE identified the system displaying the highest lake–stream differentiation (COE) as consisting of two genetically distinct populations. The four other systems qualified as a single population (details not presented). Analyzing all 11 samples together suggested two distinct genetic clusters. The first cluster involved RHI and the stream site of COE, the second involved all other populations from the LC basin plus the DAN sample. However, the STRUCTURE algorithm can perform poorly when faced with highly imbalanced sample sizes (Kalinowski 2011). Indeed, most samples from the LC basin were genetically so similar that they essentially formed one single large sample, which probably caused RHI and COE stream to cluster together despite strong genetic differentiation (F_{ST} = 0.16). However, when analyzing only RHI, COE stream, and a *single* lake sample together, three distinct populations were indicated, as expected based on F_{ST}.

Our mitochondrial D–loop sequencing identified six total SNPs, defining five distinct haplotypes (Fig. 1.5). One of these haplotypes was clearly predominant; it was either the only one discovered, or at least very frequent, in *all* samples from the LC basin. Notably, this haplotype was also the only one found in the DAN sample. By contrast, all individuals from RHI exhibited a different haplotype shared only with some individuals from three stream samples of the LC basin. Three additional haplotypes occurred at low frequency, mainly in stream fish.

Table 1.3: Pairwise genetic differentiation among the nine lake and stream stickleback samples from the Lake Constance basin, and the two solitary samples, based on eight microsatellite markers.

	CON lake	CON stream	COE lake	COE stream	COS lake	COS1 stream	COS2 stream	COW lake	COW stream	RHI	DAN
CON lake		0.00 (0.676)	0.01 (0.071)	0.18 **(0.001)**	0.01 (0.240)	0.02 (0.041)	0.10 **0.001**	0.00 (0.305)	0.05 **(0.001)**	0.27 **(0.001)**	0.03 **(0.002)**
CON stream	0.00		0.00 (0.587)	0.15 **(0.001)**	0.00 (0.386)	0.01 (0.132)	0.06 **(0.001)**	0.00 (0.759)	0.03 **(0.004)**	0.25 **(0.001)**	0.02 (0.011)
COE lake	0.02	0.00		0.18 **(0.001)**	0.00 (0.543)	0.02 **(0.003)**	0.07 **(0.001)**	0.00 (0.744)	0.04 **(0.001)**	0.28 **(0.001)**	0.03 **(0.001)**
COE stream	0.55	0.46	0.50		0.20 **(0.001)**	0.17 **(0.001)**	0.21 **(0.001)**	0.17 **(0.001)**	0.13 **(0.001)**	0.16 **(0.001)**	0.17 **(0.001)**
COS lake	0.02	0.00	0.00	0.56		0.01 (0.160)	0.08 **(0.001)**	0.00 (0.478)	0.03 **(0.001)**	0.28 **(0.001)**	0.04 **(0.001)**
COS1 stream	0.05	0.02	0.05	0.47	0.02		0.06 **(0.001)**	0.02 (0.053)	0.03 **(0.002)**	0.24 **(0.001)**	0.08 **(0.001)**
COS2 stream	0.22	0.13	0.15	0.52	0.17	0.12		0.08 **(0.001)**	0.11 **(0.001)**	0.29 **(0.001)**	0.12 **0.001**
COW lake	0.00	0.00	0.00	0.48	0.00	0.05	0.17		0.02 **(0.007)**	0.26 **(0.001)**	0.02 (0.023)
COW stream	0.13	0.08	0.10	0.40	0.07	0.07	0.25	0.05		0.21 **(0.001)**	0.06 **(0.001)**
RHI	0.69	0.64	0.66	0.46	0.66	0.56	0.62	0.62	0.54		0.26 **(0.001)**
DAN	0.08	0.05	0.07	0.50	0.00	0.19	0.27	0.05	0.16	0.65	

The upper semimatrix gives Weir and Cockerham's F_{ST} estimator (Weir and Cockerham 1984), with P–values based on 999 permutations in parentheses (bold if P < 0.01). The lower semimatrix presents F_{ST} standardized by the maximum differentiation possible given the observed magnitudes of within–population heterozygosity (Hedrick 2005).
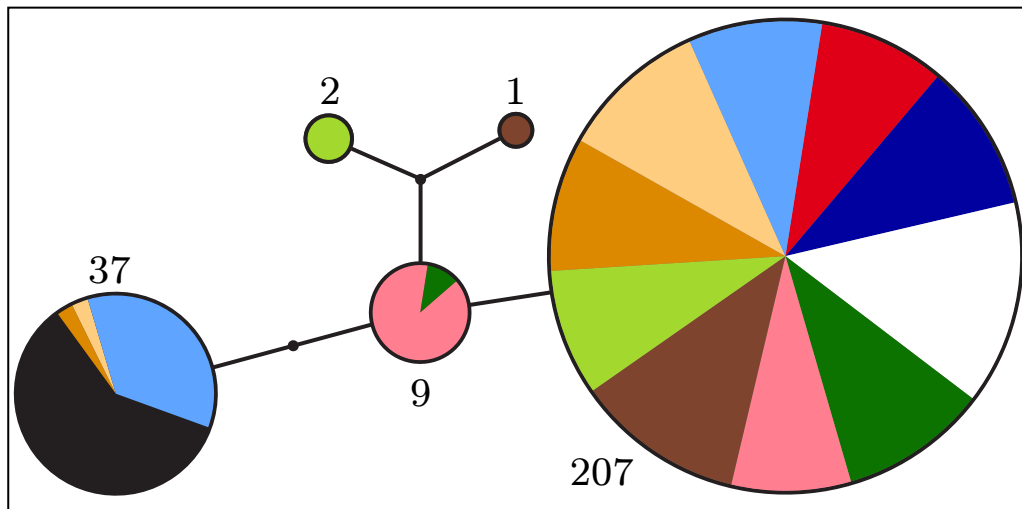
Figure 1.5: Haplotype network for the lake–stream stickleback pairs in the Lake Constance basin and the solitary populations. The network is based on six single nucleotide polymorphisms in the mitochondrial D–loop. The numbers give the total count for each haplotype. Color codes are as in Fig. 1.1.

1.5 Discussion

1.5.1 Life history divergence and implications for reproductive isolation

Divergence in life history traits might strongly contribute to reproductive isolation, and yet its role in speciation is little explored. We here investigated life history in stickleback residing in Lake Constance and multiple tributary streams, revealing dramatic divergence between the two habitats: lake fish reproduce at much greater age and size than their conspecifics in the streams, and these patterns coincide with much greater fecundity in females from the lake. These findings parallel concurrent shifts in age and size at reproduction and in reproductive investment reported from North American lake populations (Reimchen 1992; Baker et al. 2011; Gambling and Reimchen 2012). The only life history trait that proved stable between lake and stream stickleback was egg size, possibly indicating similar stabilizing offspring viability selection in both habitats (Parker and Begon 1986; Bernardo 1996).

Divergence in age and size at reproduction was highly consistent across multiple replicate habitat pairs in the LC basin, and our genetic data indicate clearly that this results from repeated evolution in stream stickleback. The reason is that the stream samples consistently displayed strong mutual microsatellite differentiation, contrary to the lake samples exhibiting negligible differentiation. This pattern clearly rules out the possibility that the different stream populations originate from a common ancestral stream stickleback population. Moreover, the rare D–loop haplotypes found in the LC basin were mostly unique to specific stream samples (Fig. 1.5), consistent with independent founder events (i.e., haplotype frequency shifts caused by strong genetic drift in the small stream founder populations). Together, our life history and genetic data thus argue strongly for the independent colonization of the different tributaries by an essentially panmictic LC population, followed by repeated life history evolution in stream stickleback.

Given the great magnitude of lake–stream divergence in body size, and the general importance of this trait in mate choice and male aggressive interactions in the species (Dufresne 1990; Nagel and Schluter 1998; Ishikawa and Mori 2000; McKinnon et al. 2004, 2012; Albert 2005; Boughman et al. 2005), the observed life history shifts might well contribute to reducing gene flow across the lake–stream habitat transitions. Indeed, our F_{ST}–based analysis revealed substantial lake–stream differentiation within some systems (with values reaching 0.18), and STRUCTURE identified two distinct populations in one of them. This allows us to infer the presence of strong reproductive barriers at a small spatial scale, consistent with findings from lake–stream

systems in Pacific North America (Berner et al. 2009; Deagle et al. 2012; Kaeuffer et al. 2012; Roesti et al. 2012a). Note that the weak marker divergence seen in some of our systems (CON, COS1; $F_{ST} \leq 0.01$) does not conflict with this conclusion; because the colonization of the LC basin is presumably relatively recent (see below), detecting reproductive isolation with neutral markers is expected to be difficult (Berner et al. 2010a; Thibert–Plante and Hendry 2010). The presence of effective habitat–related reproductive barriers is also supported by the consistent and sometimes substantial (COE, COW) lake–stream divergence in plate morph frequency (Fig. S3 (Supplementary material)). This divergence has a strong genetic basis (Berner et al. 2010a) and would not have arisen, or be maintained, in the absence of effective barriers to gene flow. Nevertheless, the extent to which the observed lake–stream shifts in life history actually contribute to reproductive isolation cannot be evaluated based on the present data.

1.5.2 Mechanisms of life history divergence

In many organisms, the transition of resource allocation from growth to reproductive life is governed by critical maturation size thresholds (reviewed in Bernardo 1993; Berner and Blanckenhorn 2007). Although not investigated in detail, this seems to hold for stickleback as well (Craig–Bennett 1931; Baggerman 1972): as long as an individual has not attained this threshold, environmental cues signaling spring conditions will not trigger maturation and reproductive behavior. On the basis of this maturation control, we propose two not mutually exclusive hypotheses explaining life history divergence in lake–stream stickleback in the LC basin. First, assuming similar growth rates in both habitats, lake fish might exhibit a relatively higher maturation size threshold (due to genetic divergence and/or phenotypic plasticity) that they generally cannot attain within one year. Only after two years of growth, lake fish would exceed their maturation threshold and start reproducing – and at that time also be much larger than the stream fish reaching their threshold size within one year (Berner and Blanckenhorn 2007). This hypothesis is plausible: body size divergence among populations of ninespine stickleback is attributable to genetically–based divergence in maturation size thresholds (Herczeg et al. 2009; Shimada et al. 2011).

Alternatively, maturation size thresholds might be similar among the populations, but growth rates might be lower in lake fish than in tributary stream populations (again due to genetic divergence, phenotypic plasticity, or both). The consequence would be the same as above: lake fish would require two years of growth to attain their maturation threshold, but mature larger (Berner and Blanckenhorn 2007). Indeed, our study provides evidence

of differential growth rates between the habitats. As the analysis of stomach content suggests, stickleback inhabiting LC exploit exclusively zooplankton prey outside the breeding grounds. These fish are also an occasional by–catch in off–shore drift nets (personal communications from LC fishermen), and are absent from littoral habitat outside the breeding season (DM, personal observation). Moreover, for a freshwater population, stickleback in LC display extremely long gill rakers (Berner et al. 2010a), a character state generally associated with zooplankton exploitation (Robinson and Wilson 1994) and typical of pelagic marine stickleback (Berner et al. 2010b). Stickleback residing within LC thus display a pelagic life style, with a foraging niche shift during the reproductive period (see also Bentzen et al. 1984). Note also that the LC fish provide a rare example of a freshwater population almost fixed for the full lateral plate morph (Fig. S3 (Supporting information)), a phenotype presumably favored in pelagic populations highly exposed to vertebrate predation (Reimchen 1994a). (We found no evidence, however, for a direct relationship between plate phenotype and life history traits.).

By contrast, stream populations in the LC basin exploit exclusively benthic resources. Within the LC basin, we thus find similarly strong divergence in foraging modes as seen in the most ecologically divergent lake–stream pairs on Vancouver Island, Canada (Berner et al. 2008, 2009; Kaeuffer et al 2012). This difference in resource use might directly induce differential growth performance between the habitats, as benthic foraging generally seems to allow for a higher growth rate than pelagic foraging (Schluter 1995; Taylor et al. 2012). Direct evidence for divergence in growth rates comes from a small sample of juvenile stickleback captured during the breeding season at the edge of the breeding ground at the COE lake site (non–reproductive status was confirmed by dissection; testes and ovaries were poorly developed). These fish displayed body sizes clearly below those of stream stickleback (43–49 mm, N = 3), and yet otolith analysis confirmed that they were already one year old. It thus appears plausible that a lower growth rate in lake stickleback, induced by a relatively poor pelagic resource base, underlies the lake–stream divergence in life history observed within the LC basin (acknowledging the possibility that differential growth rates in the two habitats has a genetic component).

The direct induction or genetically based evolution of an annual life cycle in response to more profitable benthic resources in streams would explain the relatively low variance in average body size across stream populations from different geographic regions (Fig. 1.4). The reason is that the resource spectrum used by stream stickleback is highly consistent across global populations, while lake populations are more variable in resource use (Gross and Anderson 1984; Berner et al. 2008, 2009; Kaeuffer et al. 2012). If variation

in population mean size was (at least partly) a consequence of resource–dependent variation in growth rate, we would indeed expect lake population means to be more variable than stream means. We note, however, that small–sized lake populations are not necessarily benthic–foraging. For instance, the lake population with the smallest average size in Fig. 1.4 (Pye Lake, Vancouver Island) exploits a strictly pelagic food base (Berner et al. 2008). Hence, factors other than food resources (e.g., predation in Moodie and Reimchen 1976; McPhail 1977) likely contribute to the presumably greater life history diversity in lake (and perhaps marine) stickleback than in stream stickleback.

Body size divergence through resource–mediated plasticity in growth rate might play a particularly important role in reproductive isolation. The reason is that this divergence would occur, and potentially influence sexual interactions, within a single generation after the colonization of a stream by lake fish (West–Eberhard 2003; Thibert–Plante and Hendry 2011). It would therefore be crucial to quantify environmental and genetic contributions to life history divergence in stickleback from the LC basin and elsewhere.

1.5.3   Origin of stickleback in the lake constance basin

Consistent with a previous population genetic investigation (Lucek et al. 2010), our genetic analyses indicate that the populations in the LC basin do not originate from colonization by stickleback residing in the Rhine downstream of LC. However, we find that stickleback in the LC basin are genetically very closely related to those occurring in the nearby Danube drainage: pairwise differentiation between Lake Constance samples and DAN was consistently low ($F_{ST} \leq 0.04$), and the only D–loop haplotype found in DAN was the one also predominant in the LC basin. Is it possible that LC stickleback derive from a source population from the Black Sea region that colonized naturally via the Danube? A population genetic study in European perch (*Perca fluviatilis*) (Behrmann–Godel et al. 2004) and geological data (Keller and Krayss 2000) suggest the existence of such a temporary colonization route during the last glacial retreat. In fact, a connection between the Danube drainage and the LC basin still persists today, as the source of the stream sampled at the CON stream site is formed by water captured from the Danube headwaters through a sinkhole and a 12 km underground stream (Hötzl 1996). Whether this allows for fish dispersal has not been investigated.

A scenario of colonization via the Danube, however, is challenged by the absence of stickleback from the entire Danube drainage reported in the nineteenth century (Heller 1971), p. 319; the species was already present in the LC basin at that time), although the reliability of this information is un-

known. Moreover, stream–resident stickleback are generally low–plated (e.g., Hagen 1967; Reimchen et al. 1985; Hendry and Taylor 2004; Raeymaekers et al. 2007; Gelmond et al. 2009). The incomplete shifts toward the low–plated morph in our stream samples from the LC basin, along with the low haplotype diversity within the basin, might thus be taken as tentative support of a relatively recent origin, perhaps due to human introduction. More extensive phylogeographic data from Central and Eastern European populations are needed for a better understanding of the origin and age of stickleback in the LC basin and the Danube drainage.

1.5.4   Conclusion

We have shown strong, repeated, and possibly rapid life history divergence between lake and stream stickleback in the Lake Constance basin, sometimes coinciding with substantial differentiation in neutral markers. Our comparison of body size patterns across global populations and habitats, combined with data from other stickleback systems, further suggests that life history divergence is very common in this species. Our study opens up several important avenues for further investigation: first, experimental work should uncover the mechanistic basis of life history shifts; are they due to differences in maturation size thresholds, in growth rate, or both? Second, the relative contribution of phenotypic plasticity *versus* genetic change to life history divergence should be quantified, and the ecological basis of divergence (e.g., contrasting trophic environments, differential predation regimes) should be identified. Finally, great efforts will be needed to understand whether life history divergence is primarily an aspect of adaptive divergence facilitated by already existing barriers to gene flow, or whether life history divergence itself is a major source of reproductive isolation between lake and stream populations.

1.6   Acknowledgments

and N. Boileau facilitated wet lab work. M. Matschiner created the haplotype network with his unpublished software. W. Salzburger and L. Schärer provided valuable suggestions on the manuscript. We are most grateful for all this support.

1.7   Author contributions

Conceived and designed the experiments: DB DM MR. Performed the experiments: DM DB MR. Analyzed the data: DM DB. Wrote the paper: DB DM.

Chapter 2

Lake–stream divergence in stickleback life history: A plastic response to trophic niche differentiation?

Authors: DARIO MOSER, Benjamin Kueng & Daniel Berner

Published in: Evolutionary Biology

Date of publication: May 26, 2015

Preface: The three experiments in chapter 2 were all done in parallel. Hence, I learned very valuable lessons in scheduling and fish husbandry. Additionally, I largely improved my field expertise during that time. First, I had to find suitable creeks for my transplant experiment. Second, I had to convince the fisheries authorities, tenants, local fishermen and farmers from three countries with different regulations that my experiment would not interfere with their activities. Finally, I had to design, build and install the cages. Luckily, my cage design worked out, making it possible to recycle the cages for the main experiment in chapter 3.

2.1 Abstract

Speciation can be promoted by phenotypic plasticity if plasticity causes populations in ecologically different habitats to diverge in traits mediating reproductive isolation. Although this pathway can establish reproductive barriers immediately and without genetic divergence, it remains poorly investigated. In threespine stickleback fish, divergence in body size between populations represents a potent source of reproductive isolation because body size often influences reproductive behavior. However, the relative contribution of phenotypic plasticity and genetically based divergence to stickleback body size evolution has not been explored. We here do so by using populations residing contiguously in Lake Constance (Central Europe) and its tributaries, a system where lake fish exhibit strikingly larger size and greater age at maturity than stream fish. Laboratory experiments reveal the absence of substantial genetic divergence in intrinsic growth rates and maturation size thresholds between lake and stream fish. A field transplant experiment further demonstrates that lake fish display the life history typical of stream fish when exposed to stream habitats for one year, confirming that life history divergence in this system is mainly plastic. This plasticity appears to be driven by restricted food availability in the lake relative to the stream habitat. We thus propose that in this stickleback system, the exploitation of different trophic niches immediately promotes reproductive isolation via resource–based plasticity in life history.

2.2 Introduction

The formation of new species is often initiated by the divergence of populations into selectively different habitats (Rice 1987; Schluter 2000; Rundle and Nosil 2005; Sobel et al. 2010; Nosil 2012). Generally, two key elements are implicitly assumed to govern this process: first, divergent selection on phenotypes between habitats drives allele frequency shifts between populations at underlying genetic loci. Second, this genetically based (i.e., heritable) divergence generates some degree of reproductive isolation between the populations, for instance through performance tradeoffs between the habitats (Hendry 2004; Nosil et al. 2005; Thibert–Plante and Hendry 2009), or divergence in reproductive behavior (Coyne and Orr 2004; Ritchie 2007; Maan and Seehausen 2011; Thibert–Plante and Gavrilets 2013). Although it is debatable how fast reproductive isolation through this pathway can emerge (Hendry et al. 2007; Gavrilets et al. 2007; Nosil 2012), selection over multiple generations is certainly needed to achieve the underlying genetic divergence

– even when selection is strong and genetic variation is abundant.

However, a faster pathway to speciation can occur when the exposure to ecologically different habitats directly causes divergence between populations through phenotypic plasticity (i.e., not via allele frequency shifts), and this divergence drives reproductive isolation. For example, if plasticity generates adaptive population differentiation prior to dispersal, gene flow between habitats will be impeded by selection against migrants (Crispo 2008; Thibert–Plante and Hendry 2011; Fitzpatrick 2012). Similarly, plasticity might cause phenotypic divergence in traits mediating reproductive interactions, such as mating cues or phenology (Levin 2009), and thereby produce assortative mating. In all these scenarios involving phenotypic plasticity, reproductive barriers will arise *within a single generation* and set the stage for further divergence through allele frequency changes. Despite this potentially important role of plasticity in speciation, however, research efforts are generally directed to deciphering how *genetically based* trait differences between diverging populations contribute to reproductive isolation (e.g., Hatfield 1997; Hawthorne and Via 2001; Lexer et al. 2004; Rogers and Bernatchez 2006; Terai et al. 2006; Rego et al. 2007; Fuller 2008; Kitano et al. 2009; Lowry and Willis 2010; Berner et al. 2011; Streisfeld et al. 2013; Arnegard et al. 2014; Chung et al. 2014; but see Payne et al. 2000; Kozak et al. 2011; Smith et al. 2013).

In the present study, we begin an investigation of the potential role of phenotypic plasticity in speciation by using populations of threespine stickleback fish residing in contiguous lake and stream habitats (Reimchen et al. 1985; Lavin and McPhail 1993; Hendry and Taylor 2004; Berner et al. 2009; Ravinet et al. 2013). We focus on lake–stream stickleback populations occurring in the Lake Constance basin in Central Europe (Berner et al. 2010a; Lucek et al. 2010; Chapter 1). In this system, stickleback exploit two distinct trophic niches: lake fish feed pelagically (i.e., in the open–water) on zooplankton during most of their life, whereas stream fish feed exclusively on benthic (bottom–dwelling) macroinvertebrates (Berner et al. 2010a; Lucek et al. 2012; Chapter 1). This differential habitat use is paralleled by substantial divergence in putatively neutral genetic markers over small geographic scales (Berner et al. 2010a; Chapter 1). Because Lake Constance stickleback invade tributaries during the breeding season, providing the opportunity for genetic exchange between lake and stream fish, the small–scale genetic structure indicates the presence of at least partial barriers to gene flow between the habitats.

The nature of these barriers is presently unknown but might be related to divergence in life history. Specifically, stickleback in the Lake Constance basin display strong lake–stream divergence in age and size at reproduction:

Lake Constance fish generally start reproducing when they are 2 years old and large, while their counterparts in the tributaries typically die after reproducing at one year of age and at only half the body mass of the lake fish (Fig. 2.1a) (Lucek et al. 2012; Chapter 1). Experimental evidence from other threespine stickleback systems suggests that this life history divergence might be an important component of reproductive isolation. The reason is that stickleback mate choice has often been found to be positively size–assortative, with both females and males mating preferably with conspecifics of matching size (Nagel and Schluter 1998; Ishikawa and Mori 2000; McKinnon et al. 2004, 2012; Albert 2005; Boughman et al. 2005; Conte and Schluter 2013; but see Raeymaekers et al. 2010). Similarly, the outcome of aggressive territorial interactions among males has been shown to be body size–dependent (Dufresne et al. 1990; Nagel and Schluter 1998). We have therefore suggested that the divergence in body size observed in the Lake Constance system might contribute to reproductive isolation between lake and stream populations (Chapter 1). An important step in exploring this idea is to understand the relative contribution of adaptive genetic divergence versus phenotypic plasticity to life history divergence, since these alternative mechanisms determine how rapidly reproductive isolation can emerge.
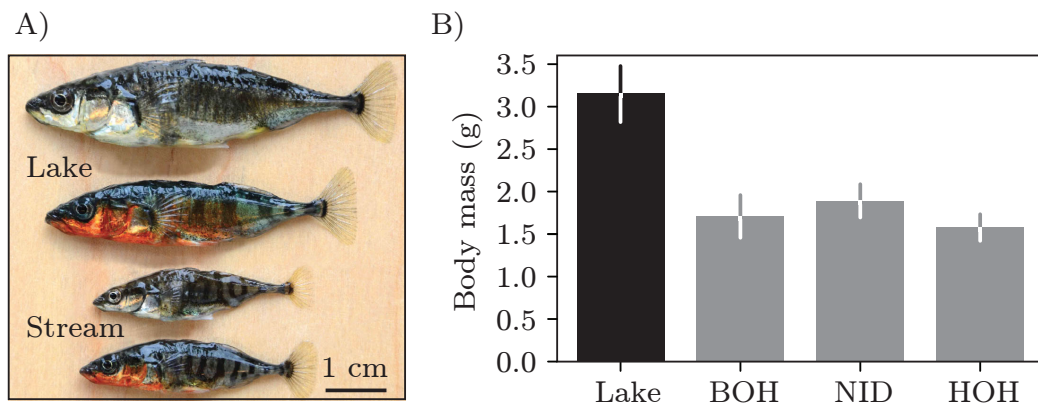
Figure 2.1: a) Reproductive stickleback from Lake Constance and an inlet stream (NID). Females are on top, males (in breeding dress) on the bottom. b) In the wild, Lake Constance stickleback display roughly twice the body size of stickleback populations residing in tributaries (BOH, NID, HOH). Error bars are parametric 95% confidence intervals.

We here present such an investigation based on predictions from a mechanistic model of resource allocation. In particular, it is a general feature of animal ontogeny that the transition from a primarily somatic growth phase to the reproductive stage is governed by a maturation size threshold (reviewed in Bernardo 1993; Nijhout 2003; Berner and Blanckenhorn 2007; for evidence from threespine stickleback see Craig–Bennett 1931). Based on this recogni-

tion, the divergence in life history between lake and stream stickleback might be achieved in two ways: first, lake and stream fish share a common maturation size threshold, but lake fish grow more slowly than stream fish (Fig. 2.2a). As a consequence, only stream stickleback reach the maturation size threshold within one year of growth and can thus respond to the photoperiodic cue (critical day length) that triggers reproduction (Craig–Bennett 1931; Baggerman 1985). Second, lake and stream fish exhibit similar growth trajectories but lake fish have a higher maturation size threshold than stream fish (Fig. 2.2b; see also Shimada et al. 2011). Consequently, again only stream stickleback manage to enter the reproductive stage after one year of growth. It is important to note that these two mechanisms of life history divergence are not mutually exclusive, and that both may be influenced by genetically based divergence, phenotypic plasticity, or a combination of the two.

To shed light on these different possibilities, we use laboratory experiments examining if lake and stream populations have evolved genetically based differences in the intrinsic growth rate, and/or in the maturation size threshold. These experiments are complemented by a field transplant experiment to evaluate to what extent life history is phenotypically plastic. As we will show, these experiments together indicate a key role of plasticity in life history divergence between lake and stream stickleback, with potentially important consequences for speciation in the face of gene flow.

2.3 Material and methods

2.3.1 Study populations and generation of experimental lines

All our experiments described below were performed by using F_1 individuals derived in the laboratory from stickleback caught from one Lake Constance site and from three inlet stream populations. Consistent with previous work, the lake population was sampled in Romanshorn (for geographic details see Berner et al. 2010a or figure 1.1 and table 1.1 in chapter 1). A single sample was adequate to represent Lake Constance stickleback because they are known to form a large, genetically well–mixed population (Berner et al. 2010a; Chapter 1). The stream populations are those from Bohlingen (BOH), Nideraach (NID), and Hohenems (HOH) (Berner et al. 2010a; Chapter 1). Sampling occurred with unbaited minnow traps during the breeding season (early May 2013). The collected individuals were immediately transferred to the laboratory to perform artificial crosses. All crosses were made within
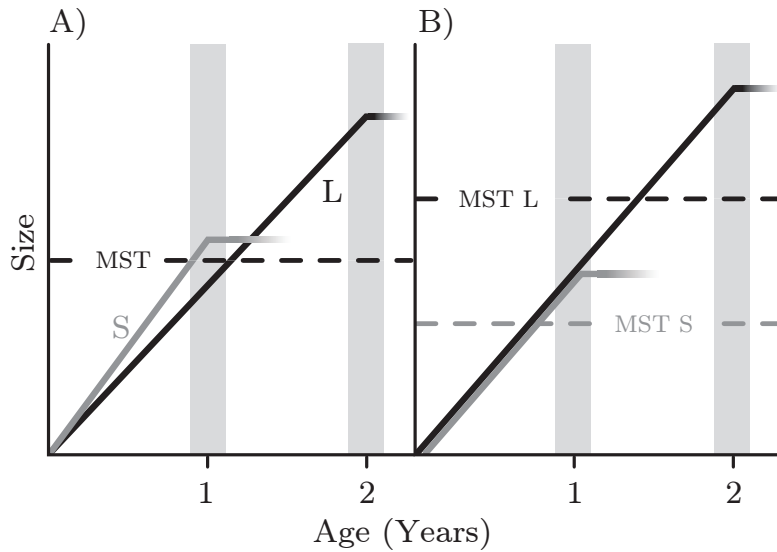
Figure 2.2: Alternative models of life history divergence between lake and stream stickleback. a) Lake (L) and stream (S) fish share a common maturation size threshold (MST) but differ in growth rates. Stream fish grow fast and reach critical size by one year of age. They thus respond to the first photoperiodic cue (gray vertical bar) by maturing and reproducing, followed by senescence and death. By contrast, body size in the relatively slow–growing lake fish is still below the maturation size threshold after one year, so that the first photoperiodic cue cannot trigger reproduction. Instead, lake fish continue to invest in somatic growth. After 2 years, the lake fish have grown beyond critical size (and beyond the size of reproductive stream fish) and are ready to mature. b) Lake and stream fish share similar growth rates but exhibit different maturation size thresholds. A relatively low size threshold in stream fish allows them to mature after one year, whereas a higher critical size in lake fish allows reproduction after 2 years only. Both models lead to the joint divergence in age and size at maturity.

a window of 3 weeks, and each specimen was used for a single cross only. We generated 12 pure lake crosses and ten pure crosses for each stream population. The 84 total parental individuals and some surplus fish not used for crossing (lake: N = 11; BOH: N = 10; NID: N = 6; HOH: N = 7) were killed with an overdose of Koi Med Sleep (phenoxyethanol; Fishmed, Rain, Switzerland), weighed to the nearest 0.01 g, and stored in absolute ethanol. Following the protocol described in chapter 1, we subsequently determined otolith–based age at reproduction. All these field–caught fish (grand total N = 118) were used to confirm that the lake–stream divergence found in chapter 1 was constant across years (i.e., samples from 2010 vs 2013), and to compare life histories between experimental and wild fish.

Embryonic development of the F_1 generation occurred in four well aerated 100 L tanks, with 2 g NaCl and 80 μl Fungol (JBL, Neuhofen, Germany)

per liter to prevent fungus infection (none observed). For hatching, each clutch (family; N = 42) was transferred to an individual 15 L 'hatching tank' connected to a flow–through system. We used a rearing temperature of 16 °C and a 16:8 h light–dark (LD) summer photoperiod. Hatchlings were fed live *Artemia* nauplii *ad libitum* twice a day during the first 2 weeks, and then additionally frozen copepods (*Cyclops*).

2.3.2 Laboratory experiment 1: genetically based divergence in growth trajectories

In our first laboratory experiment, we tracked stickleback body mass (our body size measure) over one year to investigate whether lake and stream populations have evolved different intrinsic growth trajectories. Based on the ontogenetic model above, our specific prediction was that stream fish display steeper trajectories (Fig. 2.2a).

This experiment involved the Lake Constance (hereafter simply 'lake') population and two stream populations (BOH and NID). Three weeks after hatching, we haphazardly selected 40 individuals from each hatching tank and divided this sample into two replicate 15 L tanks connected to the same flow-through system (resulting in 84 total tanks with 20 individuals each). As a resource for the other experiments described below, the remaining fish were transferred from the hatching tanks to 100 L 'stock tanks', pooling all families within each population. Although this precluded subsequent tracking of the source families, the number of individuals per family was relatively similar and mortality was near zero, thus ensuring a balanced contribution to the stock tanks across families. The fish used for the growth trajectory experiment and those in the stock tanks received exactly the same temperature, light, and food treatment. Specifically, the temperature was 16 °C throughout the experiment. The photoperiod was initially 16:8 h LD ('summer') but was reduced to 12:12 16 weeks post–hatch and to 8:16 ('winter') 22 weeks post–hatch until the end of the experiment. The winter photoperiod was used to avoid the transition to reproduction toward the end of the experiment. All fish were fed *ad libitum* twice a day. We provided a mix of live *Artemia* nauplii and frozen *Cyclops* during the first 9 weeks, and then a combination of frozen bloodworms (chironomid larvae), frozen *Cyclops*, and decapsulated *Artemia* eggs. This latter diet included prey taxa consumed by both limnetically foraging lake stickleback and benthically foraging stream stickleback populations in the wild (e.g., Berner et al. 2008, 2010a; Chapter 1).

In the course of the growth trajectory experiment, the number of individ-

uals per tank was reduced from initially 20 down to 15 (10 weeks post–hatch), 13 (29 weeks), and 11 (32 weeks), eliminating individuals haphazardly. The rationale of this reduction was to avoid excessive crowding, and to maintain similar densities of individuals across the tanks (although mortality was very low). Starting 9 weeks post–hatch, ten fish per tank were chosen haphazardly, weighed to the nearest 0.01 g, and returned to their tank. This was repeated every 5 weeks, resulting in nine rounds of measurement and a total experimental period of one year. In each round except the last, measurements were conducted within 7 days or less. The ninth round was performed in the exact order of hatching over a window of 14 days and included all remaining fish per tank (mean: 10.7).

2.3.3 Laboratory experiment 2: genetically based divergence in maturation size thresholds

The second laboratory experiment tested the prediction derived from the ontogenetic model that lake fish have evolved an elevated maturation size threshold relative to stream fish (Fig. 2.2b). Our experimental strategy was to transfer stickleback from both habitats from a winter to a summer photoperiod (i.e., to provide the photoperiodic maturation cue) at body sizes well below the size of reproductive lake fish in the wild. Our expectation was that if maturation size thresholds have diverged between the habitats, lake fish would display a lower propensity to respond to the cue and become mature than stream fish.

This experiment used lake and NID stream individuals chosen haphazardly from the corresponding stock tanks and was conducted in a separate room with 16 °C and a summer photoperiod. The room was equipped with fifty 15 L tanks. Each tank was furnished with 400 ml of sand and fine gravel, 200 nylon threads of 5 cm length (both to allow males to build a nest), and a plastic plant. To start the experiment, each tank was stocked with a single individual whose body mass had been recorded. Visual contact among tanks was allowed. The fish were fed *Cyclops* and frozen bloodworms *ad libitum* twice a day. Before feeding, we inspected the reproductive status of each individual. Females were considered reproductive if they produced a ripe clutch that could be stripped. Males qualified as reproductive if they displayed breeding dress (bluish iris and orange jaw and throat) and maintained a nest. In a few cases where the latter criterion was ambiguous, we presented a gravid female to the male. If the male then displayed and entered its nest, it was considered reproductive. The sex of individuals not mature at the end of the experiment was determined by dissection.

The experiment was conducted in three rounds, starting 32, 39, and 46 weeks post–hatch, each lasting 45 days. All experimental fish had thus experienced at least 10 weeks of winter photoperiod in the stock tanks. Total sample size was 150, with 81 lake fish (N = 34, 20, and 27 in the rounds 1, 2, and 3) and 69 NID stream fish (N = 16, 30, 23). Mortality was zero, but eight fish showed low food uptake and apathy and were excluded from analysis.

2.3.4 Field transplant experiment: life history plasticity

The above experiments were performed under standardized environmental conditions to detect genetically based differences in ontogenetic determinants between lake and stream stickleback. However, to explore phenotypic plasticity in life history, a field experiment was needed. Our approach was to release juvenile lake stickleback produced in the laboratory into stream enclosures, and to track growth and the propensity to mature until the beginning of the subsequent reproductive season. Our expectation was that if the observed life history divergence in the wild is primarily genetically based, lake fish should maintain their typical life history phenotype (i.e., large size and delayed maturation) even when developing in stream habitats. Conversely, a strong phenotypically plastic component to life history divergence would cause transplanted lake fish to express the typical stream phenotype (i.e., reproduction at small size after one year). We note that ideally, this experiment would have included reciprocally transplanting stream fish to lake enclosures. However, technical constraints and difficulties in maintaining an adequate pelagic foraging environment within lake enclosures over a long time period (e.g., avoiding the establishment of zoobenthos on enclosure walls) precluded transplants in this direction.

Our field experiment involved nine total enclosures, three of which were constructed near each of our three stream sampling sites (details given in Table S1 (Supplementary material)). Trapping confirmed that stickleback occurred naturally at each site. The enclosures were built by fitting perforated metal plates (4 mm diameter holes; 58% passage) vertically in the stream bed and shore, enclosing stream segments of 6 m length. The enclosures were oriented parallel to the shore, such as to reach approximately 1 m from the water's edge into the streams (Fig. S4 (Supplementary material)). The bottom and shore area within the enclosures was natural, and to minimize disturbance, construction work was performed 6 weeks prior to fish release (early June 2013). At this point, we also removed all adult and as many juvenile stickleback as possible by extensive minnow trapping and electrofishing. All enclosures were covered with a fine 40 mm nylon net to

prevent bird predation.

To begin the experiment, two enclosures per site were stocked with (foreign) lake stickleback. As a control, the third enclosure at each site was stocked with individuals from the corresponding stream population (locals). The number of individuals released was 30 per enclosure, selected haphazardly from the laboratory stock tanks. Since the enclosures allowed the entrance of small juvenile stickleback from outside, we marked all experimental fish by clipping the second dorsal spine. The same treatment was also applied to 80 fish from the stock tanks that were subsequently maintained in the laboratory. This confirmed that clipping had no growth or survival consequences, and that this marking was irreversible and unambiguous. The releases occurred 8 weeks post–hatch (July 23, 2013). At that point, the mean mass of the released fish was 0.1 g (approximately 20 mm standard length) and did not differ among the populations (details not presented).

The enclosures were subjected to minnow trapping 10, 14, 18, 23, 31, and 36 weeks after the release at the HOH site, and after 10, 14, 31, and 36 weeks at the BOH and NID sites. (To reduce work load, and because we expected little growth during winter, only one site was sampled during wintertime.) Unmarked resident fish that had entered the enclosures were always removed. Experimental fish were counted, weighed, and returned to their enclosure. During the last visit (March 27–April 2, 2014), all experimental fish were additionally inspected for reproductive status, euthanized, and stored in absolute ethanol. Individuals were considered reproductive if they displayed mature ovaries (females), or breeding dress (males), the former determined by dissection.

2.3.5 Data analysis

To compare growth trajectories among the laboratory populations, we first averaged individual body mass measurements across the two replicate tanks, yielding a single data point per family and measurement round. Because hatching of the experimental families extended over 3 weeks but body mass measurements were generally performed within one–week windows irrespective of hatching date, combining body mass data across families within populations required standardizing for age. We did so by using locally weighted scatterplot smoothing (LOESS, a non–parametric regression; Cleveland 1979). Based on a first–order polynomial and a smoothing span of 0.75, we predicted for each family the body mass at standardized ages defined by the latest–hatching families. We also used LOESS to visualize population–specific mean growth trajectories and their associated 95% confidence bands (implemented in the *ggplot2* R package; Wickham 2009).

To examine if the lake and the NID populations differed in their propensity to mature at the endpoint of the experiment (i.e., after 45 days), we analyzed the individual incidence of maturation in a generalized linear model with binomial error structure and experimental round and population as predictors. Because females and males differ in their reproductive physiology, this analysis was performed separately for each sex. P–values of the model terms and their interaction was established through (non–parametric) permutation (Manly 2007). We here randomized the response over the predictors 9999 times and used the distribution of the z–value of each model term across the iterations to derive P–values.

To test for differences in body mass among the enclosures at end of the field transplant experiment (week 36 post–release), we used a linear model with body mass as response and enclosure as predictor. Data from each site were analyzed separately. P–values were established by permutation as above, using the model's F–value as test statistic. We also tested for each site if the stream fish raised in the (control) enclosure differed in size from their wild local counterparts at the end of the experiment. P–values were again generated by permutation, using the difference in population means (wild minus enclosure) as test statistic. All analyses and graphing were performed in the R statistical environment (R Development Core Team 2014).

2.4 Results

2.4.1 Life history divergence in the field

The field specimens collected in 2013 for the present study displayed life histories fully consistent with those observed earlier (Chapter 1): body mass at reproduction was roughly twice as high in Lake Constance fish as in stream fish (Fig. 2.1b). Similarly, the lake population displayed an average age at reproduction of 2.1 years (range 1–3 y), as opposed to 1.2 years in stream fish (range 1–2 y). Life history divergence between lake and stream stickleback in the Lake Constance basin is thus temporally stable.

2.4.2 Laboratory experiments

Our first hypothesis, a genetically determined lower growth rate in lake fish compared to stream fish, was clearly refuted by the analysis of growth trajectories. Although growth trajectories diverged in the course of the experiment, with the NID population growing slower than the other two populations, this

difference was in the direction opposed to our prediction (Fig. 2.3). If anything, the intrinsic growth rate is higher in lake than stream fish.

In the maturation size threshold experiment, mean body mass in the beginning of all experimental rounds was substantially below the mean mass at reproduction observed in any population in the wild (range across all combinations of population, sex, and experimental round: 0.63–1.28 g, Table S2 (Supplementary material); compare to Fig. 2.1b). Because body mass tended to increase from the first to the third experimental round (Table S2 (Supplementary material), we also observed an increasing propensity to mature over the experimental rounds (Fig. 2.4) (experimental round term, females: $P < 0.001$; males: $P = 0.16$). Combining across the sexes and populations, the incidence of maturation rose from 46%(round 1) to 84%(round 2) and 93%(round 3).

The key outcome of the maturation size threshold experiment, however, was a lack of a difference in the propensity to mature between Lake Constance and NID stream in males (population term: $P = 0.68$; round by population interaction: $P = 0.33$), and a difference in the direction opposed to our prediction in females (population: $P = 0.007$; interaction: $P = 0.99$) (Fig. 2.4). However, the latter population difference should be taken with caution; due to slight differences in growth trajectories between the lake and NID populations (see above), lake fish were slightly larger than stream fish in the beginning of each experimental round. Combining across the sexes and experimental rounds, the overall propensity to mature was similar between lake and stream fish (75 and 72%). We further observed that across all experimental fish, individuals larger than 1 g at the start of an experimental round ($N = 41$) always matured (Fig. S5 (Supplementary material)). The minimum mass absolutely required for maturation could not be determined with confidence because the number of very small experimental individuals was insufficient, but is clearly below 0.5 g (Fig. S5 (Supplementary material)).

Taken together, the maturation size threshold experiment demonstrates that both lake and stream fish can mature at body sizes much smaller than the typical size at reproduction seen in all populations in the wild. We find no support for the hypothesis that the switch to the reproductive stage is genetically determined to occur at a larger size in lake than in stream fish.

2.4.3 Field transplant experiment

At the NID field site, no individual in the two lake transplant enclosures survived longer than 10 weeks. Since we were interested in life history phenotypes expressed over longer time frames, this site had to be omitted from analysis.
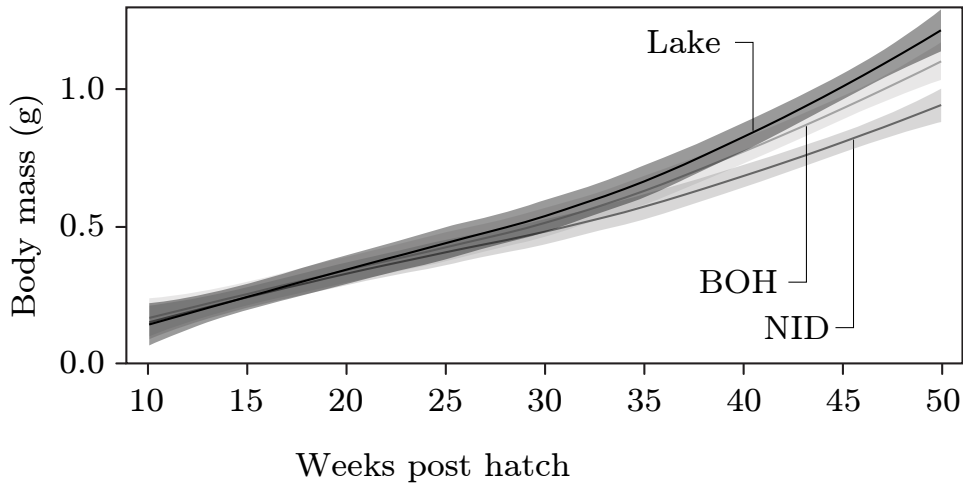
Figure 2.3: a) Growth trajectories of the Lake Constance and two stream stickleback populations over 40 weeks under common garden conditions. Shown are mean trajectories across the replicate families within each population, along with the associated 95% confidence bands.

At the BOH site, the transplanted lake stickleback were larger at the end of the experiment (week 36) than their stream conspecifics in the enclosures (Fig. 2.5; P = 0.005). However, this result was based on a single lake enclosure because sometime between week 31 and 36, damage to the other lake enclosure allowed all experimental fish to escape. Analyzing the data from week 31, when both lake enclosures were still intact, we detected no body mass difference among the enclosures (P = 0.07). Similarly, there was no indication of body mass differences among the enclosures at the end of the experiment at the HOH site (P = 0.3).

At both the BOH and HOH site, control stream stickleback in the enclosures displayed slightly lower body mass at the end of the experiment than the corresponding resident stream population (Fig. 2.5, compare to Fig. 2.1b; BOH P < 0.001, HOH P = 0.02). However, this difference is not surprising because the enclosure experiment ended in March whereas the field populations (parental fish used to create the experimental fish) were sampled in May. We thus conclude that the growth trajectories displayed by stickleback within the enclosures are qualitatively similar to those of the wild local stream populations.

In all enclosures, stickleback started to mature toward the end of the experiment. At the BOH site, this was true for all individuals in the remaining lake enclosure (N = 4), and for 64% of the individuals in the stream enclosure (N = 17). At HOH, 28 and 50% of the transplanted lake fish matured (N =
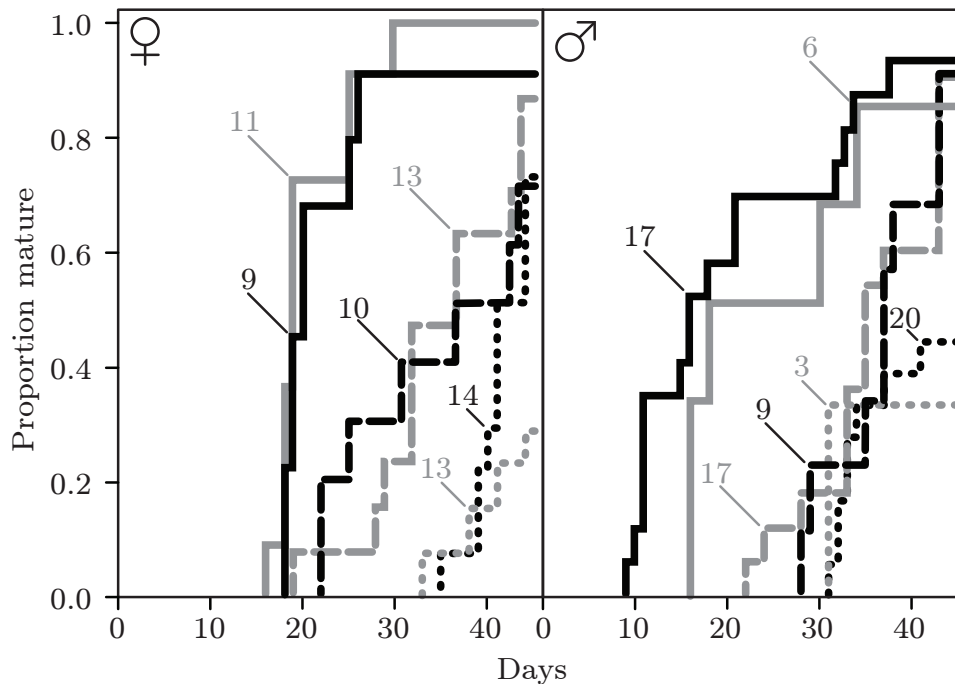
Figure 2.4: a) The proportion of stickleback from the Lake Constance population (*black*) and a stream population (NID; *gray*) becoming reproductive during the maturation size threshold experiment, presented separately for females and males. The line styles designate the three experimental rounds (*dotted*, *dashed*, and *solid* for round 1, 2, and 3) and the numbers indicate sample sizes.

18 and 22), and a similar proportion of stream fish (44%, N = 27).

To summarize, the main insight from the field transplant experiment is that lake fish raised in replicated stream environments readily start reproducing after a single growing season. Further, they do so at body sizes typical of stream fish – that is, much smaller than the typical reproductive lake fish. Phenotypic plasticity thus causes a major life history shift within a single generation in Lake Constance stickleback.

2.5   Discussion

2.5.1   The mechanism of life history divergence between lake and stream stickleback

The objective of this study was to combine multiple experiments to identify the mechanism(s) underlying life history divergence among stickleback populations in the Lake Constance basin. In this system, lake fish have been
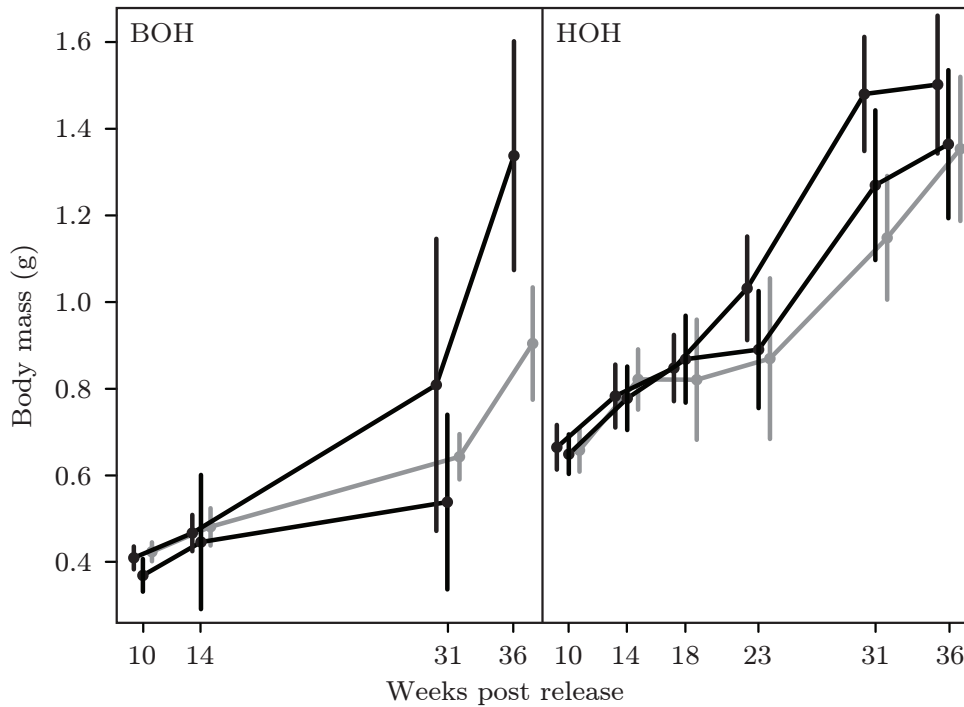
Figure 2.5: a) Reproductive stickleback from Lake Constance and an inlet stream (NID). Females are on top, males (in breeding dress) on the bottom. b) In the wild, Lake Constance stickleback display roughly twice the body size of stickleback populations residing in tributaries (BOH, NID, HOH). Error bars are parametric 95% confidence intervals.

shown to reproduce at much larger size and later in life than neighboring stream populations (Lucek et al. 2012; Chapter 1), a pattern here confirmed based on temporally independent samples.

Studying growth trajectories under controlled laboratory conditions revealed some degree of genetically based differentiation among the study populations, with Lake Constance fish displaying the fastest growth. This result agrees with a previous laboratory study based on a different lake–stream population pairing from the Lake Constance basin that also suggested slightly faster growth in lake than stream fish (Lucek et al. 2012). The difference in growth among the populations might be due to divergence in the rate of food consumption, in the efficiency of food conversion, or both (Present and Conover 1992; Silverstein et al. 1999; Jonassen et al. 2000; Trudel et al. 2001). Tentative support for the former derives from the qualitative observation during our laboratory growth experiment that Lake Constance fish were bolder and foraged more actively than stream fish. However, formal experiments would be needed to quantify the relative contribution of foraging behavior and physiology to the genetic variation in growth, ideally includ-

ing different food availability treatments to explore if stronger divergence is apparent when food is restricted.

Whatever the cause(s) for the different growth trajectories under laboratory conditions, these differences clearly cannot explain the variation in age and size at reproduction among the wild populations: first, the intrinsic differences in growth trajectories are too subtle to explain the large body size divergence within the Lake Constance basin. Second and most importantly, faster growth would make lake fish more likely than stream fish to attain the maturation size threshold within a single growing season, hence conflicting with the observation of delayed reproduction in Lake Constance stickleback relative to the stream populations (Fig. 2.2a).

Furthermore, our investigation of maturation size thresholds in the laboratory makes clear that both lake and stream genotypes can reproduce at body sizes well below the size of wild reproductive stream stickleback. The delayed reproduction of Lake Constance stickleback relative to their conspecifics in streams thus cannot be caused by the genetically based evolution of an elevated critical maturation size. Collectively, our laboratory experiments indicate that life history divergence within the Lake Constance basin primarily represents phenotypic plasticity. This view is confirmed by our field transplant experiment, demonstrating that Lake Constance fish developing in stream habitats display life history phenotypes similar to typical stream fish – i.e., maturity within one year at small size.

Which specific ontogenetic determinants (i.e., growth rate, the maturation size threshold, or both) and ecological factors conspire to generate this life history plasticity cannot be inferred directly from our experiments. However, additional evidence allows us to propose that differential growth rates resulting from different resource availabilities between the lake and stream habitat are responsible for life history plasticity, consistent with model A in Fig. 2.2. Support for this view is offered by quantitative data on the temporal development of zooplankton availability in Lake Constance, revealing a single zooplankton abundance peak from late spring to early summer (Sommer 1985). During the rest of the year, zooplankton abundance is low. Juvenile lake stickleback thus appear to be born into a habitat where resource availability is rapidly declining, and they additionally have to compete for food with larger individuals from previous age cohorts. This suggests that compared to its tributaries, Lake Constance is a relatively poor foraging environment over most of the year, generally supporting a growth rate too low to reach critical maturation size within one growing season. (Nevertheless, the large body size reached by Lake Constance fish after two years suggests that during peak zooplankton abundance, growth rate is high.) The demonstration of a large proportion of very small (i.e., below 0.5 g) non–reproductive

stickleback during the breeding season in the Lake Constance population would provide definitive evidence of this scenario.

By contrast, stomach content analysis in a supplementary sample of stream stickleback from the NID population taken in late December 2014 indicates that in streams, prey resources are abundant throughout the year (Table S3 (Supplementary material)). Also, in this habitat, competitors from previous age cohorts are rare (Chapter 1). Accordingly, our field transplant experiment demonstrates that stream habitats allow for substantial growth over fall and winter (i.e., between the weeks 14 and 31 in Fig. 5). Streams thus appear to be relatively profitable habitats generally allowing stickleback to attain critical maturation size within one growing season. If this proves generally true, it offers a plausible explanation for the convergence in body size among stream stickleback populations observed at a worldwide scale (see Fig. 1.4 in Chapter 1).

2.5.2 Implications

Overall, we provide strong evidence that life history divergence between lake and stream stickleback in the Lake Constance basin is the outcome of resource–mediated phenotypic plasticity in growth trajectories between the habitats. Our study challenges the suggestion that divergence in size at reproduction within the Lake Constance basin is due to the genetically based adaptive evolution of faster growth in lake fish (Lucek et al. 2012). The different conclusions emerging from Lucek et al. (2012) and the present work emphasize three important aspects: first, understanding life history evolution requires explicitly considering the mechanisms through which growth and reproductive function are coordinated (Day and Rowe 2002; Berner and Blanckenhorn 2007). In our stickleback system, this concerns the interplay between growth rate, the maturation size threshold, and the photoperiodic maturation cue (Baggerman 1985). Considering these determinants jointly makes clear that large size at reproduction in Lake Constance fish cannot readily be attributed to faster growth, but – perhaps counterintuitively – to slower growth early in life.

Second, caution is warranted when interpreting phenotypic divergence in natural populations based on laboratory experiments alone. While stickleback in the Lake Constance basin certainly exhibit some genetically based differences in growth rate detectable in the laboratory, these differences are overwhelmed by phenotypic plasticity in the wild.

Third, adaptationist interpretations of phenotypic divergence in nature should be made with caution. We recognize that the slightly elevated growth rate of lake fish under laboratory conditions might represent a genetically

based adaptation partly compensating for the generally low resource availability in that habitat, and thus might provide an example of countergradient variation (Conover and Schultz 1995). Nevertheless, most of the life history divergence between our lake and stream populations is plastic, and whether this plasticity is adaptive or simply an unavoidable response of the ontogenetic machinery to ecological differences between the habitats (Berner and Blanckenhorn 2007; Fitzpatrick 2012) requires experimental investigation.

Finally, our study has important potential implications for speciation. Lake Constance stickleback enter tributaries for reproduction. The breeding grounds of lake and stream fish thus certainly overlap (at least in streams where physical dispersal barriers are absent), providing the opportunity for lake–stream gene flow. However, phenotypic plasticity maintains a prominent body size difference between the habitats, and body size to govern reproductive interactions in several population within this species (Dufresne et al. 1990; Nagel and Schluter 1998; Ishikawa and Mori 2000; Albert 2005; Boughman et al. 2005; McKinnon et al. 2004, 2012; Conte and Schluter 2013). We therefore propose that in lake and stream stickleback in the Lake Constance basin, the colonization of ecologically distinct habitats immediately promotes reproductive isolation via sexual barriers. Experimentally evaluating the role of body size in sexual isolation in this system thus emerges as on obvious avenue for future research.

2.6   Acknowledgments

2.7   Author contributions

Conceived and designed the experiments: DB DM. Performed the experiments: DM BK DB. Analyzed the data: DM DB. Wrote the paper: DB DM.

Chapter 3

Fitness differences between parapatric lake and stream stickleback revealed by a field transplant

Authors: DARIO MOSER, Anja Frey & Daniel Berner

Preface: I name the field transplant experiment of chapter three as the core study of my PhD. I like the degree of replication, the inclusion of F_1 hybrids and of course the outcome, which would not have been possible without some luck. Interestingly, this was the least work intensive project. Crossing, some husbandry in the lab and five field trips were enough to begin with the analysis. This experiment also enabled future research. The numerous positive interactions with the fisheries authorities in this region during chapter 1–3 made an approval for a F_2 hybrid release in autumn 2015 possible.

3.1 Abstract

Molecular comparisons of populations diverging into ecologically different environments often find strong differentiation in localized genomic regions, with the remainder of the genome being weakly differentiated. This pattern of heterogeneous genomic divergence, however, is rarely connected to direct measurements of fitness differences among populations. We here do so by performing a field enclosure experiment in threespine stickleback fish residing in a lake and in three replicate adjoining streams, and displaying weak yet heterogeneous genomic divergence between these habitats. Tracking survival over 29 weeks, we consistently find that lake genotypes transplanted into the streams suffer greatly reduced viability relative to local stream genotypes, and that the performance of F_1 hybrid genotypes is intermediate. This observed selection against migrants and hybrids combines to a total reduction in gene flow from the lake into streams of around 80%. Overall, our study identifies a strong reproductive barrier between parapatric stickleback populations, and cautions against inferring fitness differences between populations from the overall magnitude of genomic differentiation.

3.2 Introduction

Genomic studies exploring how molecular variation is influenced during adaptive divergence between populations residing in ecologically different habitats have become frequent (e.g. Nadeau et al. 2012; Roesti et al. 2012a; Renaut et al. 2013; Evans et al. 2014; Soria–Carrasco et al. 2014; Fraser et al. 2015; Lamichhaney et al. 2015). A common emerging pattern is heterogeneous genomic differentiation – that is, relatively strong population differentiation in localized regions of the genome and weak differentiation outside these regions. This pattern is typically interpreted as ecologically important loci experiencing divergent natural selection within a genomic background relatively homogenized by gene flow (Wu 2001; Nosil et al. 2009; Feder et al. 2012). While such descriptions of genomic differentiation are valuable to shed light on the molecular complexity of adaptive divergence and to discover adaptation genes, they generally remain incomplete in that direct information about the fitness consequences of heterogeneous genomic divergence in nature is lacking (Barrett and Hoekstra 2011). Establishing the link between genomic divergence and fitness differences among populations, however, is crucial to evaluate the promise of ecological genomics that mechanistic insights about adaptation and speciation can be derived from the examination of DNA sequence variation (Feder et al. 2012).

In the present study, we address this link by experimentally quantifying fitness differences in nature among populations in which genomic divergence has been characterized. Specifically, we study populations of threespine stickleback fish residing in contiguous lake and stream habitats (i.e., in parapatry) within the Lake Constance basin in Central Europe (Berner et al. 2010a; Lucek et al. 2010, 2012; Chapter 1). These populations have diversified ecologically: lake fish display a pelagic life style, exploiting zooplankton in the open water, while stream fish forage on benthic (substrate–dwelling) macroinvertebrates. This difference in foraging niches coincides with phenotypic divergence in foraging, predator defense, and life history traits. However, some of the phenotypic divergence has been shown to be mainly plastic (Chapter 2), and traits generally exhibiting strong and consistent parallel lake–stream divergence in stickleback at a global scale (i.e., overall body shape, gill raker number; Reimchen et al. 1985; Berner et al. 2008, 2009; Kaeuffer et al. 2012; Ravinet et al. 2013) have not evolved among lake and stream populations from the Lake Constance basin (Berner et al. 2010a; Lucek et al. 2013). The relatively weak phenotypic divergence among our focal stickleback populations is mirrored by weak molecular differentiation: genome–wide high–density single–nucleotide polymorphism (SNP) markers revealed baseline differentiation (i.e., genome–wide median F_{ST}) in multiple lake–stream population comparisons to range between 0.005 and 0.06 only (Chapter 6). However, genomic differentiation appeared highly heterogeneous, with some genetic markers exhibiting strong differentiation (see below).

A crucial question is now whether weak but heterogeneous genomic differentiation in stickleback from the Lake Constance basin is sufficient to cause substantial fitness tradeoffs between the lake and stream habitats. This question is important because lake and stream stickleback populations in close contact have established as a strong system for studying the relationship between adaptive divergence and speciation (McKinnon and Rundle 2002; Hendry 2009;). Nevertheless, adaptive divergence has so far been inferred only from the combination of phenotype–environment correlations (Reimchen et al. 1985; Hendry and Taylor 2004; Berner et al. 2008, 2010; Kaeuffer et al. 2012; Ravinet et al. 2013) and information on the genetic basis of trait divergence (Lavin and McPhail, 1993; Sharpe et al. 2008; Berner et al. 2011; Chapter 5); unambiguous experimental demonstrations of whole–organism fitness differences between lake and stream stickleback are lacking (but see Hendry et al. 2002 for suggestive results from Canadian populations, and Eizaguirre et al. 2012 for adaptive divergence in immune genes). Furthermore, it remains uncertain how adaptive divergence contributes to the reproductive isolation assumed to drive and maintain the (sometimes strong) marker–based genetic differentiation between lake and stream populations in

close contact (Hendry et al. 2009).

To inform these questions, we subject lake and stream stickleback from the Lake Constance basin to a transplant experiment to quantify fitness differences in nature. Combining the emerging results with recent genomic data, our study reveals the fitness correlate of heterogeneous genomic divergence and identifies powerful reproductive barriers between contiguous but ecologically different populations.

3.3 Material and methods

3.3.1 Study design

The logic of our transplant study was to release juvenile stickleback from multiple stream populations into field enclosures in their stream of origin, together with lake fish and lake–stream F_1 hybrids, and to track fitness until adulthood. We thus performed replicate 'local versus foreign' experiments of local adaptation (Turesson 1922; Clausen et al. 1940; Kawecki and Ebert 2004; Blanquart et al. 2013). We expected that in the presence of adaptive divergence between the habitats, local stream fish should outperform foreign lake fish. Furthermore, assuming an overall additive genetic basis to potential fitness differences (which does not imply additivity at the underlying genetic loci; Lynch and Walsh 1998), F_1 hybrid performance should be intermediate between the pure populations. Although including the reciprocal experimental setup – that is, transplanting stream fish into the lake – would have been desirable, the challenge of adequately reproducing pelagic foraging habitat in lake enclosures over many weeks imposed a unidirectional approach.

Our investigation considers four stickleback populations, including the one inhabiting Lake Constance (hereafter simply 'lake') and three from independent tributaries to the lake (NID, BOH and HOH; Fig. 3.1) (see also Berner et al. 2010a; Chapter 1, 2 & 6). A single sample was adequate to represent the lake fish because this population is genetically well mixed (Chapter 1 & 6).

3.3.2 Experimental fish

For our experiment, we used F_2 individuals derived from the laboratory populations established in chapter 2. In brief, we first generated an F_1 laboratory cohort in the spring of 2013 by artificially crossing field–caught reproductive individuals from each of the four study populations. We thus obtained 12 pure lake families and ten pure families from each of the three stream popu-

lations. Individuals were then pooled across families within each population, taking care to ensure an approximately similar contribution among families to each pool (details on the production of this F_1 cohort and on husbandry is given in chapter 2). After one year in the laboratory (i.e., between April 26 and May 19, 2014), individuals from the F_1 cohort were sampled haphazardly to generate an F_2 laboratory cohort. The latter again included the four pure populations, and additionally F_1 hybrids between the lake and each stream population (i.e., seven cross types in total). The number of replicate families was 16, 10, 16, and 5 for the lake, NID, BOH, and HOH cross types; and 10, 6, and 6 for lake–NID, lake–BOH, and lake–HOH F_1 hybrids. The juveniles of the F_2 cohort were raised by pooling individuals from all replicate families of a given cross type into a single aquarium. Rearing temperature was 16 °C, the light–dark photoperiod was 16:8, and the juveniles were fed live *Artemia* nauplii and frozen *Cyclops*, *Daphnia* and chironomid larvae ('bloodworms') *ad libitum*. Mortality in the laboratory was negligible.

3.3.3 Transplant experiment

Approximately 8–11 weeks post–hatch (July 24, 2014), juveniles from the F_2 cohort were transferred to field enclosures constructed in 2013 in each of the focal streams (Chapter 2). The enclosure sites were near the sites where the parental individuals of the laboratory lines had been sampled (Fig. 3.1), displayed similar habitats as the latter, and harbored resident stickleback. Each stream site comprised three replicate enclosures. The enclosures were 6 m long and 1.5 m wide and were built along the stream shore by using perforated metal plates (4 mm diameter holes, 58% passage), thus allowing the flow of water and small organisms across the enclosure walls (see Fig. S6 (Supplementary material) for enclosure photographs, and chapter 2 for further details on the study sites and construction).

Prior to fish release, adult resident stickleback were removed from the enclosures by extensive minnow trapping (although small resident juveniles could enter and leave the enclosures). We then stocked each enclosure with a total of 90 juvenile stickleback from our laboratory lines, including 30 individuals from the focal stream, 30 lake individuals, and 30 individuals from the corresponding F_1 hybrid cross type. To distinguish our experimental fish from residents, each cross type was marked by clipping the first dorsal, the left pelvic, or the right pelvic spine, using each clipping type once for every cross type at each study site.

Starting five weeks post–release, the enclosures were visited on four occasions in intervals of eight weeks. The last visit occurred at the end of February 2015, after more than 200 days of experimental time, just before the onset

of the breeding season (i.e., March; chapter 2). During each visit, the enclosures were sampled in a standardized way by setting 14 minnow traps per enclosure two hours before dusk and removing them two hours after dawn on the following day. Recaptured experimental (i.e., marked) individuals were then assigned to cross type, counted, and weighed, providing survival and body mass as fitness measures. The number of non–experimental fish captured in the enclosures (hereafter 'competitors') was also recorded. After this, all fish (experimental and competitors) were released back into their enclosures (except for the last visit when the experimental fish were killed with an overdose of Koi Med Sleep (phenoxyethanol; Fishmed, Rain, Switzerland) and preserved in Ethanol). Across all study sites, this procedure was always completed within three days.
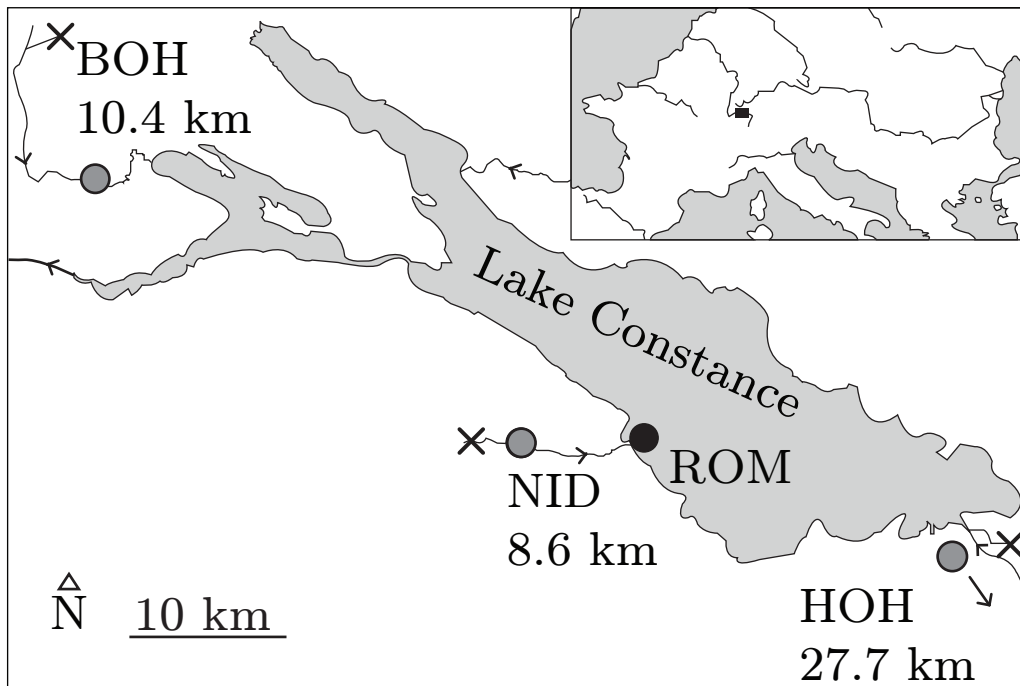
Figure 3.1: Geographical situation of the study sites in the Lake Constance region (black rectangle in the insert map). The circles indicate the location of the three stream sites (NID, BOH, and HOH) and the lake (ROM) site where stickleback were sampled to generate the experimental populations. The numbers indicate the approximate water distance from each stream site to the lake. The crosses indicate the location of the experimental stream enclosures.

3.3.4   Supplementary measurements

To ensure the robustness of our experiment, three checks were performed. First, we haphazardly sampled and weighed 20 individuals from each cross type the day before the release into the enclosures, which confirmed the absence of body mass differences among the cross types at the onset of the experiment (Fig. S2). Second, after the standard sampling of the enclosures (see above) during the last field inspection, we continued sampling each enclosure with the same method. This extended sampling yielded few additional individuals (Fig. S7 (Supplementary material)), indicating that our standard trapping scheme captured stickleback in the enclosures effectively. For consistency across the four sampling periods, these additional individuals were not considered for analysis (except in the calculation of reproductive isolation, see below), although including them would only have strengthened our results (Fig. S8 (Supplementary material)). Finally, we tested whether lake and stream stickleback differed in their intrinsic propensity to be captured by minnow traps. This test was conducted in mid–April 2015, after completing the field transplant experiment. We here stocked the three enclosures at the NID site with a similar number of marked, adult, field-caught lake and NID stream stickleback, each enclosure with a different total density (8, 16, and 24 individuals). After 12 hours, we sampled the enclosures using the standard method described above, which recovered every single released individual in each enclosure. This again confirmed the effectiveness of minnow trapping, and showed that lake and stream fish were equally likely to be recaptured (this test was likely conservative, as the different growth environments of these field–caught lake and stream fish can be expected to exaggerate any genetically–based behavioral difference). Together, these checks confirmed that our transplant experiment was very unlikely to be affected by methodological artifacts.

Furthermore, to characterize the natural abundance of resident stream stickleback at each study site, we applied our standard trapping scheme in the immediate area outside the enclosures in April 2014, and recorded the number fish. Although this census was made outside our experimental period (i.e., July–February), the resulting counts should be roughly comparable to the number of competitors observed within the enclosures at the end of the experiment.

3.3.5   Data analysis

Our first prediction was that resident stream stickleback survive better in stream enclosures than foreign lake fish, and that F_1 hybrid survival falls

between the pure lines. We therefore tested for differential survival among the experimental lines by fitting the number of survivors in the enclosures in a linear model with the terms cross type, study site, and their interaction. P–values for the model terms were obtained by permuting the number of survivors 9999 times and evaluating the observed F–statistics against their random distributions (Manly 2007). For this test, we considered survival data from the fourth (last) sampling period only. Our second prediction was that body mass attained during the experiment – an indirect fitness measure – was higher in stream than lake and hybrid fish. We thus tested for differences in body mass among the cross types and study sites at the end of the experiment by permutation, using the same model structure as for survival. This test, however, considered only stream fish and hybrids because only a single lake survivor was recovered at the NID and BOH sites. Differences among the study sites and sampling periods in the number of competitors present in the enclosures were tested analogously based on a repeated measures model with study site as factor and sampling time as within–enclosure effect.

To examine to what extent performance differences among the experimental lines reduced gene flow from the lake into the streams, we calculated the strength of unidirectional reproductive isolation using the formula 4A from (Sobel and Chen 2014):

$$RI = 1 - 2 \times \left(\frac{H}{H+C} \right)$$

We here substituted the number of lake and stream survivors at the end of the experiment for H and C to quantify the reproductive barrier due to viability selection against lake immigrants. Analogously, substituting the number of hybrid survivors for H expressed reproductive isolation due to selection against hybrids. Note that RI varies linearly from 1 (complete reproductive isolation, here corresponding to an absolute barrier to gene flow from the lake into the streams) to –1 (maximum possible gene flow from the lake into the streams). We calculated this metric both globally, combining survival data from all enclosures and streams, and separately for each stream, combining data from all enclosures. All graphing and analyses were performed in R (R Development Core Team 2014).

3.4   Results

As predicted for local adaptation, survival in the stream enclosures was consistently higher in local stream stickleback than in foreign lake fish, and F_1 hybrid survival was intermediate (Fig. 3.2, upper row) (cross type effect,

permutation P = 0.0151). Most strikingly, at the NID site, experimental lake fish were already essentially eliminated 13 weeks after the release, while stream and hybrid fish were still present in all enclosures. Survival also differed among the streams (P = 0.0006; cross–site interaction: P = 0.134), with the highest survival occurring at the HOH site. At all sites, mortality was most severe during the first sampling interval.

On average, body mass of experimental stickleback increased more than threefold in the course of the experiment. However, contrary to our expectation, we found no difference in body mass between the pure stream and the F_1 hybrid crosses, nor among the study sites (all model terms P > 0.162) (Fig. 3.2, middle row).

The number of competitors in the enclosures differed clearly among the stream sites (P = 0.0006), declining from NID (mean over enclosures and time points: 81) to BOH (61) and HOH (10) (Fig. 3.2, bottom row). We also observed a decrease over time (P = 0.0031), driven primarily by the NID and BOH sites (site–time interaction: P = 0.0016). We suspect that this temporal decline is underestimated by our methodology, as a proportion of small juvenile fish in the beginning of the experiment escaped our trapping. The number of competitors within the enclosures further mirrored the natural abundance of stickleback present among the study sites, as revealed by sampling outside the enclosures (Fig. 3.2, bottom row, week 29).

The survival differences among the cross types by the end of the experiment implied a substantial barrier to gene flow: in the global analysis, reproductive isolation attributable to selection against lake immigrants and against lake–stream hybrids was 0.67 and 0.4. The corresponding site–specific values were 0.71 and 0.1 for NID, 0.82 and 0.54 for BOH, and 0.63 and 0.42 for HOH.

3.5   Discussion

3.5.1   Local adaptation in lake–stream stickleback

Our objective was to test for fitness differences between lake and stream stickleback and their hybrids through a replicated transplant experiment in nature. The emerging pattern is clear and consistent: local stream fish display higher survival than lake fish, and F_1 hybrids are intermediate between these populations. Although our experimental individuals were confined in field enclosures, this is unlikely to compromise the generality of our findings: the enclosures were relatively large and permeable to prey organisms, and importantly, stickleback densities within the enclosures were compara-
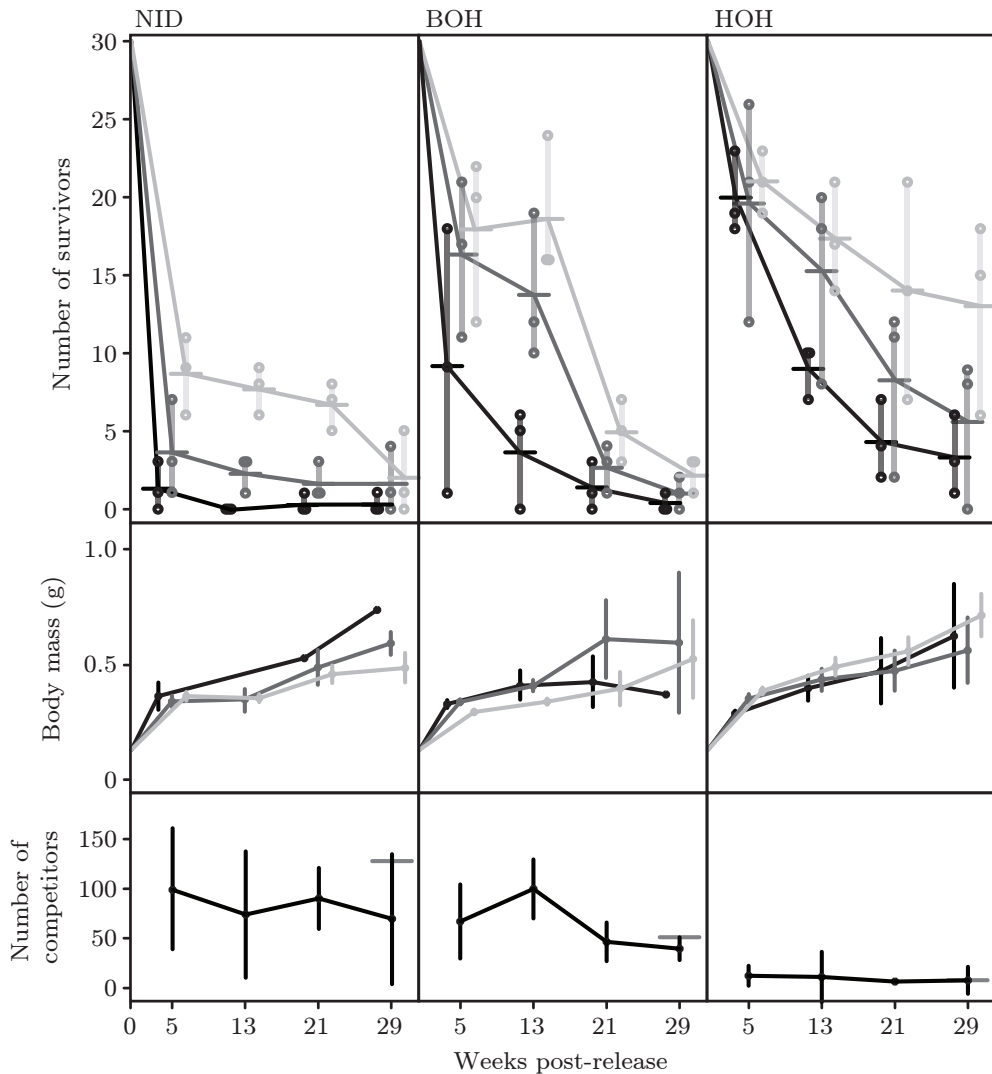
Figure 3.2: Upper row: Number of lake (black), stream (light gray), and F_1 hybrid (dark gray) stickleback surviving in the field enclosures during the transplant experiment at each study site. The circles represent the raw survivor counts in each replicate enclosure, the vertical bars connect the minima and maxima, and the horizontal bars are the means across the enclosures. Middle row: Change in body mass along the experiment. Dots are means across the replicate enclosures (using within–enclosure averages as data points), error bars are the associated parametric 95% confidence intervals (note that after week 5, lake stickleback at the NID site are represented by a single individual only). Bottom row: Number of competitors (i.e., non–experimental stream-resident stickleback) captured within the enclosures during the experiment. Dots and error bars are means and 95% confidence intervals across the replicate enclosures. The gray horizontal bars at week 29 indicate the number of stickleback captured outside the enclosures (this latter census was made slightly outside our experimental period, see Materials and methods).

ble to those outside the enclosures. The experiment can be expected to have reproduced the selective conditions in the streams adequately.

We thus provide the first demonstration of adaptive divergence between lake and stream stickleback at the level of whole–organism performance, and contribute to the scant body of direct experimental evidence for fitness differences among natural populations of vertebrates (e.g., Schluter 1995; Gomez–Mestre and Tejedo 2003). Our finding of strong fitness differences between lake and stream stickleback within stream habitats differs from merely suggestive differences found in a transplant study using Canadian lake–stream populations (Hendry et al. 2002). The different outcomes, however, are likely attributable to different methodologies, as the latter study used adult, field–caught experimental fish and ran for a much shorter time, thus perhaps missing the life stage under intense selection.

Having conducted our experiments in streams only, we recognize that for a formal demonstration of local adaptation (as opposed to stream fish being unconditionally fitter than lake fish), a reciprocal transplant of lake and stream populations across both habitats would have been needed (Kawecki and Ebert 2004; Blanquart et al. 2013). However, molecular analyses have established that the Lake Constance population is evolutionarily derived from a stream ancestor and has experienced genomically wide–spread selective sweeps in its novel habitat (Chapter 6). This makes clear that the lake habitat is challenging for stream fish. Moreover, Lake Constance fish have diverged from the tributary populations in ecologically important traits such as defensive lateral plating and gill raker length (Berner et al. 2010a; Lucek et al. 2013; Chapter 1), differentiation generally known to have a strong genetic basis in stickleback (Colosimo et al. 2005; Glazer et al. 2015; Chapter 5 & 6). The reciprocal expectation of higher fitness of lake than stream or hybrid fish in the lake habitat thus appears highly plausible.

Contrary to our prediction, body mass, our indirect fitness measure, did not differ among the experimental populations in the end of the experiment. An obvious explanation is that individuals achieving poor growth were eliminated continuously, a possibility we cannot evaluate because our population–level marking did not allow tracking survival and growth of individual fish.

Our experiment further suggests an interesting detail about the nature of selection in lake-stream stickleback. Specifically, selection against lake fish (and hybrids) appeared relatively relaxed at the study site HOH that also displayed the lowest density of resident stickleback, as observed both within and outside the enclosures. This is most evident when considering the proportion of surviving lake fish relative to the total number of individuals (experimental and competitors) recovered at the end of the experiment, pooled across all replicate enclosures. This proportion was vanishingly low

(0.005 and 0.008) in the NID and BOH systems displaying relatively high competitor densities, but substantial (0.12) at HOH where resident stickleback were much less abundant. (We suspect that the low natural abundance of stream–residents at HOH is due to a shortage of breeding habitat; this stream site exhibits higher water flow and less organic litter and vegetation than the two other sites; DM and DB, personal observation). Similarly, the overlap in survival among the cross types early in the experiment was highest at the HOH site. This suggests that dispersing lake fish perform well in relatively unoccupied streams, but are eliminated rapidly from streams in which a dense locally adapted population is present. We thus hypothesize that selection is density-dependent and driven by intraspecific resource competition – a factor generally considered important to ecologically–based reproductive isolation (Schluter 2000; Nosil 2012). Although density–dependent selection in this stickleback system needs to be confirmed more directly, our study highlights the value of replicating selection studies across multiple habitats (Wade and Kalisz 1990).

3.5.2 Genomic differentiation and reproductive isolation

Our laboratory stickleback populations producing the experimental fish had spent more than an entire life cycle under standardized conditions. The fitness differences observed in the field enclosures must therefore be attributed largely to genetic differentiation between the lake and stream populations. Fortunately, genome–wide information about this differentiation is available: the lake and two of the three stream populations (NID and BOH) have been genotyped previously at high–density SNP markers for demographic analysis, and to study signatures of selection in the genome (Roesti et al. 2015). This provides the opportunity to relate fitness differences to genomic divergence in the same populations. To this end, we here reuse the SNP data to characterize the genome–wide distribution of genetic differentiation (F_{ST}) for both the lake–NID and the lake–BOH population comparisons. These distributions (Fig. 3.3) highlight the weak overall lake–stream differentiation in both population comparisons (genome–wide median F_{ST}, lake–NID: 0.013; lake–BOH: 0.005), the absence of complete allele frequency shifts (i.e., F_{ST} = 1), but that a small proportion of loci nevertheless exhibit strong lake–stream differentiation (up to 0.84 and 0.67 in the two comparisons). (A very similar F_{ST} distribution can be expected for the lake–HOH comparison, as microsatellite–based differentiation in this population pairing is intermediate between the lake–NID and lake–BOH comparisons; Chapter 1) We thus

find strong fitness differences in population pairs in which overall genetic differentiation would generally be considered very weak. For example, using fully comparable methodology, genome–wide baseline F_{ST} was estimated as high as 0.15 in neighboring lake and stream stickleback population from Vancouver Island, Canada (Roesti et al. 2012).

The weak and heterogeneous genomic differentiation in our lake–stream systems directly translates to powerful pre– and postzygotic reproductive barriers: averaged across the streams, selection against migrants (Coyne and Orr 2004; Hendry 2004; Nosil et al. 2005) reduces gene flow from the lake into the stream populations by approximately 70% relative to the absence of fitness differences between the populations. Furthermore, the ecological inferiority of F_1 hybrids resulting from mating between dispersers from the lake and stream residents reduces gene flow by another 40%. Combining these two reproductive barriers sequentially (Coyne and Orr 1989; Sobel and Chen 2014), adaptive divergence drives total reproductive isolation in the order of 0.8. This strong ecological barrier to gene flow offers a partial answer to the long–standing question of how lake and stream stickleback pairs can maintain (often striking) genetic and phenotypic integrity in close contact (Reimchen et al. 1985; Berner et al. 2009; Bolnick et al. 2009; Eizaguirre et al. 2009; Hendry et al. 2009).

We emphasize, however, that it remains unclear to what extent the components of reproductive isolation identified in our study actually operate in nature, as they require that lake stickleback disperse into tributaries (selection against migrants) and reproduce with stream fish (selection against hybrids). This assumption appears plausible because the Lake Constance population invades tributaries during the reproductive period. Indeed, anecdotal evidence indicates overlap in breeding habitat between lake and stream stickleback at least in the BOH stream. Nevertheless, our present insights should be complemented by experimental information on how the opportunity for gene flow is modified by dispersal behavior (Edelaar and Bolnick 2012; Webster et al. 2012; Berner and Thibert–Plante 2015; see Bolnick et al. 2009 for a habitat preference study in Canadian lake–stream stickleback) and by sexual interactions (Eizaguirre et al. 2009; Raeymaekers et al. 2010; Chapter 3).

3.6 Conclusion

We demonstrate strong genetically–based fitness differences between neighboring lake and stream stickleback populations despite weak – but heterogeneous – genomic differentiation. Our study thus highlights the risk of predict-
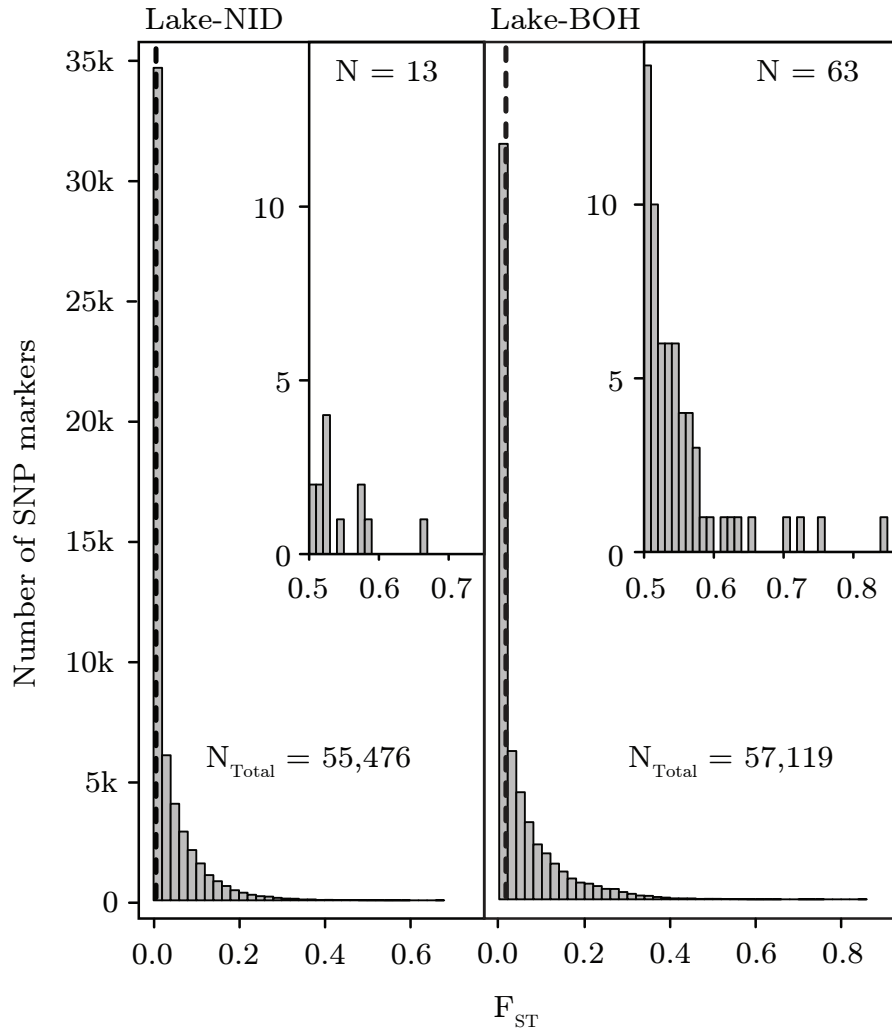
Figure 3.3: Geographical situation of the study sites in the Lake Constance region (black rectangle in the insert map). The circles indicate the location of the three stream sites (NID, BOH, and HOH) and the lake (ROM) site where stickleback were sampled to generate the experimental populations. The numbers indicate the approximate water distance from each stream site to the lake. The crosses indicate the location of the experimental stream enclosures.

ing the magnitude of adaptive divergence based on genetic markers only. We further show that adaptive divergence translates to strong ecologically–based reproductive barriers. Future studies are needed to compare the relative importance of these and other reproductive barriers in stickleback from the Lake Constance basin, and to experimentally measure fitness differences in other lake–stream systems, including those known to exhibit stronger genomic differentiation.

3.7 Acknowledgments

3.8 Author contributions

DB and DM designed the experiment; DM, AF and DB performed the experiment; DM and DB analyzed the data; DB and DM wrote the paper.

Chapter 4

Recombination in the threespine stickleback genome – patterns and consequences

Authors: Marius Roesti, **DARIO MOSER** & Daniel Berner

Preface: Besides working on my Master thesis, I could help out Dani in the aquaria room, where his F_2 hybrids needed food and the aquaria had to be maintained. Besides fish husbandry, I was in charge of the DNA extraction and was able to prepare my first RAD libraries with Marius' help and supervision. Finally, I was part of the genotype correcting progress for the genetic map construction, which we did manually.

4.1 Abstract

Heterogeneity in recombination rate may strongly influence genome evolution and entail methodological challenges to genomic investigation. Nevertheless, a solid understanding of these issues awaits detailed information across a broad range of taxa. Based on 282 F_2 individuals and 1'872 single nucleotide polymorphisms, we characterize recombination in the threespine stickleback fish genome. We find an average genome–wide recombination rate of 3.11 cM/Mb. Crossover frequencies are dramatically elevated in the chromosome peripheries as compared to the centers, and are consistent with one obligate crossover per chromosome (but not chromosome arm). Along the sex chromosome, we show that recombination is restricted to a small pseudoautosomal domain of c. 2 Mb, spanning only 10% of that chromosome. Comparing female to male RAD sequence coverage allows us to identify two discrete levels of degeneration on the Y chromosome, one of these 'evolutionary strata' coinciding with a previously inferred inverted region. Using polymorphism data from two young (<10'000 years old) ecologically diverged lake–stream population pairs, we demonstrate that recombination rate correlates with both the magnitude of allele frequency shifts between populations and levels of genetic diversity within populations. These associations reflect genome–wide heterogeneity in the influence of selection on linked sites. We further find a strong relationship between recombination rate and GC content, possibly driven by GC–biased gene conversion. Overall, we highlight that heterogeneity in recombination rate has profound consequences on genome evolution and deserves wider recognition in marker–based genomic analyses.

4.2 Introduction

Meiotic recombination is a fascinating process because of its pivotal role in multiple biological contexts. For instance, recombination is generally considered instrumental to the proper segregation of homologous chromosomes during meiosis (Mather 1938; Baker et al. 1976; Roeder 1997; Smith and Nicolas 1998; Hassold and Hunt 2001). At the same time, recombination breaks the linkage between DNA segments located on the same chromosome. This allows selection to operate more effectively on multiple loci, and hence promotes adaptation (Hill and Robertson 1966; Felsenstein 1974; Otto and Barton 1997; Burt 2000; Otto and Lenormand 2002). Conversely, the suppression of recombination can initiate chromosome degeneration, a process believed to be common during sex chromosome evolution (Bull 1983; Charlesworth and Charlesworth 2000; Charlesworth et al. 2005; Wilson and

Makova 2009).

Variation in recombination rate may also explain genome–wide heterogeneity in the magnitude of genetic divergence between populations, and genetic diversity within populations. The reason is that linkage between selected loci and their physical neighborhood is tighter in regions exhibiting relatively low recombination rate. Selectively neutral polymorphisms will therefore be affected by selection more often and more strongly when located in low–recombination regions. As a consequence, hitchhiking under positive and background selection is predicted to increase allele frequency shifts between populations, and to reduce genetic diversity within populations, in low–relative to high–recombination genomic regions (Maynard Smith and Haigh 1974; Kaplan et al. 1989; Begun and Aquadro 1992; Nordborg et al. 1996; Charlesworth et al. 1997; Charlesworth 1998; Nachman 2002). Similarly, loci under divergent selection between ecologically distinct habitats should impede neutral gene flow more extensively in low–recombination regions (Barton and Bengtsson 1986; Feder and Nosil 2010). Finally, recombination may have direct effects on the constitution of chromosomes, for instance through biased gene conversion or mutagenesis (Galtier et al. 2001; Duret and Galtier 2009; Webster and Hurst 2012).

Despite the recognition of recombination as a major evolutionary factor, our understanding of both the mechanisms governing the process, and its consequences on genome evolution, remains highly incomplete (Nachman 2002; Smukowski and Noor 2011; Webster and Hurst 2012). Moreover, detailed investigations of recombination outside genetic model organisms are needed for the discovery of general patterns. The goal of our study is to provide the first comprehensive analysis of meiotic recombination in threespine stickleback fish.

A thorough understanding of recombination in this powerful model organism for ecological genetics is particularly valuable for two reasons. First, the species has been shown to display a relatively young (<10 Myr old) XY (male–heterogametic) sex determination system (Peichel et al. 2004). Information on the extent of XY recombination and associated patterns of Y degeneration, however, remains highly incomplete, but promises exciting insights into sex chromosome evolution (Peichel et al. 2004; Ross and Peichel 2008; Shikano et al. 2011). Second, performing genome scans in stickleback populations residing contiguously in selectively distinct lake and stream habitats, we have shown recently that population divergence (F_{ST}) is elevated in chromosome centers and argued that this effect is caused by a lower recombination rate within these regions (Roesti et al. 2012a). Because robust information on recombination was lacking, however, this hypothesis could not be evaluated definitively. Our study therefore combines single nucleotide

71

polymorphism (SNP) data from a laboratory F_2 cross and natural populations to characterize the stickleback recombination landscape; to explore the role of recombination in sex chromosome evolution; to examine the relationship between recombination rate and the magnitude of divergence among and genetic diversity within populations; and to investigate the association between recombination rate and nucleotide composition.

4.3 Material and methods

4.3.1 Laboratory cross

We generated an F_2 population for linkage map construction by artificially crossing a male and a female from the Central European ROM and CHE populations (described in Berner et al. 2010; Roesti et al. 2012b; Chapter 1) in the spring 2009. The resulting F_1 were raised in two 50 L tanks on a mixed Artemia (live, decapsulated cysts, frozen) and bloodworm diet under 'summer' laboratory conditions (18–20 °C with a 16:8 h day/night photoperiod). After a 'winter' phase (15 °C, 8:16 h photoperiod) of 3 months, summer conditions were reestablished in the spring 2010 to initiate reproduction. The F_2 population was generated by performing 20 artificial F_1 full–sib crosses, each involving a unique male–female combination. After 1 year, 282 adult F_2 (140 males, 142 females) were haphazardly chosen, killed with an overdose of MS–222 and stored in absolute ethanol.

4.3.2 Marker generation

DNA was extracted from pectoral fin tissue on a MagNA Pure LC278 extraction robot (Roche) by using the tissue Isolation Kit II. We then prepared restriction site–associated DNA (RAD; Baird et al. 2008) libraries, involving SbF_1 restriction, the fusion of 5–mer individual barcodes and pooling DNA of 62 individuals per library. The final enrichment PCR was performed in duplicate to reduce random amplification variation. Each library was single–end sequenced to 100 base reads in a separate Illumina HiSeq lane. In addition to the F_2 individuals, the two founder individuals of the cross were also sequenced, each twice in different libraries. The Illumina sequences were sorted according to barcode and aligned to the stickleback reference genome (release Broad S1; Jones et al. 2012) by using Novoalign v2.07.06, accepting a total of approximately eight high–quality mismatches and/or indels along a read. Alignments were converted to BAM format using SAMtools (Li et al. 2009). Each replicate alignment of each grandparent was then screened

independently for homozygous RAD loci. A locus qualified as homozygous if it was either invariant or if the binomial probability for the two dominant haplotypes to reflect a heterozygous locus was <0.001. We here ignored loci with <129 coverage (average coverage per locus varied between 31 and 47 among the grandparents and replicate alignments). RAD loci proving homozygous in both replicates of a given grandparent were then screened for SNPs (here subsuming both SNPs and microindels) fixed for different alleles between the grandparents, accepting only one SNP per RAD locus. This conservative SNP detection strategy yielded a total of 2'223 markers. The F_2 population was then genotyped at each SNP detected in the grandparents. We considered a SNP homozygous when only one grandparent allele was present and occurred in at least 20 copies, or heterozygous when both alleles were present in at least 20 copies each (average sequence coverage per RAD locus was 55.6 among the F_2 individuals). Loci not satisfying these criteria received an ambiguous genotype based on the dominant allele or were treated as missing data when the total allele count was below six (<0.5% of all genotypes). Next, we eliminated 58 SNPs displaying clearly skewed allele frequencies across the F_2 and ordered the remaining 2165 markers according to their physical position in the Broad S1 stickleback reference genome.

4.3.3 Genome reassembly

Visual inspection of the genotypes ordered according to the reference genome indicated marker intervals exhibiting extremely high crossover frequency. Without exception, these intervals coincided perfectly with scaffold boundaries, indicating genome assembly errors. This conclusion was also supported by comparing physical and genetic map positions in a low–resolution data set extracted by Roesti et al. (2012a) from genetic maps available for North American stickleback (Albert et al. 2008; Greenwood et al. 2011): markers on scaffolds found to be inverted in the current study showed opposite genetic and physical map order in the latter data set as well (details not presented). An accurate characterization of recombination thus required genome reassembly. For this, we created de novo linkage groups in R/qtl (Broman and Sen 2009) by including markers unanchored to any linkage group in the Broad S1 genome. We used a maximum recombination frequency of 0.3 or less and a LOD score of 8 or greater and further optimized marker order along linkage groups through permutation within a sliding window of seven markers. The resulting genetic map allowed us to invert 13 total scaffolds (size range: 0.7–17.1 Mb; 98.2 Mb in total) within the known linkage groups (hereafter 'chromosomes') and to incorporate 18 previously unanchored scaffolds with a total length of 20.1 Mb into the chromosomes. We ignored unanchored

scaffolds smaller than 140 kb, as this was below our average marker resolution. We then recalculated the physical position for every marker. These assembly corrections are described in Fig. S9 (Supplementary material). All physical map positions in this study refer to our improved genome assembly, which is available in FASTA format on the Dryad digital repository (doi:10.5061/dryad.846nj).

For final genetic map construction, we first corrected genotyping errors and ambiguous calls by hand, making the common and well–supported assumption that the vast majority of tight double–recombinants reflect genotyping errors. We then clipped the most peripheral marker at each chromosome end because here phase shifts were most difficult to distinguish from genotyping errors. Next, we discarded all markers not assigned to linkage groups, and one (redundant) marker in cases where two SNPs formed a pair derived from sister RAD loci (i.e. loci flanking the same SbF_1 restriction site). The final data set used for genetic mapping comprised 1'872 markers (59–150 per chromosome), with an average spacing of 217 kb. We note that this data set is expected to slightly underestimate recombination rate along chromosomes. The reason is that with our marker resolution, a few tight double–crossovers may have escaped detection altogether, and a few others may have been captured by one or two markers but taken as genotyping error and eliminated. Moreover, our markers never covered the full physical chromosome span because of the randomness of SbF_1 restriction sites; because we ignored unanchored scaffolds mapping to one or both ends of many chromosomes when these scaffolds were small and represented by only one to three markers; and because we discarded the peripheral marker on each end of the initially generated linkage groups.

4.3.4 Analysis of recombination

Genetic distances along the 20 autosomes were estimated in R/qtl using the Kosambi map function (assuming crossover interference) and the full F_2 panel. For the sex chromosome (chromosome 19; Peichel et al. 2004), final map construction used genotype data from females only (N = 142). The reason is that sequence degeneration of the Y relative to the X chromosome precluded reliable genotyping in males (the reference sex chromosome sequence is the X). R/qtl was also used to count the number of crossovers for each individual and chromosome.

We visualized recombination rate along the chromosomes by plotting genetic distance (cM) against physical distance (Mb). Moreover, we calculated the average recombination rate for every interval between adjacent markers as the ratio of genetic distance to physical distance (cM/Mb) and plotted

this rate against the physical midpoint of the marker interval. We also calculated average recombination rate across each chromosome, and across each chromosome arm, using for the latter information on centromere positions extracted from Urton et al. (2011). Throughout this paper, effective physical chromosome (and chromosome arm) spans are defined by the position of our most peripheral markers. The only exception is Fig. S9 (Supporting material) where we show the full physical chromosome lengths.

Crossover counts were used to examine the relationship between recombination frequency and chromosome length. We here determined for each chromosome the average crossover number across the 282 F_2 (or the 142 females for chromosome 19) and calculated the correlation coefficient r between this variable and chromosome length. The magnitude of this test statistic was evaluated against its empirical random distribution established by permuting the crossover data 9'999 times (Manly 2007; all statistical tests in this study are based on analogous permutation tests). A similar analysis was performed by using chromosome arm length, rather than total chromosome length, as a predictor of crossover number. In this latter analysis, six chromosome arms with low marker coverage were excluded, which had a trivial influence on the results. Also, these analyses were performed with and without the sex chromosome. As this did not materially influence the results, we report the former.

Individual crossover counts across all autosomes were used to test for a difference in overall recombination rate between the sexes, using as test statistic the F–ratio of a linear model with crossover count as response and sex as fixed factor. Analogous tests were also performed to explore sex differences in crossover number for each chromosome separately. Finally, individual crossover counts were used to scan the genome (including chromosome 19) for the presence of quantitative trait loci (QTL) determining recombination rate. We emphasize that our data are not ideal for this purpose; quantifying the recombination phenotype in the F_2 generation would have required crossover data from the F_3 generation or from F_2 gametes. Our scan was thus limited to detecting QTL heterozygous in one or both of the grandparents. The QTL scan was performed in R/qtl using the extended Haley–Knott method (other methods produced very similar results). Significance of LOD peaks was established based on 9'999 permutations, following Broman and Sen (2009).

4.3.5 Recombination and divergence within the sex chromosome

Recombination between the X and Y chromosomes was studied by determining which of the 69 SNPs along chromosome 19 occurred homozygous for the grandfather allele in F_2 females. This female genotype necessarily requires XY crossover in the F_1 father.

To explore degeneration of the Y chromosome, we haphazardly selected 100 males and 100 females from the F_2 population. For each sex separately, we determined for every RAD locus along chromosome 19 the total sequence coverage across all individual alignments. For each RAD locus, we then calculated the ratio of female to male coverage. A RAD locus not or little differentiated between the gametologs would display an expected ratio of one because both the X and Y sequences would align to the X reference. At a locus substantially diverged between X and Y, the latter would no longer align to the reference, producing twice the sequence coverage in females relative to males. To reduce noise, we restricted this analysis to RAD loci displaying a minimal total sequence coverage of 4'000 in each sex, yielding a total of 1'556 informative loci along the X chromosome (average intermarker distance: 13 kb). This analysis of Y degeneration was additionally performed by using a natural population sample from Europe (CHE) and Canada (Boot Lake, see below). These populations are derived independently from Atlantic and Pacific ancestors. Because here sample size was much smaller (N = 13–14 per sex and population), we used a minimal sequence coverage threshold of 50 per sex.

4.3.6 Genetic divergence, genetic diversity and GC content in relation to recombination rate

We tested the prediction of a negative genome–wide correlation between recombination rate and the magnitude of allele frequency shifts by using divergence data from two independent replicate lake–stream population pairs studied in Roesti et al. (2012a) (the Boot and Robert's pair; see also Berner et al. 2008, 2009). These young (postglacial, <10 000 years old) population pairs are those among the four pairs investigated in Roesti et al. (2012a) displaying the strongest divergence in phenotypes and genetic markers between the selectively distinct habitats (genome–wide median F_2 is 0.15 and 0.03 for Boot and Robert's; Roesti et al. 2012a). Each of the four samples was represented by 27 individuals (balanced sex ratio). Polymorphism data were generated through RAD sequencing, yielding 3'930 and 7'992 genome–wide SNPs for the Boot and Robert's pair (details on library preparation,

sequencing, genotyping, SNP detection and access to the raw data are given in Roesti et al. 2012a, b). The magnitude of divergence between the lake and stream population was quantified by F_2 based on haplotype diversity (Nei and Tajima 1981; formula 7), tolerating only informative SNPs with a minor allele frequency of 0.25 or greater (Roesti et al. 2012b). F_2 was then averaged across the intervals defined by adjacent markers from the mapping cross, resulting in the same resolution as our recombination rate data (see Fig. 4.1). This allowed us to explore the genome–wide correlation between the magnitude of divergence and recombination rate, using r as statistic for significance testing.

Next, we examined the prediction of a positive correlation between recombination rate and levels of genetic diversity within each population. For this, we screened each of the four population samples separately for polymorphisms and calculated genetic diversity (haplotype diversity, Nei and Tajima 1981; singletons were omitted to exclude technical artefacts). RAD loci were allowed to contribute a single SNP only, keeping the one with the highest diversity at loci with multiple SNPs (drawing a SNP at random produced very similar results). The resulting total number of SNPs varied between 4'938 and 17'649 among the populations. As a complementary analysis, we also counted the number of polymorphisms (excluding singletons) on each RAD locus, with the number of RAD loci varying between 6'440 and 25'186 among the populations. We considered these data, hereafter referred to as SNP density, a valuable alternative genetic diversity metric because selection should not only skew allele frequencies in linked regions, but also reduce the density of polymorphisms in those regions. Both the genetic diversity and SNP density data were averaged to the resolution of the genetic map and tested for an association with recombination rate as described for F_2.

Finally, we investigated a possible association between recombination rate and GC content in an analogous way. However, to maximize precision, we calculated the proportion of GC nucleotides for each marker interval based on the full reference genome sequence rather than our RAD sequences. Moreover, we here detected a clear nonlinear relationship and therefore used as test statistic the ratio of residual to total sum of squares of a nonparametric regression (LOESS–robust locally weighted scatterplot smoothing; Cleveland 1979; a linear fit with r as test statistic produced similar results). We note that this analysis assumes that patterns of nucleotide composition in the reference genome, which was built based on a Pacific–derived freshwater stickleback, are also representative of Atlantic–derived European populations. This assumption is justified; repeating the correlation analysis using genome–wide GC content estimated from consensus sequences at 27'396 RAD loci derived from the cross grandmother produced similar results (details not presented).

In the above correlation analyses (F_2, genetic diversity, SNP density, GC content), marker intervals with an extreme recombination rate (below 0.01 and above 40) were excluded, although analyses including all intervals produced very similar results. The final data sets thus comprised 1'783 genome–wide marker intervals. Also, including or excluding the sex chromosome did not materially influence the analyses; we thus report the former. Apart from sequence alignment and BAM conversion, all analyses and plotting were carried out in the R language (R Development Core Team 2012), benefiting greatly from the Bioconductor packages ShortRead (Morgan et al. 2009), Rsamtools and Biostrings. Data smoothing was performed with R's implementation of LOESS.

4.4   Results

The 21 stickleback chromosomes accounted for a total genetic map length of 1'251 cM, yielding a genome–wide average recombination rate of 3.11 cM/Mb (this number is based on the total physical genome length effectively covered by our markers: 401.8 Mb). However, recombination rate proved highly heterogeneous across the genome: crossovers occurred primarily in the chromosome peripheries, with a greatly reduced rate in the chromosome centres (Fig. 4.1). Except for two of the smallest chromosomes (5, 21), this pattern was consistent and was particularly pronounced in the larger ones. For instance, the average recombination rate in the first and last 5 Mb of the largest chromosome (4) was 7.8 and 6.8 cM/Mb, whereas the segment ranging from 10 to 25 Mb exhibited an c. 20–fold lower rate (0.4 cM/Mb). The general pattern of periphery–biased recombination proved essentially insensitive to centromere position (e.g., compare chromosomes 7 and 8 in Fig. 4.1). Our data also suggested a tendency for the recombination rate to drop again right at the chromosome ends (e.g., chromosomes 1, 2, 4, 17 in, Fig. 4.1). Formally testing this observation, however, would have required higher–resolution data, sampling the terminal domains more densely.

Comparing mean crossover number per meiosis among chromosomes revealed a lower limit of approximately one crossover for the chromosomes at the lower end of the size range (around 15 Mb) (Fig. 4.2A). With increasing chromosome length, the crossover number also increased (r = 0.92, permutation P = 0.0001), with the largest chromosomes (around 30 Mb) displaying c. 1.5 crossovers per meiosis. We also found a positive association between chromosome arm length and crossover number (r = 0.87, P = 0.0001) (Fig. 4.2B). Along the short arms of telocentric and acrocentric chromosomes, crossovers occurred rarely. These relationships caused the average recombi-
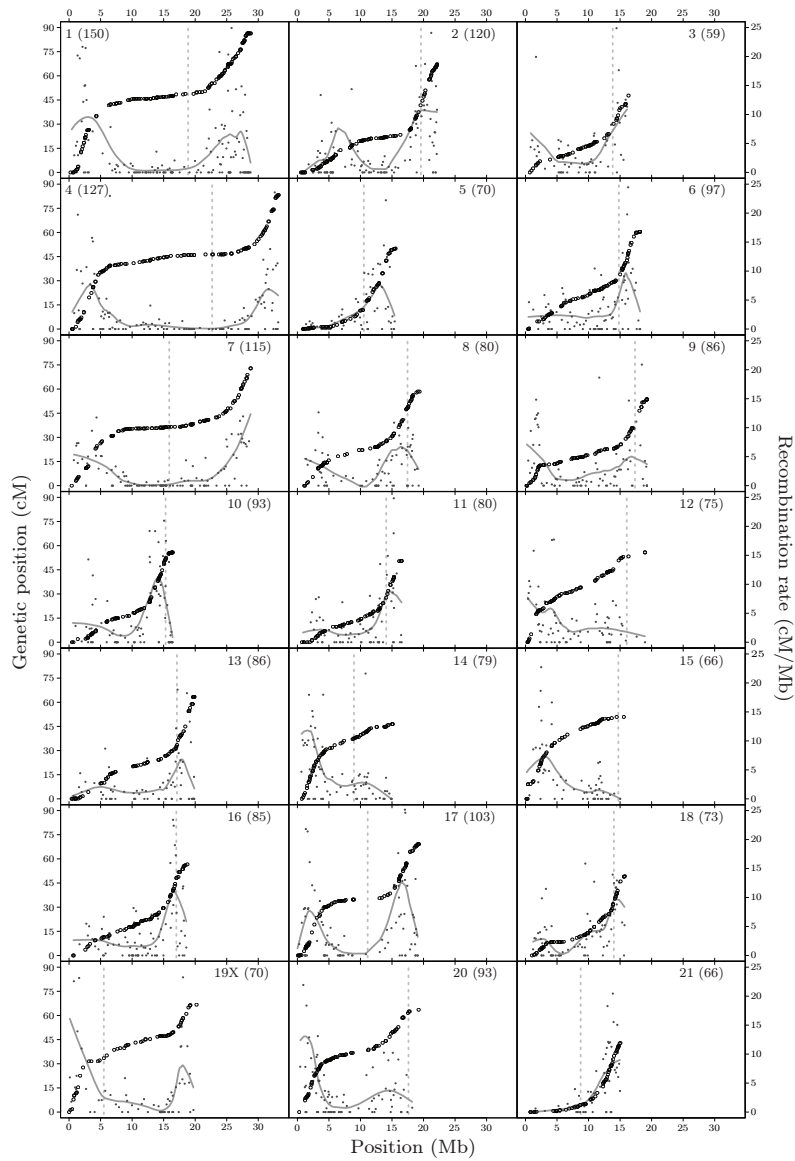
Figure 4.1: Recombination along the 20 threespine stickleback autosomes (based on 1'872 total markers and 282 F_2 individuals) and along the X chromosome (chromosome 19; based on 142 females). Marker number per chromosome is given in parentheses. The open circles (referring to the left axis) indicate the genetic map position of the markers in Kosambi centimorgan, plotted against their physical position in the genome (in megabases). The smaller grey dots (right axis) represent the average recombination rate in cM/Mb for the intervals defined by pairs of adjacent markers, plotted against the intervals' physical midpoint. The grey curves show the latter data smoothed by LOESS, with a polynomial degree of one and the smoothing span decreasing from 0.33 to 0.149 from the smallest to the largest chromosome to ensure a constant smoothing resolution across the panels. Dashed vertical lines specify centromere positions. Note the striking trend towards elevated recombination rate in the peripheral chromosome regions.

Table 4.1: Genome–wide associations between re combination rate and genetic population divergence, and between recombination rate and within–population genetic diversity. Divergence was quantified as F_{ST} between the lake and stream sample within the Boot and Robert's population pair. Genetic diversity within each of the four populations was expressed as both haplotype diversity (capturing allele frequency shifts) and the density of single nucleotide polymorphisms (SNPs) per RAD locus. All these metrics were averaged within the physical intervals defined by adjacent markers in the SNP panel used for genetic mapping (N = 1'783 intervals)

	Population(s)	r	P
Genetic divergence (F_{ST})	Boot lake–stream	-0.2699	0.0001
	Robert's lake–stream	-0.1127	0.0001
Haplotype diversity	Boot lake	0.1184	0.0001
	Boot stream	0.0925	0.0022
	Robert's lake	0.0400	0.0929
	Robert's stream	0.0665	0.0113
SNP density	Boot lake	0.1873	0.0001
	Boot stream	0.1810	0.0001
	Robert's lake	0.2593	0.0001
	Robert's stream	0.1882	0.0001
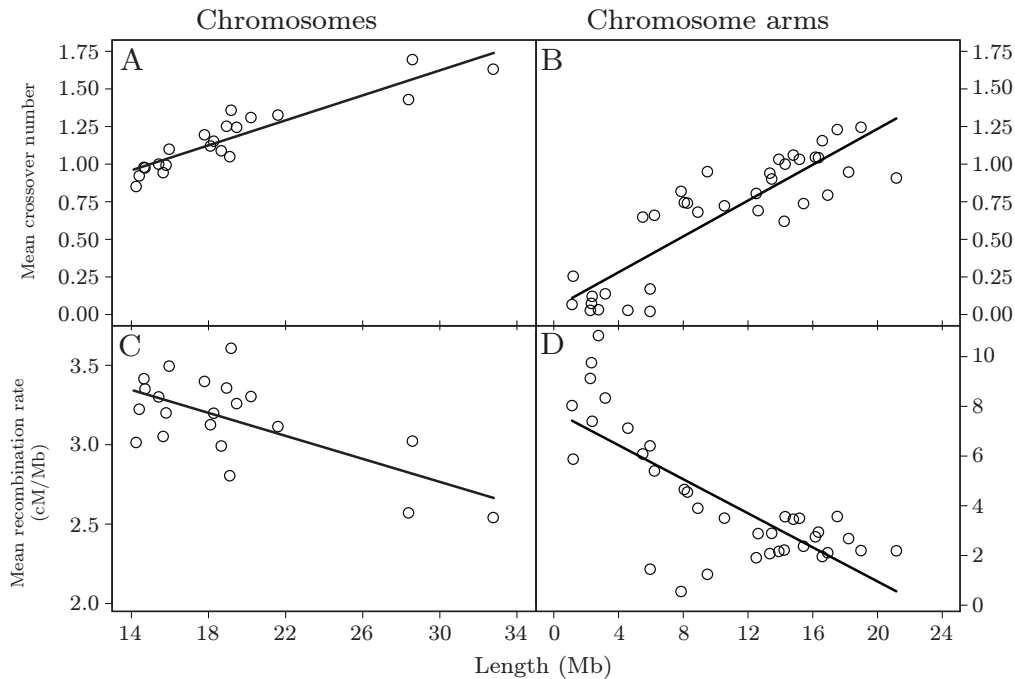
Figure 4.2: Stickleback chromosomes display an approximate minimal crossover number of one per meiosis, and crossover number is related positively to chromosome length (A). A similar positive relationship exists between crossover number and chromosome arm length (B). Because the increase in crossover number with increasing chromosome length is not proportional, longer chromosomes display a lower average recombination rate (C). The same holds for chromosome arms (D). Note that (C) and (D) have different scales on the Y–axis.

nation rate to be higher on short chromosomes and chromosome arms than on longer ones (Fig. 4.2C, 4.2D; chromosomes: r = –0.66, P = 0.0026; arms: r = –0.76, P = 0.0001). We found no indication of an overall difference in recombination rate between the sexes (P = 0.982); total autosomal map length was almost identical (1'190 cM) for males and females. Analyzing each chromosome separately also revealed only trivial sex–related differences in recombination rate (none of them remained significant when correcting for multiple testing). We further detected no significant QTL driving overall recombination rate on any of the 21 chromosomes (maximum LOD = 2.98; P = 0.261), keeping in mind the methodological limitations mentioned above.
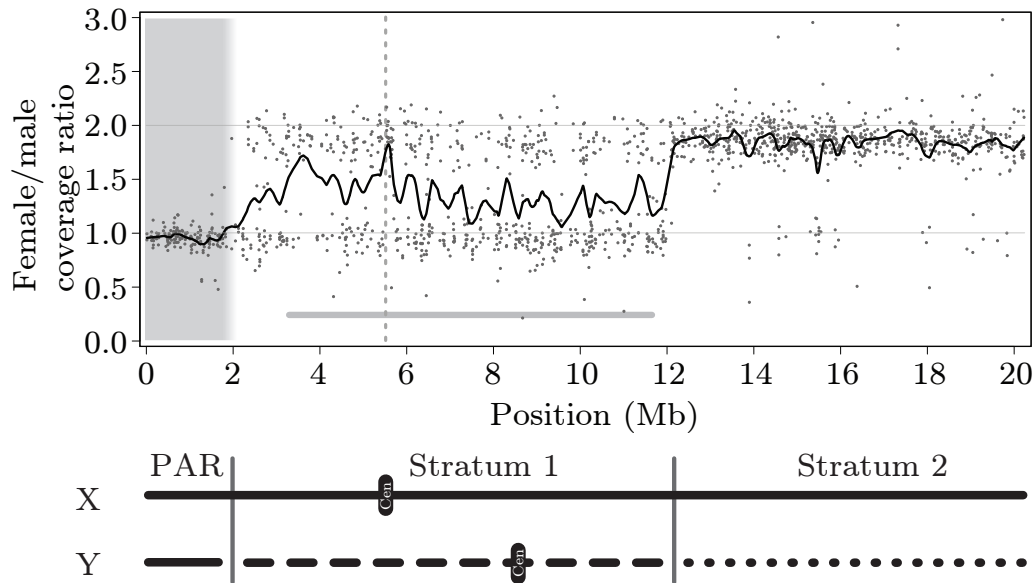
Figure 4.3: Patterns of recombination and divergence between the X and Y chromosome. In the top panel, the abscissa gives the physical position along the reference X chromosome. The centromere is indicated by the dashed grey vertical line. The domain on the left shaded in grey indicates the extent of the pseudoautosomal region (PAR) where the gametologs still recombined in our cross (the PAR boundary lies between 1.75 and 2.22 Mb). The dots show the ratio of female to male sequence coverage across 100 individuals per sex for 1'556 RAD loci (the black curve shows these data smoothed; degree = 1, span = 0.025). Within the PAR, the coverage ratio approximates unity (lower grey horizontal line), as expected for a DNA segment homochromatic between X and Y. Outside the PAR, many RAD loci display twofold higher sequence coverage in females than males (upper grey horizontal line), consistent with strong degeneration or loss of the X sequence on the Y. Note that two levels of Y degeneration ('evolutionary strata') are indicated (abutting at 12 Mb), the left one coinciding with the minimal size of a pericentric inversion on the Y inferred by Ross and Peichel (2008; visualized as heavy grey horizontal bar). On the bottom, we present the patterns of XY divergence inferred from our data in schematic form. Highly consistent patterns were also found when analyzing natural population samples from Europe and Canada (see Fig. S10 (Supplementary material)).
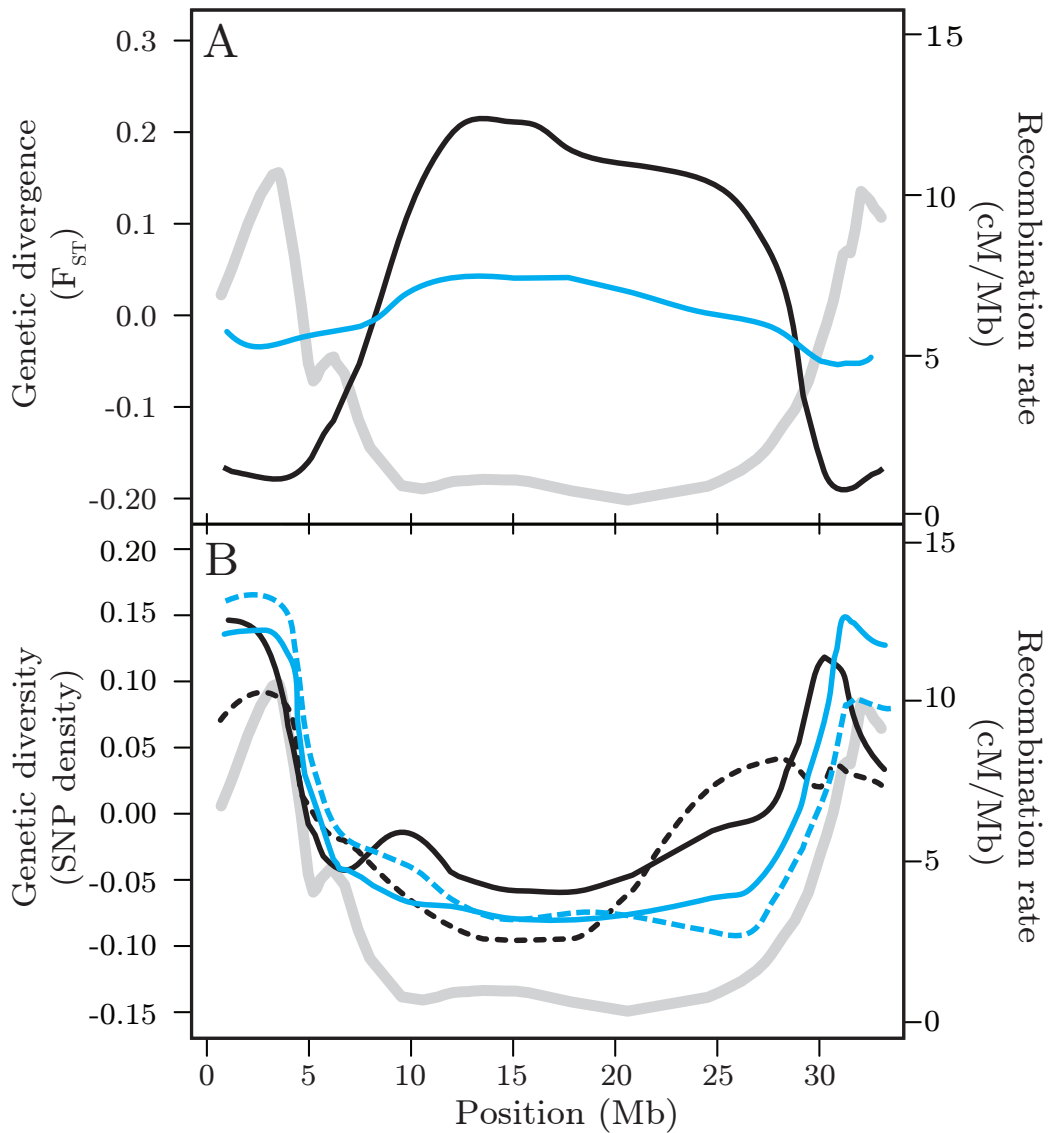
Figure 4.4: Genetic divergence and genetic diversity in relation to recombination rate (shown as heavy grey line referring to the right axis in both panels) in natural lake and stream stickleback populations, exemplified for the largest chromosome (4). In (A), we show the smoothed (degree = 0, span = 0.35) magnitude of lake–stream divergence (F_{ST}) for the Boot (black) and Robert's (blue) population pair (for the sake of clarity, the underlying raw data points are not shown). To facilitate comparison, the data were centered to a mean of zero before smoothing. Note that divergence is greatest in the chromosome centre where recombination rate is lowest, an effect more pronounced in the Boot population pair showing much stronger overall divergence. In (B), we display smoothed genetic diversity, quantified as single nucleotide polymorphism density, for the lake (solid line) and stream (dashed line) population in the Boot (black) and Robert's (blue) population pair (data also centered). Note the strong and consistent positive association between genetic diversity and recombination rate.
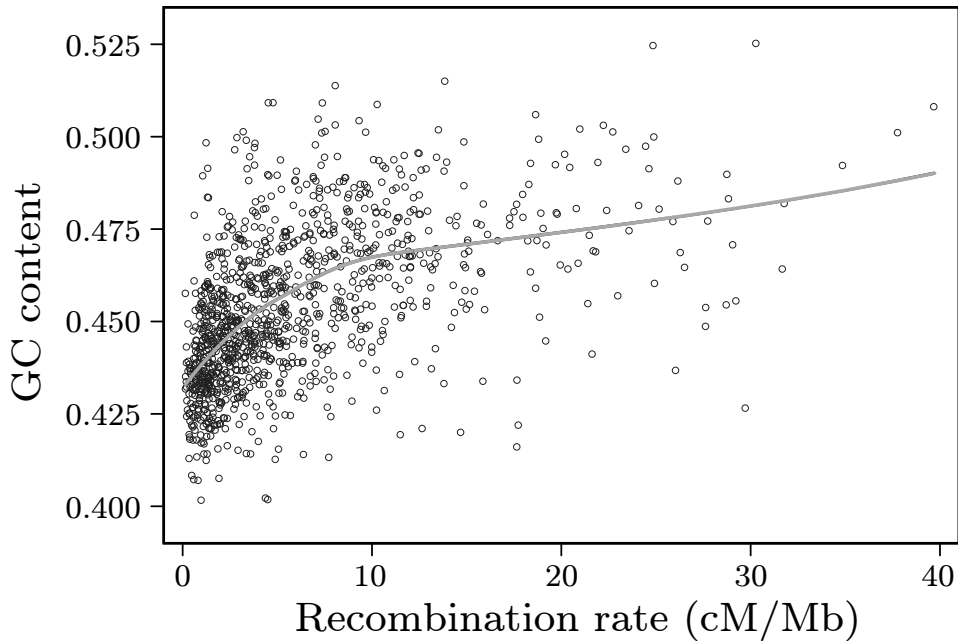
Figure 4.5: Genome–wide relationship between GC content and recombination rate. The data points are the intervals defined by adjacent markers in the single nucleotide polymorphism panel used for genetic mapping (N = 1'783 intervals). GC content was calculated for each marker interval by using information from the stickleback reference genome. The grey line shows the smoothed data (degree = 2, span = 0.85; a standard correlation produces r = 0.49).

4.4.1 Recombination and degeneration along the sex chromosome

In our F_2 population, XY recombination never occurred beyond the marker located at 1.75 Mb (Fig. 4.3). We thus demonstrate the presence of a small pseudoautosomal region (PAR), spanning c. 10% of the entire X chromosome only. The comparison of female with male RAD sequence coverage along the sex chromosome clearly revealed Y degeneration outside the PAR (Fig. 4.3). Moreover, the extent of degeneration was not uniform outside the PAR: within the segment from c. 12 Mb to the chromosome end opposed to the PAR, Y sequences generally did not align to the X reference. By contrast, the segment ranging from c. 2 to 12 Mb showed weaker degeneration. Despite small sample size and hence more random noise, analogous analyses in the two natural populations produced very similar results supporting identical conclusions (Fig. S10 (Supporting material)).

4.4.2 Genetic divergence, genetic diversity and GC content

The prediction of a negative genome–wide association between recombination rate and F_2 was clearly confirmed (Table 4.1; Fig. 4.4A). Shifts in allele frequencies between populations were thus greater in low–recombination regions. As expected, this effect was stronger in the Boot lake–stream pair showing greater overall divergence (and hence higher variance in F_2) than the Robert's pair (see Roesti et al. 2012a). The two complementary analyses of genetic diversity within populations also agreed with the prediction: all correlations were positive and generally highly significant (Table 4.1; Fig. 4.4B). Genetic diversity was thus reduced in marker intervals exhibiting a relatively low recombination rate. Finally, we found a striking positive broad–scale association between recombination rate and GC content across the genome (Fig. 4.5; P = 0.0001). Marker intervals showing relatively high recombination rates (around 10 cM/Mb or greater) displayed an c. 10% higher average GC content than intervals at the lower end of recombination rates (around 1 cM/Mb or lower).

4.5 Discussion

A major finding of our analysis of recombination in the threespine stickleback genome is the strong bias of crossover to occur primarily in the chromosome peripheries. This pattern confirms preliminary evidence from vertebrates (Borodin et al. 2008; Chowdhury et al. 2009; Backström et al. 2010; Wong et al. 2010; Bradley et al. 2011; Auton et al. 2012; Sandor et al. 2012; Tortereau et al. 2012), invertebrates (Rockman and Kruglyak 2009; Niehuis et al. 2010), plants (Akhunov et al. 2003; Anderson et al. 2003; but see Salomé et al. 2012) and yeast (Barton et al. 2008). This striking consistency across taxa implies a common mechanistic basis: crossovers seem to be initiated from the peripheries. Indeed, peripheral clustering of chromosomes during the meiotic prophase I is believed to play a key role in proper homolog pairing and probably also in crossover initiation (Scherthan et al. 1996; Roeder 1997; Harper et al. 2004; Brown et al. 2005; Naranjo and Corredor 2008). Peripheral crossover might also favor proper homolog dissociation (Colombo and Jones 1997; Hassold and Hunt 2001). Whatever the exact cause, the observed periphery bias in the distribution of crossovers in the stickleback genome (and many other genomes) implies strong mechanistic constraints on the distribution of recombination. Therefore, genetic information is reshuffled much more effectively in some genomic regions than

in others.

Moreover, taking into account a slight underestimation of recombination (see Materials and methods), our data indicate that stickleback chromosomes display at least one crossover per meiosis. This is consistent with the notion that one crossover per chromosome and meiosis is generally required for proper homolog segregation (Mather 1938; Baker et al. 1976; Roeder 1997; Smith and Nicolas 1998; Hassold and Hunt 2001), and reflects another mechanistic constraint on recombination. The widely accepted idea of one obligate crossover per chromosome arm, however, is not supported by our data (see also Borodin et al. 2008; Fledel–Alon et al. 2009): on acrocentric and telocentric stickleback chromosomes, the shorter arm rarely crosses over. We further find that the number of crossovers beyond one is a function of chromosome length. Standardized by their length, however, large chromosomes still exhibit a lower recombination rate than small chromosomes, the same also being true for chromosome arms.

4.5.1 Sex chromosome evolution

Sex chromosomes are generally thought to evolve from an ordinary pair of homologous autosomes that partly stop crossing over to prevent alleles at loci with sexually antagonistic effects from recombining (Bull 1983; Charlesworth and Charlesworth 2000; Charlesworth et al. 2005; Wilson and Makova 2009). This cessation of recombination should initiate the differentiation of the gametologs. While early karyotypic investigations in threespine stickleback found no evidence of heteromorphic sex chromosomes (Chen and Reisman 1970; Cuñado et al. 2002), recent investigations have indicated reduced recombination, chromosomal rearrangements and sequence divergence between the X and Y (Peichel et al. 2004; Ross and Peichel 2008; Shikano et al. 2011; Natri et al. 2013). These observations, based on a small number of markers, are greatly refined and extended by our sex chromosome analysis. We confirm that XY recombination is restricted to a small PAR, as suggested by Ross and Peichel (2008). The requirement of at least one crossover per meiosis thus implies a very high average recombination rate (c. 25 cM/Mb) across the PAR in males. This agrees with the estimation by Peichel et al. (2004) of a much greater distance between markers lying within the PAR in male than in female genetic maps (e.g., the genetic distance in the Paxton cross between the microsatellites Stn303 and Stn186, located at 0.4 and 1.9 Mb, is 27.3 cM in females and 47.7 cM in males).

A consequence of the cessation of recombination along most of the sex chromosome is that the region on the Y outside the PAR occurs in permanently heterozygous state and at lower population size than the X. Both

conditions are predicted to make selection on the Y less effective and hence to promote its degeneration (Felsenstein 1974; Charlesworth and Charlesworth 2000; Otto and Lenormand 2002; Charlesworth et al. 2005; Wilson and Makova 2009). Our results strongly support this view: outside the PAR, RAD loci often display only half the sequence coverage in males relative to females, consistent with substantial sequence degeneration (or loss) on the Y. Interestingly, our analysis further indicates two discrete levels of Y degeneration, with much stronger degeneration along the c. 8 Mb towards the chromosome end opposed to the PAR than along the c. 10 Mb adjacent to the PAR. Such 'evolutionary strata' (Lahn and Page 1999) have been found in mammals (Lahn and Page 1999; Sandstedt and Tucker 2004; Pearks Wilkerson et al. 2008), birds (Lawson Handley et al. 2004; Nam and Ellegren 2008) and plants (Bergero et al. 2007; Wang et al. 2012). To our knowledge, we here provide the first evidence for evolutionary strata in fish.

Evolutionary strata are generally taken as evidence that XY recombination ceased simultaneously across large domains of the evolving sex chromosome. An obvious way how this may happen is through chromosomal inversion. Indeed, a recent study using in situ fluorescent hybridization argued for a large pericentric inversion on the Y relative to the X, with breakpoints at c. 3 and 12 Mb (Ross and Peichel 2008). The evolutionary stratum adjacent to the PAR identified in our work matches this inversion almost perfectly and allows us to refine its physical boundaries. Threespine stickleback thus reinforce the view that recombination suppression along evolving sex chromosomes will primarily occur through inversion rather than crossover rate modifier genes (Charlesworth et al. 2005).

It would now be interesting to date the two bouts of recombination suppression underlying the evolutionary strata in the species based on sequence divergence between homologous loci on the X and Y (Lahn and Page 1999; Lawson Handley et al. 2004; Nam and Ellegren 2008; Pearks Wilkerson et al. 2008; Wang et al. 2012). We note that this might be difficult for stratum 2 if the remarkably strong degeneration detected in our analysis actually reflects deletion (Peichel et al. 2004). Clearly, however, patterns of XY divergence were already established prior to the split into Pacific and Atlantic stickleback clades (Fig. 10 (Supplementary material)).

4.5.2 Consequences of heterogeneous recombination rate on genome evolution

The rate of recombination within a genomic region determines to which extent selection on a locus influences allele frequencies at neutral loci, and

interferes with selection on other loci, in its physical neighborhood (Hill and Robertson 1966; Maynard Smith and Haigh 1974; Barton and Bengtsson 1986; Kaplan et al. 1989; Begun and Aquadro 1992; Nordborg et al. 1996; Charlesworth et al. 1997; Charlesworth 1998; Nachman 2002; Feder and Nosil 2010). Several types of selection (divergent, positive and background) should therefore increase divergence among populations and reduce genetic diversity within populations in low–recombination genomic regions relative to regions where recombination rate is higher.

Consistent with these predictions, we have recently shown that the magnitude of divergence between neighboring lake and stream stickleback populations is dramatically biased towards chromosome centers (Roesti et al. 2012a). (Note that divergence in these young populations essentially reflects differential sorting of standing variation rather than novel mutations.) Using robust recombination rate data, we here demonstrate that elevated divergence in these population pairs is related to reduced recombination. Because lake and stream stickleback occupy selectively distinct environments (Berner et al. 2008, 2009), the divergence–recombination association almost certainly arises from within–chromosome variation in hitchhiking and/or introgression.

The present study further demonstrates reduced within–population genetic diversity in the chromosome centers relative to the peripheries, resulting in a genome–wide positive correlation between diversity and recombination rate. A similar correlation has previously been reported in a broad range of organisms (Begun and Aquadro 1992; Kraft et al. 1998; Nachman 2001; Tenaillon et al. 2001; Takahashi et al. 2004; Roselius et al. 2005; McGaugh et al. 2012). Given that a positive correlation between recombination rate and genetic diversity may also arise if recombination is directly mutagenic (Spencer et al. 2006; Webster and Hurst 2012; but see McGaugh et al. 2012), caution is generally warranted when inferring from the above correlation that recombination rate modulates the influence of selection on linked sites across the genome. In our lake–stream stickleback systems, however, the colocalization of elevated population divergence and reduced genetic diversity within young populations residing in selectively distinct environments provides clear support for such an indirect influence of recombination on genome evolution (see also Stoelting et al. 2013). The precise selective processes driving these patterns, however, remain to be elucidated.

In addition to these indirect (selective) effects, our study perhaps also points to a direct effect of recombination on stickleback genome evolution: large–scale bias in nucleotide composition. Across the genome, GC content is higher in regions displaying relatively elevated recombination rate – that is, in the chromosome peripheries. Interestingly, the positive association between GC content and recombination rate seems as widespread as periphery bias

in recombination rate; it has been reported in mammals (Jensen–Seaman et al. 2004; Spencer et al. 2006; Duret and Arndt 2008; Auton et al. 2012; Tortereau et al. 2012), birds (ICGSC 2004; Backström et al. 2010), insects (Niehuis et al. 2010; Stevison and Noor 2010; but see Comeron et al. 2012), plants (Muyle et al. 2011) and yeast (Gerton et al. 2000; Birdsell 2002). As hypothesized in other organisms, elevated GC content in the stickleback genome might represent a direct causal consequence of elevated recombination rate, given evidence of GC bias in the machinery correcting nucleotide mismatch in heteroduplex DNA formed during crossover initiation (GC–biased gene conversion; Brown and Jiricny 1987; Bill et al. 1998; Galtier et al. 2001; Birdsell 2002; Meunier and Duret 2004; Mancera et al. 2008; Duret and Galtier 2009; Muyle et al. 2011). Our correlational data, however, cannot address this causal hypothesis conclusively; direct experimental evidence is needed.

4.5.3 Methodological implications

In addition to the above influences on genome evolution, heterogeneous recombination rate within the genome has important methodological implications. Marker–based genome scans searching for signatures of divergent selection in the form of locally elevated divergence between ecologically distinct populations (Lewontin and Krakauer 1973; Beaumont and Nichols 1996; Luikart et al. 2003; Beaumont 2005; Nielsen 2005; Storz 2005) are becoming commonplace. What is generally ignored is that the distortion between physical and genetic maps will dilute the link between the selection coefficient on a locus and the magnitude of hitchhiking produced in its neutral neighborhood (Roesti et al. 2012a; this chapter). In other words, a locus under selection is more likely to be detected when located in a low–recombination region where hitchhiking is more extensive. This bias should increase with decreasing marker resolution and with increasing sliding window size. The generality of chromosome periphery–biased recombination rate across taxa therefore raises a potential caveat to the interpretation of differentiation outliers in genome scans when combined physical and genetic map information is missing (i.e. 'anonymous' approaches; for one strategy to alleviate this difficulty when a physical map is available, see Roesti et al. 2012a). An analogous issue arises when interpreting the number and effect size of mapped QTL: within low–recombination regions, multiple loci of small effect are more likely to emerge as a single large–effect locus (Noor et al. 2001).

Finally, our study highlights the need for a reliably assembled genome for investigations of recombination and linkage. Assembly errors will inflate the genome–wide average crossover frequency, distort the recombination land-

scape and bias analyses of linkage disequilibrium along chromosomes. For instance, we find that a high–recombination island on chromosome 4 inferred in Hohenlohe et al. (2012) coincides with the boundary of a scaffold anchored in the wrong sense within that chromosome (see Fig. S9 (Supporting material)) and hence represents an artifact. The same assembly error also mimics long–distance linkage disequilibrium along this chromosome (Hohenlohe et al. 2012).

To summarize, our analysis of recombination in threespine stickleback indicates strong constraints on the frequency and location of crossovers imposed by the mechanistic requirements of meiosis. At the same time, we demonstrate that recombination influences the genome profoundly, both by modulating the consequences of selection across the genome and perhaps by directly influencing nucleotide composition. We anticipate that our characterization of the recombination landscape will facilitate interpretations of genome scans and QTL mapping in the species, promote further investigations on sex chromosome evolution and pave the way for more detailed investigations of the determinants and consequences of recombination.

4.6 Acknowledgments

4.7   Author contributions

Conceived and designed the experiments: DB MR. Performed the experiments: DB DM & MR. Analyzed the data: DB MR. Wrote the paper: DB MR.

Chapter 5

Genetic architecture of skeletal evolution in european lake and stream stickleback

Authors: Daniel Berner, **DARIO MOSER**, Marius Roesti, Heinz Buescher & Walter Salzburger

Preface: The raw RAD data from the fourth chapter were also used for the QTL–mapping in chapter 5. Together with Dani, I photographed all F_2 fish. This was necessary for centroid size estimation and size correction. The traits I fully or partially phenotyped were vertebrae number, snout length and head length.

5.1 Abstract

Advances in genomic techniques are greatly facilitating the study of molecular signatures of selection in diverging natural populations. Connecting these signatures to phenotypes under selection remains challenging, but benefits from dissections of the genetic architecture of adaptive divergence. We here perform quantitative trait locus (QTL) mapping using 488 F_2 individuals and 2011 single nucleotide polymorphisms (SNPs) to explore the genetic architecture of skeletal divergence in a lake–stream stickleback system from Central Europe. We find QTLs for gill raker, snout, and head length, vertebral number, and the extent of lateral plating (plate number and height). Although two large–effect loci emerge, QTL effect sizes are generally small. Examining the neighborhood of the QTL–linked SNPs identifies several genes involved in bone formation, which emerge as strong candidate genes for skeletal evolution. Finally, we use SNP data from the natural source populations to demonstrate that some SNPs linked to QTLs in our cross also exhibit striking allele frequency differences in the wild, suggesting a causal role of these QTLs in adaptive population divergence. Our study paves the way for comparative analyses across other (lake–stream) stickleback populations, and for functional investigations of the candidate genes.

5.2 Introduction

Exploring the genetic basis of adaptation promises to illuminate several long–standing issues in biological diversification. These include the number and genomic location of genetic changes underlying adaptation, their role in developmental pathways, their phenotypic effects and resulting ecological consequences, and their predictability (Orr 1998; Barton and Keightley 2002; Phillips 2005; Hoekstra and Coyne 2007; Mitchell–Olds et al. 2007; Wray 2007; Arendt and Reznick 2008; Stern and Orgogozo 2008; Mackay et al. 2009; Rockman 2011; Wake et al. 2011; Yeaman and Whitlock 2011). Currently, perhaps the most popular approach to investigating the genetics of adaptation is divergence mapping (Nielsen 2005; Storz 2005; Oleksyk et al. 2010). Here a large set of genome–wide molecular markers is screened for putative signatures of divergent selection between ecologically distinct populations. In well–developed empirical systems, this is proving a powerful method for the discovery of genomic regions or candidate genes involved in adaptive divergence (e.g., Akey et al. 2002; Voight et al. 2006; Hohenlohe et al. 2010; Lawniczak et al. 2010; Jones et al. 2012; Nadeau et al. 2012; Roesti et al. 2012a, 2014; Mateus et al. 2013; Stölting et al. 2013). A

short coming of divergence mapping, however, is that in general molecular signatures alone cannot tell us much about the traits actually targeted by selection (Mitchell–Olds et al. 2007; Stinchcombe and Hoekstra 2008; Storz and Wheat 2010). In the years to come, we can thus anticipate a surge of information about genome regions putatively influenced by divergent selection in many organisms, but knowledge about the phenotypes transferring selection to the molecules is likely to lag behind. Understanding the genetics of adaptation will thus benefit greatly from the combination of purely genomic investigations with extensive data on the genetic architecture of phenotypic divergence, as for instance obtained by quantitative trait locus (QTL) mapping.

In the present study, we report a QTL mapping experiment performed in a powerful system for studying adaptive divergence: lake and stream populations of threespine stickleback fish. Following the retreat of the last Pleistocene ice sheets, the colonization of freshwater by ancestral marine stickleback has resulted in the establishment of numerous populations occurring in adjacent lake and stream habitats (Reimchen et al. 1985; Lavin and McPhail 1993; Thompson et al. 1997; Hendry and Taylor 2004; Berner et al. 2008, 2010a; Aguirre 2009; Bolnick et al. 2009; Deagle et al. 2012; Lucek et al. 2013; Ravinet et al. 2013; Chapter 1). Lake and stream stickleback are often ecologically divergent, with the most consistent difference concerning their foraging modes: lake stickleback partly or exclusively exploit pelagic food resources (zooplankton), whereas stream stickleback generally use benthic prey (macroinvertebrates; Gross and Anderson 1984; Berner et al. 2009; Kaeuffer et al. 2012; Ravinet et al. 2013; Chapter 1). This divergence in foraging modes is associated with relatively consistent phenotypic differences in traits presumably important for prey capture and handling, such as overall body shape and gill raker structure (Reimchen et al. 1985; Lavin and McPhail 1993; Berner et al. 2008, 2009, 2010a; Kaeuffer et al. 2012; Lucek et al. 2013; Ravinet et al. 2013). The existence of replicate, ecologically and phenotypically divergent population pairings makes lake–stream stickleback an appealing system for the search of molecular signatures of divergent selection. Indeed, divergence mapping has already been performed in some lake–stream stickleback systems (Deagle et al. 2012; Roesti et al. 2012a).

By contrast, very little is known about the genetics of phenotypic divergence between lake and stream stickleback. Quantitative genetic (common–garden) experiments have demonstrated a genetic basis to divergence in some foraging traits (Lavin and McPhail 1993; Sharpe et al. 2008; Berner et al. 2011), but QTL dissections of the genetic architecture of phenotypic divergence have yet to be performed. We here take up this challenge by using QTL mapping to explore the genetic basis of divergence in skeletal features

between lake and stream stickleback populations from Central Europe.

5.3 Material and methods

5.3.1 Cross

Our study is based on an F_2 intercross population derived from a single *in vitro* cross of a male from Lake Constance (sampled at the ROM lake site described in Berner et al. 2010a) with a female from a stream draining into Lake Geneva (the CHE stream site in Berner et al. 2010a). The F_2 panel comprises 492 individuals (251 males, 237 females) selected haphazardly at one year of age from 35 separate F_1 crosses, each produced by a unique full–sib pairing. All details on crossing, husbandry, and handling are exactly as described in chapter 4, a recombination study based on a subset of 282 individuals from the full F_2 population used here for QTL mapping.

All fish were euthanized with an overdose of MS–222, photographed immediately as described in Berner et al. (2009), and stored in absolute EtOH. After six months of preservation, a fin clip was taken for genetic analysis and each individual was subjected to a digital X–ray scan of the whole body and a higher resolution scan of the head. This was performed by using a Faxitron Digital Specimen Radiography System LX–60 (tube voltage 35 kV, tube current 0.3 mA), including a reference size scale in all scans

5.3.2 Phenotyping

Our study focuses on aspects of skeletal morphology, here defined broadly as bone traits. The first trait of interest was the length of the gill rakers (bony tubercles) located on the first branchial arch (Fig. 5.1). Gill rakers are important to foraging because they influence prey retention and handling performance (Gerking 1994; Sanderson et al. 2001). In particular, longer gill rakers generally promote foraging on small prey items (such as zooplankton), whereas shorter gill rakers are favored in fish foraging on larger prey (such as macroinvertebrates). Indeed, the natural source populations of our cross are highly divergent in this trait, with the lake population displaying 25% longer size–corrected gill rakers than the stream population (standardized mean difference: 0.99; see Fig. 5.2 in Berner et al. 2010a), and this divergence coincides with distinct foraging modes: Lake Constance stickleback forage pelagically on zooplankton (Lucek et al. 2012; Chapter 1), whereas their conspecifics from the CHE stream site feed on larger benthic macroinvertebrates (Berner et al. 2010a). Given that such concurrent divergence in gill

raker length and prey utilization has also been found in other (lake–stream) stickleback systems (Gross and Anderson 1984; McPhail 1984; Schluter and McPhail 1992; Bolnick 2004; Berner et al. 2008, 2010a,b; Matthews et al. 2010; Ravinet et al. 2013), and even in distantly related fish species (Kahilainen and Ostbye 2006; Pfaender et al. 2011), the divergence between ROM and CHE stickleback is very likely adaptive. We note that benthic versus pelagic resource specialization often coincides with additional divergence in gill raker *number*, but because the source populations are not divergent in this trait (Berner et al. 2010a), we did not include this trait in the current analysis. Gill raker length was measured on the left first branchial arch of the preserved specimens under a stereomicroscope fitted with an ocular micrometer at $50\times$ magnification (precision: 0.01 mm). We measured and then averaged the length of the rakers two to five (counted from the joint with the dorsal arch bone, see Berner et al. 2008).
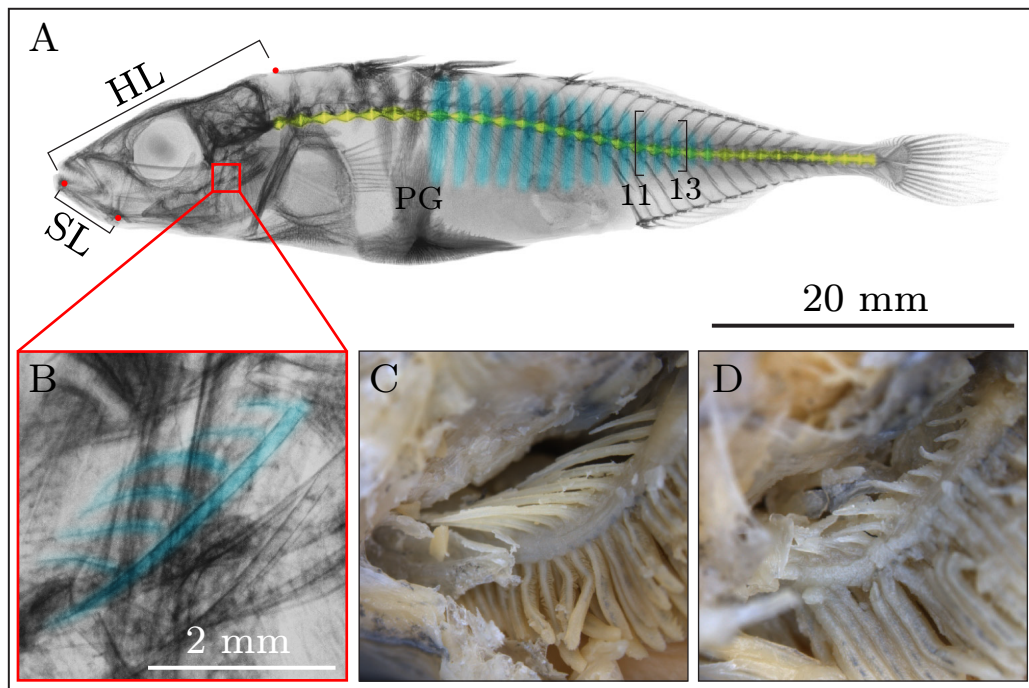
Figure 5.1: Traits subjected to QTL mapping in lake and stream stickleback. (A) X–ray scan of a partially plated stickleback visualizing snout length (SL), head length (HL), the vertebrae, and the lateral plates. Plate height was measured on the plates 11 and 13 posterior to the pelvic girdle (PG). (B) Detail of the head, showing the gill rakers (GR) on the first lower branchial arch (BA). The subpanels (C) and (D) display, on the same scale as (B), the gill rakers of two size–matched individuals from the upper and lower end of the gill raker length distribution.

Next, we considered two aspects of head morphology: snout length and

overall head length (Fig. 5.1). The pelagic ROM lake population displays lower values for both traits relative to the CHE stream population foraging on benthic prey (Berner et al. 2010a), and similar foraging–related divergence is also seen in other stickleback systems (Caldecutt and Adams 1998; Albert et al. 2008). Moreover, head morphology typically shows sexual dimorphism (Caldecutt and Adams 1998; Kitano et al. 2007; Albert et al. 2008; Aguirre and Akinpelu 2010; Berner et al. 2010a, 2011; Ravinet et al. 2013). This dimorphism is possibly also related to differential foraging modes. The reason is that in stickleback, males tend a nest and provide parental care. The (presumably ancestral) necessity of males to forage on benthic resources during the breeding season while females can continue to exploit pelagic prey may have driven divergence in head structure between the sexes (Bentzen and McPhail 1984; Bentzen et al. 1984). Both snout length and head length were measured from the head X–ray scans. The former was defined as the distance from the joint to the tip of the lower jaw, the latter as the distance from the tip of the lower jaw to the dorsal posterior edge of the cranium.

The next trait quantified was vertebral number. Stickleback populations often differ in the number of vertebrae (Hagen and Gilbertson 1972; Moodie and Reimchen 1976; Reimchen et al. 1985). Although the functional basis of this variation remains poorly understood (but see Swain 1992), genetic analysis in stickleback may provide insights into vertebral diversification in other fish (Ward and Brainerd 2007; McDowall 2008) and vertebrates in general. As a first step, we thus produced whole–body X–ray scans of 14 specimens from each natural source population, counted all vertebrae excluding the urostyle (Fig. 5.1), and tested for a population difference in mean count using 9'999 random permutations of the trait over the populations (Manly 2007; all significance testing in this study was performed using analogous permutation procedures). This analysis made clear that ROM stickleback have a higher number of vertebrae than CHE fish (see Results). Following the same methods, we therefore quantified vertebral number for the full F_2 panel. Because of skeletal anomalies, 18 individuals could not be scored unambiguously, leaving 474 datapoints.

Finally, our phenotypic analysis included elements of lateral plating. Ancestral marine stickleback display a complete series of bony plates along their body, whereas the number of plates is typically greatly reduced in freshwater populations (Bell and Foster 1994). This difference is presumably attributable to differential exposure to predators (Hagen and Gilbertson 1972; Reimchen 1994a; Bergstrom 2002; Leinonen et al. 2011a), although other ecological factors targeting plate number or other traits correlated with plate number due to pleiotropy or genetic linkage might influence plate evolution as well (e.g., Heuts 1947; Giles 1983; Barrett et al. 2009; Myhre and Klepaker

2009; Leinonen et al. 2011b; Roesti et al. 2014). Interestingly, Lake Constance stickleback are a rare example of a freshwater population almost completely fixed for the fully plated phenotype (Berner et al. 2010a; Chapter 1). Because plating is reduced in several tributary streams to Lake Constance, the persistence of full plating in the lake likely reflects an adaptation to high predator exposure associated with a pelagic life style. By contrast, CHE stickleback represent a typical low–plated freshwater population (Berner et al. 2010a), thus providing the opportunity to map variation in lateral plating in the F_2 cross. Consistent with previous work (Berner et al. 2010a; Chapter 1), we scored the extent of lateral plating using three discrete phenotypic classes (low, partially, and fully plated).

Previous mapping efforts and subsequent functional analysis in Pacific marine and freshwater stickleback have already identified the *Ectodysplasin* (*EDA*) gene as a major driver of evolutionary shifts in the extent of lateral plating (Colosimo et al. 2004, 2005; Cresko et al. 2004; Baird et al. 2008). Moreover, targeted sequencing of the entire *EDA* coding region revealed distinct haplotypes in fully plated Lake Constance versus low–plated CHE stream fish (Berner et al. 2010a). Our primary objective in mapping plate morph was therefore to assess if genomic regions beyond *EDA* contribute to plating divergence between these European freshwater populations. To this end, we additionally counted the total number of lateral plates posterior to the pelvic girdle (including the plates forming the caudal keel) across both body sides in the subset of F_2 individuals genotyped unambiguously as heterozygotes at our single SNP marker located within *EDA*. Focusing on this particular subset (N = 209) allowed us to screen for loci influencing the extent of plating while controlling rigorously for the effect of the known major locus.

As an alternative to reducing the extent of lateral plating via a reduction in the *number* of plates (see above), stickleback sometimes appear to evolve *shallower* plates (Leinonen et al. 2012). Although differences in plate size between ROM and CHE stickleback could not be examined adequately because the latter are low–plated, a preliminary inspection of the F_2 population indicated substantial variation in plate height. We therefore measured the maximal height of the plates 11 and 13, as counted from the pelvic girdle, perpendicular to the anterior–posterior axis on the left body side (Fig. 5.1). Measurements were taken with a digital caliper (precision: 0.01 mm) handled under a stereomicroscope at 10–$30\times$ magnification. As plate height could only be quantified in the fully and most of the partially plated individuals, sample size was 358 and 342 for plate 11 and 13.

All metric (length) traits considered in our study scaled strongly with overall body size (Pearson's r: 0.49–0.84), whereas the meristic (count) traits

did not (vertebral number: r = 0.042; lateral plate number: r = 0.045). Prior to QTL mapping, we therefore subjected the former traits to size correction by regressing each trait separately against body size, and treating the residuals as size–independent variables (Reist 1985; Berner 2011). These variables were shifted back into the original measurement range by adding the trait value predicted by the regression at mean body size across all individuals. To obtain a robust size metric for these procedures, we used tpsDig (Rohlf 2001) to digitize 16 landmarks as described in Berner et al. (2010a) on the digital photographs of all individuals, and extracted geometric morphometric centroid size using TpsRelw (Rohlf 2001).

Finally, we assessed measurement precision for all traits by remeasuring 30 haphazardly selected individuals on a second occasion, and calculating the repeatability (Lessells and Boag 1987). Repeatability was consistently very high, ranging from 0.96 (plate number) to 1 (vertebral number, plate morph).

5.3.3 Marker generation

As markers for mapping, we used single nucleotide polymorphisms (SNPs) discovered by RAD sequencing (Baird et al. 2008). In brief, this involved DNA restriction with the *Sbf1* enzyme, and sequencing pools of 62 barcoded individuals in eight lanes with 100 cycles on an Illumina HiSeq 2000 instrument. RAD library preparation and the bioinformatics pipeline used for SNP discovery and genotyping were exactly as described in chapter 4. From the 2165 markers thus obtained, we excluded 154 to avoid *Sbf1* restriction sites being represented by more than one SNP. We also discarded four individuals exhibiting more than 10% missing genotypes across all markers. Our final mapping dataset thus comprised 488 F_2 individuals (recall that sample size was lower for some traits) and 2'011 SNPs.

5.3.4 QTL mapping

All SNPs were ordered physically according to the stickleback genome reassembly performed in chapter 4, resulting in 61–152 markers per chromosome and a median marker spacing of 118 kb. Next, we excluded 111 individuals with relatively low genotyping quality, as judged by clearly inflated genome–wide crossover count (we here used 2.5 times the median autosomal crossover count across all 488 individuals as threshold). The remaining 377 individuals were used to estimate the genetic map in R/qtl (Broman and Sen 2009), applying the Kosambi map function (assuming crossover interference). The resulting genetic map proved highly consistent with that

provided in chapter 4 based on fewer individuals but with genotype errors corrected manually, and was used to specify the genetic marker distances for QTL mapping. Mapping with genetic distances estimated by using the full F_2 panel produced very similar results (details not presented).

All phenotypes were subjected to single–QTL interval mapping in R/qtl using the extended Haley–Knott regression method (Broman and Sen 2009) and the full F_2 panel. Head length was mapped both with and without snout length entered as covariate, as our head length measure included the snout tip. We present the former analysis only, noting that both approaches produced quantitatively very similar results. QTL significance was established based on the distribution of genome–wide maximum LOD (logarithm of the odds ratio for QTL likelihood) scores across 1000 random permutations of the phenotype data over the genotype data (Broman and Sen 2009). In the Results, we present only QTLs significant at the 0.05 level, but additional loci are considered in the Discussion, and a table including suggestive QTLs ($0.05 \leq P < 0.1$) is provided as Table S4 (Supplementary material). QTL effect sizes were quantified both as the percentage of the total phenotypic variance in the F_2 cross explained by the QTLs (percent variance explained, PVE), and as their allelic substitution effect (i.e. the phenotypic difference between the two homozygous genotype classes). We present the latter both in the traits' original measurement scale (millimeter for all length traits), and standardized by the average standard deviation within the homozygous genotype classes. All statistics and plotting were carried out with the R language (R Development Core Team 2013).

5.3.5   Exploring QTLs

Following QTL detection, we retrieved from the Ensembl Genome Browser all genes located in the physical window spanned by the two SNPs flanking the marker displaying the LOD peak (this interval usually coincided with the 1.5 LOD support interval). We then scanned these gene lists for strong causative candidates, as judged by information on protein function in vertebrate model organisms (chicken, mice, rats, humans) compiled in the UniProt database (The UniProt Consortium 2013).

In addition, the availability of RAD sequences generated previously for the ROM and CHE population allowed us to inspect the magnitude and direction of allele frequency shifts in the wild at QTLs discovered in the F_2 population. Although this type of follow–up analysis has, to our knowledge, not previously been carried out, it promised stronger QTL inference because a genotype–phenotype association shared between a cross and its natural source populations suggests that the focal QTL is effectively contributing to

divergence in the wild, as opposed to being specific to the cross. As a caveat, we note that this approach assumes that the tight linkage detected between marker and QTL alleles in the cross also persists in the wild. Specifically, we here capitalized on RAD sequence data from 27 individuals sampled from each source population. Details on the wet laboratory protocol, the analysis pipeline, and access to the sequence data are provided in Roesti et al. (2012b; this reference describes data generation for the ROM population only; the CHE dataset has not previously been analyzed but was generated in exactly the same way). Because the RAD libraries of both the cross and the natural populations were generated using the *Sbf1* restriction enzyme, all RAD loci of interest were shared among the two datasets. However, the latter libraries were Illumina–sequenced to 76 bases as opposed to 100 bases for the cross, thus precluding the examination of allele frequencies in the natural populations at QTL–linked SNPs located distal to the restriction site. We further ignored SNPs linked to lateral plate height QTLs because we here lacked information on the direction and magnitude of divergence between the natural populations (see above).

For those SNPs represented in both the cross and the natural population datasets (four SNPs in total), we first determined from which population each of the two alleles present in the cross originated. This assignment was unambiguous because our study considered only markers homozygous within each grandparent (Chapter 4). Next, we arbitrarily converted the two alleles to integers (0, 1) and tested for frequency shifts by random permutation, using the difference in the population means as test statistic. While providing a formal test for population divergence at QTL–linked SNPs, this approach yielded no information regarding the potential cause of divergence at these SNPs. To gain insights into the latter, we performed a second analysis comparing the SNP allele frequency shifts between the natural populations to the magnitude of genome–wide baseline divergence between the populations. The rationale was that an allele frequency shift clearly exceeding baseline divergence – reflecting the magnitude of differentiation by drift – offers evidence for divergent selection having acted in the close neighborhood of the QTL–linked marker. We recognize the possibility, however, that selection may not have target the detected QTL itself, but a nearby locus unrelated to the mapped phenotype.

We thus translated allele frequency differences at the QTL–linked SNPs to F_{ST} (Nei and Tajima 1981, eq. 7), and estimated the confidence interval for F_{ST} as the 95 percentile of the distribution produced by bootstrap resampling the observed alleles 10'000 times within each population (Manly 2007). This confidence interval was then evaluated against the magnitude of baseline differentiation between the ROM and CHE population samples, defining

baseline differentiation as genome–wide median F_{ST} (Roesti et al. 2012a). Following Roesti et al. (2012a,b), the estimation of baseline differentiation ignored SNPs with a minor allele frequency < 0.25 to avoid polymorphisms with low information content, and for RAD sites harboring multiple polymorphisms used only the one SNP yielding the highest F_{ST} value. Baseline differentiation thus calculated was 0.37 across 5'429 informative SNPs.

5.4 Results

5.4.1 Gill raker length

We found two significant QTLs influencing gill raker length (Table 5.1; an additional suggestive QTL is described in Table S4 (Supplementary material); genome–wide LOD profiles for all traits are presented as Fig. S11 (Supplementary material)). Both showed a modest effect size. The SNP associated with the QTL exhibiting the greater effect size (located on chromosome 6) produced a phenotypic shift in the predicted direction (longer gill rakers associated with the ROM lake allele), while the other one did not. Only the chromosome 6 marker could be analyzed for allele frequency shifts in the natural populations, revealing almost complete fixation of the expected SNP allele within the ROM and CHE sample (permutation $P = 0.0001$). This frequency shift ($F_{ST} = 0.77$, lower and upper 95% confidence limits: 0.65, 0.92) was much stronger than expected from the populations' baseline divergence.
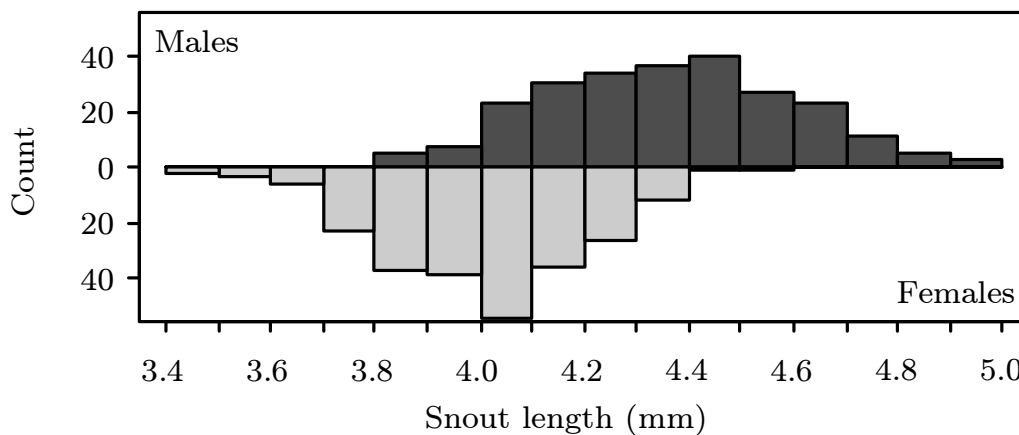

Figure 5.2: Distribution of size–adjusted snout length in male (dark gray, pointing upward) and female (light gray, pointing downward) stickleback from the F_2 panel.

Table 5.1: Characterization of the QTLs for skeletal divergence between lake and stream stickleback.

Trait	Marker	Chr.	Position (bp)	LOD	P	PVE	HSE	Dir.	Cand. gene
GRL	chrVI-12733534	6	13'735'445	4.52	0.027	6.5	0.19(0.73)	L*	
	chrIV-570692	4	570'692	4.60	0.019	4.3	0.08(0.33)	S	*BAPX1*(15)
SL	chrXIX-19432535	19	69'077(contig 1'730)	45.1	0.001	42.9	0.38(1.87)	M	
HL	chrXIX-19432535	19	69'077(contig 1'730)	5.70	0.002	7.7	0.33(0.58)	M	
	chrUn-11709633	5	464'792	5.57	0.004	6.9	0.45(0.72)	S*	
	chrXV-11777081	15	11'777'081	5.01	0.015	4.4	0.38(0.58)	S*	
	chrXIV-6849438	14	6'849'438	4.55	0.031	3.2	0.24(0.37)	S*	
VNo	chrXXI-2306628	21	4'955'041	7.82	0.001	9.2	0.43(0.85)	L*	*COL11A1*(6)
	chrXVII-1670571	17	1'670'571	7.64	0.001	6.4	0.44(0.78)	L*	*ASPN,OGN*(11)
PM	chrIV-12797213	4	12'797'213	155	0.001	76.0	-	L*	*EDA*(15)
P11H	chrXI-10140558	11	10'140'558	9.69	0.001	12.7	0.79(1.04)	S	*AXIN2*(36)
	chrXI-6239999	11	6'239'999	8.94	0.001	12.0	0.71(0.97)	S	*PHOSPHO1*(36)
	chrIV-4185607	4	4'185'607	4.54	0.041	5.5	0.47(0.6)	L	
P13H	chrIV-6474941	4	6'474'941	8.20	0.001	11.8	0.58(1.07)	L	
	chrXI-10140558	11	10'140'558	5.96	0.002	9.4	0.6(0.8)	S	*AXIN2*(36)
	chrXI-6239999	11	6'239'999	5.79	0.002	8.4	0.47(0.69)	S	*PHOSPHO1*(36)
	chrIX-9659641	9	12'543'749	4.99	0.012	7.7	0.53(0.71)	L	

The first column lists traits with the following abbreviations: Gill raker length = GRL; Snout lenght = SL; Head length = HL; Vertebral number = VNo; Plate morph = PM; Plate 11 height = P11H; Plate 13 height = P13H. The marker names specify genomic locations (chromosome and base pairs) according to the Broad S1 genome assembly, whereas the chromosome numbers (Chr.) and positions given in separate columns refer to the improved assembly (Chapter 1). The position of the marker on chromosome 19 (sex chromosome) is unclear (it proved linked relatively loosely to the other markers within the nonrecombining domain of this chromosome), hence we provide the position within its contig. Effect sizes are expressed as percent variance explained (PVE), and as homozygous substitution effect (HSE; in measurement unit, and standardized in parentheses). HSE is not given for plate morph, as this trait has an ordinal scale, and effect sizes for the two plate height QTLs on chromosome 11 are probably inflated because of linkage. The QTLs are ordered by PVE within each trait. The Direction column (Dir.) indicates whether ROM lake (L), CHE stream (S), or male (Y–linked; M) alleles cause higher trait values, and asterisks indicate allelic effects in the direction expected from the divergence between the natural populations (note that this could not be determined for the plate height QTL). The last column lists candidate genes (Cand. gene) found in the marker intervals around the QTL SNPs, with the numbers in parentheses indicating the total number of genes in each interval (including predicted genes). This table reports only QTLs reaching P < 0.05; additional suggestive loci are presented in Table S4 (Supplementary material).
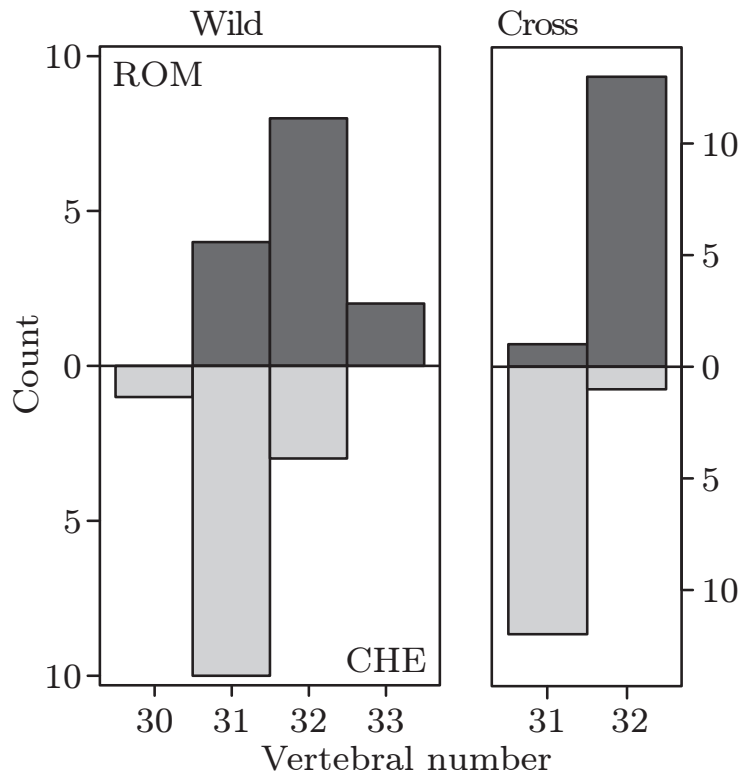
Figure 5.3: Vertebral number in ROM lake and CHE stream stickleback. The left panel shows vertebral count histograms based on a sample (N = 14) from the lake population (dark gray, pointing upward) and the stream population (light gray, pointing downward). The right panel displays the distribution of vertebral number in individuals from the F_2 cross concurrently homozygous for either the lake alleles (dark gray; N = 14) or the stream alleles (light gray; N = 13) at the two QTLs identified on chromosomes 17 and 21.

5.4.2 Head morphology

The analysis of snout length detected a single large–effect QTL only (43 PVE; Table 5.1, Fig. S11 (Supplementary material)). This QTL mapped to the domain on the sex chromosome (19) where the X and Y gametologs do not recombine (Chapter 4). Males of the F_2 population further displayed strikingly longer snouts than females (Fig. 5.2). Together, these observations indicated very strong sex–linked control of snout length. Indeed, mapping sex as a binary trait produced a single significant QTL (LOD = 380) coinciding exactly with the snout length QTL, whereas mapping snout length separately within each sex produced no QTL (details not presented).

Some sex–linked control was observed for overall head length as well, as the snout length QTL was also the strongest QTL affecting head length (Tables 5.1, S4, Fig. S11 (Supplementary material); recall that head length was
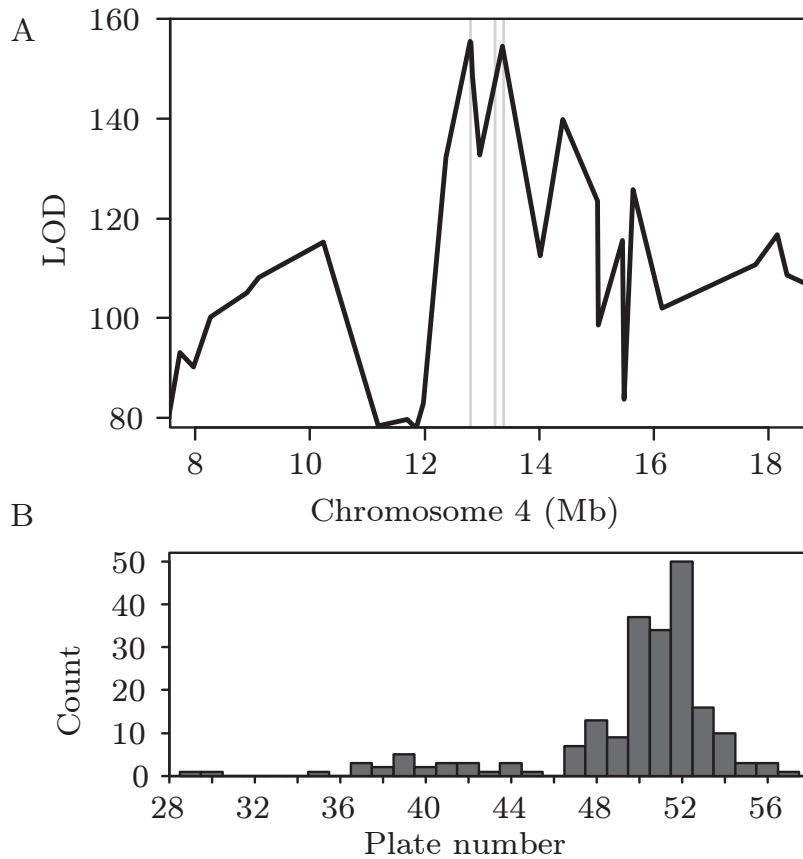
Figure 5.4: (A) LOD profile for the segment on chromosome 4 containing the detected QTL for lateral plate morph. The gray vertical lines indicate, from left to right, the position of *EDA* and the two candidate genes *PDLIM7* and *ANXA6*. The two LOD peaks (>150) are separated by two markers. (B) Distribution of the total number of lateral plates posterior to the pelvic girdle in F_2 individuals heterozygous at the *EDA* marker.

mapped with snout length as covariate, so this finding is not a methodological artifact). Three additional minor head length QTLs were detected on the autosomes, all of them (and also the suggestive locus) exhibiting an effect in the direction predicted from previous phenotypic work (a larger head associated with the CHE stream alleles). Allele frequencies in the natural populations could be inspected for the marker linked to the QTL on chromosome 15 only, which again revealed a shift in the predicted direction (P = 0.0001; F_{ST} = 0.51, CLs: 0.35, 0.68) and exceeding the baseline level.

5.4.3 Vertebral number

Most stickleback from the ROM lake sample displayed 32 vertebrae, as opposed to 31 vertebrae predominating in CHE stream fish (P = 0.0085; Fig. 5.3). In the cross, vertebral number mapped to two QTLs, with their effects being in the expected direction (ROM lake alleles associated with greater vertebral number; the same is true for the suggestive loci; Tables 5.1, S4, Fig. S11 (Supplementary material)). Despite moderate effect sizes of the two QTLs when estimated separately (9.2 and 6.4 PVE), their joint effect was striking: individuals homozygous for the ROM lake or CHE stream alleles at both QTL–linked SNPs simultaneously exhibited almost consistently 32 versus 31 vertebrae (Fig. 5.3). Comparing a subset of F_2 individuals with 31 and 32 vertebrae (N = 30 each) showed unambiguously that the variation was in the number of caudal as opposed to abdominal vertebrae (details not presented). Moreover, testing for a difference in mean body size between individuals with 31 versus 32 vertebrae (together accounting for 97% of all F_2 individuals) revealed clearly that vertebral number and body size were unrelated (P = 0.36, standardized mean difference in size between the two groups: 0.06; visualized in Fig. S12 (Supplementary material)). Allele frequency shifts could be examined for the marker linked to the QTL on chromosome 21 only, revealing divergence in the expected direction (P = 0.0001; F_{ST} = 0.41, CLs: 0.15, 0.71), but not stronger than expected from the baseline.

5.4.4 Lateral plating

Mapping lateral plate morph detected a locus of large effect (76 PVE) on chromosome 4, located precisely in the *EDA* region (LOD = 155.4 for the SNP 3 kb from the start position of *EDA*, and LOD = 155.2 for the SNP within *EDA*; Table 5.1, Fig. 5.4A). An almost equally strong marker–phenotype association (LOD = 154.6), however, occurred at 13.35 Mb. Inspecting the genotype frequencies at the two SNPs separating these high–LOD regions indicated that the drop in the strength of marker–phenotype association was not due to low genotyping quality (details not presented). At the *EDA* SNP, the natural populations were relatively close to fixation for the expected alternative alleles (P = 0.0001; F_{ST} = 0.60, CLs: 0.42–0.79), a shift clearly exceeding the baseline divergence level. No additional plate morph QTL was found (Fig. S11 (Supplementary material)).

Lateral plate number was variable among the F_2 individuals heterozygous at *EDA*, but never lower than 29 (Fig. 5.4B). Hence, *EDA* heterozygotes in our cross always classified as either partially or fully plated. We found no

significant QTL for plate number when only considering *EDA* heterozygotes (Fig. S11 (Supplementary material); a single suggestive QTL is described in Table S4 (Supplementary material)). The height of lateral plate 11 mapped to two QTLs (Tables 5.1, S4, Fig. S11 (Supplementary material)). The locus on chromosome 11 displayed a substantial effect size (12.7 PVE), with the ROM lake allele associated with shorter plates. However, this effect size was probably slightly inflated, as inspecting the LOD profile along chromosome 11 revealed the presence of an additional, nearly equally strong QTL 4 Mb (9.4 cM) away (LOD = 8.94; this second QTL is included in Table 5.1). Lacking information on plate height divergence between the natural populations, we did not investigate population–level shifts in allele frequencies.

The genetic architecture of lateral plate 13 height overlapped partly with that of plate 11 (Table 5.1, Fig. S11 (Supplementary material)), which is not surprising, given the relatively strong phenotypic correlation of the two plate height traits within the F_2 population (r = 0.84). Specifically, we detected exactly the same two QTLs located on chromosome 11. However, the strongest effect (11.8 PVE) was now seen in a QTL on chromosome 4. This locus was 2.3 Mb away from the QTL on the same chromosome driving plate 11 height (Fig. S11 (Supplementary material)), and thus perhaps represents a distinct locus, although this cannot be determined with confidence. In addition, plate 13 height was influenced by a QTL on chromosome 9.

5.5 Discussion

We have used an F_2 intercross to investigate the genetic architecture of divergence in skeletal traits between lake and stream stickleback. A first suite of traits considered included gill raker, snout, and head length, traits believed to mediate trophic specialization. In particular, gill raker length displays a highly predictable association with prey use in stickleback and other fish species. To our knowledge, variation in gill raker length has not previously been mapped in any species, but common garden experiments in stickleback indicated a heritable basis to the phenotypic divergence between benthic and pelagic populations (McPhail 1984; Day et al. 1994; Wund et al. 2008). In line with these quantitative genetic observations, our study discovered QTLs for gill raker length. Despite a mutation screen in zebrafish, implicating the *Ectodysplasin* (*EDA*) signaling pathway in gill raker formation (Harris et al. 2008), the detected QTLs showed no obvious relationship to that pathway. However, screening the marker interval around the QTL on chromosome 4 suggested *BAPX1* as a strong candidate gene, given that *BAPX1* is crucial to the formation of the first branchial arch in zebrafish (Miller et al. 2003).

We also found several autosomal QTLs explaining variation in head length. The effect sizes were consistently in the direction expected from the phenotypic divergence between the source populations (Berner et al. 2010a) and other benthic–pelagic stickleback systems (Caldecutt and Adams 1998; Albert et al. 2008). Nevertheless, in accordance with greater male than female overall head length found in many stickleback studies (Caldecutt and Adams 1998; Kitano et al. 2007; Albert et al. 2008; Aguirre and Akinpelu 2010; Berner et al. 2010a, 2011; Ravinet et al. 2013), the strongest head length QTL was sex–linked and also turned out to be the only (large–effect) locus driving snout length. Hence, while contrasting foraging habitats likely drive the evolution of stickleback head morphology among populations, the footprint of sex–specific selection is much stronger.

5.5.1 Vertebral number

The source populations of the cross showed clear divergence in the number of vertebrae, with a higher average count in lake than stream fish. This trend has also been found in other studies comparing lake and stream stickleback (Hagen and Gilbertson 1972; Reimchen et al. 1985) and thus likely represents an adaptive response to divergent selection on locomotion (Swain 1992). Although further functional evidence is needed, our finding that vertebral number is genetically unrelated to body size (as also found in a different stickleback system; Alho et al. 2011) indicates that population divergence in the number of vertebrae is unlikely to reflect a correlated response to selection on size (note that the ROM lake and CHE stream populations differ in size; Chapter 1).

In our cross, vertebral number mapped to two QTLs. These loci explained a moderate proportion of the total phenotypic variance when considered in isolation, but in combination had a high explanatory power: their joint homozygous substitution accounted for an approximate shift of one vertebra, roughly the magnitude of divergence between the natural populations. To our knowledge, vertebral number has previously been mapped only in two fish species (medaka and trout) and in pigs. The former studies detected QTLs but were performed with a marker resolution too low to allow candidate gene identification (Nichols et al. 2004; Kimura et al. 2012). QTLs also emerged in pigs, where fine mapping produced strong candidate genes (*NR6A1*, *VRTN*, *PROX2*, *FOS*; Mikawa et al. 2007, 2011; Ren et al. 2012). The stickleback homologues of these genes, however, are not located on the chromosomes 17 and 21 where we found QTLs for vertebral number. Instead, screening the target marker interval on chromosome 17 identified *OGN* (Madisen et al. 1990) and *ASPN* as candidate genes. Both genes are involved in bone

formation. In particular, *ASPN* regulates osteoblast collagen mineralization in vitro (Kalamajski et al. 2009) and is implicated in human degenerative diseases of skeletal joint regions, including intervertebral disks (Kizawa et al. 2005; Song et al. 2008). Also, a strong candidate gene (*COL11A1*) emerged in the focal chromosome 21 segment. Mutations in *COL11A1* cause skeletal disorders, including the malformation of vertebrae (Li et al. 1995; Tompson et al. 2010; Koyama et al. 2012).

5.5.2 Lateral plating

At first glance, our mapping of lateral plate morph produced an expected result: the LOD maximum mapped to the *EDA* gene, and the corresponding SNP explained 76% of the total variance, a value very similar to that reported in Colosimo et al. (2004) for the plate morph QTL on chromosome 4 (77.6 PVE). Interestingly, however, a nearly equally strong LOD score emerged at 13.35 Mb (roughly 0.5 Mb from *EDA*), a region identified as high differentiation outlier in a divergence mapping study using fully plated marine and low–plated freshwater stickleback from Alaska (Hohenlohe et al. 2010). Our marker interval in that region contains two strong candidate genes, *PDLIM7* and *ANXA6* (see also Hohenlohe et al. 2010). *PDLIM7* has been shown to initiate bone formation de novo, and also to interact with bone morphogenetic protein (*BMP*) signaling (Boden et al. 1998; Liu et al. 2002). Similarly, *ANXA6* plays a critical role during the calcification of skeletal tissue (Kirsch et al. 2000; Wang and Kirsch 2002; Thouverey et al. 2009). It is thus possible that the strong effect seen at the *EDA* marker in our cross captures variation in lateral plating driven by polymorphism in one or more additional genes in its close neighborhood. Unfortunately, the paucity of crossovers between the SNPs at these QTLs in our cross precludes disentangling their relative effect sizes.

Outside chromosome 4, we found no QTL substantially influencing plate morph or number. This is surprising, given that such QTLs were discovered previously on chromosomes 7, 10, and 21 (Colosimo et al. 2004; but see Baird et al. 2008). This difference in genetic architecture likely explains why *EDA* heterozygotes in our cross were never low–plated, although low–plated heterozygotes occurred in the mapping panel studied by Colosimo et al. (2004). As a complementary route to the adaptive reduction in lateral plating, stickleback might evolve shallower plates (Leinonen et al. 2012). Mapping the height of the plates 11 and 13 posterior to the pelvic girdle, we found QTLs on chromosomes 4, 9, and 11. These results differ from the previous report of plate height QTLs on the chromosomes 4 (at around 2 Mb, hence in a different region than in our cross), 7, and 20 (Colosimo et

al. 2004). However, that study measured plates immediately adjacent to the pelvic girdle. Combined with our observation that the relative influence of the QTLs on chromosomes 4 and 11 on the height of the plates 11 and 13 was inverted, and that the QTL on chromosome 9 (and the additional suggestive QTLs) influenced one of the plates only, we conclude that plate height has a fairly complex genetic architecture, with several loci acting relatively locally.

Examining the plate height QTL regions produced strong candidate genes. Notably, the marker interval around the highest LOD peak observed (chromosome 11) included *AXIN2*. Loss of function mutations in *AXIN2* lead to ectodermal dysplasia in humans (Lammi et al. 2004; Mostowska et al. 2006; Callahan et al. 2009; Bergendal et al. 2011) – the same disorder also observed for disruptions of the *EDA* pathway (Kere et al. 1996; Bayes et al. 1998; Monreal et al. 1999; Headon et al. 2001; Chassaing et al. 2006). The SNP interval around 6.2 Mb on the same chromosome, in turn, proved close to *PHOSPHO1*, a gene involved in skeletal tissue mineralization (Houston et al. 1999, 2004; Roberts et al. 2007). Candidate genes involved in bone formation also emerged at the suggestive plate height QTLs on chromosomes 5 (*PLEKHM1*; Van Wesenbeeck et al. 2007) and 17 (*ALPL*; Weiss et al. 1988; Henthorn et al. 1992; Table S4 (Supplementary material)).

5.5.3   QTL effect size

Mapping lateral plate morph and snout length identified QTLs of very large effect (acknowledging that the effect size of the plate morph QTL is possibly confounded by the presence of multiple tightly linked loci, see above). The majority of our detected QTLs, however, had a relatively minor effect, a typical result in QTL mapping studies (Mackay et al. 2009). Moreover, for some traits (e.g., gill raker length, head length), inspecting the genome–wide LOD profile (Fig. S11 (Supplementary material)) suggested the presence of additional loci with even smaller effect that were missed in our experiment due to insufficient power – a well–known issue in QTL mapping (Lande and Thompson 1990; Beavis 1994; Xu 2003; Rockman 2011). To explore this issue further, we compiled the effect sizes of all the QTLs (including marginally significant ones) detected in our study across all traits. This revealed that despite relatively large F_2 sample size, we lacked the power to identify QTLs with an effect size below 3–4 PVE (Fig. 5.5). (We are aware of the additional complication that the effect sizes of our detected minor QTLs are likely to be biased upward; Beavis 1994; Göring et al. 2001; Xu 2003.) We thus argue that although QTL mapping provides interesting insights into the genetic architecture of phenotypic divergence among stickleback populations, our understanding of adaptive variation in many traits will continue to benefit

from quantitative genetic investigation.

5.5.4   Allele frequency shifts in the source populations

The availability of marker data from the natural populations underlying our cross made it possible to assess if associations between trait values and QTL–linked SNP alleles were replicated at the population level. Such an association is expected under two conditions. First, SNP alleles must tag QTL alleles reliably at the population level (as opposed to merely in the grandparents used for the cross). Second, allele frequency shifts at the focal QTL need to make some contribution to the trait divergence between the natural populations. Moreover, a shift at an SNP tightly linked to a QTL is expected to exceed the level of baseline population divergence attributable to drift if the QTL has been influenced by divergent selection between the populations.

All these conditions are indeed met by the *EDA* locus: phylogenetic analysis revealed that alleles at SNPs within *EDA* are tightly linked to their corresponding causative variants (which remain unknown) in the two study populations, and that adaptive population divergence in plate morph frequency is paralleled by frequency shifts at these SNPs (Berner et al. 2010a; see also Colosimo et al. 2005). We thus predicted very strong population–level shifts at our *EDA* maker, which were indeed observed. Similar analyses could be performed only in a small subset of the other QTL–linked SNPs, because some relevant markers were missing at the population level due to a different sequencing protocol, and because plate height could not be quantified in the (low–plated) stream population. Nevertheless, all three additional SNPs that were examined (associated with gill raker length, head length, and vertebral number) showed clear enrichment for the expected allele within each source population. Moreover, in three of the four total cases (including *EDA*), the observed allele frequency shifts were stronger than baseline divergence. We thus conclude that the phenotypic divergence between our study populations is probably attributable at least partly to allele frequency shifts at the QTL discovered in the cross, and that some of these shifts have been driven by divergent selection.

5.5.5   Conclusions

We subjected skeletal traits in European lake and stream stickleback to QTL mapping. Although this revealed a few large–effect QTLs, the majority of the loci detected across all traits exhibited a modest to small effect size. At least for some traits, QTL mapping seems to permit a relatively incomplete

characterization of genetic architecture. Nevertheless, the close neighborhood around the QTLs that were discovered often contained genes involved in bone formation, which thus emerge as strong candidate drivers of skeletal evolution. Manipulative functional experiments are now needed to confirm the causative role of these genes, and comparisons across numerous phenotypically well–characterized stickleback populations should investigate how consistently these genes are involved in diversification. Excitingly, a region containing two novel candidate genes for lateral plate morph evolution in our study coincided with an outlier region identified in a divergence scan using geographically independent stickleback populations divergent in lateral plating (Hohenlohe et al. 2010). This illustrates how understanding adaptation can benefit from the combination of phenotype–based and purely molecular genome scans. Finally, we attempted to move beyond mere QTL identification within a cross by screening for QTL–linked SNP allele frequency shifts in the natural source populations. These analyses indicated that at least some of our identified QTLs may indeed contribute to population divergence, and suggested that allele frequency shifts have been driven by divergent selection. A deeper understanding of the nature of this selection, however, will require extensive ecological investigation.

5.6 Acknowledgments

5.7 Author contributions

DB designed the study, produced the cross, measured phenotypes, generated the genotype data, performed all mapping, and wrote the paper, with input from all co–authors. DM contributed to fish husbandry. DM and MR did the molecular wet lab work and measured phenotypes. MR contributed to study design and did the candidate gene search. HB generated all X–ray scans. WS contributed to study design and provided resources and infrastructure.

Chapter 6

The genomics of ecological vicariance in threespine stickleback fish

Authors: Marius Roesti, Benjamin Kueng, **DARIO MOSER** & Daniel Berner

Preface: My contribution to this chapter was rather small. However, it somehow closed the circle, which I opened at the very beginning in chapter 1. The fish used for this study were caught in the very first sampling trip, which I organized for my Master thesis. Additionally, Beni and I extracted DNA and prepared the RAD libraries together.

6.1 Abstract

Populations occurring in similar habitats and displaying similar phenotypes are increasingly used to explore parallel evolution at the molecular level. This generally ignores the possibility that parallel evolution can be mimicked by the fragmentation of an ancestral population followed by genetic exchange with ecologically different populations. Here we demonstrate such an ecological vicariance scenario in multiple stream populations of threespine stickleback fish divergent from a single adjacent lake population. On the basis of demographic and population genomic analyses, we infer the initial spread of a stream–adapted ancestor followed by the emergence of a lake–adapted population, that selective sweeps have occurred mainly in the lake population, that adaptive lake–stream divergence is maintained in the face of gene flow from the lake into the streams, and that this divergence involves major inversion polymorphisms also important to marine–freshwater stickleback divergence. Overall, our study highlights the need for a robust understanding of the demographic and selective history in evolutionary investigations.

6.2 Introduction

Parallel (or convergent (Arendt and Reznick 2008)) phenotypic evolution – that is, the repeated independent emergence of a specific phenotype associated with a specific habitat, can provide important insights into the determinism of natural selection. The reason is that similar phenotypes are unlikely to evolve repeatedly in association with an environment by chance. An aspect of parallel evolution now made amenable to investigation through advances in molecular techniques is to what extent the repeated evolution of similar phenotypes involves the same genetic loci (Arendt and Reznick 2008; Conte et al. 2012; Martin and Orgogozo 2013). A common analytical framework adopted to address this question is to compare multiple population pairs, each believed to represent an independent replicate of adaptive population divergence between two ecologically different habitats. The evolutionary independence of these population pairs is generally established by demonstrating that the genetic relatedness between the populations within pairs, as inferred from markers little influenced by selection (for simplicity hereafter called 'neutral markers'), exceeds that seen among the pairs. If so, the population pairs are assumed to represent replicates of independent ecological divergence and are screened for genomic loci exhibiting signatures of divergent selection between the habitats (for example, high divergence relative to some genome–wide baseline). Finally, the resulting lists of such

loci are compared to draw conclusions about the extent of parallel evolution at the genomic level (for example, Tennessen and Akey 2011; Roesti et al. 2012a; Gagnaire et al. 2013; Foll et al. 2014; Soria–Carrasco et al. 2014 and Westram et al. 2014; for closely related inferential approaches see Hohenlohe et al. 2012, Jones et al. 2012 and Roesti et al. 2014).

A possibility rarely considered in such investigations is that the demographic and selective history of the study populations may complicate or preclude inferences about parallel evolution. Such a situation occurs when multiple patches of two ecologically different habitats are initially colonized by a single ancestor already adapted to one habitat type. Subsequently, local adaptation in the alternative habitat drives ecologically based reproductive isolation between the habitats, although some genetic exchange across habitat boundaries will continue in the absence of absolute geographic barriers. The outcome of such 'ecological vicariance' (Hardy and Linder 2005) with genetic exchange will mimic parallel evolution (Bierne et al. 2013). The reason is that gene flow between ecologically different populations in contact will cause genetic differentiation at neutral markers to be lower within than among population pairs – the pattern also expected under parallel divergence. Moreover, under both scenarios, loci under divergent selection will be relatively protected from exchange between the populations in contact and can therefore maintain stronger differentiation between the habitats than neutral loci (Barton and Bengtsson 1986; Bierne 2010; Feder and Nosil 2010; Roesti et al. 2014). In situations involving ecological vicariance with gene flow, comparing multiple population pairs can permit the reliable identification of selected loci and thus confirm divergent selection, but inference about the genetic basis of independent parallel evolution will be inappropriate because divergence did not occur repeatedly.

Distinguishing parallel divergence from ecological vicariance scenarios is thus crucial when attempting to explore how deterministically selection acts at the genomic level during evolution. While this distinction is not possible based on phylogenetic relationships at neutral markers (Endler 1977; Coyne and Orr 2004), it can be achieved by combining thorough analyses of molecular signatures around the loci under divergent selection with robust reconstructions of the populations' demographic history (Barrett and Schluter 2008; Bierne et al. 2013). We here present such an investigation based on populations of threespine stickleback fish adapted to lake and stream habitats within the Lake Constance basin in Central Europe.

This stickleback system comprises a large and genetically well–mixed population residing in Lake Constance – with 571 km^2 the third largest lake in Central Europe – and multiple adjoining stream–resident populations inhabiting the lake's tributaries (Berner et al. 2010a; Lucek 2010; Chapter 1).

116

The lake and stream habitats are ecologically different, as mirrored by the lifestyles of the stickleback populations: lake fish forage pelagically (that is, in the open water) on zooplankton, whereas the stream populations feed on benthic (substrate–dwelling) macroinvertebrates. This different resource use is paralleled by divergence in foraging morphology and life history (Berner et al. 2010a; Chapter 1 & 2). Lake and stream populations in the Lake Constance basin also differ predictably in their extent of lateral plating (Berner et al. 2010a; Chapter 1). Just like marine stickleback (Bell and Foster 1994), pelagic Lake Constance fish exhibit a series of bony plates covering their entire flank, providing protection from vertebrate predators in the open water (Reimchen 1994b). By contrast, multiple stream populations show a reduction in the extent of lateral plating, the phenotype predominant in freshwater stickleback on a global scale.

Although the Lake Constance stickleback system has certainly formed post–glacially (that is, within the last 12'000 years (Keller and Krayss 2000), its origin is not resolved. One view is that a human introduction during the nineteenth century initially led to the establishment of a large lake population, and that subsequently multiple stream populations diverged independently from the lake population (Berner et al. 2010a; Chapter 1). This scenario thus implies parallel divergence. An alternative is a more ancient natural colonization of the Lake Constance region by an already stream–adapted ancestral population from the Danube drainage (Chapter 1) (now draining into the Black Sea, hence disconnected from the Lake Constance basin), providing the potential for an ecological vicariance scenario.

The first goal of our study is to combine multiple lines of molecular evidence, based on dense genome–wide single–nucleotide polymorphisms (SNPs) obtained through restriction site–associated (RAD) sequencing (Baird et al. 2008), to resolve the demographic and selective history of lake–stream divergence in the Lake Constance stickleback system. We demonstrate that adaptive divergence has occurred in the face of gene flow in an unexpected historical context, pointing to limitations in the standard interpretation of repeated phenotypic evolution. Based on these insights, we then dissect the molecular consequences of divergent selection in target regions, including the prime locus underlying divergence in lateral plating, and finally examine the role of chromosomal inversions in adaptive divergence.

Next, we compared population–specific allele frequency spectra and found that across almost all minor allele frequency (MAF) classes, the lake exhibited the lowest and GRA the highest number of polymorphisms, with BOH and NID being intermediate (Fig. S15 (Supplementary material)). The lake also displayed the highest proportion of monomorphic SNPs, and the lowest proportion of tri–allelic SNPs (Table S5 (Supplementary material)). These

findings clearly demonstrate that genetic diversity is lowest in the lake and increases from BOH to NID to GRA. Moreover, because the divergence among our study populations is recent (Fig. 6.1b, Fig. S14 (Supplementary material)) and the sharing of polymorphisms is extensive (Table S5 (Supplementary material)), most of the genetic variation in the present populations must have been standing in their common ancestor.

Calculating genome–wide baseline differentiation (that is, median F_{ST}) for each of the three lake–stream pairings revealed an increase in population differentiation from 0.005 in the lake–BOH comparison to 0.013 and 0.061 in the lake–NID and lake–GRA comparisons, whereas no stream–stream population comparison yielded baseline F_{ST} higher than 0.056 (BOH–GRA; NID–GRA: 0.047; BOH–NID: 0.012). In a rooted phylogeny, the lake population emerged as a distal branch nested within the more basal stream fish (Fig. 6.1c, Fig. S16 (Supplementary material)). An unrooted phylogeny further confirmed the close relatedness of the lake and BOH populations and the lower genetic diversity in the lake than in the streams (Fig. S17 (Supplementary material)).

6.3 Results and discussion

6.3.1 Demography and population genomic analyses

Our investigation focuses on four stickleback populations, including the panmictic (Fig. S13 (Supplementary material)) Lake Constance population (hereafter simply 'lake') and three stream populations residing in tributaries (referred to as Bohlingen (BOH), Nideraach (NID) and Grasbeuren (GRA); see also Berner et al. 2010a and Chapter 1) (Fig. 6.1a), each represented by 22–25 individuals. To reconstruct the demographic history of these populations, we parameterized a divergence with gene flow model by using coalescent simulations based on the populations' joint allele frequency spectra (Excoffier et al. 2013) derived from 14.8 million nucleotide positions on 166'711 RAD loci across the 460 Mb stickleback genome. This analysis indicated that the study populations – exhibiting relatively small estimated effective population sizes (extremely small in the lake, largest in GRA) – split from an at least 20 times larger ancestral population a few thousand generations (and years, since the typical life span of stickleback in this system is $1 - 2$ years (Chapter 1 & 2)) ago (Fig. 6.1b). Qualitatively similar estimates were obtained with an alternative model including only two stream populations (Fig. S14 (Supplementary material)). Also, long–term rates of lake–stream gene flow differed approximately tenfold, being highest between the lake and

the BOH population, and lowest between the lake and the GRA population.
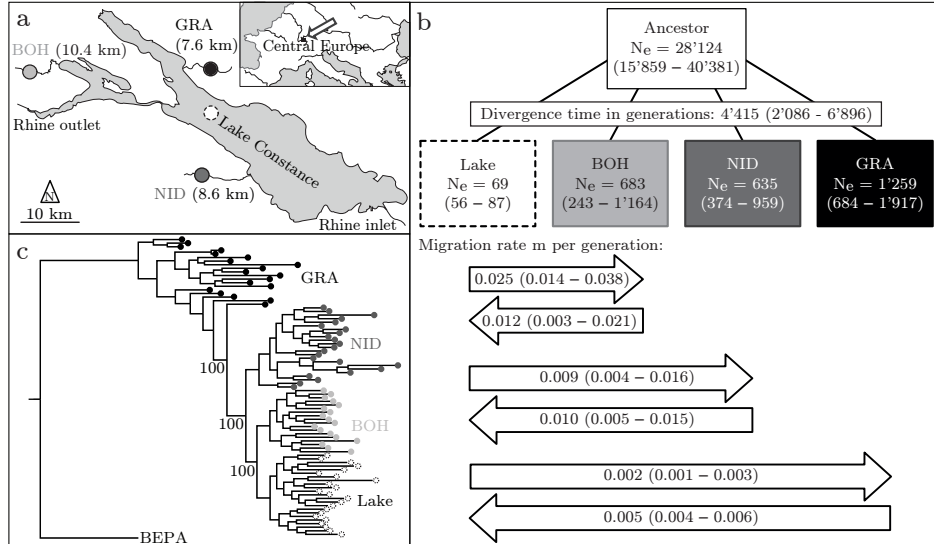
Figure 6.1: Geographic context, demography and phylogeny of the study populations. (a) Location of the study populations from the Lake Constance basin, including the panmictic lake population and the three tributary stream populations (BOH, NID and GRA; the same color coding and line types identifying the populations are used throughout the paper). Numbers in parentheses indicate the water distance between each stream site and the lake. (b) Estimated age of the split of the study populations from their common ancestor (divergence time), effective population sizes (numbers within boxes), and bi–directional migration rates between the lake and each stream population (numbers in horizontal arrows, representing the long–term proportion of immigration into the target population from the source population per generation forward in time). The values are based on an estimated SNP mutation rate of 6.8×10^{-1}. Numbers in parentheses are 95% bootstrap confidence intervals. (c) Phylogenetic relationship among the study populations visualized by a maximum likelihood tree rooted using a North American stickleback (BEPA, Bear Paw Lake, Alaska) as outgroup. Bootstrap support in per cent is given for the key nodes.

Finally, we quantified linkage disequilibrium (LD) between all pairwise combinations of SNPs within all chromosomes in each population and found that strong allelic associations between SNPs occurred only over a scale of 1 kb or less; beyond this distance, LD was much weaker (Fig. 6.2a). The peak in LD at the smallest physical scale was driven by those SNPs exhibiting a high MAF; low–MAF SNPs exhibited more homogeneous and generally weaker LD at all distances (Fig. 6.2a, insert). Another striking result was that the extent of LD across the genome was substantially greater in the lake population (and the two stream populations little divergent from the lake, that is, BOH and NID) than in GRA. A similar result was obtained by exploring average LD among marker pairs within non–overlapping chromosome
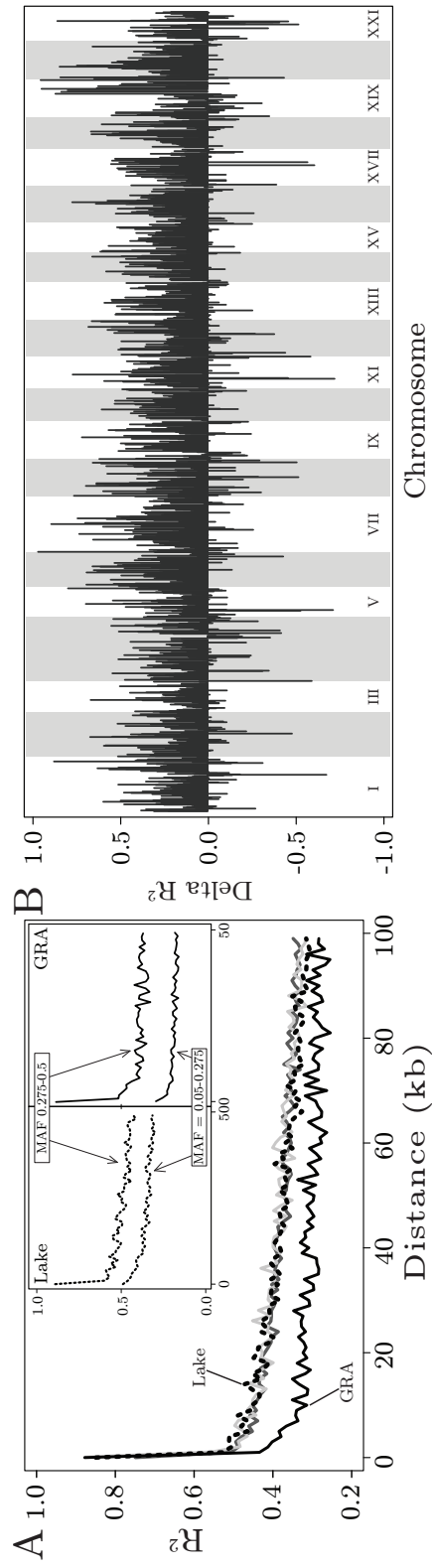
Figure 6.2: Linkage disequilibrium across the stickleback genome. (a) Magnitude of LD (squared correlation of allele frequencies) between SNP pairs in relation to their distance on a chromosome, shown for the lake (dotted black line), BOH (solid light grey line), NID (solid dark grey line) and GRA (solid black line) population. The main panel uses a minimal MAF threshold of 0.05. The insert panels display LD separately for low–MAF (0.05–0.275) and high–MAF (0.275–0.5) SNPs in the lake and GRA population. (b) Difference in LD between the lake and GRA population along the genome. The data points represent the average LD in the lake minus the average LD in GRA across non–overlapping 200 kb chromosome windows, yielding a measure called Delta R^2.

windows: across most of the genome, LD was much stronger in the lake than in GRA (Fig. 6.2b), a result insensitive to the MAF threshold (Fig. S18 (Supplementary material)). Finally, the similarity in the local magnitude of linkage across the genome between the lake and each stream population, expressed as the correlation of LD between the chromosome windows, declined from the lake–BOH (r = 0.17) to the lake–NID (r = 0.15) and the lake–GRA pairing (r = 0.12) (all P < 0.001).

In combination, the above analyses resolve the demographic and selective history of stickleback in the Lake Constance basin. First, the demography is inconsistent with the view that the populations originate from a recent introduction of (presumably few) founder individuals, and instead supports an earlier postglacial and extensive natural colonization, presumably via the Danube drainage (Chapter 1). Second, the demographic estimates of effective population size and all metrics of genetic variation make clear that the stream populations – and not the lake – represent the main reservoirs of genetic variation. This result is unexpected because Lake Constance is very large, and even conservative estimates of the present census size of its stickleback population range in the millions (personal communications from fishermen and fisheries authorities), which is certainly much greater than the size of any single stream population. (The streams investigated here are small, with an approximate average depth and width of 0.5 and 4 meters) Third, we observe the strongest genome–wide differentiation (F_{ST}) between a stream and the adjoining lake population, and not in any of the comparisons between the stream populations separated by dozens of kilometers of lake habitat. Fourth, the lake population proves to be phylogenetically derived from stream fish. All these observations can be brought in line by the biogeographically plausible perspective that the Lake Constance basin was initially colonized by ancestral stream–adapted stickleback. This colonization gave rise to multiple stream–resident populations isolated from each other by the adjoining, ecologically different lake habitat – that is, an ecological vicariance scenario. Subsequently, the lake fish started to adapt to their
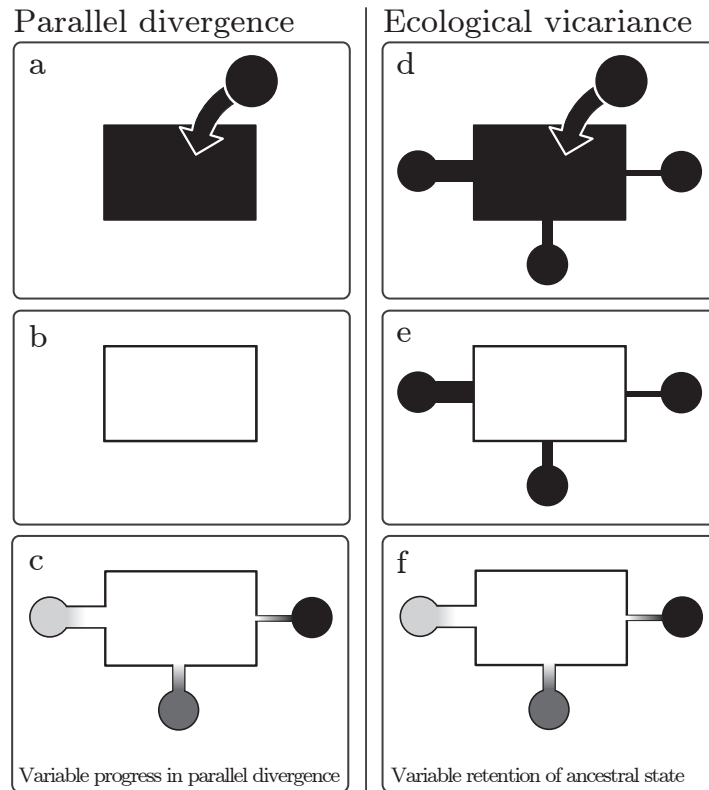
Figure 6.3: Alternative demographic scenarios explaining repeated population divergence. The alternatives are exemplified by multiple stream populations divergent from the adjacent lake population in the Lake Constance basin. In the 'parallel divergence' scenario (panels a–c), a (stream–adapted) ancestor enters the lake (a) and becomes locally adapted (b). Subsequently, multiple stream populations derive independently via parallel evolution from the lake population (c), the latter thus representing their most recent common ancestor. The magnitude of lake–stream divergence in (c) (visualized as different grey shades) is determined by a combination of the time since colonization of each stream, the strength of local selection within each stream, and the extent of homogenizing gene flow from the lake into each stream. In this scenario, genetic variation available to local adaptation in the streams has been filtered during the adaptation of the lake population. Predictions here include greater genetic diversity in the lake than the stream populations, that F_{ST} is highest in stream–stream as opposed to lake–stream comparisons (due to founder events and relatively strong drift in these small populations), and that LD is highest in the streams (due to selective sweeps during adaptive divergence from the lake). In contrast, the 'ecological vicariance' scenario (panels d–f) involves the colonization of the entire study region by an already stream–adapted ancestor (d), followed by local adaptation in the lake (e). The magnitude of lake–stream divergence is then primarily determined by the extent to which the stream populations can maintain their genetic integrity in the face of gene flow from the large lake population (f). Predictions here include greater genetic diversity in the streams than in the lake, highest F_{ST} in lake–stream as opposed to stream–stream comparisons, and strongest LD in the lake due to extensive selection. All these latter predictions are confirmed by our analyses.
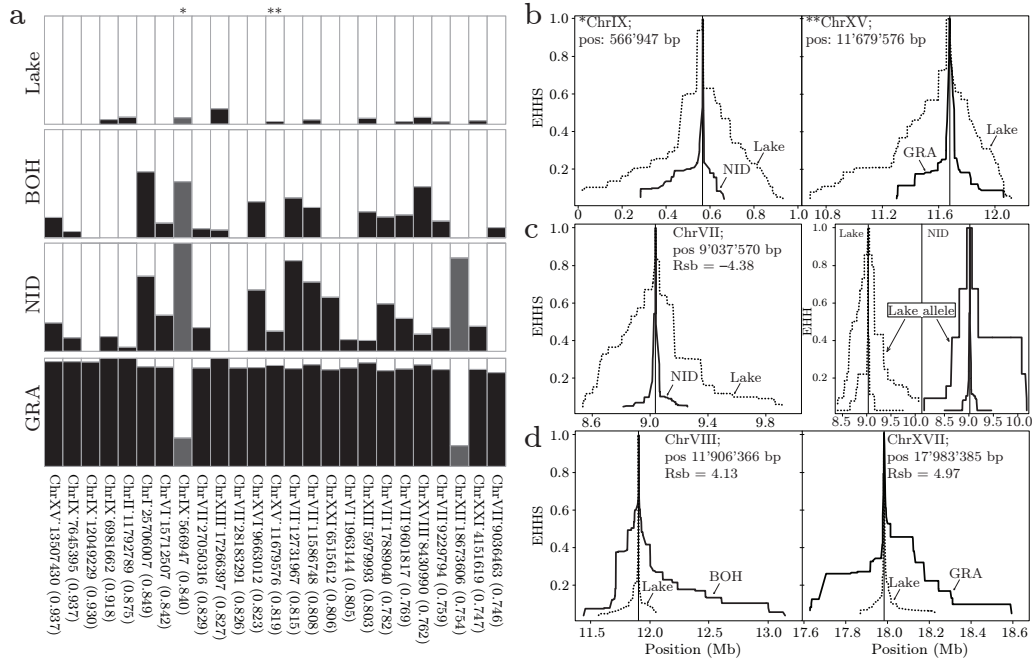
Figure 6.4: Localized signatures of selection. (a) Allele frequencies within each population at the 25 F_{ST} extremes (columns). The proportion of the SNP alleles predominant in the lake are shown in white, while the proportion of the alleles predominant in the streams are either black (when the extreme F_{ST} value emerged from the lake–GRA genome scan, N = 23) or dark grey (extreme F_{ST} value observed in the lake–NID scan, N = 2). On the bottom, the genomic position and the highest F_{ST} value observed across all lake–stream comparisons are given for each F_{ST} extreme. (b) Lake and stream haplotype decay (EHHS) around representative F_{ST} extremes (flagged by asterisks in a) identified in the lake–NID F_{ST} scan (left panel) and in the lake–GRA scan (right panel). (c) Haplotype decay in the lake and the NID stream population around a representative negative Rsb extreme identified in the lake–NID Rsb scan (left panel). For the same Rsb extreme, the right panel displays allele–specific haplotype decay (EHH) around each allele within each population separately (both alleles occur in both populations; the allele predominant in the lake is labelled 'Lake allele'). (d) Lake and stream haplotype decay around two representative positive Rsb extremes identified in the lake–BOH Rsb scan (left panel) and in the lake–GRA scan (right panel). Note that the scale of the x axis varies in b–d.

123
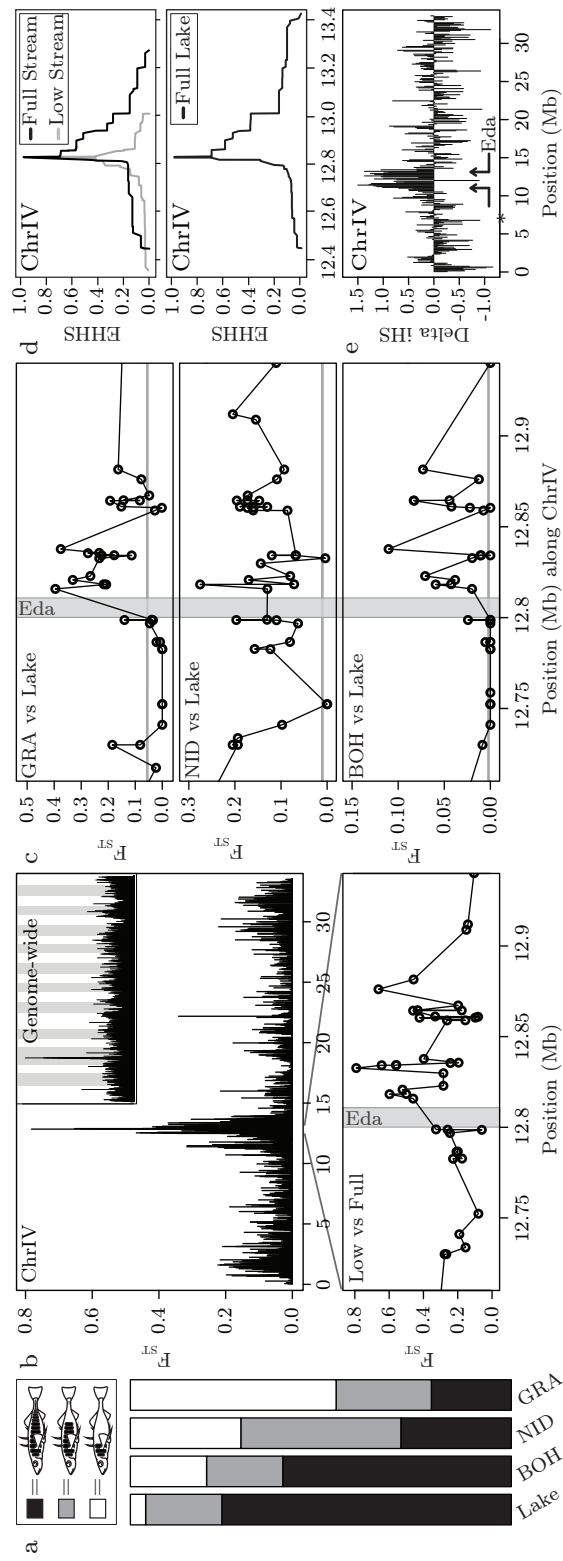
Figure 6.5: Lake–stream divergence in lateral plating and the associated molecular signatures. (a) Frequency of the three plate phenotypes (completely, partially and low–plated) in the four study populations. (b) Genetic differentiation (F_{ST}) between completely and low–plated stream stickleback reveals a peak on chromosome IV, with the highest F_{ST} value immediately downstream of the *Eda* coding region (grey vertical bar). (c) Divergence (F_{ST}) profiles around the plate locus for all lake–stream comparisons, with the horizontal grey lines indicating baseline differentiation (note that the scale of the y axes varies). (d) Haplotype decay (EHHS) in completely and low–plated stream stickleback around the *Eda*–associated SNP exhibiting the strongest phenotype–genotype association in the bulk segregant analysis (see b, bottom) (upper panel). The lower panel shows haplotype decay around the completely plated allele at the same SNP in the lake population. (e) Profile of the difference in the rate of haplotype decay between completely and low–plated stream stickleback along chromosome IV. High positive values of this 'Delta iHS' metric, indicating more extensive haplotype tracts in completely plated individuals, occur across a broad region centred at the *Eda* locus, and in a second genomic region nearby (indicated by an asterisk; note the corresponding F_{ST} peak in the upper panel of b).

novel habitat and thereby experienced strong genome–wide selection. This selection should not only have reduced genetic variation in the lake relative to the streams, but also have driven relatively elevated LD within the lake, predictions clearly borne out by our analyses.

A key implication of this ecological vicariance scenario (visualized in Fig. 6.3d–f) is that the stream populations cannot be considered independent products of parallel divergence from an ancestral lake population. The stream fish are closer to the ancestral state while the lake population is the most derived. (Note that the phylogeny in Fig. 6.1c also rules out the possibility that the lake population results from a secondary colonization; in this case, the lake fish would branch basally from the stream populations.) Variation in the magnitude of genetic and phenotypic lake–stream divergence thus reflects different levels of homogenizing gene flow (that is, introgressive hybridization) from the large lake to the stream populations rather than variable progress in repeated parallel divergence (Fig. 6.3a–c). Supporting this view, typical lake phenotypes can sometimes be found at our BOH stream sample site during the breeding season (personal communication from fishermen). This highlights the potential for extensive genetic exchange in the one lake–stream pairing also exhibiting the highest migration rate estimates and the lowest genetic differentiation.

The strong genome–wide footprint of selection in the lake population, observed as relatively reduced genetic diversity and elevated LD, also raises an important methodological caveat. Marker–based approaches to demographic inference generally assume that allele frequencies reflect selectively neutral processes (Becquet and Przeworski 2009; Excoffier et al. 2013; Cornuet et

126
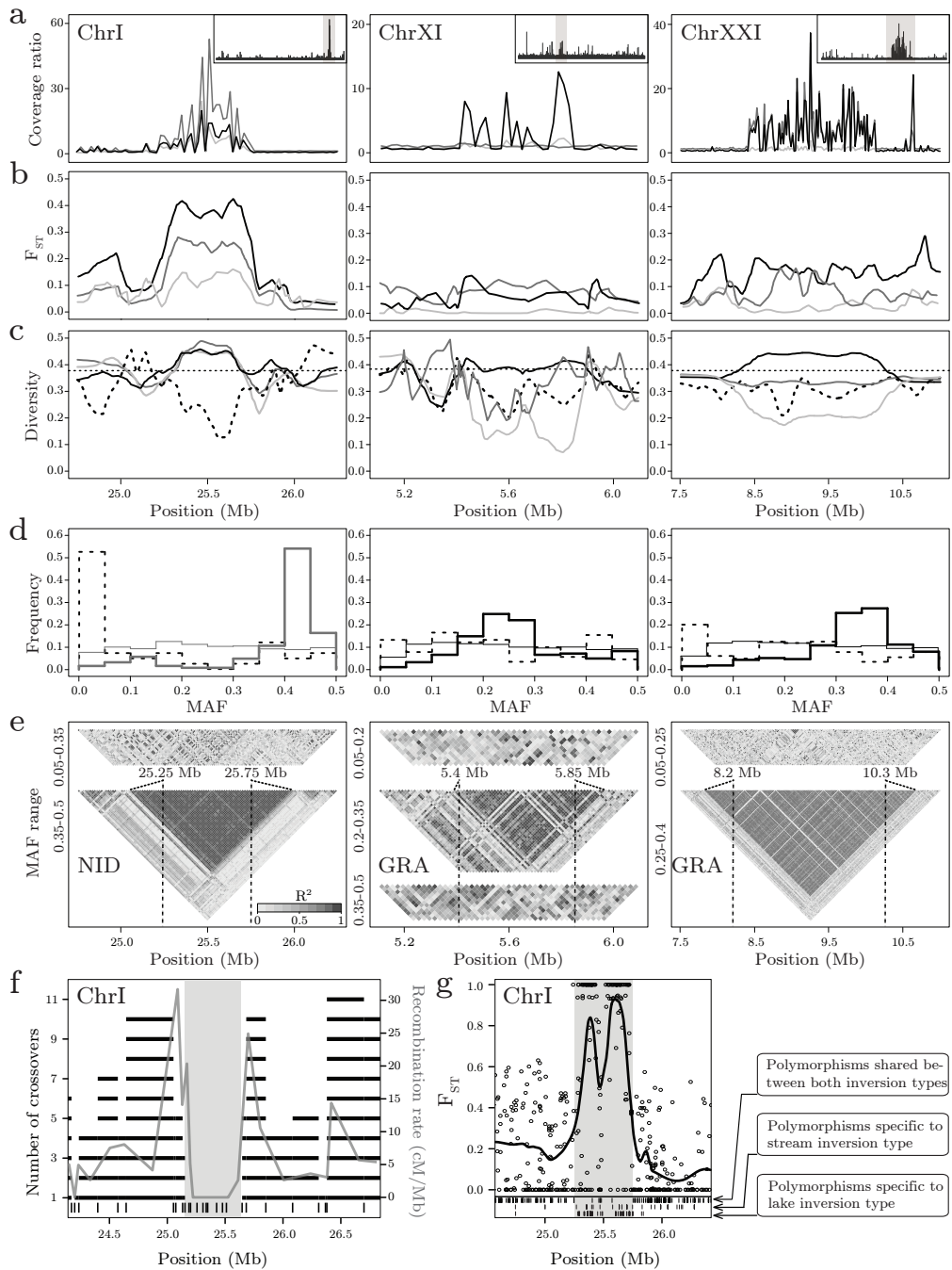
Figure 6.6: Detecting and characterizing large chromosomal inversions in lake and stream stickleback. (a) RAD sequence coverage of the stream populations relative to the lake population (coverage ratio), shown separately for each lake–stream population pair (lake–BOH light grey, lake–NID dark grey and lake–GRA black) along focal segments of the chromosomes I, XI and XXI harboring an inversion. The inserts show the coverage ratio along the entire chromosomes (focal segments shaded grey), based on the coverage data pooled across the three stream populations. (b) Genetic differentiation between the lake and each stream population, and (c) allelic diversity at SNPs within each of the four populations, around the three inversions. (d) MAF distribution for SNPs located within each inversion, shown for the stream population exhibiting the strongest coverage ratio distortion relative to the lake (see a) (thick solid line). For comparison, the genome–wide MAF distribution for the same stream population (thin solid line), and the MAF distribution for all inversion SNPs in the lake population (dotted line) are also plotted. (e) Linkage disequilibrium heat maps based on SNPs from distinct MAF classes shown for the same stream populations as in d. (f) Recombination between the ChrI inversion types (the inverted segment is shaded grey) in a laboratory cross. Black horizontal bars indicate the number of crossovers observed between two neighboring markers (vertical bars on the bottom), and the grey profile shows the corresponding recombination rate. (g) Genetic differentiation (raw values and smoothed profile) between individual pools of ChrI inversion homozygotes. The bottom part indicates the position of SNPs shared between the two inversion types, and of those unique to each.

al. 2014). In our study, the reduction of genetic variation by widespread selection in the lake clearly dissociates marker–based estimates of effective population size from biologically plausible census population sizes; the lake population, and to a lesser extent also the two stream populations strongly influenced by gene flow from the lake (BOH and NID), certainly have their estimated effective population sizes biased downward relative to the GRA stream population. This highlights the benefit of backing up genetic inferences of demography with analyses of the selective history and with qualitative information from the field.

6.3.2 Genomically localized characterization of selection

The above genome–wide analyses indicated that the lake population has been particularly strongly influenced by widespread selective sweeps. To confirm this asymmetry in selection at a finer scale, we inspected localized signatures of selection at two classes of loci within the genome. The first, called F_{ST} extremes, included the 25 independent SNPs displaying the strongest lake–stream differentiation across all three lake–stream F_{ST} scans combined (79'770 total SNPs). None of these extreme SNPs showed fixed allelic differences between the habitats, but nearly so: F_{ST} ranged from 0.94 to 0.75 – remarkably high values given the low baseline differentiation (Fig. 6.4a;
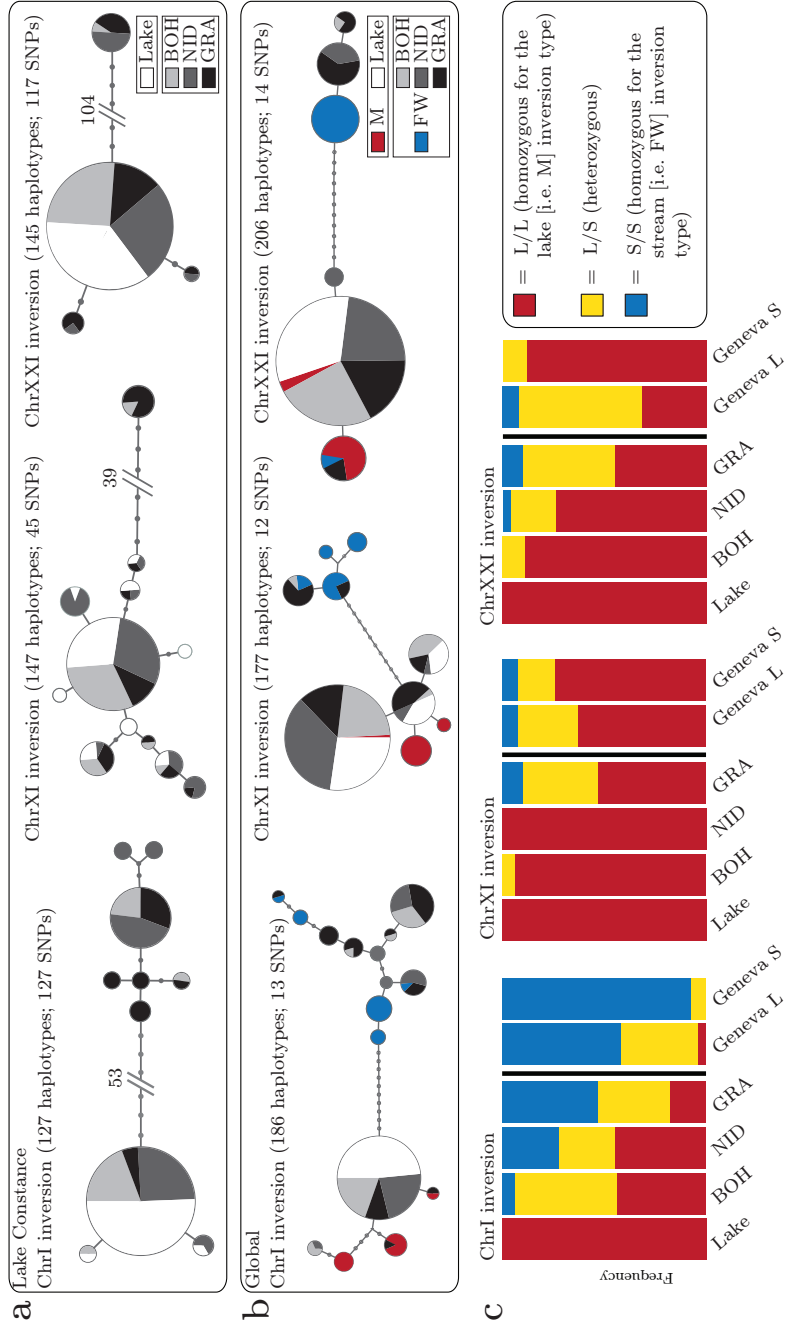
Figure 6.7: Phylogenies and habitat associations of the inversions. (a) Haplotype phylogenies restricted to SNPs located within the inversions, based on individuals from the Lake Constance basin. Pie sizes reflect the relative frequency of each haplotype, and internodes are mutational steps. Only haplotypes recovered more than twice are shown (total haplotype numbers are given above the networks). (b) Haplotype networks as in a, but additionally including individuals from marine and freshwater populations across the species' global range (Jones et al. 2012). (c) Frequency of the three diploid genotype classes at each inversion in the four populations from the Lake Constance basin, and in the lake–stream pair from the Lake Geneva basin. The color coding follows b.

genome–wide F_{ST} profiles visualizing the strikingly heterogeneous genomic divergence in all three lake–stream comparisons are provided in Fig. S19 (Supplementary material)). The F_{ST} extremes were found on 11 different chromosomes and derived mostly from the lake–GRA comparison that also produced the greatest baseline differentiation. Inspecting allele frequencies at the F_{ST} extremes showed that the MAF was generally lower in the lake population (14 out of the 25 SNPs were monomorphic) than in the corresponding stream population (with only four monomorphic SNPs; binomial test for similar occurrence of monomorphic SNPs: P = 0.007; Fig. 6.4a), suggesting that selection has mainly occurred, or has been more effective, in the lake. At the F_{ST} extremes, those alleles near fixation in one of the stream populations were generally also present in the other stream populations, with the frequency of these stream alleles increasing from BOH to NID to GRA (Fig. 6.4a). Finally, we found that haplotype decay around the F_{ST} extremes was slower in the lake than in the focal stream population (binomial P = 0.004; Fig. 6.4b).

The F_{ST} extremes represented genomic regions with nearly complete lake–stream allele frequency divergence, hence reflecting strong selection. To search for weaker or ongoing selective sweeps, we delimited a second class of loci based on haplotype structure (Sabeti et al. 2006; Oleksyk et al. 2010). Specifically, we used Rsb (Tang et al. 2007) to compare the rate of haplotype decay between the lake and the streams at 87'738 SNPs for each lake–stream comparison. Following the convention that positions with an absolute Rsb value >4 provide compelling evidence of selection (for example Flori et al. 2012), we identified a total of 22 such 'Rsb extremes' on 11 chromosomes across all three lake–stream comparisons (lake–stream Rsb profiles are presented in Fig. S20 (Supplementary material); in contrast to the F_{ST} extremes, Rsb extremes emerged from all lake–stream contrasts, Fig. 9 (Supplementary material)). Interestingly, examining allele–specific haplotype structure revealed that within both habitats, the lake alleles were surrounded by relatively longer haplotype tracts than the alternative stream

alleles (Fig. 6.4c). This indicates that alleles selected positively in the lake, but presumably negatively in the streams, are maintained at substantial frequency in the streams by gene flow from the lake population. Finally, our haplotype–based analysis also revealed signatures of selective sweeps that have occurred in the stream habitat (Fig. 6.4d, Fig. S21 (Supplementary material)).

Overall, our analyses of localized signatures of selection provide strong support for the selective scenario indicated by the genome–wide signatures: selection is wide–spread across the genome and is asymmetric, with more extensive sweeps having occurred in the lake than in the stream populations. Moreover, lake–stream divergence in the Lake Constance basin has clearly occurred in the face of gene flow. Consistent with the census size (but not the estimated effective population size) of the Lake Constance population being orders of magnitude larger than the stream populations, introgression occurs primarily from the lake into the streams. Nevertheless, many loci resist gene flow and maintain substantial differentiation from the lake (Barton and Bengtsson 1986; Bierne 2010; Feder and Nosil 2010; Roesti et al. 2014), thereby generating heterogeneous genomic divergence between the lake and the stream populations (Wu 2001).

6.3.3 Signatures of selection around a known adaptation locus

Our analyses of localized signatures of selection within the genome focused on regions likely important to adaptation to the lake and stream habitats, yet it is unknown what phenotypes the polymorphisms in these regions influence. For the extent of lateral plating, however, it was possible to take an alternative route and to investigate the molecular signatures produced by selection on a trait known a priori to be important to lake–stream divergence. We started at the phenotypic level by establishing that lake individuals were mostly completely plated, whereas plating was relatively reduced in all stream populations, most clearly so in NID and GRA (lake–BOH permutation test for similar plating: P = 0.420; lake–NID: P = 0.002; lake–GRA: P < 0.001) (Fig. 6.5a). This agrees with earlier work using different populations and/or samples from the same basin (Berner et al. 2010a; Chapter 1). Next, we performed a bulk segregant analysis (BSA) by pooling all completely and all low–plated stream fish into two separate groups. Genetic differentiation between these groups across genome–wide SNPs revealed a region on chromosome four (ChrIV) harboring markers with a very strong association between allelic state and phenotype (Fig. 6.5b). The peak association (F_{ST}

= 0.78) occurred immediately downstream of the Ectodysplasin (*Eda*) gene. This locus is known as major determinant of lateral plating (Colosimo et al. 2005; Chapter 5), with a causative cis–regulatory polymorphism having been identified 1 kb downstream of the coding region (O'Brown et al. 2015). No SNP outside this region on ChrIV displayed $F_{ST} > 0.38$.

Combined, the phenotypic data and BSA indicate that differentiation in plating among our study populations involved adaptive lake–stream divergence at the *Eda* locus. We thus predicted molecular footprints of selection at this locus. To evaluate this prediction, we inspected all three lake–stream F_{ST} scans for the magnitude of differentiation around *Eda* (Fig. 6.5c). As expected from the plate morph distribution (Fig. 6.5a), the strongest differentiation occurred in the lake–GRA comparison ($F_{ST} = 0.40$), just 5.7 kb downstream of *Eda*. However, in this particular comparison, the most divergent SNP near *Eda* ranked only within the upper 3.5 percentile of the genome–wide F_{ST} distribution (lake–BOH and lake–NID comparisons: 8.8 and 2.3 percentile). Similarly, the highest absolute Rsb value around *Eda* (1.17) also emerged from the lake–GRA comparison but fell only within the upper 23 percentile of the genome–wide Rsb distribution. Hence, thousands of SNPs displayed a stronger deviation from selective neutrality than the *Eda* locus. Accordingly, subjecting the lake–GRA pairing to a standard selection outlier detection analysis (BayeScan (Foll and Gaggiotti 2008)) failed to provide any evidence of selection at SNPs surrounding *Eda* (Fig. S22 (Supplementary material)).

More nuanced insights into the evolution of lateral plating were obtained by analysing haplotype structure around the *Eda* locus: in the streams, where both *Eda* alleles (still) occur at substantial frequencies, haplotype decay was slower around the allele associated with complete plating (Fig. 6.5d, top). Moreover, the haplotype structure around the completely plated allele in the streams matched the haplotype structure around this allele in the lake (where the low–plated allele was too rare to characterize LD) (Fig. 6.5d, bottom). Together, this indicates that selection for complete plating in the lake has been more effective than selection against plates in the streams, and again suggests the maintenance of an unfavourable variant – and the associated phenotype – in the streams by gene flow from the lake (see also Fig. 6.4c). To fully appreciate the extent of LD driven by selection on lateral plating, we again took a bulk segregant approach by treating all completely and low–plated stream fish as separate groups, and looked for distortions between these groups in the rate of haplotype decay along ChrIV. This confirmed that selection on the *Eda* variant driving complete plating has been much more intense than selection on the low–plated variant, and showed that the associated sweep has influenced haplotype structure at the scale of megabases

(Fig. 6.5e). Unexpectedly, this scan also detected a second, similarly strong selective sweep in completely plated stickleback centred at 11.4 Mb. This latter region also exhibited a clear signature of divergence in the F_{ST}–based BSA (Fig. 6.5b, top): the differentiation peak in this region ($F_{ST} = 0.31$) fell within the top 0.06 per cent of the genome–wide distribution.

Together, the investigations at the *Eda* locus highlight our limited ability to elucidate the genetic basis of adaptive population divergence based on genetic markers when selective sweeps are incomplete. Neither the magnitude of differentiation (F_{ST}) nor haplotype structure (Rsb) among populations allowed the major plate locus to emerge as an obvious selection candidate–despite substantial evolution in the associated ecologically important phenotype, and despite an extensive selective sweep visible when comparing haplotype structure among individuals grouped by phenotype. Given that stronger signatures than those around *Eda* are numerous in our data sets, we conclude that hundreds of genomic regions must be involved in the adaptive divergence into lake and stream habitats. We further propose that lateral plate evolution in the Lake Constance basin is governed by at least one other locus besides *Eda*. Inspecting the newly detected region on ChrIV indeed produces a strong candidate gene, *Col23a1* (bp–position 11'443'468–11'468'190; this specific segment contained the highest–F_{ST} SNP observed across the new candidate region in the BSA). Like *Eda*, this gene encodes a transmembrane collagen involved in the development of the epidermis (Veit et al. 2011). Since the new candidate region and *Eda* occur in close proximity (c. 1.4 Mb apart) in a low–recombination chromosome region (Chapter 4), it is tempting to speculate that the coupling of alleles in the two regions might facilitate divergence in plating relative to the situation where each locus segregates independently (Yeaman 2013; Roesti et al. 2014).

6.3.4 Detection and characterization of inversions

Our genetic data indicate that lake–stream divergence in the Lake Constance basin has occurred in the face of gene flow. Genetic polymorphisms predicted by theory to resist homogenizing gene flow and to diverge between populations particularly well are chromosomal inversions (Rieseberg 2001; Kirkpatrick and Barton 2006; Yeaman 2013). The reason is that different inversion types can physically couple alleles promoting adaptation to different habitats across multiple loci. The integrity of these allele clusters is easily maintained, because a single crossover within the inversion generally produces unbalanced meiotic products in inversion heterozygotes (that is, heterokaryotypes), thus effectively suppressing recombination (Sturtevant 1936; Navarro 1997). Consequently, alternative inversion types can be considered

single large–effect alleles.

To test this idea, we examined if lake–stream divergence in the Lake Constance basin was promoted by chromosomal inversions. For this, we scanned the genome for extended distortions in the relative RAD sequence coverage between the lake and each stream population (Fig. S23 (Supplementary material)). This produced three strong candidates, located on ChrI (approximate length: 500 kb), ChrXI (450 kb) and ChrXXI (2.1 Mb) (Fig. 6.6a) – all coinciding with inversions recently identified in a comparison of marine and freshwater stickleback (Jones et al. 2012). For two of these candidate inversions (ChrI and ChrXI), we designed PCR primers across expected inversion breakpoints based on our RAD sequences, and the presence/absence of PCR products confirmed that these regions were inversions (Fig. S24 (Supplementary material)). We then performed several complementary analyses to characterize the three inversion polymorphisms in our populations. Inspecting inversion–specific allele frequencies revealed that the lake population was consistently fixed for one inversion type, whereas the stream populations were polymorphic at two (NID) or all three inversions (BOH and GRA). However, only at the ChrI inversion were lake–stream frequency shifts strong enough to drive clearly elevated F_{ST} relative to baseline differentiation (Fig. 6.6b). Consistent with only the stream populations being polymorphic for the inversions, the allelic diversity at polymorphic sites within the inversions tended to be elevated in the stream populations relative to the lake (Fig. 6.6c). However, the segregation of an inversion type at very low frequency within a population sometimes generated an excess of SNPs displaying reduced diversity relative to the genomic baseline within that population (BOH and NID at the ChrXI and ChrXXI inversions, Fig. 6.6c). The stream populations also exhibited a clear excess of SNPs falling into the specific MAF class mirroring the relative frequency of the minor inversion type (Fig. 6.6d). SNPs within this MAF class – but not those from other MAF classes –revealed extended blocks of nearly perfect LD caused by the inversion polymorphisms in the streams (Fig. 6.6e).

For the ChrI inversion, we experimentally confirmed suppressed recombination in inversion heterozygotes by inspecting crossover frequencies in an F_2 intercross derived from two parental individuals homozygous for either inversion type (Chaper 4 & 5). Not a single crossover occurred within the inversion, but recombination immediately adjacent to the inversion was frequent (Fig. 6.6f; see Fig. S25 (Supplementary material) for a negative control of this analysis). Nevertheless, for large inversions, theory predicts that occasional double crossovers should allow some genetic exchange between the inversion types, albeit not near the inversion breakpoints (Navarro et al. 1997; Guerrero et al. 2012). We examined this prediction for the ChrI

inversion by comparing homozygotes for one inversion type to homozygotes for the other type, considering individuals from all populations. We found that while these two groups were fixed for different SNP alleles across most of the inversion, differentiation decayed in a narrow region in the centre of the inversion (Fig. 6.6g). This region was also relatively enriched for polymorphisms shared between the two inversion types, but contained relatively few SNPs unique to either of the two types (Fig. 6.6g, bottom).

To learn more about the history and ecology of the three inversion polymorphisms, we next established the phylogenetic relationship among our study individuals using haplotype information based on SNPs located within the inverted regions only. For each inversion, this revealed the presence of two haplotype clusters separated by a deep split (Fig. 6.7a). In line with our findings from the allele frequencies at putative loci under selection (Fig. 6.4a), Lake Constance fish consistently harbored haplotypes from one of these clusters only, whereas all stream populations contained haplotypes from both clusters. Repeating the phylogenetic analysis by including SNPs extracted from 21 previously sequenced marine and freshwater stickleback sampled across the species' global distribution (Jones et al. 2012) produced a striking result: haplotypes representing the inversion type for which the Lake Constance population was fixed clustered consistently or were even identical with haplotypes recovered in marine stickleback (Fig. 6.7b). Conversely, haplotypes representing the inversion type found exclusively in the streams were closely related to, or identical with, haplotypes from global freshwater populations. To further explore how consistently these inversion polymorphisms are recruited for lake–stream divergence, we investigated SNP data for individuals sampled from Lake Geneva and from one of its tributary streams, waters documented to have been colonized by stickleback very recently (nineteenth century) and independently from the Lake Constance basin (see references in Berner et al. 2010a and Lucek et al. 2010; genome–wide divergence in this lake–stream pair is described in Fig. S26 (Supplementary material)). We here again recovered all three inversion polymorphisms (Fig. 6.7c, Fig. S26 (Supplementary material)). At the ChrI inversion, the direction of lake–stream divergence was congruent between the Lake Constance and Lake Geneva basins, whereas the ChrXI showed no divergence in the latter. Surprisingly, the direction of lake–stream divergence at the ChrXXI inversion was reversed between the two basins.

Overall, a first insight emerging from our analyses of inversions is that the relative frequencies of inversion types need to be taken into account when scanning population genomic data for the presence of such polymorphisms. Characteristic signatures like extended blocks of SNPs displaying exceptional levels of population differentiation or strong LD can become evident only

when restricting SNPs to the appropriate MAF class. Second, our analysis of the ChrI inversion shows that genetic exchange between inversion types can occur despite effective overall recombination suppression, and that this exchange is biased towards the inversion centre. To our knowledge, this has previously been demonstrated only for much larger inversions in *Drosophila* and *Anopheles* (Schaeffer and Anderson 2005; Stump et al. 2007). Our data from the laboratory cross further suggest exceptionally high recombination rates in the collinear segments immediately flanking the inversion (Fig. 6.6f). This is unexpected – double crossover encompassing a single inversion breakpoint should produce unbalanced chromatids, hence one would predict relatively reduced recombination in these regions (Navarro et al. 1997).

Finally, the distribution of inversion haplotypes in the Lake Constance basin suggests divergent lake–stream selection on these chromosomal rearrangements. Specifically, the occurrence of shared haplotypes at both inversion types within multiple, presently unconnected stream populations, and the consistent presence of only a single inversion type in the lake, indicate particularly effective sorting of ancestral standing variation in the lake population. This reinforces our conclusion of asymmetric selection based on the genome–wide analyses and the inspection of F_{ST} and Rsb extremes, and supports the view that inversion polymorphisms are ecologically relevant (Rieseberg 2001) (We note that we could not find any indication of intrinsic incompatibility or transmission disequilibrium between the inversion types, as their frequencies did not deviate from Hardy–Weinberg expectation in any inversion–population combination. Details not presented, but see Fig. 6.7c.).

All inversion haplotypes occurring within Lake Constance further coincide with haplotypes predominant in marine stickleback. This suggests the presence of shared selective features between the ocean and large lakes – possibly mediated by a pelagic lifestyle in both habitats (see Pearse et al. 2014 for similar evidence from trout) – driving genuine parallel evolution at a much larger geographic scale than our focal lake – stream system. In any case, these inversions are not (only) relevant to saltwater – freshwater adaptation (Jones et al. 2012). To further complicate functional conclusions, the ChrXXI inversion has diverged in opposed directions between lake and stream stickleback in the Lake Constance and the Lake Geneva systems. This unexpected trend is unlikely to arise from drift in the young Geneva system: among the 50 most extreme genome–wide F_{ST} values in this exceptionally weakly divergent lake–stream pair (genome–wide median $F_{ST} = 0$), 22 (44%) map to the ChrXXI inversion, including the top value observed overall ($F_{ST} = 0.338$) (Fig. S26 (Supplementary material)). This suggests intense selection on this inversion polymorphism in the Geneva system. However, given the great number of genes coupled by each inversion (∼24, 25 and 109 genes

135

for the ChrI, ChrXI and ChrXXI inversions), dissecting the precise target(s) of selection in different ecological contexts will remain a serious challenge. Finally, the detected sharing of haplotypes between our study populations (derived from Atlantic ancestors) and worldwide stickleback populations (including Pacific–derived fish), along with the vast mutational differentiation observed between the inversion types (Fig. 6.6g and Fig. 6.7b), indicates that all three inversion polymorphisms must be ancient.

To summarize, a main goal of our study was to dissect the demographic and selective history of adaptive diversification in lake and stream stickleback populations within a single lake basin. Combining demographic inference with broad scale and localized analyses of genetic differentiation and diversity, linkage disequilibrium and haplotype structure within the genome allows us to reject a standard scenario of parallel divergence of multiple stream populations from a shared ancestral lake population (Fig. 6.3a–c). Instead, our results support a history of ecological vicariance with gene flow. This latter scenario involves the widespread colonization of the Lake Constance basin by a stream–adapted ancestor, the subsequent emergence of a derived lake–adapted population through intense selection of standing variation and sustained gene flow across the lake–stream boundaries (Fig. 6.3d–f). Consequently, different magnitudes of overall divergence among the lake–stream pairings, and heterogeneous lake–stream divergence across the genome, do not mirror how strongly gene flow from the lake has constrained the emergence of adaptation in the streams, but how effectively introgression from the lake has eroded initial stream adaptation. Our work thus underscores that investigations of patterns of divergence consistent with parallel evolution should consider an alternative – that is, the repeated retention of shared ancestral variation, and should be rooted in detailed knowledge about the demographic and selective history of populations (Bierne et al. 2013). Nevertheless, nested within a vicariance background, our investigation of inversion polymorphisms indicates the recycling of the same genetic variants for adaptive divergence in seemingly different ecological contexts, and hence real parallel evolution on a large geographic scale.

Furthermore, our finding of highly heterogeneous genomic divergence conflicts with the recent theoretical prediction that adaptive divergence in the face of gene flow involving selection on extensive standing variation should produce genome–wide reproductive isolation and therefore limit heterogeneity in genome divergence (Flaxman et al. 2014). Given the numerous factors influencing adaptive divergence in natural populations, we believe that it will remain very difficult to predict how fast and to what extent heterogeneous genomic divergence should build up. However, our study clearly supports the notion that heterogeneity in genome divergence is promoted

by sustained gene flow between young populations adapting to ecologically different environments (for example Feder et al. 2012). We challenge the claim that such heterogeneity represents the divergence of populations after reproductive isolation has become complete (Cruickshang et al. 2014).

Finally, our study adds molecular evidence to the idea that chromosomal inversions promote adaptive divergence by acting as loci of large effect (Rieseberg 2001). However, lake–stream stickleback divergence certainly also involves numerous loci not located within chromosomal rearrangements, and selection on some of these loci appears at least as strong as selection on the inversions. Determining the importance of inversions relative to other adaptive polymorphisms in evolutionary diversification remains an important empirical issue.

6.4 Material and methods

6.4.1 Stickleback samples and marker generation

Specimens from the Lake Constance population were sampled at two localities (Romanshorn, Switzerland, N = 12, and Unteruhldingen, Germany, N = 13; for geographic details see Chapter 1). Genetic structure is absent at any scale within this large lake (Fig. S13 (Supplementary material); Berner et al. 2010a; Chapter 1), so the two lake samples were combined to a single 'lake' pool for all analyses. Stream stickleback were sampled from three geographically well-separated tributaries connected through the lake only (Fig. 6.1a). The stream sites correspond to the Bohlingen (BOH, N = 22), Nideraach (NID, N = 24) and Grasbeuren (GRA, N = 24) localities in chapter 1). Natural dispersal barriers are absent in all streams, but low man–made dams have likely restricted gene flow from the lake to the NID and GRA sites over the last decades. All work in this study was approved by the Veterinary Office of the Canton of Basel–Stadt (permit number: 2383).

DNA was extracted from stickleback fin and muscle tissue using either a MagNA Pure LC278 extraction robot (Roche, Basel, Switzerland) with the tissue Isolation Kit II, or the DNeasy Blood & Tissue Kit (Qiagen, Valencia, USA). After an RNase treatment, the extracts were standardized to 18 ng μl^{-1} based on multiple NanoDrop photospectrometer readings (Thermo Scientific, Wilmington, USA), and used to generate RAD DNA libraries essentially following the protocol described in Roesti et al. 2012a. The main modification was that we used the Nsi1 enzyme for DNA restriction, exhibiting a 7.5 times higher recognition site density (that is, c. 164'000 sites across the 460 Mb stickleback genome) compared with the commonly used Sbf1

restriction enzyme. We prepared 12 total RAD libraries, each combining individually 5mer–barcoded DNA from seven or eight of the 95 total individuals. For final enrichment, we pooled six replicate PCRs per library to reduce amplification bias.

Each library was single–end sequenced with 100 cycles on a separate Illumina HighSeq2000 lane. Raw sequence reads were parsed by individual barcodes and aligned to the improved assembly (Chapter 4) of the threespine stickleback reference genome11 by using Novoalign v2.07.06. We enforced unique alignment, tolerating an equivalent of ∼8 high–quality mismatches or gaps (flags: –t236, –g40, –x15). Alignments were BAM–converted in Samtools v0.1.11 (Li et al. 2009). For individual consensus genotyping, we first applied two effective filters to further exclude RAD loci located on repeated elements. First, loci were excluded if they displayed a read coverage exceeding three times the mean coverage across all loci within an individual. Second, if a RAD locus was polymorphic, it was excluded if the two dominant haplotypes failed to account for >70% of all reads.

Loci passing the above filters were subjected to consensus genotyping using a refinement of our earlier haplotype–based algorithm (Roesti et al. 2012a), which has been demonstrated to perform highly accurately (Nevado et al. 2014). The main novelty was that instead of building genotypes quality–aware base–by–base, we discarded sequence quality and treated the entire read as the genotyping unit. A diploid genotype was called if the read coverage contributed by the two dominant haplotypes, or the total coverage for monomorphic loci ('effective coverage'), was 15 or greater (median total coverage across all RAD loci and individuals was $38.5\times$). Because we observed in our previous work that the distribution of the two haplotypes for heterozygous loci was over–dispersed relative to the binomial expectation, we avoided distinguishing homozygote from heterozygote genotypes based on a theoretical distribution. Instead, a locus was considered heterozygous if the ratio of the second most frequent haplotype to the sum of the first and second was >0.25. Otherwise, a locus was considered homozygous. If the effective coverage was below 15 but at least two, we called a haploid genotype only, based on the dominant haplotype. Loci with single–read coverage were discarded. Inspection of the haplotype distribution at RAD loci showed that with our sequence data, this defensive algorithm maximized both the detection of truly heterozygote loci and the exclusion of polymorphisms reflecting technical artifacts (Fig. S27 (Supplementary material)). To create the raw SNP matrix for downstream analyses, we pooled the consensus genotypes across all populations and extracted a maximum of six SNPs per RAD site, provided the haploid consensus genotype coverage across all individuals and populations was at least $80\times$.

6.4.2 Demography and phylogenetics

To explore the evolutionary history of our four study populations, we reconstructed their demography using the coalescent simulator *fastsimcoal2.1* (Excoffier et al. 2013). As input, we computed the observed joint site frequency spectrum (SFS) for each of the six pairwise population combinations. For this, we first sampled at random exactly 30 haploid consensus genotypes per RAD locus from each population. Loci with sparser coverage and those harboring more than two polymorphisms with an identical frequency of the less common allele (that is, the 'minor allele frequency' (MAF)) across the last 30 positions were ignored. The latter excluded uninformative sequential pseudo–SNPs from RAD loci harboring a micro–indel polymorphism, and hence ensured that only true SNPs were considered. Next, we counted the occurrence of the minor allele at each of the 89 positions per RAD locus in each population to populate the SFS. This considered both monomorphic positions and bi–allelic SNPs. For the latter, the minor allele was defined based on the pool of all four populations. If the MAF of a SNP was exactly 0.5, both alleles were treated as minor and entered the SFS, but with a weight of 0.5 only (personal recommendation by L. Excoffier). The resulting joint SFS were based on 14.837 million base positions on 166'711 RAD loci. We additionally computed all population–specific SFS with the same resolution.

Using the observed joint SFS, we then performed simulations with *fastsimcoal2.1* to estimate the most likely parameter values for an evolutionary scenario in which the four focal populations split under gene flow from an ancestral population colonizing the Lake Constance basin. We here assumed that the populations in the different habitats established rapidly, justifying a single splitting time. We estimated the age of the split, all effective population sizes (including the ancestor), migration rates between the lake and each stream population (but not among stream populations) and the SNP mutation rate. The simulation was run in 80 replicates, each including 40 estimation loops with 100'000 coalescent simulations. To determine the best parameter estimates, we selected the 10 most likely replicate runs (that is, those with the smallest difference between the estimated and observed likelihood) and used this subset to calculate the mean for all parameters, along with their 95% confidence intervals (95 percentiles from bootstrap distributions based on 100'000 resamples). Because the lake population turned out to be particularly strongly influenced by selection, we explored an analogous model in which just the two stream populations most divergent from the lake (NID and GRA) split from an ancestor under gene flow.

To explore phylogenetic relationships among populations, we first reduced individual genotypes to single–letter code and eliminated individuals with

>75% and SNPs with >15% missing data. We then used the R (R Core Team 2013) package *phangorn* (Schliep 2011) to infer the most appropriate model of sequence evolution (Posada 2008) (GTR + G + I). (The R language was used for all analytical procedures in this paper, unless noted otherwise.) Finally, we constructed unrooted maximum likelihood trees to infer the phylogeny of all four populations (based on 51,188 SNPs) and of the two lake samples only (55'561 SNPs). These analyses used no more than one SNP per RAD locus and required a MAF > 0.2 across all populations (MAF > 0.05 resulted in very similar results). Node support was assessed with 200 bootstrap replicates. The same data were also used to visualize genetic structure based on a principal coordinates analysis as implemented in the R package *ape* (Paradis et al. 2004). Rooted phylogenies were constructed analogously by incorporating genotype data from geographically distant outgroup stickleback individuals, including the Pacific BEPA reference genome individual, at 14'429 SNPs ascertained in the populations from the Lake Constance basin.

6.4.3 Genetic diversity

Two analyses were conducted to compare genetic diversity among the populations. For both, we only considered SNPs from our raw SNP matrix that occurred alone on a given RAD locus (that is, data from RAD loci harboring multiple polymorphisms were ignored). Using only such 'loner SNPs' avoided potential bias in the estimation of genetic diversity due to pseudo–SNPs caused by micro–indels. We further ignored those loner SNPs displaying a minor allele count <2 across all individuals pooled, thereby avoiding sequencing artifacts. We thus obtained a total of 62'332 genome–wide loner SNPs. As a first measure of diversity, we determined for each population the proportion of the total loner SNPs actually being polymorphic. To obtain a second diversity measure, we screened all loner SNPs for the presence of three alleles across all individuals pooled ('tri–allelic loner SNPs'; the least frequent allele had to occur at least twice across all individuals). On average, one out of 169 loner SNPs proved tri–allelic (genome–wide total: 368). We then determined for each population the proportion of the total tri–allelic loner SNPs actually displaying all three alleles.

6.4.4 Genome–wide LD

We quantified LD within each population using the squared correlation coefficient (R^2) between pairs of SNPs. From the raw SNP matrix, we excluded SNPs that were tri–allelic or had >25% missing genotypes, and individuals with >75% missing diploid genotype calls. The remaining SNPs were filtered

for two different MAF ranges (0.05–0.275 and 0.275–0.5). Only a single randomly chosen SNP was retained if multiple SNPs passed these thresholds for a pair of sister RAD loci (that is, the two RAD loci flanking the same restriction site). The final number of SNPs was 16'088 and 18'787 for the former and latter MAF range (marker number was adjusted to be equal for all populations). We then ran PLINK (Purcell et al. 2007) with the command line '–ld-window 100 –ld-window–kb 100 –ld–window–r2 0' to calculate R^2, enabling R^2 values even below the default threshold of 0.2 to be reported. On average, this resulted in 142'249 R^2 values for the 0.05–0.275 MAF range, and in 241'154 R^2 values for the 0.275–0.5 MAF range. We then assigned the R^2 values to 1 kb bins according to the physical distance between the two focal SNPs, and plotted the mean R^2 for each bin from 1 to 100 kb. For the analysis of genome–wide LD decay with the full MAF range (0.05–0.5), we pooled the two MAF range specific PLINK outputs (one generated for the 0.05–0.275 and one for the 0.275–0.5 MAF range) before binning. Setting a MAF range of 0.05–0.5 right at the filtering step of the raw SNP matrix produced very similar results. To investigate more localized LD along chromosomes, we considered only R^2 values between SNPs > 2 kb but < 50 kb apart (a range between 2 kb and 30 kb, or considering pairwise R^2 values only produced similar results supporting identical conclusions). We determined the physical midpoints for all SNP pairs, binned the respective R^2 values in non–overlapping 200 kb windows along the genome, and calculated average R^2 for each window and population. Different window sizes (that is, 50 or 100 kb) yielded similar results supporting identical conclusions. To visualize localized differences in LD along the genome between the lake and GRA populations, we subtracted for each window the GRA R^2 value from its lake counterpart, yielding a metric referred to as Delta R^2'. We further calculated the correlation of R^2 values between the lake and each stream population, using the above windows as data points. The magnitude of this correlation was evaluated against its empirical random distribution generated by permuting the R^2 data over the windows 10'000 times.

6.4.5 F_{ST}–based identification of selected regions

Scans for genomic regions exhibiting strong differentiation were performed for each lake–stream combination. (We decided to refer to particularly high differentiation values as 'extremes' rather than 'outliers', as the outlier terminology implies a distinct class of loci.) Consistent with Roesti et al. (2012a, 2014), F_{ST} was calculated based on haplotype diversity. We considered only polymorphisms exhibiting a nucleotide coverage of at least $21\times$ in each population. To achieve adequate information to calculate genetic differentiation

(Roesti et al. 2012b), we further ignored SNPs with a MAF <0.2 across the focal lake and stream population pool. If multiple SNPs derived from the same RAD locus, we selected only the single one yielding the highest F_{ST} value (selecting instead based on maximum MAF, or at random, had no material influence on the results). Applying these stringent filters, we obtained 55'476, 57'119 and 60'052 genome–wide F_{ST} values for the BOH–lake, NID–lake and GRA–lake comparisons. To obtain regions suited for a detailed characterization of signatures of selection, we chose the 25 autosomal SNPs displaying the highest F_{ST} values across the three F_{ST} data sets combined (that is, 172'647 F_{ST} estimates from 79'770 unique SNPs). To ensure that each of these differentiation extremes represented an independent genomic region, SNPs were ignored if they were closer than 200 kb to a SNP already accepted as extreme.

6.4.6 Haplotype–based identification of selected regions

Our F_{ST}–based search for evidence of positive selection was complemented with haplotype–based statistics proving particularly powerful to detect incomplete selective sweeps (Sabeti et al. 2006; Oleksyk et al. 2010). However, they rely on relatively high marker resolution and robust sequence coverage in many individuals; requirements met by our study (see above). From the raw SNP matrix, we first excluded SNPs that were tri–allelic, had >40% missing genotypes, or did not reach a MAF of 0.05. We further excluded individuals with >75% missing diploid genotype calls after SNP–filtering. *fastPHASE* (Scheet and Stephens 2006) was then used to reconstruct haplotypes and missing genotypes separately for each chromosome. We classified individuals according to their population (–u option) and increased the number of iterations of the EM algorithm to 50 (–C option; default is 25) and the number of sampled haplotypes to 100 (–H option; default is 20). *fastPHASE* output files were then imported into the R package *rehh* (Gautier and Vitalis 2012) to obtain the following haplotype–based statistics: EHH (Sabeti et al. 2002) (allele–specific 'Extended Haplotype Homozygosity'), EHHS (Sabeti et al. 2002) (population–specific weighted average of EHH across both alleles), iHH (Voight et al. 2006) ('integrated Haplotype Homozygosity'), iHS (Voight et al. 2006) ('integrated Haplotype Score') and Rsb (Tang et al. 2007) (the standardized ratio of integrated EHHS from two populations). iHS was calculated separately for each of the four populations using the 'scan–hh' and 'ihh2ihs' commands ('minmaf', the MAF threshold, was set to 0.05; '–freqbin' was set to 0, but setting this option to 0.05 or 0.1 resulted in qualitatively similar results supporting identical conclusions). Rsb was calculated for each of the three possible lake–stream comparisons

by applying default parameters ('ies2rsb' command). We obtained a total of 87'738 Rsb values (corresponding to an average marker distance of 4.8 kb), which were screened for extremes (that is, values below – 4 or above 4 (Tang et al. 2007; Flori et al. 2012)). Haplotype decay around F_{ST} and Rsb extremes was calculated and visualized using the 'calc–ehh' and the 'calc–ehhs' option at default.

6.4.7 Analyses specific to lateral plating

To screen the genome for loci influencing the lateral plate phenotype, we performed a BSA by assigning 24 completely plated stream individuals to one phenotypic group, and 24 low–plated stream individuals to another group (lateral plate phenotyping followed chapter 1). This assignment considered all three stream populations but ignored the (mostly completely plated) lake fish, thus avoiding confounding signals of lake–stream divergence (that is, signals unrelated to plate phenotype). Based on 61'822 SNPs, we then carried out a genome–wide F_{ST} scan by treating the phenotypic groups as populations, but otherwise following all conventions described above for the population–based F_{ST} calculations.

To examine if *Eda* was recognized as a selected locus in a standard F_{ST} scan, we applied BayeScan (Foll and Gaggiotti 2008) to the SNP data set from the GRA–lake comparison (60'052 markers), that is, the population pair with the strongest differentiation at *Eda*. BayeScan was run with default settings except that we used 300 as prior odds for neutrality–according to the software manual an appropriate value for this data set. However, a second analysis was performed with the default prior odds of 10, which is expected to produce more liberal results.

For the *Eda*–specific analyses of haplotype structure, we created three pools: a first pool with all completely plated stream individuals, a second pool with all low–plated stream individuals (both N = 24), and a third pool with all completely plated lake individuals (N = 19). We calculated and plotted EHHS for each pool around the SNP exhibiting the highest F_{ST} value in the above bulk segregant genome scan (bp–position 12'832'658 on chromosome IV). Finally, we subtracted iHS values from the completely plated stream individuals from the corresponding values in the low–plated stream individuals ('Delta iHS') across chromosome IV (N = 5'626; average marker distance = 6 kb). Delta iHS was then averaged and plotted in non–overlapping 100 kb windows (different window sizes led to identical conclusions).

6.4.8 Identification and characterization of inversions

Our approach to detecting inversions was based on the expectation that the two inversion types (collinear and inverted), representing two isolated populations, differ in their magnitude of divergence from the reference genome. This should cause differential read alignment success across inverted genomic regions. Inversions should thus be revealed by a physically extended distortion of the relative RAD locus sequence coverage between two populations if these populations differ in the frequency of the inversion types (Fig. S23 (Supplementary material)). The same logic recently enabled the identification of evolutionary strata on the stickleback sex chromosome (Chapter 4). We therefore screened all 372'884 RAD loci for population–specific sequence coverage, excluding those with a total sequence coverage below 200 across all populations and those located in genomic regions unanchored to chromosomes, thus obtaining 290'170 informative loci. For each stream population, we calculated the RAD locus–specific stream to lake coverage ratio. Next, we divided the chromosomes in non–overlapping 20 kb windows (21'048 in total) and calculated the average coverage ratio among the RAD loci for each one of them (using the coverage variance among RAD loci within windows produced very similar results). The median number of RAD loci per window was 13. Finally, we looked for distortions in the coverage ratio extending over multiple adjacent windows, suggesting the presence of an inversion. We note that this analysis based on read coverage was limited to the detection of relatively large inversions exhibiting substantial sequence divergence.

To confirm that the above sequence coverage method reliably detects inversions, we used RAD loci near an expected inversion breakpoint in two of the three emerging candidate regions to design PCR primer pairs across the breakpoint boundaries. These primer pairs were expected to yield a PCR product only for the inversion type occurring in the streams. Ten to 13 individuals representing a given inversion type were subjected to long–range PCR and inspected for the presence or absence of amplification (further details are given in Fig. S24 (Supplementary material)).

Next, we examined allelic diversity and minor allele frequencies (MAFs) around the three detected inversions. For this, we screened each of the four population samples separately for polymorphisms with >50% available genotype calls (singletons were omitted to exclude technical artifacts) and calculated haplotype diversity (that is, an analogue of heterozygosity ranging from 0 to 0.5) and the MAF at each SNP. RAD loci were allowed to contribute a single SNP only, keeping the one with the highest diversity when multiple SNPs occurred on the same locus (drawing a SNP at random or averaging diversity estimates of multiple SNPs per RAD locus yielded very similar re-

sults). Diversity was visualized using R's implementation of LOESS (locally weighted scatterplot smoothing; LOESS was used for all smoothing in this paper). The MAF frequency distribution within the inversions was plotted for the lake and for the stream population displaying the strongest inversion frequency shift from the lake. For this population, we also plotted the genome–wide MAF distribution.

To investigate LD patterns around the three inversions and to refine their physical boundaries, we calculated LD as the correlation among unphased SNP alleles using the R^2 statistic implemented in mcld (Zaykin et al. 2008). Only bi–allelic SNPs with $<25\%$ missing data and individuals with $<50\%$ missing diploid genotype calls were considered. When multiple SNPs were located on sister RAD loci, only a single randomly picked SNP was retained. For the calculation of LD, we applied different MAF filters, including a 0.15 MAF range centered on the MAF peak reflecting the relative frequency of the two variants at each inversion (see MAF analysis above). Patterns of LD around the inversions were visualized using the LDheatmap (Shin et al. 2006) R package for the stream population displaying the strongest inversion frequency shift from the lake (analyzing the other stream populations yielded very similar estimates of the inversion breakpoint positions).

To construct haplotype genealogies for the inversions using individuals from the Lake Constance basin only, we first extracted the SNPs in each inversion, (SNPs closer than 20 kb to the inversion breakpoints identified in the LD analysis above were not considered). Next, we excluded SNPs with a MAF <0.05 and with $>25\%$ missing genotypes. Different MAF ranges (that is, 0.1–0.5 or 0.2–0.4) led to identical conclusions. Individuals with $>75\%$ missing diploid genotypes after removing low–quality SNPs were excluded. When multiple SNPs per sister RAD loci passed the above filters, we only retained the one with the highest MAF (choosing a random SNP yielded similar results). For the largest inversion (located on ChrXXI), we randomly subsampled the resulting SNP panel to a total of 173 SNPs to reduce complexity. Haplotype reconstruction used PHASE 2.1 (Stephens et al. 2001), optimized by specifying the physical position of all polymorphisms and increasing the number of search iterations to >99. Five independent runs were performed with different seeds to confirm consistency among the results. Haplotype alignments were used to infer phylogenetic trees with RAxML v.8.0.0 (Stamatakis 2014), using the GTRCAT model of sequence evolution with rate heterogeneity among sites. Based on sequence alignments and phylogenetic trees, we constructed and visualized haplotype genealogies with Fitchi (Matschiner, M.: Fitchi: Haplotype genealogy graphs based on Fitch distances. http://www.evoinformatics.eu/fitchi, 2015), using a minimal node size of two haplotypes for display (–n option). To construct haplo-

type networks including individuals from across the stickleback's geographic range, we randomly selected 20 SNPs from the Lake Constance–specific haplotype genealogies, and inferred the genotypes at these SNPs for a total of 11 freshwater and 10 marine stickleback specimens (Jones et al. 2012) based on the ENSEMBL and the UCSC Stickleback Genome Browsers. The resulting SNPs (12, 13 and 14 for the ChrI, ChrXI and ChrXXI inversions) were used for haplotype network construction and visualization as described above.

The Lake Constance–specific haplotype networks allowed us to unambiguously infer diploid genotypes at all three inversions for our main study individuals. Of these individuals, 33 had already been RAD sequenced previously using the Sbf1 restriction enzyme (Roesti et al. 2012b), allowing us to determine SNPs on Sbf1 RAD loci diagnostic for the two variants at each inversion. At these diagnostic SNPs, we then determined the diploid genotypes in 27 lake and 27 stream stickleback from the Lake Geneva basin (Berner et al. 2010a). For the stream individuals, Sbf1 RAD data were already available (Chapter 4). For the Lake Geneva individuals, however, RAD sequence data were generated specifically for this study, following the protocol described in (Roesti et al. 2012a). The SNP data from all individuals from the Lake Geneva basin were then used to search for the presence of inversion polymorphisms in this lake–stream system, to determine the frequencies of the inversion types in each population, and additionally to conduct an F_{ST}–based lake–stream genome scan.

To explore the short–term recombination rate at the inversions, we inspected genotype data from an F_2 laboratory intercross (Chapter 4). This revealed that the two parental stickleback individuals used to initiate the cross (a male from Lake Constance and a female from a tributary stream of Lake Geneva) were fixed for different inversion types at the ChrI inversion (but not at the two other inversions). We therefore counted crossovers between SNPs across the ChrI inversion region in all 282 F2 individuals. As a negative control, we did the same around the ChrXI and ChrXXI inversions. To address the theoretical prediction that large inversions should maintain some genetic exchange due to double crossovers (gene conversion is considered less important)(Navarro et al. 1997), we assigned stream individuals from the Lake Constance basin homozygous for one or the other inversion type at the ChrI inversion to separate groups (N = 15 and 20 for the stream and lake inversion type, defined according to Fig. 6.7c). These groups were then used to perform an F_{ST}–based differentiation scan. Additionally, using the same groups, we determined the number and location of loner SNPs specific to each inversion type, or shared between the types, within and around the ChrI inversion. Analogous analyses for the ChrXI and ChrXXI inversions were not possible because here individuals homozygous for the stream

inversion type were too rare (Fig. 6.7c).

6.5 Acknowledgements

6.6 Author contributions

MR designed the study, conducted field sampling, did wet lab work, analysed the data, interpreted and visualized results, and contributed to paper writing. BK did wet lab work and contributed to data analysis. DM conducted field sampling and wet lab work. DB designed the study, conducted field sampling, developed the genotyping pipeline, analysed data, interpreted results and wrote the paper.

Chapter 7

Methane emission by camelids

Authors: Marie T. Dittmann, Ullrich Runge, Richard A. Lang, **DARIO MOSER**, Cordula Galeffi, Michael Kreuzer & Marcus Clauss

Preface: Chapter 7 & 8 are rather 'far'–outreach I must say. Marie, which became a good friend over the years, asked me to help her out on Kamelhof Olmerswil for her llama measurements. During that time she had to attend an advanced training at ETH Zürich, making it impossible for her to do the work by herself.

7.1 Abstract

Methane emissions from ruminant livestock have been intensively studied in order to reduce contribution to the greenhouse effect. Ruminants were found to produce more enteric methane than other mammalian herbivores. As camelids share some features of their digestive anatomy and physiology with ruminants, it has been proposed that they produce similar amounts of methane per unit of body mass. This is of special relevance for country-wide greenhouse gas budgets of countries that harbor large populations of camelids like Australia. However, hardly any quantitative methane emission measurements have been performed in camelids. In order to fill this gap, we carried out respiration chamber measurements with three camelid species (*Vicugna pacos*, *Lama glama*, *Camelus bactrianus*; n = 16 in total), all kept on a diet consisting of food produced from alfalfa only. The camelids produced less methane expressed on the basis of body mass (0.32 ± 0.11 L kg^{-1} d^{-1}) when compared to literature data on domestic ruminants fed on roughage diets (0.58 ± 0.16 L kg^{-1} d^{-1}). However, there was no significant difference between the two suborders when methane emission was expressed on the basis of digestible neutral detergent fiber intake (92.7 ± 33.9 L kg^{-1} in camelids vs 86.2 ± 12.1 L kg^{-1} in ruminants). This implies that the pathways of methanogenesis forming part of the microbial digestion of fiber in the foregut are similar between the groups, and that the lower methane emission of camelids can be explained by their generally lower relative food intake. Our results suggest that the methane emission of Australia's feral camels corresponds only to 1 to 2% of the methane amount produced by the countries' domestic ruminants and that calculations of greenhouse gas budgets of countries with large camelid populations based on equations developed for ruminants are generally overestimating the actual levels.

7.2 Introduction

The quantification and abatement of methane (CH_4) emissions from domestic ruminants have received major attention from the scientific community during the last decades (Johnson and Johnson 1995; Hackstein and van Alen 1996; Beauchemin et al. 2008; Martin et al. 2010) Ruminants digest fibrous carbohydrates by microbial fermentation of plant material in their gastrointestinal tract (Stevens and Hume 1998). One of the side products of this fermentation process is CH_4, a greenhouse gas (GHG) that also represents a loss of energy to the host animal (Johnson and Johnson 1995).

Among mammals, ruminants (*Ruminantia*) produce the highest amounts

of CH_4 in relation to body mass, yet explanations for this finding remain speculative (Franz et al. 2010). Some of the features that characterize ruminants, like the ability to ruminate and a chambered foregut that enables the sorting of food particles according to size, are shared with another artiodactyl suborder, the camelids (*Tylopoda*) (Vallenas et al. 1971; Lechner–Doll and von Engelhardt 1989; von Engelhardt et al. 2006a; Wang et al. 2000). Given these similarities in digestive anatomy and physiology, it has been assumed that camelids produce similar amounts of CH_4 as ruminants when compared at the same body mass range (IPCC 2006; Lerner et al. 1988; Franz et al. 2010) and are thus responsible for the release of significant amounts of this GHG. However, despite the similarities to the ruminant digestive anatomy and physiology, there are some important differences between the two suborders:

1. The camelid foregut can be separated into three compartments (Vallenas et al. 1971; Wang et al. 2000). The first two compartments (C1 and C2) represent a fermentation chamber similar to the reticulorumen of ruminants. The last elongated tubular compartment (C3) shows similarities to the abomasum of ruminants (Wang et al. 2000). Despite structural similarities with the ruminant foregut, the camelid compartments cannot be considered as direct homologues (Vallenas et al. 1971).

2. Camelids have a lower food intake compared to ruminants (Meyer 2010), which corresponds to their lower energy requirements (NRC 2007). This can be interpreted as an adaptation to environments with low resource availability.

3. Food particles are retained longer in the camelid foregut than in the ruminant foregut (Heller et al. 1986a). This could be explained by the lower intake of food, and results in a longer time of fermentation, which is a prerequisite for effective fiber digestion. It has also been suggested that longer particle retention is achieved by the delayed start of rumination after feeding compared to ruminants (von Engelhardt 2006).

4. The mechanism of particle sorting in the forestomach appears to be similarly density–dependent in camelids and ruminants (Lechner–Doll and von Engelhardt 1989). However, some proportions of large particles are found in the last camelid forestomach compartment (C3), where no further breakdown of particles takes place. Large particles are not

found in the distal digestive tract or feces, these large particles need to be returned to the C1/C2 compartments from which they can be re–submitted to further size reduction via rumination (Lechner–Doll and von Engelhardt 1989). This particularity of retaining very large particles in the last compartment could represent a limitation for food intake.

5. Camelids were reported to have a higher efficiency in dry matter and fiber digestion than ruminants (Hintz et al. 1973; Kayouli et al. 1993; Dulphy et al. 1997; Sponheimer et al. 2003). This is probably achieved by a longer retention of particles and not by different fermentation pathways, as composition of the microbial community in the camel gut resembles the one in ruminants (Ghali et al. 2004, 2011). The longer particle retention and the consequently longer exposition to microbial fermentation could result in a higher CH_4 production per unit food ingested when compared to ruminants.

Taken together, there are notable differences in the anatomy and physiology of the digestive tract between camelids and ruminants, which may influence microbial CH_4 production. Relatively little is known about CH_4 emission by camelids. Hackstein and Van Alen 1996 detected methanogenesis in the feces of Bactrian camels (*Camelus bactrianus*), alpacas (*Vicugna pacos*) and guanacos (*Lama guanaicoe*). A study on methanogenic archeae in the alpaca foregut revealed the presence of *Methanobrevibacter* strains, which are the most common methanogens in ruminants, at similar densities as reported for ruminants (St–Pierre and Wright 2012). The occurrence of production of enteric CH_4 was confirmed for dromedaries (*Camelus dromedarius*) (Schulze et al. 1997; Guerouali and Laabouri 2013), llamas (*Lama glama*) (Carmean et al. 1992; Vernet et al. 1997) and alpacas (Pinares–Patiño et al. 2003, 2009; Liu et al. 2009a, 2009b).

Including livestock emissions into global GHG surveys revealed that enteric fermentation, mostly of ruminants, contributes approximately 20 to 25% to the observed increase in atmospheric CH_4 (Lassey 2007). Such estimates are generally developed based on equations for ruminants and animal population sizes of the respective countries (IPCC 2006). Therefore, specific data for CH_4 emission from camelids are interesting for calculating GHG budgets of countries that harbor large populations of camelids like several African and South American countries as well as Australia (Saalfeld and Edwards 2010; FAO 2013).

To fill this gap of knowledge, we measured CH_4 emission in three camelid species and compared them with literature data from ruminants. Our hypotheses were that (i) camelids produce less CH_4 than ruminants per kg of

body mass (BM) because it is known that their food intake per capita is lower than that of ruminants of similar size (NRC 2007; Meyer et al. 2010). Given the longer time of particle retention camels (Heller et al. 1986a), which results in a longer time available for fermentation of the digesta and, thus, in a higher nutrient digestibility (Hintz et al. 1973; Kayouli et al 1993; Dulphy et al. 1997), (ii) CH_4 production per unit food ingested was expected to be higher in camelids than in ruminants. The same was expected for methane expressed as percentage of digestible energy intake (DEI) as a higher digestibility might result in a production of higher amounts of CO_2 and H_2, the substrates for CH_4. This has already been shown in sheep (Blaxter and Clapperton 1965) (iii). As fiber is the main substrate for methanogens (Moe and Tyrell 1979), CH_4 emission should be determined especially by the amount of digestible fiber ingested by the animal. Despite the differences in digestive anatomy and physiology between ruminants and camelids, we further assumed that the process of fiber digestion itself and the pathways of methanogenesis are similar in both groups and that, therefore, (iv) camels produce the same amount of CH_4 when expressed on a basis of digestible neutral detergent fiber intake (dNDFI).

7.3   Material and methods

7.3.1   Ethics statement

Animal trials in this study were approved by the Kantonales Veterinäramt Zürich, Switzerland, and took place under the Swiss Cantonal Animal Experiment Licence no. 142/2011.

7.3.2   Study species

Measurements were carried out on three camelid species that were chosen to cover a range of body mass corresponding that of domestic ruminants. The smaller two species, alpacas and llamas, belong to the SAC. Despite uncertainties about their taxonomic affiliations, llamas and alpacas are considered to be the domesticated forms of the guanaco (*Lama guanicoe*) and vicugna (*Vicugna vicugna*), originating in the Andean region (Wheeler 1995). The third species selected was the Bactrian camel, the largest member of this suborder, which was originally distributed over the Asian continent, while nowadays only few remaining free–ranging individuals roam small desert areas in Mongolia and China (Tulgat and Schaller 1992).

Table 7.1: Nutrient composition of the diet items used in the present study (in g/kg dry matter and MJ/kg dry matter for GE).

Diet item	Species	TA	CP	EE	CF	NDF	ADF	ADL	GE
Alfalfa hay	Alpaca	8.3	14.8	1.0	37.8	58.5	38.5	8.4	18.3
	Llama	9.6	13.3	0.9	40.0	59.2	44.6	9.2	18.1
	Bactrian camel	9.6	16.3	1.0	41.4	56.2	45.6	9.9	17.9
Alfalfa pellets*	All camelids	11.9	16.6	1.6	26.6	40.8	33.3	7.9	18.3

TA total ash, CP crude protein, EE ether extracts, CF crude fiber, NDF neutral detergent fiber, ADF acid detergent fiber, ADL acid detergent lignin, GE gross energy.
*No. 2805, Provimi Kliba SA, Kaiseraugst, Switzerland.

7.3.3   Respiration measurements

Five alpacas kept at Zoo Zürich, and six llamas and five Bactrian camels kept on a private camel farm in Switzerland were separated and kept in individual pens. Animals had access to a diet consisting of alfalfa hay provided at *ad libitum* access and a limited amount of alfalfa pellets (Table 7.1). Alfalfa pellets made up 53±10, 33±6 and 21±2% of DMI in alpacas, llamas and Bactrian camels respectively. They had unrestricted access to water. Details on the experimental animals are given in Table 7.2.

In order to determine DMI, digestible NDF intake (dNDFI), and DEI, food supply, refusal and feces amounts were weighed daily during one week before the CH_4 measurements, and representative samples were taken. After the animals were weighed on a mobile scale (alpacas) or a truck scale (llamas, Bactrian camels), they were put separately into the respiration chambers for one 24 h period. For the alpacas, a transport box of a size of 1.9×0.7×1.3 m was used as chamber, for the llamas and the Bactrian camels a part of a building was separated by wooden panels to build boxes of 2.9×1.6×2.4 m and 4.5×2.9×2.4 m, respectively. To prevent air leaks, the chambers were sealed with plastic foil (Building and covering film, 0.2 mm, Folag AG Folienwerke, Sempbach, CH), silicone and tape. In the chambers the animals also had free access to alfalfa hay and water, and a limited amount of alfalfa pellets.

Chambers were fitted with a series of air inlets at the bottom and a series of air outlets at the top of the chamber, that were connected to an air pump (Flowkit 500, Sable Systems, Las Vegas, USA), which ensured a slight under–pressure in the chamber and constant flow rates of 48 to 72 L min^{-1} for alpacas, 116 to 148 L min^{-1} for llamas and 362 to 460 L min^{-1} for Bactrian camels, respectively. Levels of CH_4, oxygen, carbon dioxide, water vapor pressure and barometric pressure were measured by gas analyzers (MA–10 and Turbofox, Sable Systems) from ambient air and air sampled from the chambers at alternating intervals of 90 seconds each. Wash out times for the system ranged at 10 seconds and readings were corrected for this time

Table 7.2: Animals used in the present study and individual data on body mass, food and digestible energy intake, and methane production.

Species	Age	Sex	BM	DMI	NDFI	dNDFI	DEI	CH₄				Estimate based on Kirchgessner et al.*	Ratio measured to estimated	Ratio to CO₂ produced
								L d⁻¹	L kg⁻¹ DMI	% DEI	L kg⁻¹ dNDFI			
	y		kg	kg d⁻¹	kg d⁻¹	kg d⁻¹	MJ d⁻¹					L d⁻¹		
Vicuna pacos	2	F	50	0.9	0.4	0.2	9.6	13.1	14.7	5.2	9.4	64.2	0.20	0.084
Vicuna pacos	4	F	53	1.3	0.6	0.4	15.3	33.2	26.1	8.4	23.8	74.5	0.45	0.100
Vicuna pacos	3	F	64	1.0	0.4	0.1	8.6	27.1	27.7	12.2	19.4	66.0	0.41	0.082
Vicuna pacos	15	F	71	1.4	0.6	0.3	16.0	22.1	15.9	5.3	15.8	75.7	0.29	0.102
Vicuna pacos	10	M	79	1.2	0.5	0.2	12.1	17.3	15.0	5.5	12.4	70.0	0.25	0.081
Lama glama	4	F	110	2.3	1.1	0.6	24.2	51.1	22.3	8.1	36.6	99.1	0.52	0.082
Lama glama	7	M	140	2.2	1.0	0.5	20.4	41.1	19.1	7.8	29.4	95.2	0.43	0.068
Lama glama	4	F	140	2.4	1.2	0.6	24.1	48.1	19.9	7.7	34.4	102.0	0.47	0.074
Lama glama	11	M	150	1.9	0.9	0.3	15.6	47.5	24.6	11.7	34.0	89.2	0.53	0.075
Lama glama	5	F	160	2.5	1.3	0.6	24.2	46.5	18.3	7.4	33.3	105.7	0.44	0.084
Lama glama	7	M	190	3.4	1.8	0.9	34.6	71.0	20.8	7.9	50.8	128.7	0.55	0.088
Camelus bactrianus	13	M	590	9.4	4.8	2.2	89.0	154.2	16.4	6.7	110.4	284.6	0.54	0.080
Camelus bactrianus	5	M	600	9.3	4.8	2.0	84.6	185.5	20.0	8.5	132.8	282.0	0.66	0.086
Camelus bactrianus	6	M	640	8.6	4.4	1.8	80.4	117.8	13.8	5.6	84.3	262.1	0.45	0.069
Camelus bactrianus	7	M	700	7.5	3.9	1.5	65.0	131.3	17.5	7.8	94.0	233.7	0.56	0.084
Camelus bactrianus	7	F	760	7.9	4.2	1.7	73.9	154.5	19.5	8.1	110.6	244.6	0.63	0.070

BM body mass, DMI dry matter intake, NDFI neutral detergent fiber intake, dNDFI digestible neutral detergent fiber intake, DEI digestible energy intake, y years, F female, M male. *Estimated based on a regression equation developed from domestic ruminants that uses information about diet nutrient composition (see Methods).

lag. For data analysis, we only used measurements recorded after gas levels in the chamber had reached a stable plateau, which occurred 60 to 150 min after the animals had been placed in the boxes. Animals were under constant monitoring throughout the measurements.

Gas analyzers were calibrated prior to each measurement by using pure nitrogen and a calibration gas (PanGas, 19.91% O_2, 0.51% CO_2, 0.49% CH_4 dissolved in nitrogen). Data obtained by the respiratory system were analyzed with the software ExpeData (Sable Systems) where the mean CH_4 concentration was calculated and corrected for CH_4 concentration in ambient air, partial pressures of oxygen, carbon dioxide and water vapor as well as barometric pressure.

7.3.4 Sample analysis

Nutrient contents of the samples from food, refusals and feces were analyzed using standard procedures (AOAC 1997; Van Soest et al. 1991). All samples were oven–dried at 65 °C and ground to 0.75 mm with a mill (Retsch GmbH, Haan, Germany). Samples were analyzed for dry matter content by drying at 103 °C to constant weight. Gross energy (GE) was determined by bomb calorimetry (IKA–Calorimeter C4000, Ika, Stauffen, Germany). Total ash (TA) was analyzed using a muffle furnace (Naumann and Bassler 1976). For determinations of nitrogen by the Dumas method, an Elementar rapid N III Analyzer (Elementar Analysensysteme, Hanau, Germany) was used. Crude protein (CP) was calculated as 6.25×N (Robbins 1993). Crude fiber (CF), NDF (after treatment with α–amylase), ADF and ADL contents were determined using the Fibertec System M (Tecator, 1020 Hot Extraction, Flawil, Switzerland; AOAC 962.09). The fiber data were corrected for ash content. Ether extract (EE) was analyzed with a Soxhlet extractor system (Extraktionsapparatur B–811, Büchi, Flawil, Switzerland; AOAC 963.15). Nitrogen free extract (NfE) was calculated as 100 – TA (%) – CP (%) – EE (%) – CF (%).

Nutrient data were used to predict the expected amount of CH4 produced by domestic cattle on the corresponding diet using the equation of Kirchgessner et al. 1991: CH_4 (g d^{-1}) = 63 + 80×CF (kg d^{-1}) + 11×NfE (kg d^{-1}) + 19×CP (kg d^{-1}) – 195×EE (kg d^{-1}).

7.3.5 Literature data

Apart from the scarce CH_4 data on camelids, where the animals had received a roughage–only diet, literature data were collated from the three most common domestic ruminant species, i.e. cattle (*Bos taurus* and *Bos indicus*),

sheep (*Ovis aries*) and goat (*Capra hircus*). Only measurements that could be related to BM, DMI, and, if possible, DEI and dNDFI (see Table S6 (Supplementary material) for data and sources) were used. Because of the differences in the level of detail reported in the various literature sources, the corresponding datasets differed distinctively in sample size. We only selected data from animals that were fed on roughage to allow comparison to the data obtained from our respiration measurements, and to broadly exclude the effect of diet (as in roughage vs concentrate feeds). Only data obtained by measurements in respiration chambers were used.

7.3.6 Statistical evaluation

In order to investigate how much CH_4 camelids produce in relation to domestic ruminants, we applied general linear models (GLM) with CH_4 production (L per day, L per kg DMI, % of DEI, and L per kg dNDFI) as the dependent variable, and body mass, suborder (SO, ruminant or camelid) and, when available for the majority of the data points within a dataset, NDF content of the diet as fixed effects. The interaction between BM and SO was also included as fixed effect, but was removed from the model when it was not statistically significant. In the case of a significant interaction, we performed separate analyses on two subgroups of different body mass ranges consisting of alpaca and llama (SAC) in comparison to sheep and goats (subgroup: small) and Bactrian camels in comparison to cattle (subgroup: large) by applying either GLMs or, when there was no significant effect of BM, Wilcoxon ranked sum tests. Analyses were carried out with lntransformed values for BM and the dependent variables.

In addition to that, we tested whether the data obtained by our camelid measurements were actually in the range that would be expected for ruminants on the experimental diet by subjecting our data to the equation of Kirchgessner et al. 1991 and by applying a Mann–Whitney–U–test to compare the correspondingly estimated data with the measured data. In order to test whether CH4 emissions correlate with indicators of energy metabolism, we incorporated emissions of CH_4 and CO_2 (L d^{-1}) into a linear model and calculated the average ratio of CH_4:CO_2 to compare it to ruminant values from the literature. All statistical tests were carried out with R 3.0.2 (R Core Team 2012) and significance levels were set to $\alpha = 0.05$, with values between 0.05 and 0.10 considered as trends.

7.4　Results

The dataset on CH_4 in L d^{-1} contained 18 camelid and 48 ruminant data points. In this dataset, the interaction of body mass and suborder (BM×SO) was significant ($F_{1,65} = 8.40$; P = 0.005), which is why the two animal subgroups (small and large) were tested separately. For the smaller animals, there was no significance for the interaction of BM×SO but an effect of BM ($F_{1,49} = 40.80$; P < 0.001) and a trend ($F_{1,49} = 3.42$; P = 0.071) towards lower CH_4 emission from the SAC compared to the smaller ruminants. Within the larger animals, camels produced significantly less CH_4 per day than cattle (W = 2; P = 0.002) (Fig. 7.1; Table 7.3 for means). The dietary NDF contents were available for 17 camelid and 18 ruminant data points in this dataset. The analysis of this reduced dataset revealed that the NDF content of the diet was no significant covariable ($F_{1,34} < 0.001$; P = 0.99).

The dataset on CH_4 in L per kg DMI contained 18 camelid and 34 ruminant data points. In this dataset, there was an interaction of BM×SO ($F_{1,51} = 5.58$; P = 0.022). Testing the two subgroups separately revealed no effect of BM in SAC ($F_{1,39} < 0.001$; P = 0.987), and lower CH_4 emissions per kg DMI in both large and small camelids compared to ruminants (small: W = 73; P = 0.005; large: W = 0; P < 0.001). Dietary NDF contents in this dataset were available for 17 camelid and 18 ruminant data points. In this reduced dataset, NDF content of the diet was a significant covariable ($F_{1,34} = 2.67$; P = 0.012), suggesting that in the case of expressing CH_4 per DMI the difference between the suborders is due to the different fiber levels of the forages used in the experiments evaluated. In this context, the NDF content in the diet was on average higher in ruminants (59%) than in camelids (50%) (W = 71; P = 0.007).

The dataset on CH_4 in % DEI contained 17 camelid and 23 ruminant data points. In this dataset, there was no BM×SO interaction ($F_{1,39} = 0.24$; P = 0.625) and no effect of BM ($F_{1,39} = 0.05$; P = 0.827). Methane emissions in % DEI were lower in camelids than in ruminants (W = 59; P < 0.001). Dietary NDF contents in this dataset were available for 17 camelid and 12 ruminant data points and proved to be a significant covariable ($F_{1,28} = 16.2$; P < 0.001). This again suggests that when expressing CH_4 per DEI, any difference between animals is due to the fiber content of the forages used in the experiments. In this dataset, NDF content in the diet was on average 57% in ruminants and 50% in camelids (W = 152; P = 0.028).

The dataset on CH_4 per kg dNDFI contained 17 camelid and 10 ruminant data points. In this dataset, there was no interaction of BM×SO ($F_{1,23} = 0.19$; P = 0.663) and no effects of BM ($F_{1,23} = 0.47$; P = 0.501) and NDF content ($F_{1,23} = 0.01$; P = 0.927). There were also no differences between
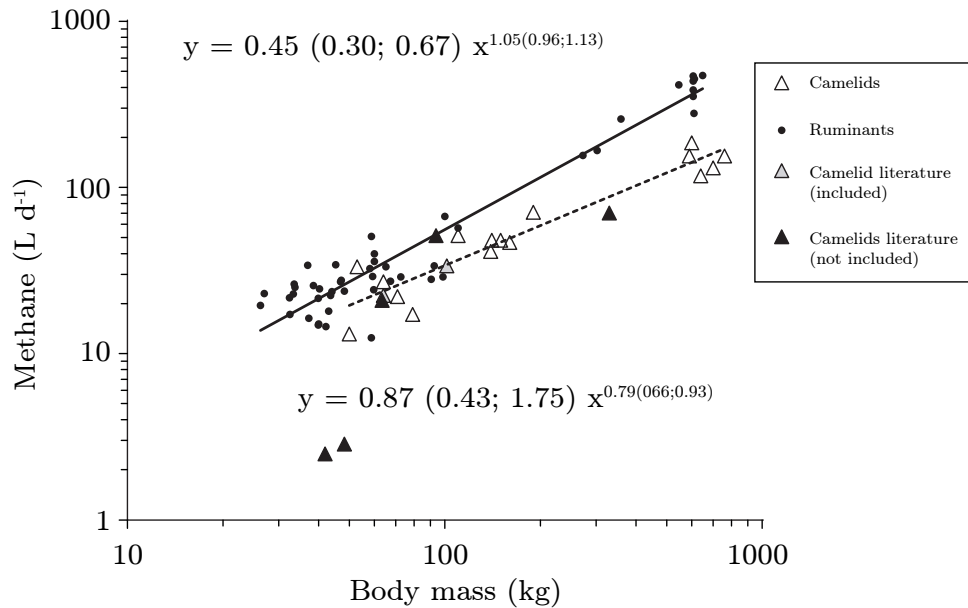
Figure 7.1: Methane emission in L d^{-1} of domestic ruminants (literature data) and camelids (own measurements, literature data included in the regression analysis and literature data not included due to differences in methodology) in relation to body mass. 95% confidence intervals of the regression lines are given in brackets. R^2 values of the regression lines are 0.93 for ruminants and 0.91 for camelids. For data sources see Table S6 (Supplementary material).

ruminants and camelids (W = 83; P = 0.941) (Fig. 7.2).

In order to test whether the sample of the domestic ruminants influenced the results, we repeated all analyses (for CH_4 per kg BM, per kg DMI and in % DEI) using only the 10 data points for domestic ruminants for which data in CH_4 per kg dNDFI were available. The outcome did not differ from the results based on the larger datasets.

The amount of CH_4 measured from the Bactrian camels in this experiment on average amounted only to 46% of the CH_4 production estimated from the equation derived from ruminant data (Kirchgessner et al. 1991) (U = 0; P < 0.001). This was very similar to the difference found in absolute CH_4 production in the larger animals, where Bactrian camels produced 47.5% of the level of CH_4 production described for cattle in L d^{-1}. The CH_4 emission of the camelids correlated highly with CO_2 emissions ($R^2 = 0.98$; P < 0.001) and the CH_4:CO_2 ratio was 0.082±0.010.
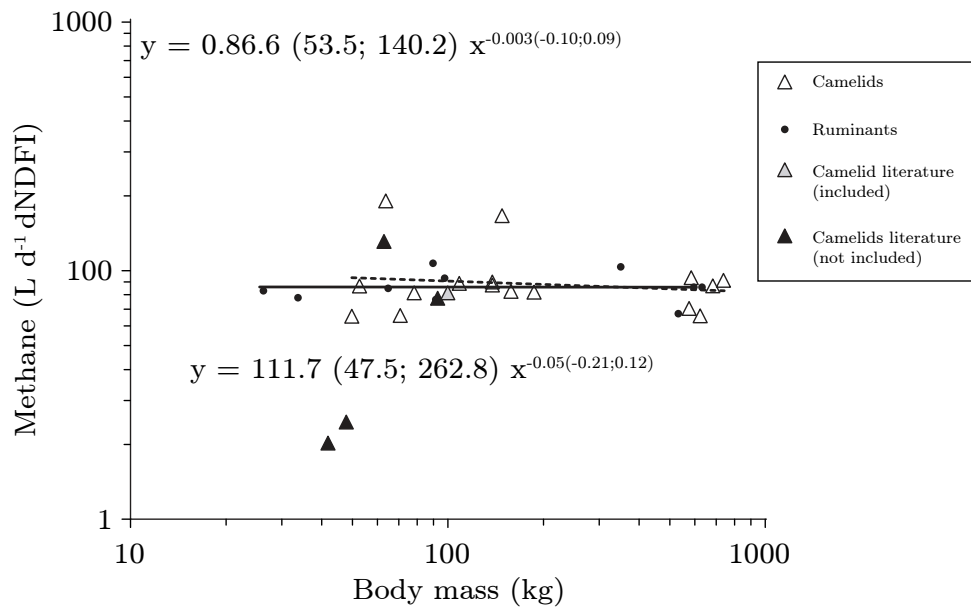
Figure 7.2: Methane emission in L per kg digestible neutral detergent fiber intake (dNDFI) of domestic ruminants (literature data) and camelids (own measurements, literature data included in the regression analysis and literature data not included due to differences in methodology) in relation to body mass. 95% confidence intervals of the regression lines are given in brackets. R^2 values of the regression lines are 0.02 for ruminants and <0.001 for camelids. For data sources see Table S6 (Supplementary material).

7.5 Discussion

7.5.1 Level of methane emissions by camelids

Only few comparable literature data on CH_4 emissions by camelids are available for inclusion into the overall analysis. To the knowledge of the authors, no CH_4 measurements have been obtained in Bactrian camels before. We are aware that limiting measurements to 24 h, as done for the animals in the present study, might be somewhat biased due to variation between days in physical condition, feeding behavior or stress of the animals remaining unaccounted for. However, literature data on CH_4 measurements obtained in llamas (Vernet et al. 1997) and alpacas (Pinares–Patiño et al. 2013) kept on a roughage–only diet were incorporated in our analysis and turned out to be in the range of the values measured in this study, indicating the reliability of data derived under similar conditions from respiration measurements. Besides these scarce data, some CH_4 measurements in camelids have been published that were not obtained by chamber respirometry or not on a roughage–only diet (Carmean et al. 1992; Pinares–Patiño et al. 2003; Liu et

al. 2009a, 2009b; Guerouali and Laabouri 2013). Despite the different measurement conditions, these values are mostly consistent in magnitude with our measurements (Fig. 7.1 and 7.2).

7.5.2 Methane emissions by camelids in comparison to ruminants

Our evaluation demonstrated that camelids produce less CH_4 than ruminants when expressed on a basis of BM, but that CH_4 production does not differ when expressed on a basis of digestible NDF intake. The differences observed in CH_4 production between suborders when expressed per unit of dry matter or digestible energy intake are most likely due to the disparity in average fiber contents of the forages fed in the studies evaluated to either camelids (lower in fiber content) or ruminants. Total CH_4 production per day in camelids, expressed per kg body mass, were on average only 56% of that reported for ruminants. In contrast, when expressed per unit of dry matter intake, camelid CH_4 production was on average 73% of that in ruminants, which mirrors the lower fiber content of the diet the camelids received compared to the ruminants. In contrast to our prediction, the putatively higher digestive efficiency of camelids did not lead to higher methane values when expressed per unit food intake.

The least biased variable to compare methanogenesis from nutrient digestion is the amount of CH_4 produced per unit of NDF digested. Because, in ruminants, methane is formed from CO_2 and H_2, which are products of microbial fermentation of carbohydrates (Moss et al. 2000; Morgavi et al. 2010), fiber is considered the major substrate for methanogenesis (Moe and Tyrell 1979). Analyzing CH_4 produced per unit of NDF digested excludes other influences on digestive efficiency, such as different fermentation conditions or a different digesta passage rate. Indeed, from the present evaluation it is obvious that camelids produce as much CH_4 per unit of digestible NDF as ruminants. This suggests that the pathways of methanogenesis via microbial fermentation might not differ between the two suborders. Differences between suborders in the amount of CH_4 produced therefore reflect the amount of fiber the animal digested, which in turn is determined by the general intake level. The most likely explanation for the lower absolute CH_4 production in camelids, therefore, is their generally lower metabolism associated with lower nutrient requirements and thus a lower food intake per unit of body mass (NRC 2007; Meyer et al. 2010). This can be assumed to reflect an adaptation to environments characterized by low resource availability. A low metabolism and intake is also indicated by a low CO_2 production per

Table 7.3: Data on average CH_4 production of camelids and ruminants obtained by respiration measurements sorted by animal size. SA camelids stands for South American camelids

Group		Mean BM (SD); n	Mean CH_4 production (SD); n			
		kg	L d^{-1} kg BM^{-1}	L kg DMI^{-1}	% DEI	L kg dNDFI^{-1}
All	Camelids	259($\pm$260);18	0.32($\pm$0.11);18	20.1($\pm$4.4);18	8.0($\pm$2.3);17	92.7($\pm$33.9);17
	Ruminants	161($\pm$211);48	0.58($\pm$0.16);48	28.1($\pm$6.0);34	11.7($\pm$2.8);23	86.2($\pm$12.1);10
Small	SA camelids	106($\pm$46);13	0.35($\pm$0.10);13	21.2($\pm$4.6);13	8.3($\pm$2.6);12	97.4($\pm$39.1);12
	Sheep & goats	53($\pm$22);37	0.55($\pm$0.17);37	26.4($\pm$5.1);24	11.6($\pm$2.4);17	86.8($\pm$11.5);6
Large	Bactrian camels	658($\pm$72);5	0.23($\pm$0.05);5	17.4($\pm$2.5);5	7.3($\pm$1.1);5	81.5($\pm$12.7);5
	Cattle	525($\pm$140);11	0.66($\pm$0.10);11	32.0($\pm$6.6);10	12.0($\pm$4.2);6	85.3($\pm$14.9);4

Note that sample size corresponds to the number of individuals used for measurements in the present study but to means from different publications for ruminants. Data sources are Table 7.2 for the present study and in Table S6 (Supplementary material) for literature data. BM body mass, DMI dry matter intake, DEI digestible energy intake, dNDFI digestible neutral detergent fiber intake.

unit of BM. Therefore a similar CH_4:CO_2 ratio can be expected in camelids and ruminants, which was actually the case. Levels reported for ruminants are ranging between 0.050 and 0.096 (Sauer et al. 1998; Madsen et al. 2010; Lassen et al. 2012; Hellwing et al. 2013) compared to the average of 0.082 found in the camelids of the present study.

7.5.3 Implications of the findings of low methane emissions by camelids

Methane production estimates for camelids, derived from an often–used equation developed for ruminants based on nutrient composition of the diet (Kirchgessner et al. 1991), were more than twice as high as the actually measured methane amounts. Therefore, this and similar equations do not seem appropriate to predict CH_4 emissions of camelids. Even conventional estimates based on the IPCC (IPCC 2006) default equation based on Ym (the ratio of CH_4 energy to GE intake) are often applied incorrectly because the proportionately lower GE intake as a consequence of the camelids' lower food intake is not considered. This is important when calculating GHG budgets for countries that harbor large populations of camelids, such as in northeastern Africa, South America (FAO 2013) or Australia (Saalfeld and Edwards 2010). In general, equations developed for livestock to estimate CH_4 emissions from any non–domestic species have to be applied carefully and assessments should rather rely on specific measurements.

Numerous approaches have recently been considered to reduce the contribution of enteric CH_4 from livestock to the greenhouse effect. Among others, the mitigation of emissions from introduced feral one–humped camels has been discussed in Australia, a country that harbors the fifth largest population of dromedaries in the world (Zeng and McGregor 2008). The increasing

negative impacts of these non–endemic animals on the Australian ecosystem initiated the search for appropriate management solutions (Coventry et al. 2010; McGregor and Edwards 2010). Statements that camels emit large amounts of CH_4 and thereby intensively contribute to the GH effect (Northwest Carbon Pty Ltd 2011) promoted calls for large–scale culling of these animals. However, the assumptions made concerning methane emission from the camels were based on estimates following the IPCC guidelines for national GHG inventories (IPCC 2006), with their limited applicability for camelids. While there is little doubt that the culling of any herbivore will reduce GHG emissions, the quantity of that reduction must be balanced against the costs of the culling. Our data suggest that a 570 kg dromedary emits approximately 131 L CH_4 d^{-1}, i.e. less than half as much as cattle of a similar size (approx. 357 L d^{-1}). This corresponds to an annual amount of 36 kg CH_4 per camel, which is clearly below the 46 kg assumed by Gibbs and Johnson 1994 for a camel of the same weight and the 58 kg assumed by Crutzen et al. 1986. In total, Australia harbors 28.4 million cattle, 75.7 million sheep (Australian Bureau of Statistics 2013) and 1 million feral dromedaries (Saalfeld and Edwards 2010). This is equivalent to an estimated annual amount of 4'500 billion L CH_4 emissions from the domestic ruminants and only 48 billion L produced by the dromedary population. Culling of all feral camels would thus have a similar effect as reducing the livestock ruminant population by 1 to 2%. However, other detrimental impacts caused by the feral camels on the Australian environment underline the continued importance of management strategies.

7.5.4 Conclusions

Methane emission was measured from three camelid species, including, for the first time, Bactrian camels. Our findings indicate that, in absolute values, camelids produce clearly less CH_4 than ruminants, and that this difference is most likely due to the generally reduced metabolism, food and (digestible) fiber intake of this group. Therefore, when calculating GHG budgets, equations developed for ruminants are not applicable for the estimation of CH_4 emissions from camelids.

7.6 Acknowledgments

during the sampling period, Carmen Kunz, Muna Merghani and Elisabeth Wenk for sample analysis.

7.7   Author contributions

Conceived and designed the experiments: MC MK. Performed the experiments: MTD, UR, RAL, DM, CG and MC. Analyzed the data: MTD and MC. Wrote the paper: MTD and MC. Manuscript review: UR, RAL, DM, CG and MK. Animal husbandry: UR, RAL and DM.

Chapter 8

Digesta retention patterns of solute and different–sized particles in camelids compared with ruminants and other foregut fermenters

Authors: Marie T. Dittmann, Ulrich Runge, Sylvia Ortmann, Richard A. Lang, **Dario Moser**, Cordula Galeffi, Angela Schwarm, Michael Kreuzer & Marcus Clauss

8.1 Abstract

The mean retention times (MRT) of solute or particles in the gastrointestinal tract and the fore–stomach (FS) are crucial determinants of digestive physiology in herbivores. Besides ruminants, camelids are the only herbivores that have evolved rumination as an obligatory physiological process consisting of repeated mastication of large food particles, which requires a particle sorting mechanism in the FS. Differences between camelids and ruminants have hardly been investigated so far. In this study we measured MRTs of solute and differently sized particles (2, 10, and 20 mm) and the ratio of large–to–small particle MRT, i.e. the selectivity factors ($SF_{10/2mm}$, $SF_{20/2mm}$, $SF_{20/10mm}$), in three camelid species: alpacas (*Vicugna pacos*), llamas (*Llama glama*), and Bactrian camels (*Camelus bactrianus*). The camelid data were compared with literature data from ruminants and non–ruminant foregut fermenters (NRFF). Camelids and ruminants both had higher $SF_{10/2mm}$FS than NRFF, suggesting convergence in the function of the FS sorting mechanism in contrast to NRFF, in which such a sorting mechanism is absent. The $SF_{20/10mm}$FS did not differ between ruminants and camelids, indicating that there is a particle size threshold of about 1 cm in both suborders above which particle retention is not increased. Camelids did not differ from ruminants in MRT_{2mm}FS, MRT_{solute}FS, and the ratio MRT_{2mm}FS/MRT_{solute}FS, but they were more similar to 'cattle–' than to 'moose–type' ruminants. Camelids had higher $SF_{10/2mm}$FS and higher $SF_{20/2mm}$FS than ruminants, indicating a potentially slower particle sorting in camelids than in ruminants, with larger particles being retained longer in relation to small particles.

8.2 Introduction

The digestive strategy of non–ruminant foregut fermenters has historically been considered 'ruminant–like' (e.g., Moir et al. 1954; Bauchop and Martucci 1968), but the process of rumination clearly sets ruminants apart from non–ruminant foregut fermenters (Fritz et al. 2009; Schwarm et al. 2009a; Clauss et al. 2010). True rumination has evolved in only two artiodactyl lineages, the ruminants and the camelids, while sporadic regurgitation and repeated mastication of stomach contents (merycism) have been reported in a variety of mammals such as koala (*Phascolarctos cinereus*) (Logan 2001, 2003), macropods (Moir et al. 1956; Mollison 1960; Barker et al. 1963; Hendrichs 1965), hyrax (*Procavia capensis*) (Hendrichs 1965), capybara (*Hydrochoerus hydrochaeris*) (Lord 1994), and proboscis monkeys (*Nasalis larvatus*) (Matsuda et al. 2011, 2014). In contrast to merycism, rumination is an

obligatory, regular behavioural and physiological process (Gordon 1968) that is characterised not only by 'repeated mastication' but also by a density–dependent sorting mechanism in the fore–stomach (FS) of ruminants and camelids (Lechner–Doll et al. 1991). This mechanism is absent in non–ruminant foregut fermenters (Schwarm et al. 2008, 2009b, 2013). In ruminants and camelids, this mechanism ensures that only those particles are ruminated that require further comminution.
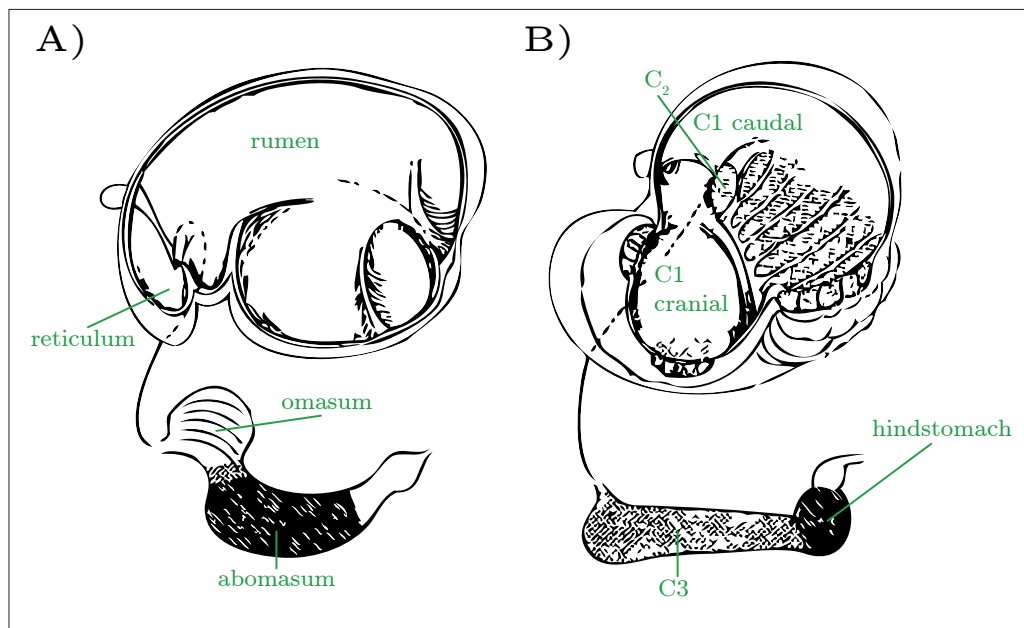

Figure 8.1: Schematic comparison of the morphology of the fore–stomach complex (viewed from its left side, with parts that cannot be viewed from the left displaced underneath) in A) ruminants and B) camelids (Lechner–Doll et al. 1995). The ruminant fore–stomach consists of the rumen (with various sub–compartments), the reticulum, the omasum and the abomasum. The reticulum and omasum are linked by the reticulo–omasal orifice. The camelid fore–stomach consists of the first compartment (C1, with a cranial and a caudal sub–compartment and typical 'glandular sacs'), the second compartment (C2, also sometimes referred to as the 'reticulum', also containing 'glandular sacs') and a third compartment (C3, consisting of a cranial part and a caudal 'hindstomach'). The C2 and the C3 are linked by a small tubular canal. White surfaces represent a stratified epithelium (in the case of ruminants, with papillae in the rumen and the typical honeycomb cells in the reticulum), dotted areas represent cardiac glands (covering the 'glandular sacs' and the cranial portion of C3), and striped areas represent acid–secreting glandular stomach epithelium.

While camelids and ruminants both ruminate, several differences set these groups apart: different chewing motions during rumination (Hendrichs 1965), the different design of the FS (Langer 1988) (Fig. 8.1), and different FS motility patterns (Heller et al. 1984, 1986a). More generally, camelids have a lower

metabolic rate (measured, e.g., via oxygen consumption) and a lower food intake than ruminants of comparable body size (Dittmann et al. 2014). The latter aspect might be related to the longer digesta retention times found in camelids (Heller et al. 1986b). In ruminants, the reticulo–omasal orifice represents a clear demarcation line before which particle sorting takes place in the reticulum, and beyond which only small particles are found (Clauss et al. 2009a, b). In camelids, particle sorting takes place in compartment C2 that is sometimes also referred to as a 'reticulum' (Langer 1988). The connection between the C2 ('reticulum') and the C3 (the 'gastric tube') is not an orifice but a short tubular canal (Vallenas et al. 1971; Langer 1988). Potentially, this canal does not represent as clear a point of demarcation as the reticulo–omasal orifice in ruminants, because large particles have been found beyond this point in the proximal part of the third compartment (Lechner–Doll and von Engelhardt 1989). These large particles are presumably transported backwards into the C2. Hence, it has been suggested that the sorting mechanism in the FS of camelids is less efficient than in ruminants and that the emptying of the FS is too slow to allow similarly high relative food intakes as those observed in some ruminant species (Clauss et al. 2010). The retention of solute as well as small and large particle markers has been investigated in camelids (Heller et al. 1986b, c; Lechner–Doll et al. 1990; Cahill and McBride 1995; von Engelhardt et al. 2006b), and a sorting mechanism in the FS, as reflected by longer retention of larger as compared with smaller particles, has been demonstrated (Heller et al. 1986b, c; Lechner–Doll et al. 1990). So far, comparative studies of retention times in ruminants and camelids are lacking. In ruminants, marked differences between species occur with respect to the retention of solute and particle markers (Dittmann et al. 2015). The efficacy of the ruminant sorting mechanism, however, is not affected by such species differences (Lechner et al. 2010). Furthermore, while the sorting mechanism of ruminants differentiates between small (<2 mm) and larger (10 mm) particles, it does not further differentiate between large particle–size classes (10 vs 20 mm) (Schwarm et al. 2009c; Lechner et al. 2010). To our knowledge, it has not yet been investigated whether the sorting mechanism in the FS of camelids is not only qualitatively, but also quantitatively similar to that in ruminants.

The aim of this study was to assess the retention patterns of solutes and differently sized particles in three camelid species, to compare retention times and the sorting mechanism within camelids, and with ruminants and non–ruminant foregut fermenters.

8.3 Material and methods

8.3.1 Animals and husbandry

The measurements were approved by the Cantonal Veterinary Office Zürich and took place under the Swiss Cantonal Animal Experiment Licence no. 142/2011 in the framework of a comprehensive experiment using respiration chambers to determine metabolic rates (Dittmann et al. 2014) and methane production (Chapter 7) in three camelid species. All experimental animals were adult and included representatives of Bactrian camels (*Camelus bactrianus*, n = 5) and llamas (*Lama glama*, n = 6) kept on a private farm in Switzerland, and alpacas (*Vicugna pacos*, n = 5) kept at Zoo Zürich. Prior to the experiment the animals were acclimated to a diet consisting of lucerne hay provided *ad libitum* and a limited amount of lucerne pellets (for a detailed nutrient analysis of diets, see Dittmann et al. 2014). The pellets eventually made up 53, 33, and 21% of total dry matter intake (DMI) in alpacas, llamas and Bactrian camels, respectively. In order to ensure comparable ad libitum intakes in all species, alpacas received a higher proportion of pellets because the voluntary daily intake of lucerne hay (per unit metabolic body mass) was comparably low in this species. All animals were weighed prior to the experiment. During the experiment, the animals were kept individually on the same diet in separate adjacent indoor pens that allowed visual and acoustic contact. Food intake was determined by weighing diet items offered and the corresponding refusals several times per day for 6–7 days. Representative samples of food and refusals were taken and dried at 60 °C. Dry matter (DM) content was analysed by drying at 103 °C following AOAC no. 942.05 (AOAC 1997). Pens were cleaned on daily basis and animals had unrestricted access to water.

8.3.2 Determination of solute and particle retention times

The principle of mean retention time (MRT) measurement is the application (typically as a single pulse–dose) of a non–absorbable marker, the excretion of which over time is then detected by analyzing fecal samples for the marker concentration (Warner 1981). To measure MRT of particles and fluid, four markers from the same batch as those used by Lechner et al. (2010) were fed, which are considered representative of four different digesta components: three different sized particle markers based on fibre from grass hay mordanted with Chromium (Cr; <2 mm), Cerium (Ce; approx. 10 mm), Lanthanum (La; approx. 20 mm), and Cobalt ethylene diaminetetracetic acid (Co–EDTA; soluble in water). Markers were prepared according to

Udén et al. (1980) and Schwarm et al. (2008, 2009c). Bactrian camels and llamas received all four markers, while alpacas received only Cr– and Ce–mordanted fibres and Co–EDTA; based on our observations of the feeding behavior of the latter species, we expected reluctance of marker ingestion if too much marker material would have been offered. Prior to the administration of the markers, three fecal samples were collected to determine baseline marker concentrations in each animal. Individuals were then fed the particle markers at 0.1 g kg^{-1} body mass (BM) each and Co–EDTA at 0.01 g kg^{-1} BM dissolved in water. Markers were fed in mixture with a small amount of lucerne pellets and were consumed within approximately 30 min. The time when the animals had completely ingested the markers was considered 0 h, after which feces of llamas and Bactrian camels were sampled every 4 h for the first 60–84 h after marker application and every 6 h for the remaining time of the 7 days. Feces of alpacas were sampled every 4 h for the first 2 days after marker application, every 6 h on day 3, every 8 h on day 4, and every 12 h on days 5, 6, and 7. Due to differences in facilities and husbandry between species, the sampling protocol differed between species. However, the method used for calculating retention times was independent of sampling intervals, as demonstrated by Van Weyenberg et al. (2006). All samples were immediately oven–dried at 60 °C and later ground to 0.75 mm. Marker analysis was performed in a similar way as in previous studies (Frei et al. 2015). For wet ashing we heated samples with 4 ml nitric acid (HNO$_3$) and 2 ml hydrogen peroxide with the microwave MLS 'START 1500' (MLS GmbH, Leutkich, Germany). Temperature was increased over 15 min to 170 °C, and over 20 min to 200 °C, and then held at 200 °C for 5 min. The wave–length was 12.25 cm and the frequency 2.45 GHz. Determination of Co, Cr, Ce, and La in the sample digests was performed using an inductively coupled plasma optical emission spectrometer (model Optima 8000, Perkin Elmer, Rodgau, Germany). Sample introduction was carried out using a peristaltic pump connected to a Meinhard nebulizer with a cyclon spray chamber. The measured spectral element lines were: Co: 228.616 nm; Cr: 267.716; Ce: 413.764 nm; La: 398.852 nm. The RF power was set to 1400 W, the plasma gas was 8 L argon min^{-1}, whereas the nebulizer gas was 0.6 L argon min^{-1}. Values were corrected for the individual baseline concentrations prior to the marker application. To avoid an artificial increase in MRT by infinite excretion curves due to variation in baseline concentrations, values below 1% of the maximum concentration of a marker in the excretion curve were set to zero (adapted from Bruining and Bosch 1992).

We estimated MRT in the gastrointestinal tract (GIT) by an algebraic equation, and the MRT of the solute marker in the fore–stomach using the descending part of the marker excretion curve, following published proce-

dures. MRT GIT was calculated according to Thielemans et al. (1978) as

$$\text{MRT GIT} = \frac{\sum t_i \times dt \times c_i}{\sum dt \times c_i}$$

where t_i is a time after marker application in h determined as the midpoint between two sampling intervals, dt is time interval represented by the marker concentration calculated as $((t_{i+1} - t_i) + (t_i - t_{i-1}))/2$, and c_i is fecal marker concentration at t_i in mg kg^{-1} DM. In contrast to equations that calculate MRT GIT without considering the time interval dt (Blaxter et al. 1956; Warner 1981), this equation has the advantage that the sampling frequency has no influence on the calculated MRT result (Van Weyenberg et al. 2006).

The mean retention time of the solute marker in the FS ($\text{MRT}_{\text{solute}}\text{FS}$) was calculated by estimating the rate constant of the descending part of the marker excretion curve using an exponential equation according to Lechner–Doll et al. (1990) as

$$y = A \times e^{-k \times t},$$

where y is fecal marker concentration at time t in mg kg^{-1} DM, A is constant, k is the rate constant of the descending part of the excretion curve in h^{-1}, and t is time after marker application in h. According to Hungate (1966), the reciprocal value of k represents the MRT within the compartment characterized by k. This approach, therefore, assumes that the fore–stomach is the major mixing compartment in the camelid GIT. Based on the assumption that fluid and particles do not differ in passage characteristics distal to the FS (empirically confirmed in ruminants by Grovum and Williams 1973; Kaske and Groth 1997; Mambrini and Peyraud 1997), $\text{MRT}_{\text{particle}}\text{FS}$ is calculated as

$$\text{MRT}_{\text{particle}}\text{FS} = \text{MRT}_{\text{particle}}\text{GIT} - (\text{MRT}_{\text{solute}}\text{GIT} - \text{MRT}_{\text{solute}}\text{FS}).$$

The selectivity factor (SF) is defined as the ratio of two MRTs, either particle to solute or large to small particles. It was calculated for both total GIT and the FS, and for the small particle marker MRTs to solute MRT (Cr:Co,), and for larger to smaller particle MRTs (Ce:Cr, La:Cr, La:Ce).

8.3.3 Comparative literature

Data on the retention of comparable passage markers obtained in various camelids, ruminants, and non–ruminant foregut fermenters (NRFF) were collected from the literature. Data on ruminant MRT_{2mm} and $\text{MRT}_{\text{solute}}$ are the same as provided in the Supplementary Table of Dittmann et al. (2015).

Data sources of 10 and 20 mm particle markers from ruminants, camelids, and NRFF are presented in Table 8.1. For the dataset on MRT_{2mm} and MRT_{solute} we classified the ruminant species as 'cattle–' or 'moose–type', based on their $SF_{2mm/solute}FS$ because 'cattle–type' ruminants are defined as having comparatively shorter solute retention times in the reticulo–rumen, and thereby higher $SF_{2mm/solute}FS$ values, than 'moose–type' ruminants (Clauss et al. 2010).

For NRFF, no data were available for large (20 mm) particle markers. Because data were available from many different species for the solute and small particle (2 mm) markers, the data incorporated in analyses with respect to these to markers were averaged per species. Species means for all measures were first calculated as an average per source and then as mean of all source averages. In total, we collated data from 32 ruminant species (consisting of 13 'moose' and 19 'cattle–type' species), four camelid species, and seven non–ruminant foregut fermenter species. For the datasets including 10 and 20 mm particle markers, fewer measurements were available and, therefore, analyses were performed with data from individual animals, not species means, and without PGLS analyses (see below).

8.3.4 Statistical evaluation

The relative dry matter intake (rDMI) was calculated using an exponent of $BM^{0.85}$, following Müller et al. (2013). This approach was supported by the data obtained from the camelids investigated in this study, in which DMI scaled at $BM^{0.85\ (95\%CI:\ 0.75;\ 0.94)}$. Data from species investigated in the present study were tested for normal distribution by applying a Shapiro–Wilk test, based on which we used ANOVAs for comparison of retention times between and within species, followed by pairwise Tukey HSD post hoc tests. Data from Bactrian camels were compared with literature data from dromedaries (Lechner–Doll et al. 1990), by applying unpaired two tailed t–tests. All statistical tests were carried out in R (R Development Core Team 2012) using the packages *ape* (Paradis et al. 2004), *caper* (Orme et al. 2010), and *nlme* (Pinheiro et al. 2011).

Correlations including data from species investigated in the present study and literature data from other herbivores were investigated by applying general least squares (GLS) models with MRT, SF or DMI as dependent variable and BM or rDMI as independent variables. In the GLS, herbivore type (camelid, ruminant (either as such or separated into 'moose–' and 'cattle–type') or NRFF) was added as a cofactor. For each model, we tested the interaction between the independent variable and the cofactor. This interaction was removed from the model when not significant. Additionally, to

Table 8.1: Sources for retention time measures of 2, 10 and 20 mm particles in ruminants, camelids and non–ruminant foregut fermenters used in the comparative evaluation (see Dittmann et al. 2015 for a complete list of ruminant species with measurements for 2 mm particles and solutes)

Species	Herbivore type	$MRT_{2mm}GIT$	$MRT_{10mm}GIT$	$MRT_{20mm}GIT$	$MRT_{2mm}FS$	$MRT_{10mm}FS$	$MRT_{20mm}FS$	MRT sources
C. dromedarius	Camelid	×		×	×		×	(Heller et al. 1986a; Lechner–Doll et al. 1990)
L. glama	Camelid	×		×	×		×	(Heller et al. 1986c)
A. alces	Ruminant	×	×	×	×	×	×	(Lechner et al. 2010)
B. javanicus	Ruminant	×	×		×	×		(Schwarm et al. 2008)
B. taurus	Ruminant	×	×	×	×	×	×	(Lirette and Milligan 1989; Lechner–Doll et al. 1990; Lechner et al. 2010)
C. hircus	Ruminant	×		×	×	×	×	(Lechner–Doll et al. 1990)
O. moschatus	Ruminant	×	×	×	×	×	×	(Lechner et al. 2010)
O. aries	Ruminant	×		×	×		×	(Lechner–Doll et al. 1990)
R. tarandus	Ruminant	×	×	×	×	×	×	(Lechner et al. 2010)
T. tajacu	NRFF	×	×		×	×		(Schwarm et al. 2009b)
H. liberiensis	NRFF	×	×		×	×		(Clauss et al. 2004; Schwarm et al. 2008)
H. amphibius	NRFF	×	×		×	×		(Clauss et al. 2004; Schwarm et al. 2008)
C. angolensis	NRFF	×	×		×	×		(Clauss et al. 2004)
C. polykomos	NRFF	×	×		×	×		(Schwarm et al. 2009a)
P. johnii	NRFF	×	×		×	×		(Schwarm et al. 2009a)
M. rufus	NRFF	×	×		×	×		(Schwarm et al. 2009a)

Different data subsets have different numbers of species depending on whether information on dry matter intake and various retention measures were available.
MRT mean retention time, GIT gastrointestinal tract, FS fore-stomach, NRFF non-ruminant foregut fermenter, Camelus dromedarius, Lama glama, Alces alces, Bos javanicus, Bos taurus, Capra hircus, Ovibos moschatus, Ovis aries, Rangifer tarandus, Tayassu tajacu, Hexaprotodon liberiensis, Hippopotamus amphibius, Coobus angolensis, Coobus angolensis, Colobus polykomos, Presbytis johnii, Macropus rufus

investigate differences in relationships between large and small particle markers between herbivore types, we applied GLS with large particle markers as dependent and small particle markers as independent variables, and with herbivore type as a cofactor (and interactions of the latter two). The respective SFs were tested for differences between herbivore types by applying ANOVA or Kruskal–Wallis tests, followed by Tukey HSD post hoc tests or non–parametric pair–wise tests as means for multiple comparisons (R function *kruskalmc*).

Species cannot be considered independent units, as they share an evolutionary history which means that similarities between species might only be an artifact of their ancestry (Felsenstein 1985). This lack of independence violates basic assumptions of many statistical tests, which is why we accounted for phylogeny by applying Phylogenetic Generalized Least Squares (PGLS) analyses. Data were linked to a supertree of extant mammals (Bininda–Emonds et al. 2007, 2008), for the same models investigated by GLS in the dataset for MRT_{2mm} for which values of many different species were available, without the inclusion of herbivore type as a cofactor. The value of the phylogenetic signal (λ) (Pagel 1999), which can be considered a measure of the phylogenetic structure in the dataset, was estimated with maximum likelihood (Revell 2010), using the PGLS command from the package caper (Orme et al. 2010). Additionally, Akaike's information criterion (AIC) for the models was determined using the R function AIC to determine which model has the better fit. Significance levels were set to $\alpha = 0.05$, with values between 0.05 and 0.10 considered as trends.
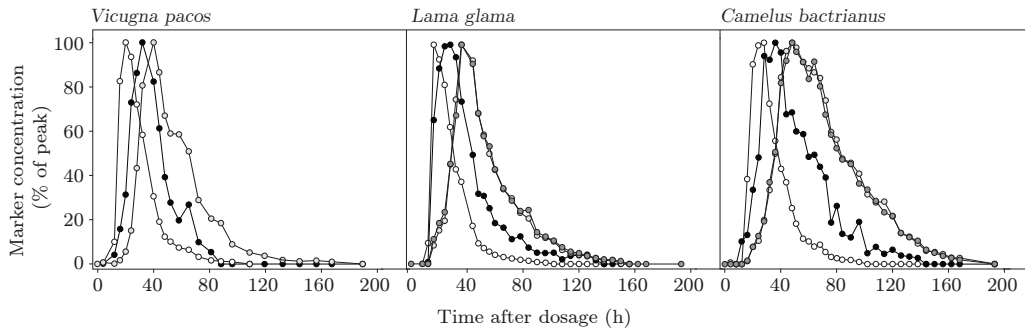

Figure 8.2: Exemplary excretion curves of the solute and particle markers of each one alpaca (*Vicugna pacos*), llama (*Llama glama*) and Bactrian camel (*Camelus bactrianus*). Solute (Co) in white, 2 mm (Cr) in black, 10 mm (Ce) in light grey and 20 mm (La) in dark grey.

Table 8.2: Body mass, dry matter intake, and retention times and selectivity factors of the gastrointestinal tract from the camelids investigated in this study and from dromedaries (*C. dromedarius*) investigated by Lechner–Doll et al. (1990)

Species	Body mass (kg)	rDMI (g kg$^{-0.85}$ d^{-1})	MRT GIT (h)				SF GIT			
			Solute	2mm	10mm	20mm	2mm/solute	10/2mm	20/2mm	20/10mm
V. pacos	63±12	34±7	34±6[1]	50±12[2]	59±12[3]	n.m.	1.46±0.13	1.20±0.14[a]	n.m.	n.m.
V. glama	148±26	35±5	29±2[1]	40±4[2]	58±4[3]	57±3[a3]	1.40±0.09	1.47±0.14[b]	1.44±0.11	0.98±0.03
C. bactrianus	658±72	35±6	34±3[1]	47±6[2]	66±5[3]	67±5[b3]	1.38±0.11	1.42±0.07[b]	1.43±0.07	1.01±0.02
C. dromedarius	453±95	n.m.	45±8*	61±7*	n.m.	88±12*	1.36±0.09	n.m.	1.43±0.10	n.m.

Superscript letters indicate significant differences (P < 0.05) between MRT measures and SFs within columns, superscript numbers indicate differences of MRT or SFs within species and asterisks indicate significant differences in the respective means between *C. bactrianus* and *C. dromedarius*

rDMI relative dry matter intake, MRT mean retention time, GIT gastrointestinal tract, SF selectivity factor, n.m. not measured, *Vicugna pacos*, *Lama glama*, *Camelus bactrianus*, *Camelus dromedarius*

Table 8.3: Retention times and selectivity factors of the fore–stomach from the camelids investigated in this study and from dromedaries (*C. dromedarius*) investigated in Lechner–Doll et al. (1990)

Species	MRT FS (h)				SF FS			
	Solute	2mm	10mm	20mm	2mm/solute	10/2mm	20/2mm	20/10mm
V. pacos	22 ± 7^1	38 ± 11^2	47 ± 11^3	n.m.	1.74 ± 0.26	1.28 ± 0.22^a	n.m.	n.m.
L. glama	17 ± 3^1	28 ± 3^2	47 ± 5^3	45 ± 4^{a3}	1.71 ± 0.23	1.66 ± 0.15^b	1.62 ± 0.12	0.97 ± 0.05
C. bactrianus	19 ± 3^1	32 ± 5^2	51 ± 4^3	51 ± 4^{b3}	1.72 ± 0.29	1.63 ± 0.14^b	1.64 ± 0.11	1.01 ± 0.04
C. dromedarius	$11\pm1^*$	$26\pm3^*$	n.m.	53 ± 7	$2.52\pm0.31^*$	n.m.	$2.01\pm0.30^*$	n.m.

Superscript letters indicate significant differences (P < 0.05) between MRT measures and SF within columns, superscript numbers indicate differences of MRT within species, asterisks indicate significant differences in the respective value between *C. bactrianus* and *C. dromedarius*, while askterisks in brackets indicate trends
n.m. not measured, MRT mean retention time, FS fore–stomach, SF selectivity factor

8.4 Results

8.4.1 Differences between camelid species

Marker elimination curves for the three species indicated a typical sequence in marker elimination peaks, with the solute marker being eliminated first, followed by the small particle marker and then by the two large particle markers (Fig. 8.2). In the two species (camels and llamas) where three particle markers had been applied, the MRTs (both in GIT and FS) of the two large particle markers did not differ from each other (P > 0.99 and P > 0.79, respectively). All other MRTs, in GIT and FS, differed significantly between each other within each species (camels: P < 0.001; llamas: P < 0.001; alpacas: P < 0.023) (Tables 8.2 and 8.3).

In general, there were no significant differences in retention times of the different markers between species; only llamas had shorter $\text{MRT}_{20\text{mm}}$GIT and FS than Bactrian camels (P < 0.036). $\text{SF}_{10/2\text{mm}}$GIT and FS were lower in alpacas than in llamas (P < 0.041) and Bactrian camels (P < 0.011).

Comparing our measurements of the large camelid, the Bactrian camel, to literature data from dromedaries (Lechner–Doll et al. 1990), revealed longer MRTs for all markers in the GIT (P = 0.000–0.002), shorter $\text{MRT}_{\text{solute}}$FS (P = 0.002) and a trend towards shorter $\text{MRT}_{2\text{mm}}$FS (P = 0.071) in dromedaries (Tables 8.2 and 8.3). Only $\text{MRT}_{20\text{mm}}$FS did not differ between the two species (P = 0.62). The SFs in the GIT were similar in the two camel species ($\text{SF}_{2\text{mm/solute}}$GIT: P = 0.73; $\text{SF}_{20/2\text{mm}}$GIT: P = 0.99), whereas $\text{SF}_{2\text{mm/solute}}$FS and $\text{SF}_{20/2\text{mm}}$FS were each higher in dromedaries than in Bactrian camels (both P < 0.001).
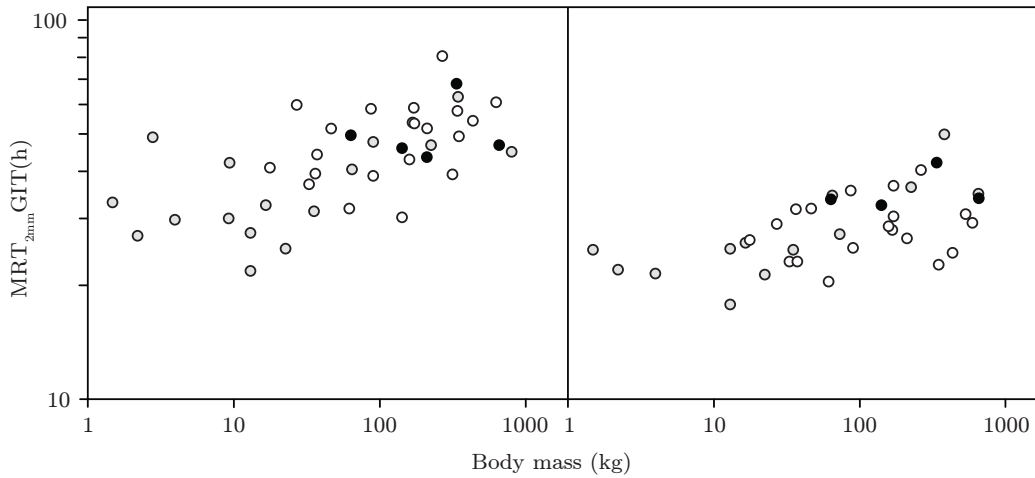
Figure 8.3: Relationships of (left) the mean retention time of 2 mm particles in the gastrointestinal tract ($MRT_{2mm}GIT$) and (right) the mean retention time of solutes in the gastrointestinal tract ($MRT_{solute}GIT$) with body mass (BM) in ruminants and camelids. *Dots* represent species means. 'Moose–type' ruminatnts in grey, 'cattle–type' ruminants in white and camelids in black.

8.4.2 Comparisons with literature data from ruminants: absolute MRTs

When relating combined data from ruminants and camelids on MRT_{2mm} and MRT_{solute}, both for GIT and FS, to body mass, there were no significant interactions ($P > 0.37$) between herbivore type and BM. There were no significant differences ($P = 0.10$–0.94) between camelids and ruminants, or between camelids, 'cattle–' and 'moosetype' ruminants in these models. Camelid values were within the range reported for ruminants (Fig. 8.3). $MRT_{2mm}GIT$ and FS, and $MRT_{solute}GIT$ were related to BM in GLS ($P < 0.035$; scaling exponents $BM^{0.07-0.12\ (0.03;\ 0.20)}$) and PGLS analyses ($P < 0.001$, $\lambda = 0.00$; scaling exponents $BM^{0.08-0.12\ (0.04;\ 0.19)}$). $MRT_{solute}FS$ was not related to BM in GLS ($P = 0.18$) and tended towards significance in PGLS with a strong phylogenetic structure ($P = 0.08$; $\lambda = 0.92$; scaling exponent $BM^{0.09\ (-0.01;\ 0.18)}$), indicating that closely related species have similar $MRT_{solute}FS$ values, independent of their BM.

8.4.3 Comparison with literature data from ruminants: 'digesta washing' in the fore–stomach

The $SF_{2mm/solute}FS$ differed between ruminants and camelids ($\chi^2 = 125$; $P < 0.001$) with significantly lower values in 'moose–type' ruminants as compared

with 'cattle–type' ruminants and camelids ($P < 0.001$) and a trend towards camelids being lower than 'cattle–type' ruminants ($P = 0.084$) (Fig. 8.4a). Correspondingly, a GLM with $MRT_{2mm}FS$ as independent and $MRT_{solute}FS$ as dependent variable revealed significant influence of herbivore type ($P < 0.001$), with 'moose–type' ruminants having higher $MRT_{solute}FS$ than 'cattle–type' or camelids at a given $MRT_{2mm}FS$ (Table 8.3; Fig. 8.4b). In a PGLS model with the same variables but without herbivore type as cofactor, there was a significant phylogenetic structure in the dataset ($\lambda = 0.781$), indicating similar values among closely related species. The fit of the GLS model with herbivore types was better than the PGLS model (AIC: –8.0 vs 11.2). Note that the camelids do not achieve the very high $SF_{2mm/solute}FS$ or short $MRT_{solute}FS$ of cattle or muskoxen (*Ovibos moschatus*) (Lechner et al. 2010).
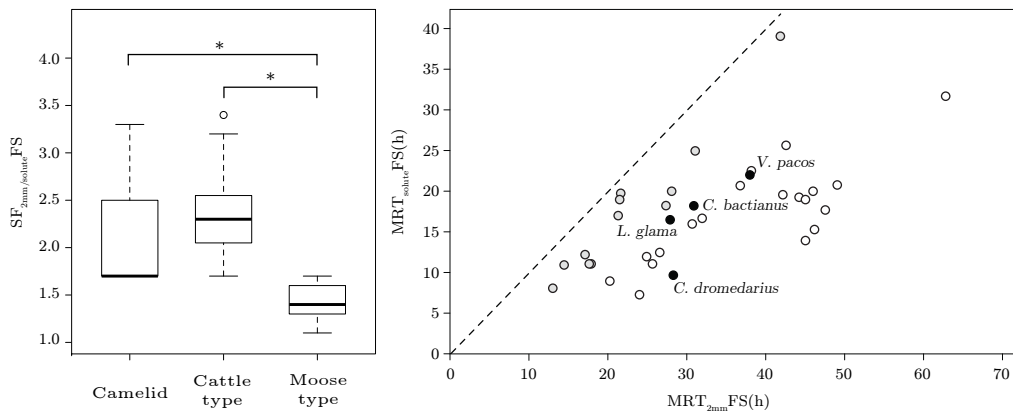

Figure 8.4: left: Comparison of the $SF_{2mm/solute}FS$ between species means from camelids and ruminats ('cattle–'or 'moose–type'). *Boxplots* indicate *median*, *upper* and *lower* quartile, as well as maximum and minimum values, *dots* indicate outliers and *asterisks* represent significant differences between herbivore types ($P < 0.05$). right: Relationship between $MRT_{solute}FS$ and $MRT_{2mm}FS$ in ruminants and camelids; *dots* represent species means; the *dashed line* represents equality of the two measures, i.e. an SF of 1). 'Moose–type' ruminatnts in grey, 'cattle–type' ruminants in white and camelids in black.

8.4.4 Comparisons with literature data from ruminants and non–ruminant foregut fermenters: sorting mechanism

The $SF_{10/2mm}GIT$ and FS differed between ruminants, camelids, and NRFF ($\chi^2 = 52.9/52.8$; $P < 0.001$) with significantly lower values (close to equality) in NRFF as compared with ruminants and camelids ($P < 0.001$) and lower values in ruminants compared with camelids (GIT: $P = 0.048$; FS: $P = 0.029$;
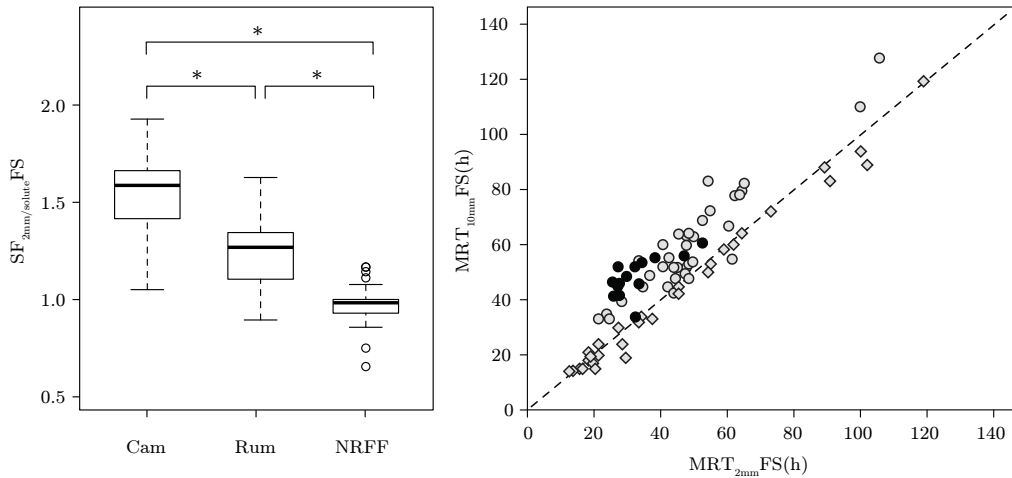
Figure 8.5: left: Comparison of individual data of the $SF_{10/2mm}FS$ between camelids (Cam; black), Ruminants (Rum; grey) and non–ruminant foregut fermenters (NRFF; open squares). right: Relationship between $MRT_{10mm}FS$ and $MRT_{2mm}FS$ in the same herbivores; *dots* represent measurements of individuals; the *dashed line* represents equality of the two measures, i.e. an SF of 1

Fig. 8.5a). In a GLM with $MRT_{2mm}FS$ as independent and $MRT_{10mm}FS$ as dependent variable, there was a significant interaction with herbivore type, irrespective of whether NRFF were included in the analyses ($P < 0.001$) or not ($P = 0.03$) (Table 8.4). While the significant interaction does not allow interpreting the exclusive effect of herbivore type in this relationship, the data analysis confirms that there is no particle sorting in NRFF and that camelids are generally within the higher range of ruminants (Fig. 8.5b).

More data could be included in the comparison of $SF_{20/2mm}FS$ between herbivore types than for $SF_{10/2mm}FS$ (n = 102 vs 85 datapoints), but no data from NRFF were available for $SF_{20/2mm}FS$. The $SF_{20/2mm}FS$ was lower in ruminants than in camelids (T = 4.5; $P < 0.001$; Fig. 8.6a). Again, in a GLS with $MRT_{2mm}FS$ as independent and $MRT_{20mm}FS$ as dependent variable, there was a significant interaction with herbivore type ($P = 0.001$). The data indicate that camelids are generally within the higher range of ruminants in this relationship (Fig. 8.6b).

In contrast, the $SF_{20/10mm}GIT$ and FS did not differ between ruminants and camelids (W = 178/177; P = 0.49/0.47) and was close to equality (Fig. 8.7a). Also, in a GLS with $MRT_{20mm}FS$ as independent and $MRT_{10mm}FS$ as dependent variable, there was no difference between camelids and ruminants (P = 0.63) (Fig. 8.7b).

In GLS models with $SF_{10/2mm}FS$ or $SF_{20/2mm}FS$ as independent variable and rDMI as dependent variable, the latter was not significant (P >

0.10), while there was again a significant difference between ruminants and camelids (P < 0.001), indicating generally higher values in camelids compared with ruminants, independent of food intake. Applying the same model for $SF_{20/10mm}FS$ revealed again no influence of rDMI (P = 0.22), but no difference between ruminants and camelids (P = 0.67). There were no significant interactions between rDMI and herbivore type in these models (P > 0.11). Note that the ranges of rDMI were overlapping for camelids and ruminants, but the range of rDMI data of the camelids were less broad (27–44 g kg $BM^{-0.85}$ d^{-1}) than the range of rDMI values from rumiants (8–107 g kg $BM^{-0.85}$ d^{-1}).
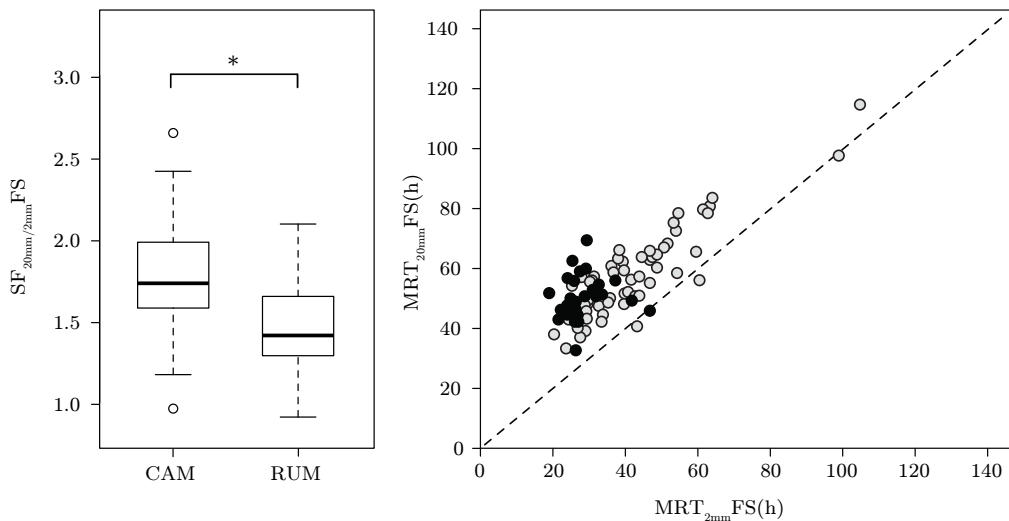

Figure 8.6: left: Comparison of individual data of the $SF_{20/2mm}FS$ between camelids (Cam; black) and ruminants (Rum; grey). right: Relationship between $MRT_{20mm}FS$ and $MRT_{2mm}FS$ in ruminants and camelids; *dots* represent measurements of individuals; the *dashed line* represents equality of the two measures, i.e. an SF of 1

8.5 Discussion

8.5.1 Differences between camelid species

In general, the absolute MRTs obtained from the camelids investigated in the present study do not confirm the particularly long retention times measured in other studies. For example, in Bactrian camels the MRTs measured in the GIT by Cahill and McBride (1995) were 50–80% longer than the ones measured in the present study ($MRT_{solute}GIT$: 50 vs 34 h; $MRT_{2mm}GIT$: 85 vs 47 h). In the llamas, $MRT_{solute}GIT$ and $MRT_{2mm}GIT$ data from Heller et al.

Table 8.4: Linear regression equations corresponding to $\log(y) = a + b\ log(x) + Cofactor$, including the interaction of cofactor $\times log(x)$ if significant

Model	Variables			n	Intercept			Independent variable			Cofactor		Interaction		AIC
	y	x	Cofactor		a	T	P	b	T	P	F	P	F	P	
GLS	MRT_{solute}FS	MRT_{2mm}FS	Cam/Rum	35	3.3	1.11	0.278	0.65	5.13	<0.001	0.17	0.682	–	ns	16.7
GLS	MRT_{solute}FS	MRT_{2mm}FS	Cam/Moose/Cattle	35	0.1	−2.14	0.041	1.04	9.48	<0.001	17.85	<0.001	–	ns	−8.0
PGLS	MRT_{solute}FS	MRT_{2mm}FS	– ($\lambda = 0.78$)	35	4.3	1.38	0.176	0.65	5.40	<0.001	–	–	–	–	11.2
GLS	MRT_{10mm}FS	MRT_{2mm}FS	Cam/Rum	54	225.0	4.50	<0.001	0.44	2.90	0.006	5.75	0.020	4.96	0.031	–
GLS	MRT_{10mm}FS	MRT_{2mm}FS	Cam/Rum/NRFF	85	225.0	4.61	<0.001	0.44	2.97	0.004	14.68	<0.001	8.72	<0.001	–
GLS	MRT_{20mm}FS	MRT_{2mm}FS	Cam/Rum	102	2968.9	7.94	<0.001	0.13	0.99	0.325	12.14	0.001	11.32	0.001	–
GLS	MRT_{20mm}FS	MRT_{10mm}FS	Cam/Rum	39	2.2	3.65	0.001	0.91	38.42	<0.001	0.53	0.470	–	ns	–

PGLS was carried out without the cofactor, instead lambda (λ), was calculated.
GLS = general least squares, PGLS = phylogenetically informed GLS, MRT = mean retention time, FS = fore–stomach, Cam = camelids, Rum = ruminants, Moose = 'moose–type' ruminants, Cattle = 'cattle–type' ruminants, NRFF = non–ruminant foregut fermenters, AIC = Akaike information criterion, ns = non–significant
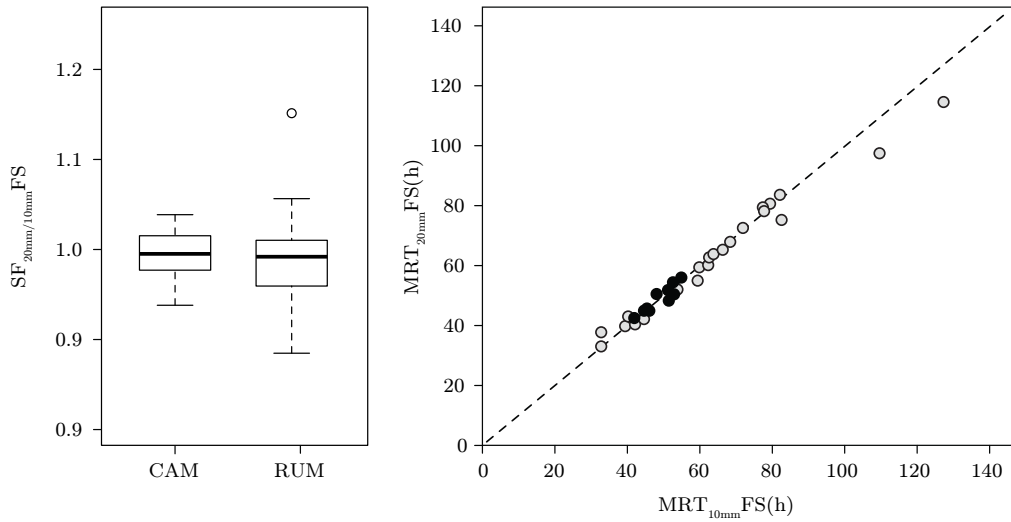
Figure 8.7: left: Comparison of individual data of the $SF_{20/10mm}FS$ between camelids (Cam; black) and ruminants (Rum; grey). right: Relationship between $MRT_{20mm}FS$ and $MRT_{10mm}FS$ in ruminants and camelids; *dots* represent measurements of individuals; the *dashed line* represents equality of the two measures, i.e. an SF of 1

(1986) exceeded the ones measured in the present study by approximately 30%. These differences might well be explained by differences in the food intake level, as described for Bactrian camels by Cahill and McBride (1995), which influence MRT within and across species (Müller et al. 2013; Clauss et al. 2014). Therefore, measurements of retention time should ideally always be accompanied by assessments of intake, and conclusions made from comparisons of absolute MRTs must account for the effect of food intake (Levey and Martínez del Rio 1999).

It would have been preferable to also include dromedaries into the experiment and feed them the same lucerne–based diet, but this was not possible due to a lack of available animals. No data on food intake or MRT_{10mm} were available for dromedaries in the literature, which is why dromedaries could not be included in the statistical comparisons between herbivores with respect to this marker. Generally, dromedary data from Lechner–Doll et al. (1990) indicated longer retention times in the GIT compared with Bactrian camels. Dromedaries had relatively short $MRT_{solute}FS$ of 11±1 h compared with 19±3 h in Bactrian camels and also shorter $MRT_{solute}FS$ than the smaller species investigated in this study. $MRT_{particle}FS$ were similar in dromedaries when compared with the camelids investigated in this study, which resulted in comparably higher SF values in the FS of dromedaries (also documented by Heller et al. 1986a). Other measurements reported for tulus (hybrids of *C. bactrianus* and *C. dromedarius*) under hydrated conditions in-

dicated short $MRT_{solute}FS$ of 12 h (von Engelhardt et al. 2006b), similar to the $MRT_{solute}FS$ in the dromedaries. Contrasting to the short $MRT_{solute}FS$ found in the camelids, long $MRT_{solute}FS$ in ruminants have been interpreted as a consequence of a proportionately large FS that serves as a water storage organ (Silanikove 1994; Hummel et al. 2008). Dromedaries, with a comparatively smaller proportionate FS volume than ruminants (Lechner–Doll et al. 1990), apparently do not use the FS to the same extent as a water reservoir. Actually, even after severe dehydration and a sudden rehydration, the camelid FS does not maintain an enlarged volume for more than 1 day (von Engelhardt et al. 2006b). Therefore, the camelids' adaptation to water shortage appears to consist in their ability to rapidly ingest large amounts of water when it is available, and to absorb this water quickly into the body, rather than retain it in the FS (von Engelhardt et al. 2006b), as for example observed in the desert–adapted addax antelope (*Addax nasomaculatus*) (Hummel et al. 2008).

8.5.2 Comparing digesta washing between camelids and ruminants

Digesta washing can be described by the difference between the $MRT_{particle}$ and the MRT_{solute}, expressed as the ratio of the two measures, the SF. In the case of high ratios, a faster–moving fluid phase washes through a slower–moving particulate digesta phase, thereby removing solutes and very fine particles, including microbes, from this plug (Lentle et al. 2006; Müller et al. 2011). This process is not restricted to ruminants as it can also be found in some NRFF and other digestion types (Müller et al. 2011). Within ruminants, species differ in rumen fluid throughput and the degree of digesta washing (Clauss and Lechner–Doll 2001; Clauss et al. 2006; Dittmann et al. 2015; Hummel et al. 2015), which led to the classification of 'cattle-' and 'moose–type' ruminants. Therefore, the finding that 'cattle-' and 'moose–type' ruminants differ significantly in the $SF_{2mm/solute}FS$ (Fig. 8.4a) is no surprise because the measure is actually used for the classification. Therefore, it appears that camelids in general have evolved a 'cattle–type' strategy, although guanacos (*Lama guanicoe*) and vicuñas (*Vicugna vicugna*) have not yet been subjected to digesta retention measurements.

The proposed major advantage of the 'cattle–type' strategy is an increased harvest of microbes from the FS, leading to a higher general yield of microbial protein, and selection for a fast–growing and particularly efficient microbial community in the FS (Clauss et al. 2010; Dittmann et al. 2015; Hummel et al. 2015). Due to this higher microbial yield, the 'cattle–type'

strategy might be particularly suitable for camelids with their greater ability to recycle urea as compared with domestic ruminants (Hinderer and von Engelhardt 1975; von Engelhardt and Schneider 1977). The 'moose–type' strategy has been linked with browse feeding and salivary defences against tannins (Hofmann et al. 2008; Codron and Clauss 2010). Because browse often represents the main component of the diet of free–ranging dromedaries (reviewed in Iqbal and Khan 2001), the 'cattle–type' dromedaries must have evolved alternative strategies to deal with tannins that are not related to saliva viscosity.

Considering only ruminants, the 'moose–type' strategy is prominent in basal groups such as the tragulids or giraffids (Clauss and Lechner–Doll 2001; Hummel et al. 2005; Darlis et al. 2012) and could, therefore, appear as the basal physiological strategy of the ruminant suborder. However, the high $SF_{2mm/solute}FS$ in the more distantly related camelids could allow the interpretation that a higher degree of digesta washing as in 'cattle–type' ruminants represents the basal situation, and that the 'moose–type' strategy may be a more derived state. Although some evidence matches the latter hypothesis, e.g., the observation of the 'moose–type' strategy in the subfamily of the Cephalophines (Clauss et al. 2011) or in dikdik (*Madoqua* spp.) (Hebel et al. 2011), which are considered derived ecomorphs (Bärmann 2014), more measurements in a larger number of species are required to confirm this concept.

8.5.3 Comparing particle sorting in camelids, ruminants, and non-ruminant foregutfermenters

The sorting of large vs small particles is crucial for the process of rumination, as it ensures that only those particles that can be efficiently further reduced in size are subjected to repeated mastication (Lauper et al. 2013). However, the actual sorting is rather based on particle density than on particle size (Baumont and Deswysen 1991; Lechner–Doll et al. 1991), because larger particles typically have a lower functional density and hence a propensity to float in a liquid medium (Sutherland 1988; Clauss et al. 2009b). In the FS of ruminants, there is a clear distinction between the reticulo–rumen on the one hand, where particles of all sizes occur, and the omasum on the other hand, where only small particles are present (Clauss et al. 2009a, b). This means that the orifice between the reticulum and the omasum is a point of demarcation. In the FS of the camelids, however, this separation is somewhat less distinct. Although there is also a clear difference in particle sizes present between compartments C1/C2 (corresponding to the reticulorumen)

and the distal part of C3/hindstomach (corresponding to the abomasum), there apparently is a more gradual transition within the proximal part of the C3 compartment, where not as many large particles as in C1/C2, but still more than those in the distal C3, are present (Lechner–Doll and von Engelhardt 1989). This suggests that the orifice between C2 and C3, although similar in its width to that of the orifice between the reticulum and omasum in ruminants (Langer 1988), may not represent an absolute demarcation point in camelids. The similar, comparatively low fecal particle sizes in ruminants and camelids (Fritz et al. 2009) leads to the assumption that the large particles in C3 must be transferred back to the more proximal parts of the FS to be ruminated and thereby eventually reduced in size.

Comparing the findings on the retention of different–sized particles in camelids with those from ruminants reveals several similarities. The marker excretion curves recorded in the present study are generally similar to those found in ruminants (compare for example, our camelid Fig. 8.2 to the excretion curves shown in Schwarm et al. 2008 or Lechner et al. 2010). As previously found in ruminants, camelids also do not discriminate between particles of 10 or 20 mm. In ruminants this pattern is independent of whether the markers are fed directly to the animal (Schwarm et al. 2009a) or inserted into the rumen via fistula (Lechner et al. 2010). In other words, this pattern is not affected by ingestive mastication. Therefore, it appears unlikely that the lack of discrimination between these sizes is due to the method of marker application in the present study, i.e. that large particle markers had been significantly reduced in size by mastication before they reached the FS. Evidently, within species for which such data are available (llamas, Bactrian camels, reindeer, muskoxen, moose, and cattle), particle size has no additional influence on particle retention above a certain threshold of about 1 cm. Whether a similar threshold exists in smaller species remains to be investigated.

The present comparison of relationships of large to small particle retention between camelids, ruminants, and NRFF suggests that a sorting mechanism sets ruminants and camelids apart from other foregut fermenters (Fig. 8.5) and represents, given the distant relatedness of camelids and ruminants, a convergent adaptation where the same function is achieved by different morphophysiological designs. This convergence not only manifests in patterns of MRT (present study), FS motility and chewing activity (Heller et al. 1986a; von Engelhardt et al. 2006a), but also in particle size reduction (Fritz et al. 2009) and the high fibre–digestibility when compared with other NRFF (Hintz et al. 1973; Sponheimer et al. 2003; Clauss et al. 2009a; Steuer et al. 2013).

The results of the present study indicate a quantitative difference in the

sorting of large vs small particles between herbivore types, with longer 10 mm or 20 mm to 2 mm particle retention in camelids as compared with ruminants (and NRFF), evident as higher $SF_{10mm/2mm}FS$ and $SF_{20mm/2mm}FS$ (Figs. 8.5, 8.6). These higher SF values appear to be caused by a longer retention of large particles rather than a shorter retention of 2 mm particles. The difference between ruminants and camelids was not explained by differences in food intake level and hence might reflect true functional differences between the morphophysiological designs of the ruminant and the camelid FS. Whether longer retention of large particles could explain the observation that, under similar experimental conditions, camelids usually have a lower food intake than ruminants (Meyer et al. 2010; Dittmann et al. 2014) and a generally lower level of metabolism (Dittmann et al. 2014) remains speculative. Interpreting the effects of morphophysiological characteristics of the GIT as constraint for other physiological functions, and ultimately for the competitiveness and diversity of taxonomic groups, could lead to instructive narratives (e.g., Janis et al. 1994; Clauss and Rössner 2014). In the case of camelids, both more functional measurements, such as particle size distributions in the different FS compartments, and a systematic evaluation of the fossil record in comparison to ruminants, are necessary to support such a narrative.

8.5.4 Conclusion

The results of this study indicate a distinct convergence between camelids and ruminants in terms of the presence of a particle sorting mechanism in their digestive tracts, as well as in the degree of 'digesta washing' between camelids and 'cattle–type' ruminants. They also provide preliminary evidence that the particle sorting mechanism differs in detail between the two groups. To explore this putative difference, more detailed studies on the retention mechanism are required.

8.6 Acknowledgments

8.7 Author contributions

Conceived and designed the experiments: MC MK. Performed the experiments: MTD RAL DM MC. Analyzed the data: MTD MC. Wrote the paper: MTD MC. Manuscript review: UR RAL DM CG SO AS MK. Animal husbandry: UR MD RAL DM

General discussion

This doctoral work led to several insights in evolutionary biology, using the threespine stickleback as a model organism (Östlund–Nilsson et al. 2006). In particular, I was working with a lake–stream model system (McKinnon and Rundle 2002), comprising populations from the Lake Constance basin in Central Europe. I wanted to answer the following main questions: Do we find divergence in the two life history traits age and size at reproduction between lake and stream populations and is it paralleled by barriers to gene flow, based on neutral genetic markers (Chapter 1)? Are the habitat–specific differences in life history genetically based or phenotypically plastic and what is the underlying mechanism – different growth rates versus different maturation size thresholds (Chapter 2)? And finally, does local adaptation exist between the contrasting habitats and how is it influencing fitness (Chapter 3)?

Life history divergence between lake and stream populations

My analyses revealed dramatic life history divergence between the two habitats lake and stream, with lake fish reproducing at a greater age and size, compared to their stream conspecifics. Lake fish exhibited approximately double the mass and normally reached maturity at the age of two, compared to an annual life–cycle in stream fish. The pattern was highly consistent across multiple population pairs. As the analysis of stomach content suggested, different food resources in the two contrasting habitats most likely promote this life history divergence: Lake fish exhibit a pelagic life–style during most of the year, exploring zooplankton as food resource. However, during breeding season, lake fish have to perform a foraging niche shift, now being constraint on benthic resources on shore. By contrast, stream populations exclusively exploit benthic resources throughout the year. These differences in resource use might lead to differential growth trajectories between habitats, since a benthic–based diet is known to allow faster growth in other

187

stickleback systems (Schluter 1995; Taylor et al. 2012). As a by–product, the great magnitude of body size divergence between lake and stream fish is expected to influence female choice and male aggressiveness, as described in other systems (Dufresne et al. 1990; Nagel and Schluter 1998; Ishikawa and Mori 2000; McKinnon et al. 2004). If so, reproductive isolation would be increased by hindering gene flow between the lake and the streams.

Population structure in the Lake Constance basin

Pairwise F_{ST} values among the four lake population samples did not exceed 0.01, indicating the presence of gene flow among them. Genetic differentiation between the panmictic lake population and the inlet stream samples were generally modest, but sometimes reached higher values (up to 0.18), suggesting reduced gene flow between lake and stream populations. Additionally, the genetic data indicated repeated lake to stream colonization: i.) highest F_{ST} values were found between different stream populations, followed by lake–stream comparisons and finally between lake samples and ii.) most of the rare D–loop haplotypes were found in stream populations. Such a pattern may emerge from random increase of rare lake alleles via drift, when streams get colonized from the lake.

The microsatellite and D–loop analyses were complemented by adding two additional populations: a Rhine sample 140 km downwards the lake outlet and a sample from the Danube rive, north of Lake Constance. As previously reported (Lucek et al. 2010), Lake Constance stickleback do not originate from downstream Rhine stickleback. The Lake Constance basin groups to the Danube watershed instead. All F_{ST} values, comparing the Danube sample to the Lake Constance samples lead to low differentiation values (≤ 0.04) and the unique D–loop haplotype found in the Danube samples was also the predominant haplotype in Lake Constance. Whether colonization occurred via human introduction or a temporary colonization route at the end of the last ice age may not be answered with this data. However, the second explanation is more likely. First, mitochondrial marker data in European perch group to Danube samples and not to the Rhine (Behrmann–Godel et al. 2004). Second, geological data show that during deglaciation some 10'000 years ago, temporal proglacial lakes existed in front of the Rhine glacier (Keller and Krayss 2000). These lakes were connected to the Danube watershed, till further glacial meltdown made draining into the Rhine possible and Lake Constance was formed.

Mechanism of life history divergence

The described pattern of life history divergence in age and size may be achieved with two alternative mechanisms: i.) Lake fish grow faster but exhibit an increased maturation size threshold compared to stream fish. ii.) Lake fish grow slower, but exhibit the same maturation size threshold as stream fish. Either way, large lake fish, breeding at age two and small stream fish, breeding at age one, are the outcome. With a combination of three experiments I identified which alternative holds true and whether it is genetically based or ecology induced.

First, growth trajectories under common garden conditions revealed genetically based differentiation, with lake fish growing slightly faster than stream fish. Possible explanations are higher rate of food consumption and/or food conversion (Present and Conover 1992; Silverstein et al. 1999, Jonassen et al. 2000; Trudel et al. 2001). However, the differences under laboratory conditions are not able to explain the divergence in the wild, since faster growth in lake fish would lead to earlier maturation in lake fish, which is obviously not the case in the wild.

A second common garden experiment found no genetic differences in maturation size thresholds between lake and stream stickleback. All fish are able to reproduce at smaller size in the lab than breeding stream fish in the wild. Combining the outcome of both laboratory experiments, I reached the conclusion that life history divergence within the Lake Constance basin is largely due to phenotypic plasticity.

Finally, a long–term field transplant experiment could confirm this view: Lake fish transplanted into streams were able to reach maturity within one year at comparable stream fish body size.

Taken together, lake fish do not reach minimum size to switch from somatic growth to reproduction within one year, and therefore exhibit an additional year of somatic growth, explaining bigger and older lake fish during breeding season in the lake. However, the specific ontogenetic determinants and ecological factors generating this life history plasticity cannot be inferred from these experiments. As discussed above, different food availabilities and resources are most likely responsible for this life history divergence. First, planktonic food is inferior when compared to benthic food (Schluter 1995; Taylor et al. 2012). Second, plankton abundance is high in spring and early summer (Sommer 1985) and low during the rest of the year. Juvenile lake fish are thus born into a poor feeding environment and additionally have to compete against older, bigger and bolder conspecifics from previous age cohorts. Third, stomach content analysis during wintertime of stream fish indicated prey abundance throughout the year. Additionally, competitors in

the streams from older age cohorts are rare, making the stream habitat a superior feeding habitat (excluding the influences of predation).

Local adaptation in lake and stream stickleback

Genome scan data based on SNP–markers comparing lake and stream populations, revealed very low overall genetic differentiation. Nevertheless, some markers expressed moderate to high differentiation between the habitats. I therefore wanted to test for fitness differences in lake and stream stickleback and their hybrids, in a replicated long–term field transplant experiment. Juvenile lab raised stickleback were transferred into field enclosures, and survival, growth and competition load over time were recorded. The outcome was highly consistent among the replicates. Stream fish displayed higher survival than lake fish, with intermediate values found in hybrids. Unexpectedly, the indirect fitness measurement body mass did not differ among cross types at the end of the experiment. Lake fish in replicates with high densities of resident stickleback (immigrants) displayed poorest survival. Density–dependent selection driven by intraspecific resource competition, which is considered to be an important factor in ecologically–driven reproductive isolation (Schluter, 2000; Nosil, 2012) might be the reason for this outcome. However, the differential survival rates directly translate into pre– and postzygotic reproductive isolation via selection against migrants and selection against hybrids and is showing strong evidence for local adaptation.

Avenues for further research

Two questions remain, which I would like to have answered. First, does divergence in size influence mate choice and male–male competition in this system and thereby further increase total reproductive isolation between the lake and the stream populations? Male size is known to influence reproductive success in this species (Dufresne et al. 1990; Nagel and Schluter 1998; Ishikawa and Mori 2000; McKinnon et al. 2004). First, small males may be inferior in territory defense. Second, female choice is known to be size–dependent in Canadian systems (Nagel and Schluter 1998). I therefore started a field experiment in spring 2015 to answer these questions. Out of logistical reasons I had to stop it though. However, we will retry to answer this questions under common garden conditions in the near future.

Second, I am interested in the speed of local adaptation based on standing

genetic variation in our system. I started an experiment in autumn 2015, which would be able to answer this question. I got the permission to release lab raised lake–stream F_2 hybrids into three stickleback free stream habitats. The plan is to do yearly samplings and then perform genome scans against a reference F_2 hybrid sample. This procedure would exhibit expected allele frequency shifts over time and thereby providing rare evidence for genetic evolution *in situ* and *in vivo*.

References

Abbot P and Withgott JH (2004) Phylogenetic and molecular evidence for allochronic speciation in gall–forming aphids (*Pemphigus*). Evolution 58:539–553.

Aguirre WE (2009) Microgeographical diversification of threespine stickleback: body shape–habitat correlations in a small, ecologically diverse Alaskan drainage. Biol J Linn Soc 98:139–151.

Aguirre WE and Akinpelu O (2010) Sexual dimorphism of head morphology in threespine stickleback (*Gasterosteus aculeatus*). J Fish Biol 77:802–821.

Akey JM, Zhang G, Zhang K et al. (2002) Interrogating a high—-density SNP map for signatures of natural selection. Genome Res 12:1805–1814.

Akhunov ED, Goodyear AW, Geng S et al. (2003) The organization and rate of evolution of wheat genomes are correlated with recombination rates along chromosome arms. Genome Rese 13:753–763.

Albert AYK (2005) Mate choice, sexual imprinting, and speciation: a test of a one–allele isolating mechanism in sympatric sticklebacks. Evolution 59:927–931.

Albert AYK, Sawaya S, Vines TH et al. (2008) The genetics of adaptive shape shift in stickleback: pleiotropy and effect size. Evolution 62:76–85.

Alho JS, Leinonen T and Merilä J (2011) Inheritance of vertebral number in the three–spined stickleback (*Gasterosteus aculeatus*). PLOS One 6:e19579.

Anderson LK, Doyle GG, Brigham B et al. (2003) High–resolution crossover maps for each bivalent of *Zea mays* using recombination nodules. Genetics 165:849–865.

Andersson M (1994) Sexual selection. Princeton: Princeton University.

AOAC (1997) Official methods of analysis of AOAC International. Association of Official Analytical Chemists, Arlington VA.

Arendt J and Reznick D (2008) Convergence and parallelism reconsidered:

what have we learned about the genetics of adaptation? Trends Ecol Evol 23:26–32.

Arnegard ME, McGee MD, Matthews B et al. (2014) Genetics of ecological divergence during speciation. Nature doi:10.1038/nature13301.

Australian Bureau of Statistics (2013) Agricultural Commodities, Australia, 2011–12. Cat. No. 7121.0. Available: http://abs.gov.au. Accessed 10 December 2013.

Auton A, Fledel–Alon A, Pfeifer S et al. (2012) A fine–scale chimpanzee genetic map from population sequencing. Science 336:193–198.

Backström N, Forstmeier W, Schielzeth H et al. (2010) The recombination landscape of the zebra finch *Taeniopygia guttata* genome. Genome Res 20:485–495.

Baggerman B (1972) Photoperiodic responses in the stickleback and their control by a daily rhythm of photosensitivity. Gen Comp Endocrinol 3:466–476.

Baggerman B (1985) The roles of daily and annual biological rhythms in the photoperiodic regulation of the breeding season in the stickleback *Gasterosteus aculeatus* L. Behaviour 93:1–7.

Baird NA, Etter PD, Atwood TS et al. (2008) Rapid SNP discovery and genetic mapping using sequenced RAD markers. PLOS ONE 3:e3376.

Baker BS, Carpenter ATC, Esposito MS et al. (1976) The genetic control of meiosis. Annu Rev Genet, 10:53–134.

Baker JA, Foster SA, Heins DC et al. (1998) Variation in female life–history traits among Alaskan populations of the threespine stickleback, *Gasterosteus aculeatus* L. (Pisces: Gasterosteidae). Biol J Linn Soc 63:141–159.

Baker JA, Cresko WA, Foster SA et al. (2005) Life–history differentiation of benthic and limnetic ecotypes in a polytypic population of threespine stickleback (*Gasterosteus aculeatus*). Evol Ecol Res 7:121–131.

Baker JA, Heins DC, King RW et al. (2011) Rapid shifts in multiple life history traits in a population of threespine stickleback. J Evol Biol 24:863–870.

Barker S, Brown GD and Calaby JH (1963) Food regurgitation in the macropodidae. Aust J Sci 25:430–432.

Barluenga M, Stolting KN, Salzburger W et al. (2006) Sympatric speciation in Nicaraguan crater lake cichlid fish. Nature 439:719–723.

Bärmann EV (2014) The evolution of body size, horn shape and social behaviour in crown Antilopini – an ancestral character state analysis. Zitteliana B 32:185–196.

Barrett RDH and Schluter D (2008) Adaptation from standing genetic variation. Trends Ecol Evol 23:38–44.

Barrett RDH, Rogers SM and Schluter D (2009) Environment specific pleiotropy facilitates divergence at the ectodysplasin locus in threespine stickleback. Evolution 63:2831–2837.

Barrett RDH and Hoekstra HE (2011) Molecular spandrels: tests of adaptation at the genetic level. Nat Rev Genet 12:767–780.

Barton AB, Pekosz MR, Kurvathi RS et al. (2008) Meiotic recombination at the ends of chromosomes in *Saccharomyces cerevisiae*. Genetics 179:1221–1235.

Barton N and Bengtsson BO (1986) The barrier to genetic exchange between hybridizing populations. Heredity 57:357–376.

Barton NH and Keightley PD (2002) Understanding quantitative genetic variation. Nat Rev Genet 3:11–21.

Bauchop T and Martucci RW (1968) Ruminant–like digestion of the langur monkey. Science 161:698–700.

Baumont R and Deswysen AG (1991) Mélange et propulsion du contenu du réticulorumen. Repr Nutr Dev 31:335–359.

Bayes M, Hartung AJ, Ezer S et al. (1998) The anhidrotic ectodermal dysplasia gene (*EDA*) undergoes alternative splicing and encodes ectodysplasin–A with deletion mutations in collagenous repeats. Hum Mol Genet 7:1661–1669.

Beauchemin KA, Kreuzer M, O'Mara FO et al. (2008) Nutritional management for enteric methane abatement: a review. Aust J Exp Agric 48:21– 27.

Beaumont MA and Nichols RA (1996) Evaluating loci for use in the genetic analysis of population structure. P Roy Soc Lond B Bio 263:1619–1626.

Beaumont MA (2005) Adaptation and speciation: what can F_{ST} tell us? Trends Ecol Evol 20:435–440.

Beavis WD (1994) The power and deceit of QTL experiments: lessons from comparative QTL studies. Pp. 250–266 in *Proceedings of the 49th annual corn and sorghum industry research conference*. American Seed Trade Association, Washington, DC.

Becquet C and Przeworski M (2009) Learning about modes of speciation by computational approaches. Evolution 63:1558–5646.

Begun DJ and Aquadro CF (1992) Levels of naturally occurring DNA polymorphism correlate with recombination rates in *Drosophila melanogaster*. Nature 356:519–520.

Behrmann–Godel J, Gerlach G and Eckmann R (2004) Postglacial colonization shows evidence for sympatric population splitting of Eurasian perch (*Perca fluviatilis* L.) in Lake Constance. Mol Ecol 13:491–497.

Belkhir K, Borsa P, Chikhi L et al. (2004) GENETIX 4.05, logiciel sous Windows pour la génétique des populations. Laboratoire Génome, Popu-

lations, Interactions, CNRS UMR 5171, Université de Montpellier II, Montpellier (France). Available: http://www.genetix.univ–montp2.fr/genetix/genetix.htm.

Bell MA and Foster SA (1994) *The evolutionary biology of the threespine stickleback*. Oxford: Oxford University.

Bentzen P and McPhail JD (1984) Ecology and evolution of sympatric sticklebacks (*Gasterosteus*): specialization for alternative trophic niches in the Enos Lake species pair. Can J Zool 62:2280–2286.

Bentzen P, Ridgway MS and McPhail JD (1984) Ecology and evolution of sympatric sticklebacks (*Gasterosteus*) – spatial segregation and seasonal habitat shfits in the Enos Lake species pair. Can J Zool 62:2436–2439.

Bergendal B, Klar J, Stecksen–Blicks C et al. (2011) Isolated oligodontia associated with mutations in *EDARADD*, *AXIN2*, *MSX1*, and *PAX9* genes. Am J Med Genet Part A 155A:1616–1622.

Bergero R, Forrest A, Kamau E et al. (2007) Evolutionary strata on the X chromosomes of the dioecious plant *Silene latifolia*: evidence from new sex–linked genes. Genetics 175:1945–1954.

Bergstrom CA (2002) Fast–start swimming performance and reduction in lateral plate number in threespine stickleback. Can J Zool 80:207–213.

Bernardo J (1993) Determinants of maturation in animals. Trends Ecol Evol 8:166–173.

Bernardo J (1996) The particular maternal effect of propagule size, especially egg size: patterns, models, quality of evidence and interpretations. Am Zool 36:216–236.

Berner D and Blanckenhorn WU (2007) An ontogenetic perspective on the relationship between age and size at maturity. Funct Ecol 21:505–512.

Berner D, Adams DC, Grandchamp A–C et al. (2008) Natural selection drives patterns of lake–stream divergence in stickleback foraging morphology. J Evol Biol 21:1653–1665.

Berner D, Grandchamp A–C and Hendry AP (2009) Variable progress toward ecological speciation in parapatry: stickleback across eight lake–stream transitions. Evolution 63:1740–1753.

Berner D, Roesti M, Hendry AP et al. (2010a) Constraints on speciation suggested by comparing lake–stream stickleback divergence across two continents. Mol Ecol 19:4963–4978.

Berner D, Stutz WE and Bolnick DI (2010b) Foraging trait (co)variances in stickleback evolve deterministically and do not predict trajectories of adaptive diversification. Evolution 64:2265–2277.

Berner D (2011) Size correction in biology: how reliable are approaches based on (common) principal component analysis? Oecologia 166:961–971.

Berner D, Kaeuffer R, Grandchamp A–C et al. (2011) Quantitative genetic inheritance of morphological divergence in a lake–stream stickleback ecotype pair: implications for reproductive isolation. J Evol Biol 24:1975–1983.

Berner D, Moser D, Roesti M et al. (2014) Genetic architecture of skeletal evolution in European lake and stream stickleback. Evolution 68:1792–1805.

Berner D and Thibert–Plante X (2015) How mechanisms of habitat preference evolve and promote divergence with gene flow. J Evol Biol 28:1641–1655.

Bierne N (2010) The distinctive footprints of local hitchhiking in a varied environment and global hitchhiking in a subdivided population. Evolution 64:3254–3272.

Bierne, N, Gagnaire PA and David P (2013) The geography of introgression in a patchy environment and the thorn in the side of ecological speciation. Curr Zool 59:72–86.

Bill CA, Duran WA, Miselis NR et al. (1998) Efficient repair of all types of single–base mismatches in recombination intermediates in Chinese hamster ovary cells: competition between long–patch and G–T glycosylase–mediated repair of G–T mismatches. Genetics 149:1935–1943.

Bininda–Emonds ORP, Cardillo M, Jones KE et al. (2007) The delayed rise of present–day mammals. Nature 456:274.

Bininda–Emonds ORP, Cardillo M, Jones KE et al. (2007) Corrigendum: The delayed rise of present–day mammals. Nature 446:507–512.

Birdsell JA (2002) Integrating genomics, bioinformatics, and classical genetics to study the effects of recombination on genome evolution. Mol Biol Evol 19:1181– 1197.

Blanquart F, Kaltz O, Nuismer SL et al. (2013) A practical guide to measuring local adaptation. Ecol Lett 16:1195–1205.

Blaxter KL, Graham NM, Wainman FW (1956) Some observations on the digestibility of food by sheep, and on related problems. Br J Nutr 10:69–91.

Blaxter KL and Clapperton JL (1965) Prediction of the amount of methane produced by ruminants. Br J Nutr 19:511–522.

Boden SD, Liu YS, Hair GA et al. (1998) *LMP–1*, a LIM–domain protein, mediates *BMP–6* effects on bone formation. Endocrinology 139:5125–5134.

Bolnick DI (2004) Can intraspecific competition drive disruptive selection? An experimental test in natural populations of sticklebacks. Evolution 58:608–618.

Bolnick DI, Snowberg LK, Patenia C et al. (2009) Phenotype–dependent native habitat preference facilitates divergence between parapatric lake and stream stickleback. Evolution 63:2004–2016.

Bonduriansky R (2011) Sexual selection and conflict as engines of ecological diversification. Am Nat 178:729–745.

Borodin PM, Karamysheva TV, Belonogova NM et al. (2008) Recombination map of the common shrew, *Sorex araneus* (eulipotyphla, mammalia). Genetics 178:621–632.

Boughman JW, Rundle HD and Schluter D (2005) Parallel evolution of sexual isolation in sticklebacks. Evolution 59:361–373.

Bradley KM, Breyer JP, Melville DB et al. (2011) An SNP–based linkage map for zebrafish reveals sex determination loci. G3 1:3–9.

Broman KW and Sen S (2009) *A Guide to QTL Mapping With R/qtl*. Springer, New York City, New York.

Brown PW, Judis LA, Chan ER et al. (2005) Meiotic synapsis proceeds from a limited number of subtelomeric sites in the human male. Am J Hum Genet 77:556–566.

Brown TC and Jiricny J (1987) A specific mismatch repair event protects mammalian cells from loss of 5–methylcytosine. Cell 50:945–950.

Bruining M and Bosch MW (1992) Ruminal passage rate as affected by CrNDF particle size. Anim Feed Sci Technol 37:193–200.

Bull JJ (1983) *Evolution of Sex Determining Mechanisms*. Benjamin Cummings, Menlo Park, CA.

Burt A (2000) Sex, recombination, and the efficacy of selection – was Weismann right? Evolution 54:337–351.

Cahill LW and McBride BW (1995) Effect of level of intake on digestion, rate of passage and chewing dynamics in hay–fed Bactrian camels. Proc Nutr Adv Group 1:3–35.

Caldecutt WJ and Adams DC (1998) Morphometrics of trophic osteology in the threespine stickleback, *Gasterosteus aculeatus* Copeia 1998:827–838.

Callahan N, Modesto A, Meira R et al. (2009) Axis inhibition protein 2 (*AXIN2*) polymorphisms and tooth agenesis. Arch Oral Biol 54:45–49.

Carmean BR, Johnson KA, Johnson DE et al. (1992) Maintenance energy requirement of llamas. Am J Vet Res 53:1696–1698.

Charlesworth B, Nordborg M and Charlesworth D (1997) The effects of local selection, balanced polymorphism and background selection on equilibrium patterns of genetic diversity in subdivided populations. Genet Res 70:155–174.

Charlesworth B (1998) Measures of divergence between populations and the effect of forces that reduce variability. Mol Evol Biol 15:538–543.

Charlesworth B and Charlesworth D (2000) The degeneration of Y chromosomes. Philos T Roy Soc B 355:1563–1572.

Charlesworth D, Charlesworth B and Marais G (2005) Steps in the evolution of heteromorphic sex chromosomes. Heredity 95:118–128.

Chassaing N, Bourthoumieu S, Cosse M et al. (2006) Mutations in *EDAR* account for one–quarter of non–ED1–related hypohidrotic ectodermal dysplasia. Hum Mutat 27:255–259.

Chen TR and Reisman HM (1970) Comparative chromosome study of North American species of sticklebacks (Teleostei – Gasterosteidae). Cytogenetics 9:321–332.

Chowdhury R, Bois PRJ, Feingold E et al. (2009) Genetic analysis of variation in human meiotic recombination. PLOS Genet 5:e1000648.

Chung H, Loehlin DW, Dufour HD et al. (2014). A single gene affects both ecological divergence and mate choice in *Drosophila*. Science 343:1148–1151.

Clausen J, Keck DD and Hiesey WM (1940) *Experimental studies on the nature of species. I. Effect of varied environment on Western North American plants.* Washington, Carnegie Institution of Washington.

Clauss M and Lechner–Doll M (2001) Differences in selective reticuloruminal particle retention as a key factor in ruminant diversification. Oecologia 129:321–327.

Clauss M, Schwarm A, Ortmann S et al. (2004) Intake, ingesta retention, particle size distribution and digestibility in the hippopotamidae. Comp Biochem Physiol A 139:449–459.

Clauss M, Hummel J and Streich WJ (2006) The dissociation of the fluid and particle phase in the forestomach as a physiological characteristic of large grazing ruminants: an evaluation of available, comparable ruminant passage data. Eur J Wildl Res 52:88–98.

Clauss M, Fritz J, Bayer D et al. (2009a) Physical characteristics of rumen contents in two small ruminants of different feeding type, the mouflon (*Ovis ammon musimon*) and the roe deer (*Capreolus capreolus*). Zoology 112:195–205.

Clauss M, Fritz J, Bayer D et al. (2009b) Physical characteristics of rumen contents in four large ruminants of different feeding type, the addax (*Addax nasomaculatus*), bison (*Bison bison*), red deer (*Cervus elaphus*) and moose (*Alces alces*). Comp Biochem Physiol A 152:398–406.

Clauss M, Nunn C, Fritz J et al. (2009c) Evidence for a tradeoff between retention time and chewing efficiency in large mammalian herbivores. Comp Biochem Physiol A 154:376–382

Clauss M, Hume ID and Hummel J (2010) Evolutionary adaptations of ruminants and their potential relevance for modern production systems.

Animal 4:979–992.

Clauss M, Lunt N, Ortmann S, Plowman A, Codron D, Hummel J (2011) Fluid and particle passage in three duiker species. Eur J Wildl Res 57:143–148.

Clauss M and Rössner GE (2014) Old world ruminant morphophysiology, life history, and fossil record: exploring key innovations of a diversification sequence. Ann Zool Fenn 51:80–94.

Clauss M, Schiele K, Ortmann S et al. (2014) The effect of very low food intake on digestive physiology and forage digestibility in horses. J Anim Physiol Anim Nutr 98:107–118.

Cleveland WS (1979) Robust locally weighted regression and smoothing scatterplots. JASA 74:829–836.

Codron D and Clauss M (2010) Rumen physiology constrains diet niche: linking digestive physiology and food selection across wild ruminant species. Can J Zool 88:1129–1138.

Colombo PC and Jones GH (1997) Chiasma interference is blind to centromeres. Heredity 79:214–227.

Colosimo PF, Peichel CL, Nereng K et al. (2004) The genetic architecture of parallel armor plate reduction in threespine sticklebacks. PLOS Biol 2:635–641.

Colosimo PF, Hosemann KE, Balabhadra S et al. (2005) Widespread parallel evolution in sticklebacks by repeated fixation of ectodysplasin alleles. Science 307:1928–1933.

Comeron JM, Ratnappan R and Bailin S (2012) The many landscapes of recombination in *Drosophila melanogaster*. PLOS Genet 8:e1002905.

Conover DO and Schultz ET (1995) Phenotypic similarity and the evolutionary significance of countergradient variation. Trends Ecol Evol 10:248–252.

Conte GL, Arnegard ME, Peichel CL et al. (2012) The probability of genetic parallelism and convergence in natural populations. Proc Biol Sci 279:5039–5047.

Conte GL and Schluter D (2013) Experimental confirmation that size determines mate preference phenotype matching in a stickleback species pair. Evolution 67:1477–1484.

Coombs JA, Letcher BH and Nislow KH (2008) CREATE: a software to create input files from diploid genotypic data for 52 genetic software programs. Mol Ecol Res 8:578–580.

Cornuet J–M, Pudlo P, Veyssier J et al. (2014) DIYABC v2.0: a software to make approximate Bayesian computation inferences about population history using single nucleotide polymorphism, DNA sequence and microsatellite data. Bioinformatics 30:1187–1189.

Coventry J, Edwards G and Zeng B (2010) The odyssey of managing feral camels and their impacts – is there an Achilles' heel? Aust Zool 35:251–264.

Coyne JA and Orr HA (1989) Patterns of speciation in drosophila. Evolution 43:362–381.

Coyne JA and Orr HA (2004) *Speciation*. Sunderland: Sinauer Associates Inc.

Craig–Bennett A (1931) The reproductive cycle of the three–spined stickleback, *Gasterosteus aculeatus*, Linn Phil Trans R Soc B 219:197–279.

Cresko, WA, Amores A, Wilson C et al. (2004) Parallel genetic basis for repeated evolution of armor loss in Alaskan threespine stickleback populations. Proc Natl Acad Sci USA 101:6050–6055.

Crispo E (2008) Modifying effects of phenotypic plasticity on interactions among natural selection, adaptation and gene flow. J Evol Biol 21:1460–1469.

Cruickshank TE and Hahn MW (2014) Reanalysis suggests that genomic islands of speciation are due to reduced diversity, not reduced gene flow. Mol Ecol 23:3133–3157.

Crutzen PJ, Aselmann I and Seiler W (1986) Methane production by domestic animals, wild ruminants, other herbivorous fauna, and humans. Tellus B 38:271–284.

Cuñado N, Barrios J, San Miguel E et al. (2002) Synaptonemal complex analysis in oocytes and spermatocytes of threespine stickleback *Gasterosteus aculeatus* (Teleostei, Gasterosteidae). Genetica 114:53–56.

Darlis NA, Liang JB and Ho YW (2012) Effects of diets of differing fiber contents on digestibility, passage rate of digesta and heat production in lesser mouse deer (*Tragulus javanicus*). Mamm Biol 77:385–390.

Darwin C (1859) *On the origin of species by means of natural selection, or the preservation of favoured races in the struggle for life.* Cows and sons, London.

Day T, Pritchard J and Schluter D (1994) Ecology and genetics of phenotypic plasticity: a comparison of two sticklebacks. Evolution 48:1723–1734.

Day T and Rowe L (2002) Developmental thresholds and the evolution of reaction norms for age and size at life–history transitions. Am Nat 159:338–350.

Deagle BE, Jones FJ, Chan YF et al. (2012) Population genomics of parallel phenotypic evolution in stickleback across stream–lake ecological transitions. Proc R Soc Lond B 279:1277–1286.

Development Core Team R (2012) R: a language and environment for statistical computing. R Foundation for Statistical Computing, Vienna.

Dittmann MT, Hummel J, Runge U et al. (2014) Characterising an artiodactyl family inhabiting arid habitats by its metabolism: low metabolism and maintenance requirements in camelids. J Arid Environ 107:41–48

Dittmann MT, Hummel J, Hammer S et al. (2015) Digesta retention in gazelles in comparison to other ruminants: evidence for taxon–specific rumen fluid throughput to adjust digesta washing to the natural diet. Comp Biochem Physiol A 185:58–68.

Dufresne F, FitzGerald GJ and Lachance S (1990) Age and size–related differences in reproductive success and reproductive costs in threespine sticklebacks (*Gasterosteus aculeatus*). Behav Ecol 1:140–147.

Dulphy JP, Dardillat C, Jailler M et al. (1997) Comparative study of forestomach digestion in llamas and sheep. Reprod Nutr Dev 37:709–725.

Duret L and Arndt PF (2008) The impact of recombination on nucleotide substitutions in the human genome. PLOS Genet 4, e1000071.

Duret L and Galtier N (2009) Biased gene conversion and the evolution of mammalian genomic landscapes. Annu Rev Genomics Hum Genet 10:285–311.

Earl DA and vonHoldt BM (2011) STRUCTURE HARVESTER: a website and program for visualizing STRUCTURE output and implementing the Evanno method. Conserv Genet Resour 4:359–361.

Edelaar P and Bolnick DI (2012) Non–random gene flow: an underappreciated force in evolution and ecology. Trends Ecol Evol 27:659–665.

Eizaguirre C, Lenz TL, Traulsen A et al. (2009) Speciation accelerated and stabilized by pleiotropic major histocompatibility complex immunogenes. Ecol Lett 12:5–12.

Eizaguirre C, Lenz TL, Kalbe M et al. (2012) Divergent selection on locally adapted major histocompatibility complex immune genes experimentally proven in the field. Ecol Lett 15:723–731.

Endler JA (1977) *Geographic variation, speciation, and clines.* Princeton: Princeton University.

Evanno G, Regnaut S and Goudet J (2005) Detecting the number of clusters of individuals using the software STRUCTURE: a simulation study. Mol Ecol 14:2611–2620.

Evans LM, Slavov GT, Rodgers–Melnick E et al. (2014) Population genomics of *Populus trichocarpa* identifies signatures of selection and adaptive trait associations. Nat Gen 46:1089–1096.

Excoffier L, Dupanloup I, Huerta–Sanchez E et al. (2013) Robust demographic inference from genomic and SNP data. PLOS Genet, 9:e1003905.

FAO (2013): Food and Agriculture Organization of the United Nations, statistical databases. Available: http://faostat3.fao.org. 10 December 2013.

Feder JL, Roethele JB, Wlazlo B et al. (1997) Selective maintenance of allozyme differences among sympatric host races of the apple maggot fly. Proc Natl Acad Sci USA 94:11417–11421.

Feder JL and Nosil P (2010) The efficacy of divergence hitchhiking in generating genomic islands during ecological speciation. Evolution 64:1729–1747.

Feder JL, Egan SP and Nosil P (2012) The genomics of speciation–with–gene–flow. Trends Genet 28:342–350.

Felsenstein J (1974) The evolutionary advantage of recombination. Genetics 78:737–756.

Felsenstein J (1981) Evolutionary trees from DNA sequences – a maximum likelihood approach. J Mol Evol 17:368–376.

Felsenstein J (1985) Phylogenies and the comparative method. Am Nat 125:1–15.

Fitzpatrick BM (2012) Underappreciated consequences of phenotypic plasticity for ecological speciation. Int J Ecol. doi:10.1155/2012/256017.

Flaxman SM, Wacholder AC, Feder JL et al. (2014) Theoretical models of the influence of genomic architecture on the dynamics of speciation. Mol Ecol 23:4074–4088.

Fledel–Alon A, Wilson DJ, Broman KW et al. (2009) Broad–scale recombination patterns underlying proper disjunction in humans. PLOS Genet, 5:e1000658.

Flori L, Gonzatti MI, Thevenon S et al. (2012) A quasi–exclusive European ancestry in the Senepol tropical cattle breed highlights the importance of the slick locus in tropical adaptation. PLOS ONE, 7:e36133.

Foll M and Gaggiotti O (2008) A genome–scan method to identify selected loci appropriate for both dominant and codominant markers: a Bayesian perspective. Genetics 180:977–993.

Foll M, Gaggiotti OE, Daub JT et al. (2014) Widespread signals of convergent adaptation to high altitude in Asia and America. Am J Hum Genet 95:394–407.

Foster SA, McKinnon GE, Steane DA et al. (2007) Parallel evolution of dwarf ecotypes in the forest tree *Eucalyptus globulus*. New Phytol 175:370–380.

Franz R, Soliva CR, Kreuzer M et al. (2010) Methane production in relation to body mass of ruminants and equids. Evol Ecol Res 12:727–738.

Fraser BA, Künstner A, Reznick DN et al. (2015) Population genomics of natural and experimental populations of guppies (*Poecilia reticulate*). Mol Ecol 24:389–408.

Frei S, Ortmann S, Reutlinger C et al. (2015) Comparative digesta retention patterns in ratites. Auk Ornithol Adv 132:119–131.

Friesen VL, Smith AL, Gomez–Diaz E et al. (2007) Sympatric speciation by allochrony in a seabird. Proc Nat Acad Sci USA 104:18589–18594.

Fritz J, Hummel J, Kienzle E et al. (2009) Comparative chewing efficiency in mammalian herbivores. Oikos 118:1623–1632.

Fuller RC (2008) Genetic incompatibilities in killifish and the role of environment. Evolution 62:3056–3068.

Gagnaire P–A, Pavey SA, Normandeau E et al. (2013) The genetic architecture of reproductive isolation during speciation–with–gene–flow in lake whitefish species pairs assessed by RAD sequencing. Evolution 67:2483–2497.

Galtier N, Piganeau G, Mouchiroud D et al. (2001) GC–content evolution in mammalian genomes: the biased gene conversion hypothesis. Genetics 159:907–911.

Gambling SJ and Reimchen TE (2012) Prolonged life span among endemic *Gasterosteus* populations. Can J Zool 90:284–290.

Gautier, M and Vitalis R (2012) *rehh*: An R package to detect footprints of selection in genome–wise SNP data from haplotype structure. Bioinformatics 28:1176–1177.

Gavrilets S, Li H and Vose MD (2000) Patterns of parapatric speciation. Evolution 54:1126–1134.

Gavrilets S (2004) *Fitness landscapes and the origin of species*. Princeton: Princeton University.

Gavrilets S, Vose A, Barluenga M et al. (2007) Case studies and mathematical models of ecological speciation. 1. Cichlids in a crater lake. Mol Ecol 16:2893–2909.

Gelmond O, von Hippel FA and Christy MS (2009) Rapid ecological speciation in three–spined stickleback *Gasterosteus aculeatus* from Middleton Island, Alaska: the roles of selection and geographic isolation. J Fish Biol 75:2037–2051.

Gerking SD (1994) Feeding ecology of fish. Academic, San Diego, CA.

Gerton JL, DeRisi J, Shroff R et al. (2000) Global mapping of meiotic recombination hotspots and coldspots in the yeast *Saccharomyces cerevisiae*. P Natl Acad Sci USA 97:11383–11390.

Ghali MB, Scott PT and Al Jassim RAM (2004) Characterization of *Streptococcus bovis* from the rumen of the dromedary camel and Rusa deer. Lett Appl Microbiol 39:341–346.

Ghali MB, Scott PT, Alhadrami GA et al. (2011) Identification and characterisation of the predominant lactic acid–producing and lactic acid–utilising bacteria in the foregut of the feral camel (*Camelus dromedaries*) in Australia. Anim Prod Sci 51:597–604.

Gibbs MJ and Johnson DE (1994) *Methane emissions from the digestive process of livestock. In: International Anthropogenic Methane Emissions: Estimates for 1990.* EPA Report 230–R–93–010. Washington DC, USA: USEPA, pp. 2–44.

Giles N (1983) The possible role of environmental calcium levels during the evolution of phenotypic diversity in Outer Hebridean populations of the three–spined stickleback, *Gasterosteus aculeatus* J Zool 199:535–544.

Glazer AM, Killingbeck EE, Mitros T et al. (2015) Genome assembly improvement and mapping convergently evolved skeletal traits in sticklebacks with genotyping–by–sequencing. G3 5:1463–1472.

Göring HHH, Terwilliger JD and Blangero J (2001) Large upward bias in estimation of locus–specific effects from genomewide scans. Am J Hum Genet 69:1357–1369.

Gomez–Mestre I and Tejedo M (2003) Local adaptation of an anuran amphibian to osmotically stressful environments. Evolution 57:1889–1899.

Gordon JG (1968) Rumination and its significance. Wrld Rev Nutr Diet 9:251–273.

Grahame JW, Wilding CS and Butlin RK (2006) Adaptation to a steep environmental gradient and an associated barrier to gene exchange in *Littorina saxatilis.* Evolution 60:268–278.

Greenwood AK, Jones FC, Chan YF et al. (2011) The genetic basis of divergent pigment patterns in juvenile threespine sticklebacks. Heredity 107:155–166.

Gross HP and Anderson JM (1984) Geographic variation in the gillrakers and diet of European sticklebacks, *Gasterosteus aculeatus.* Copeia 1:87–97.

Grovum WL and Williams VJ (1973) Rate of passage of digesta in sheep: 4. Passage of marker through the alimentary tract and the biological relevance of rate–constants derived from the changes in concentration of marker in faeces. Br J Nutr 30:313–329.

Guerouali A and Laabouri FZ (2013) Estimates of methane emission from the camel (*Camelius dromedaries*) compared to dairy cattle (*Bos Taurus*). Adv Anim Biosci 4:286 (Abstr.).

Guerrero RF, Rousset F and Kirkpatrick M (2012) Coalescent patterns for chromosomal inversions in divergent populations. Philos Trans R Soc Lond B Biol Sci 367:430–438.

Hackstein JHP and van Alen TA (1996) Fecal methanogens and vertebrate evolution. Evolution 50:559–572.

Hagen DW (1967) Isolating mechanisms in threespine sticklebacks (*Gasterosteus*). J Fish Res Bd Canada 24:1637–1692.

Hagen DW and Gilbertson LG (1972) Geographic variation and environmental selection in *Gasterosteus aculeatus* L. in the pacific northwest,

America. Evolution 26:32–51.

Hardy CR and Linder HP (2005) Intraspecific variability and timing in ancestral ecology reconstruction: a test case from the Cape flora. Syst Biol 54:299–316.

Harper L, Golubovskaya I and Cande WZ (2004) A bouquet of chromosomes. J Cell Sci 117:4025–4032.

Harris MP, Rohner N, Schwarz H et al. (2008) Zebrafish *eda* and *edar* mutants reveal conserved and ancestral roles of ectodysplasin signaling in vertebrates. PLOS Genet, 4:e1000206.

Hassold T and Hunt P (2001) To err (meiotically) is human: the genesis of human aneuploidy. Nat Rev Genet 2:280–291.

Hatfield T (1997) Genetic divergence in adaptive characters between sympatric species of stickleback. Am Nat 149:1009–1029.

Hawthorne DJ and Via S (2001) Genetic linkage of ecological specialization and reproductive isolation in pea aphids. Nature 412:904–907.

Headon DJ, Emmal SA, Ferguson BM et al. (2001) Gene defect in ectodermal dysplasia implicates a death domain adapter in development. Nature 414:913–916.

Hebel C, Ortmann S, Hammer S et al. (2011) Solute and particle retention in the digestive tract of the Phillip's dikdik (*Madoqua saltiana phillipsi*), a very small browsing ruminant: biological and methodological implications. Comp Biochem Physiol A 159:284–290.

Hedrick PW (2005) A standardized genetic differentiation measure. Evolution 59:1633–1638.

Heller C (1871) Die Fische Tirols und Vorarlbergs. Zeitschr Ferdinandeum Tir Vor 16:295–369.

Heller R, Gregory PC and von Engelhardt W (1984) Pattern of motility and flow of digesta in the forestomach of the llama (*Lama guanacoe f. glama*). J Comp Physiol B 154:529–533.

Heller R, Lechner M and von Engelhardt W (1986a) Forestomach motility in the camel (*Camelus dromedaries*). Comp Biochem Physiol A 84:285–288.

Heller R, Lechner M, Weyreter H et al. (1986b) Forestomach fluid volume and retention of fluid and particles in the gastrointestinal tract of the camel (*Camelus dromedaries*). J Vet Med A 33:396–399.

Heller R, Cercasov V and von Engelhardt W (1986c) Retention of fluid and particles in the digestive tract of the llama (*Lama guanacoe f. glama*). Comp Biochem Physiol A 83:687–691.

Hellwing ALF, Sørensen MT, Weisbjerg MR et al. (2013) Can rapeseed lower methane emission from heifers? Acta Agric Scand, A 62:259–262.

Hendrichs H (1965) Vergleichende Untersuchung des Wiederkauverhaltens. Biol Zentrbl 84:681–751.

Hendry AP, Taylor EB and McPhail JD (2002) Adaptive divergence and the balance between selection and gene flow: lake and stream stickleback in the Misty system. Evolution 56:1199–1216.

Hendry AP (2004) Selection against migrants contributes to the rapid evolution of ecologically dependent reproductive isolation. Evol Ecol Res 6:1219–1236.

Hendry AP and Taylor EB (2004) How much of the variation in adaptive divergence can be explained by gene flow? An evaluation using lake–stream stickleback pairs. Evolution 58:2319–2331.

Hendry AP, Nosil P and Rieseberg LH (2007) The speed of ecological speciation. Funct Ecol 21:455–464.

Hendry AP (2009) Ecological speciation! Or the lack thereof? Can J Fish Aquat Sci 66:1383–1398.

Hendry AP, Bolnick DI, Berner D et al. (2009) Along the speciation continuum in sticklebacks. J Fish Biol 75:2000–2036.

Henthorn PS, Raducha M, Fedde KN et al. (1992) Different missense mutations at the tissue–nonspecific alkalinephosphatase gene locus in autosomal recessively inherited forms of mild and severe hypophosphatasia. Proc Natl Acad Sci USA 89:9924– 9928.

Herczeg G, Gonda A, Merilä J (2009) Evolution of gigantism in nine–spined sticklebacks. Evolution 63:3190–3200.

Heuts MJ (1947) Experimental studies on adaptive evolution in *Gasterosteus aculeatus* L. Evolution 1:89–102.

Hill WG and Robertson A (1966) Effect of linkage on limits to artificial selection. Genet Res 8:269–294.

Hinderer S and von Engelhardt W (1975) Urea metabolism in the llama. Comp Biochem Physiol A 52:619–622.

Hintz HF, Schryver HF and Halbert M (1973) A note on the comparison of digestion by new–world camels, sheep and ponies. Anim Prod 16:30–35.

Hötzl H (1996) Origin of the Danube–Aach system. Environ Geol 27:87–96.

Hoekstra HE and Coyne JA (2007) The locus of evolution: evo devo and the genetics of adaptation. Evolution 61:995–1016.

Hofmann RR, Streich WJ, Fickel J et al. (2008) Convergent evolution in feeding types: salivary gland mass differences in wild ruminant species. J Morphol 269:240–257.

Hohenlohe PA, Bassham S, Etter PD et al. (2010) Population genomics of parallel adaptation in threespine stickleback using sequenced RAD tags. PLOS Genet, 6:e1000862.

Hohenlohe PA, Bassham S, Currey M et al. (2012) Extensive linkage disequilibrium and parallel adaptive divergence across threespine stickleback genomes. Philos T Roy Soc B 367:395–408.

Houle D (1992) Comparing evolvability and variability of quantitative traits. Genetics 130:195–204.

Houston B, Stewart AJ and Farquharson C (2004) *PHOSPHO1* – a novel phosphatase specifically expressed at sites of mineralisation in bone and cartilage. Bone 34:629–637.

Houston B, Seawright E, Jefferies D et al. (1999) Identification and cloning of a novel phosphatase expressed at high levels in differentiating growth plate chondrocytes. Biochim Biophys Acta 1448:500–506.

Hubisz MJ, Falush D, Stephens M et al. (2009) Inferring weak population structure with the assistance of sample group information. Mol Ecol Res 9:1322–1332.

Hummel J, Clauss M, Zimmermann W et al. (2005) Fluid and particle retention in captive okapi (*Okapia johnstoni*). Comp Biochem Physiol A 140:436–444.

Hummel J, Steuer P, Südekum K–H et al. (2008) Fluid and particle retention in the digestive tract of the addax antelope (*Addax nasomaculatus*)– adaptations of a grazing desert ruminant. Comp Biochem Physiol A 149:142–149.

Hummel J, Hammer S, Hammer C et al. (2015) Solute and particle retention in a small grazing antelope, the blackbuck (*Antilope cervicapra*). Comp Biochem Physiol A 182:22–26.

Hungate RE (1966) *The rumen and its microbes*. Academic Press, London.

ICGSC (2004) Sequence and comparative analysis of the chicken genome provide unique perspectives on vertebrate evolution. Nature 432:695–716.

IPCC – Intergovernmental Panel on Climate Change (2006) *Guidelines for National Greenhouse Gas Inventories*. Vol. 4. Agriculture, Forestry and Other Land Use Emissions from Livestock and Manure Management, pp. 10.11–10.87.

Iqbal A and Khan BB (2001) Feeding behaviour of camel, Review. Pakistan J Agric Sci 38:58–63

Ishikawa M and Mori S (2000) Mating success and male courtship behaviors in three populations of the threespine stickleback. Behaviour 137:1065–1080.

Janis CM, Gordon IJ and Illius AW (1994) Modelling equid/ruminant competition in the fossil record. Hist Biol 8:15–29.

Jensen–Seaman MI, Furey TS, Payseur BA et al. (2004) Comparative recombination rates in the rat, mouse, and human genomes. Genome

Res 14:528–538.

Johnson KA and Johnson DE (1995) Methane emissions from cattle. J Anim Sci 73:2483–2492.

Jonassen TM, Imsland AK, Fitzgerald R et al. (2000) Geographic variation in growth and food conversion efficiency of juvenile Atlantic halibut related to latitude. J Fish Biol 56:279–294.

Jones FC, Grabherr MG, Chan YF et al. (2012) The genomic basis of adaptive evolution in three spine sticklebacks. Nature 484:55–61.

Jones JW and Hynes HBN (1950) The age and growth of *Gasterosteus aculeatus*, *Pygosteus pungitius* and *Spinachia vulgaris*, as shown by their otoliths. J Anim Ecol 19:59–73.

Kaeuffer R, Peichel C, Bolnick DI et al. (2012) Convergence and non– convergence in ecological, phenotypic, and genetic divergence across replicate population pairs of lake and stream stickleback. Evolution 66:402–418.

Kahilainen K and Ostbye K (2006) Morphological differentiation and resource polymorphism in three sympatric whitefish *Coregonus lavaretus* (L.) forms in a subarctic lake. J Fish Biol 68:63–79.

Kalamajski S, Aspberg A, Lindblom K et al. (2009) Asporin competes with decorin for collagen binding, binds calcium and promotes osteoblast collagen mineralization. Biochem J 423:53–59.

Kalinowski ST (2011) The computer program STRUCTURE does not reliably identify the main genetic clusters within species: simulations and implications for human population structure. Heredity 106:625–632.

Kaplan NL, Hudson RR and Langley CH (1989) The hitchhiking effect revisited. Genetics 123:887–899.

Kaske M and Groth A (1997) Changes in factors affecting the rate of digesta passage through pregnancy and lactation in sheep fed on hay. Repr Nutr Dev 37:573–588.

Kawecki TJ and Ebert D (2004) Conceptual issues in local adaptation. Ecol Lett 9:1225–1241.

Kayouli C, Jouany JP, Demeyer DI et al. (1993) Comparative studies on the degradation and mean retention time of solid and liquid phases in the forestomachs of dromedaries and sheep fed on low–quality roughages from Tunisia. Anim Feed Sci Technol 40:343–355.

Keller O and Krayss E (2000) Die Hydrographie des Bodenseeraums in Vergangenheit und Gegenwart. Ber St Gallischen Naturwiss Ges 89:39–56.

Kere J, Srivastava AK, Montonen O et al. (1996) X–linked anhidrotic (hypohidrotic) ectodermal dysplasia is caused by mutation in a novel transmembrane protein. Nat Genet 13:409–416.

Kimura T, Shinya M and Naruse K (2012) Genetic analysis of vertebral regionalization and number in Medaka (*Oryzias latipes*) inbred lines.

G3 2:1317–1323.

Kirchgessner M, Windisch W, Müller HL et al. (1991) Release of methane and of carbon dioxide by dairy cattle. Agribiol Res 44:91–102.

Kirkpatrick M and Barton N (2006) Chromosome inversions, local adaptation and speciation. Genetics 173:419–434.

Kirsch T, Harrison G, Golub EE et al. (2000) The roles of annexins and types II and X collagen in matrix vesicle–mediated mineralization of growth plate cartilage. J Biol Chem 275:35577–35583.

Kitano J, Mori S and Peichel CL (2007) Sexual dimorphism in the external morphology of the threespine stickleback (*Gasterosteus aculeatus*). Copeia 2007:336–349.

Kitano J, Ross JA, Mori S et al. (2009) A role for a neo–sex chromosome in stickleback speciation. Nature 461:1079–1083.

Kizawa H, Kou I, Iida A et al. (2005) An aspartic acid repeat polymorphism in asporin inhibits chondrogenesis and increases susceptibility to osteoarthritis. Nat Genet 37:138–144.

Koyama K, Nakazato K, Min SK et al. (2012) *COL11A1* gene is associated with limbus vertebra in gymnasts. Int J Sports Med 33:586–590.

Kozak GM, Head ML and Boughman JW (2011) Sexual imprinting on ecologically divergent traits leads to sexual isolation in sticklebacks. P Roy Soc B Bio 278:2604–2610.

Kraft T, Sall T, Magnusson–Rading I et al. (1998) Positive correlation between recombination rates and levels of genetic variation in natural populations of sea beet (*Beta vulgaris subsp. Maritime*). Genetics 150:1239–1244.

Lahn BT and Page DC (1999) Four evolutionary strata on the human X chromosome. Science 286:964–967.

Lamichhaney S, Berglund J, Almén MS et al. 2015 Evolution of Darwin's finches and their beaks revealed by genome sequencing. Nature 518:371–375.

Lammi L, Arte S, Somer M et al. (2004) Mutations in *AXIN2* cause familial tooth agenesis and predispose to colorectal cancer. Am J Hum Genet 74:1043–1050.

Lande R and Thompson R (1990) Efficiency of marker–assisted selection in the improvement of quantitative traits. Genetics 124:743–756.

Langer P (1988) *The mammalian herbivore stomach*. Gustav Fischer, Stuttgart.

Lassen J, Løvendahl P and Madsen J (2012) Accuracy of noninvasive breath methane measurements using Fourier transform infrared methods on individual cows. J Dairy Sci 95:890–898.

Lassey KR (2007) Livestock methane emission: from the individual grazing animal through national inventories to the global methane cycle. Agric

Forest Meteorol 142:120–132.

Lauper M, Lechner I, Barboza P et al. (2013) Rumination of different–sized particles in muskoxen (*Ovibos moschatus*) and moose (*Alces alces*) on grass and browse diets, and implications for rumination in different ruminant feeding types. Mamm Biol 78:142–152.

Lavin PA and McPhail JD (1993) Parapatric lake and stream sticklebacks on northern Vancouver Island: disjunct distribution or parallel evolution? Can J Zool 71:11–17.

Lawniczak MKN, Emrich SJ, Holloway AK et al. (2010) Widespread divergence between incipient *Anopheles gambiae* species revealed by whole genome sequences. Science 330:512–514.

Lawson Handley L–J, Ceplitis H and Ellegren H (2004) Evolutionary strata on the chicken Z chromosome: implications for sex chromosome evolution. Genetics 167:367–376.

Lechner I, Barboza P, Collins W et al. (2010) Differential passage of fluids and different–sized particles in fistulated oxen (*Bos primigenius f. Taurus*), muskoxen ((*Ovibos moschatus*), reindeer ((*Rangifer tarandus*) and moose ((*Alces alces*): rumen particle size discrimination is independent from contents stratification. Comp Biochem Physiol A 155:211–222.

Lechner–Doll M and von Engelhardt W (1989) Particle size and passage from the forestomach in camels compared to cattle and sheep fed a similar diet. J Anim Physiol Anim Nutr 61:120–128.

Lechner–Doll M, Rutagwenda T, Schwartz HJ et al. (1990) Seasonal changes of ingesta mean retention time and forestomach fluid volume in indigenous camels, cattle, sheep and goats grazing in a thornbush savanna pasture in Kenya. J Agric Sci 115:409–420.

Lechner–Doll M, Kaske M and von Engelhardt W (1991) Factors affecting the mean retention time of particles in the forestomach of ruminants and camelids. In: Tsuda T, Sasaki Y, Kawashima R (eds) Physiological aspects of digestion and metabolism in ruminants. Academic Press, San Diego, pp 455–482.

Lechner–Doll M, von Engelhardt W, Abbas HM (1995) Particularities in forestomach anatomy, physiology and biochemistry of camelids compared to ruminants. In: Tisserand JL (ed) Elevage et alimentation du dromadaire–Camel production and nutrition Options méditerranéennes, Serie B. Etudes et Recherches Nr. 13 CIHEAM, Paris, pp 19–32.

Leinonen T, Herczeg G, Cano JM et al. (2011a) Predation–imposed selection on threespine stickleback (*Gasterosteus aculeatus*) morphology: a test of the refuge use hypothesis. Evolution 65:2916–2926.

Leinonen T, Cano JM and Merilä J (2011b) Genetics of body shape and armour variation in threespine sticklebacks. J Evol Biol 24:206–218.

Leinonen T, Cano JM, Merilä J (2011c) Genetic basis of sexual dimorphism in the threespine stickleback *Gasterosteus aculeatus*. Heredity 106:218–227.

Leinonen T, McCairns RJS, Herczeg G et al. (2012) Multiple evolutionary pathways to decreased lateral plate coverage in freshwater threespine sticklebacks. Evolution 66:3866–3875.

Lentle R, Hemar Y and Hall C (2006) Viscoelastic behaviour aids extrusion from and reabsorption of the liquid phase into the digesta plug: creep rheometry of hindgut digesta in the common brushtail possum *Trichosurus vulpecula*. J Comp Physiol B 176:469–475.

Lerner J, Matthews E and Fung I (1988) Methane emission from animals: A Global High–Resolution Data Base. Global Biogeochem Cy 2:139–156.

Lessells CM and Boag PT (1987) Unrepeatable repeatabilities – a common mistake. Auk 104:116–121.

Levey D and Martínez del Rio C (1999) Test, rejection and reformulation of a chemical reactor–based model of gut function in a fruit–eating bird. Physiol Biochem Zool 72:369–383.

Levin DA (2009) Flowering–time plasticity facilitates niche shifts in adjacent populations. New Phytol 183:661–666.

Lewontin RC and Krakauer J (1973) Distribution of gene frequency as a test of theory of selective neutrality of polymorphisms. Genetics 74:175–195.

Lexer C, Lai Z and Rieseberg LH (2004) Candidate gene polymorphisms associated with salt tolerance in wild sunflower hybrids: Implications for the origin of *Helianthus paradoxus*, a diploid hybrid species. New Phytol 161:225–233.

Li Y, Lacerda DA, Warman ML et al. (1995) A fibrillar collagen gene, *COL11A1*, is essential for skeletal morphogenesis. Cell 80:423–430.

Li H, Handsaker B, Wysoker A et al. (2009) The Sequence Alignment/Map format and SAMtools. Bioinformatics 25:2078–2079.

Lirette A and Milligan LP (1989) A quantitative model of reticulorumen particle degradation and passage. Br J Nutr 62:465–479.

Liu Q, Dong CS, Li HQ et al. (2009a) Effects of feeding sorghumsudan, alfalfa hay and fresh alfalfa with concentrate on intake, first compartment stomach characteristics, digestibility, nitrogen balance and energy metabolism in alpacas (*Lama pacos*) at low altitude. Livest Sci 126:21–27.

Liu Q, Dong CS, Li HQ et al. (2009b) Forestomach fermentation characteristics and diet digestibility in alpacas (*Lama pacos*) and sheep (*Ovis aries*) fed two forage diets. Anim Feed Sci Techol 154:151–159.

211

Liu YH, Hair GA, Boden SD et al. (2002) Overexpressed LIM mineralization proteins do not require LIM domains to induce bone. J Bone Miner Res 17:406–414.

Logan M (2001) Evidence for the occurence of rumination–like behaviour, or merycism, in koalas (*Phascolarctos cinereus*). J Zool 255:83–87.

Logan M (2003) Effect of tooth wear on the rumination–like behavior, or merycism, of free–ranging koalas (*Phascolarctos cinereus*). J Mammal 84:897–902.

Lord RD (1994) A descriptive account of capybara behavior. Stud Neotrop Fauna Environ 29:11–22.

Lowry DB and Willis JH (2010) A widespread chromosomal inversion polymorphism contributes to a major life–history transition, local adaptation, and reproductive isolation. PLOS Biol doi:10.1371/journal.pbio.1000500.

Lu G and Bernatchez L (1999) Correlated trophic specialization and genetic divergence in sympatric lake whitefish ecotypes (*Coregonus clupeaformis*): support for the ecological speciation hypothesis. Evolution 53:1491–1505.

Lucek K, Roy D, Bezault E et al. (2010) Hybridization between distant lineages increases adaptive variation during a biological invasion: stickleback in Switzerland. Mol Ecol 19:3995–4011.

Lucek K, Sivasundar A and Seehausen O (2012) Evidence of adaptive evolutionary divergence during biological invasion. PLOS ONE, 7:e49377.

Lucek K, Sivasundar A, Roy D et al. (2013) Repeated and predictable patterns of ecotypic differentiation during a biological invasion: lake–stream divergence in parapatric Swiss stickleback. J Evol Biol 26:2691–2709.

Luikart G, England PR, Tallmon D et al. (2003) The power and promise of population genomics: from genotyping to genome typing. Nat Rev Genet 4:981–994.

Lynch M and Walsh B (1998) *Genetics and analysis of quantitative traits*. Sunderland, Sinauer Associates.

Maäkinen HS, Cano JM and Merilä J (2006) Genetic relationships among marine and freshwater populations of the European three–spined stickleback (*Gasterosteus aculeatus*) revealed by microsatellites. Mol Ecol 15:1519–1534.

Maan ME and Seehausen O (2011) Ecology, sexual selection and speciation. Ecol Lett 14:591–602.

Mackay TFC, Stone EA and Ayroles JF (2009) The genetics of quantitative traits: challenges and prospects. Nat Rev Genet 10:565–577.

Madisen L, Neubauer M, Plowman G et al. (1990) Molecular cloning of a novel bone–forming compound – osteoinductive factor. DNA Cell Biol 9:303–309.

Madsen J, Bjerg BS, Hvelplund T et al. (2010) Methane and carbon dioxide ratio in excreted air for quantification of the methane production from ruminants. Livest Sci 129:223–227.

Mambrini M and Peyraud JL (1997) Retention time of feed particles and liquids in the stomachs and intestines of dairy cows. Direct measurement and calculation based on fecal collection. Repr Nutr Dev 37:427–442.

Mancera E, Bourgon R, Brozzi A et al. (2008) High–resolution mapping of meiotic crossovers and non–crossovers in yeast. Nature 454:479–485.

Manly BFJ (2007) *Randomization, bootstrap and Monte Carlo methods in biology.* 3rd ed. Boca Raton, Chapman & Hall.

Martin C, Morgavi DP and Doreau M (2010) Methane mitigation in ruminants: from microbe to the farm scale. Animal 4:351–365.

Martin A and Orgogozo V (2013) The loci of repeated evolution: a catalog of genetic hotspots of phenotypic variation. Evolution. 67:1235–1250.

Mateus CS, Stange M, Berner D et al. (2013) Strong genome–wide divergence between sympatric European river and brook lampreys. Curr Biol 23:R649–R650.

Mather K (1938) Crossing–over. Biol Rev 13:252–292.

Matsuda I, Murai T, Clauss M et al. (2011) Regurgitation and remastication in the foregut–fermenting proboscis monkey (*Nasalis larvatus*). Biol Lett 7:786–789.

Matsuda I, Tuuga A, Hashimoto C et al. (2014) Faecal particle size in free–ranging primates supports 'rumination' strategy in the proboscis monkey (*Nasalis larvatus*). Oecologia 174:1127–1137.

Matthews B, Marchinko KB, Bolnick DI et al. (2010) Specialization of trophic position and habitat use by sticklebacks in an adaptive radiation. Ecology 91:1025–1034.

Maynard Smith J and Haigh J (1974) Hitchhiking effect of a favorable gene. Genet Res 23:23–35.

McDowall RM (2008) Jordan's and other ecogeographical rules, and the vertebral number in fishes. J Biogeogr 35:501–508.

McGaugh SE, Heil CSS, Manzano–Winkler B et al. (2012) Recombination modulates how selection affects linked sites in *Drosophila*. PLOS Biol, 10:e1001422.

McGregor M and Edwards G (2010) Guest Editorial: Managing the impacts of feral camels. Rangeland J 32:i–iii.

McKinnon JS and Rundle HD (2002) Speciation in nature: the threespine stickleback model systems. Trends Evol Ecol 17:480–488.

McKinnon JS, Mori S, Blackman BK et al. (2004) Evidence for ecology's role in speciation. Nature 429:294–298.

McKinnon JS, Hamele N, Frey N et al. (2012) Male choice in the stream–anadromous stickleback complex. PLOS ONE, 7:e37951.

McPhail JD (1977) Inherited interpopulation differences in size at first reproduction in threespine stickleback, *Gasterosteus aculeatus* L. Heredity 38:53–60.

McPhail JD (1984) Ecology and evolution of sympatric sticklebacks (*Gasterosteus*): morphological and genetic evidence for a species pair in Enos Lake, British Columbia. Can J Zool 62:1402–1408.

Meirmans PG (2006) Using the AMOVA framework to estimate a standardized genetic differentiation measure. Evolution 60:2399–2402.

Meunier J and Duret L (2004) Recombination drives the evolution of GC–content in the human genome. Mol Biol Evol 21:984–990.

Meyer K, Hummel J and Clauss M (2010) The relationship between forage cell wall content and voluntary food intake in mammalian herbivores. Mamm Rev 40:221–245.

Mikawa S, Morozumi T, Shimanuki S-I et al. (2007) Fine mapping of a swine quantitative trait locus for number of vertebrae and analysis of an orphan nuclear receptor, germ cell nuclear factor (*NR6A1*). Genome Res 17:586–593.

Mikawa S, Sato S, Nii M et al. (2011) Identification of a second gene associated with variation in vertebral number in domestic pigs. BMC Genet 12:5.

Miller CT, Yelon D, Stainier DYR et al. (2003) Two *endothelin 1* effectors, *hand2* and *bapx1*, pattern ventral pharyngeal cartilage and the jaw joint. Development 130:1353–1365.

Mitchell–Olds T, Willis JH and Goldstein DB (2007) Which evolutionary processes influence natural genetic variation for phenotypic traits? Nat Rev Genet 8:845–856.

Moe PW and Tyrell HF (1979) Methane production in dairy cows. J Dairy Sci 62:1583–1586.

Moir RJ, Somers M, Sharman G et al. (1954) Ruminant–like digestion in a marsupial. Nature 173:269–270.

Moir RJ, Somers M and Waring H (1956) Studies on marsupial nutrition. I. Ruminant–like digestion in a herbivorous marsupial. Aust J Biol Sci 9:293–304.

Mollison BC (1960) Food regurgitation in Bennett's wallaby and the scrub wallaby. CSIRO Wildl Res 5:87–88.

Monreal AW, Ferguson BM, Headon DJ et al. (1999) Mutations in the human homologue of mouse dl cause autosomal recessive and dominant

hypohidrotic ectodermal dysplasia. Nat Genet 22:366–369.

Moodie GEE and Reimchen TE (1976) Phenetic variation and habitat differences in *Gasterosteus* populations of Queen Charlotte Islands. Syst Zool 25:49–61.

Morgan M, Anders S, Lawrence M et al. (2009) ShortRead: a bioconductor package for input, quality assessment and exploration of high–throughput sequence data. Bioinformatics 25:2607–2608.

Morgavi DP, Forano E, Martin C et al. (2010) Microbial ecosystem and methanogenesis in ruminants. Animal 4:1024–1036.

Moss AR, Jouany JP and Newbold J (2000) Methane production by ruminants and its contribution to global warming. Ann Zootech 49:213–253.

Mostowska A, Biedziak B and Jagodzinski PP (2006) Axis inhibition protein 2 (*AXIN2*) polymorphisms may be a risk factor for selective tooth agenesis. J Hum Genet 51:262–266.

Müller DWH, Caton J, Codron D et al. (2011) Phylogenetic constraints on digesta separation: variation in fluid throughput in the digestive tract in mammalian herbivores. Comp Biochem Physiol A 160:207–220.

Müller DWH, Codron D, Meloro C et al. (2013) Assessing the Jarman–Bell Principle: scaling of intake, digestibility, retention time and gut fill with body mass in mammalian herbivores. Comp Biochem Physiol A 164:129–140.

Muyle A, Serres–Giardi L, Ressayre A et al. (2011) GC–biased gene conversion and selection affect GC content in the *Oryza* genus (rice). Mol Biol Evol 28:2695–2706.

Myhre F and Klepaker T (2009) Body armour and lateral–plate reduction in freshwater three–spined stickleback *Gasterosteus aculeatus*: adaptations to a different buoyancy regime? J Fish Biol 75:2062–2074.

Nachman MW (2001) Single nucleotide polymorphisms and recombination rate in humans. Trends Genet 17:481–485.

Nachman MW (2002) Variation in recombination rate across the genome: evidence and implications. Curr Opin Genet Dev 12:657–663.

Nadeau NJ, Whibley A, Jones RT et al. (2012) Genomic islands of divergence in hybridizing *Heliconius* butterflies identified by large–scale targeted sequencing. Phil Trans R Soc B 367:343–353.

Nagel L and Schluter D (1998) Body size, natural selection, and speciation in sticklebacks. Evolution 52:209–218.

Nam K and Ellegren H (2008) The chicken (*Gallus gallus*) Z chromosome contains at least three nonlinear evolutionary strata. Genetics 180:1131–1136.

Naranjo T and Corredor E (2008) Nuclear architecture and chromosome

dynamics in the search of the pairing partner in meiosis in plants. Cytogenet Genome Res 120:320–330.

National Research Council – NRC (2007) *Nutrient requirements of small ruminants: Sheep, goats, cervids and New World camelids.* Washington DC, USA: National Academy of Science Press.

Natri HM, Shikano T and Merilä J (2013) Progressive recombination suppression and differentiation in recently evolved neo–sex chromosomes. Mol Biol Evol 5:1131-1144.

Naumann C and Bassler R (1976) *Die chemische Untersuchung von Futtermitteln.* Darmstadt, Germany: VDLUFA–Verlag.

Navarro A, Betran E and Barbadilla A (1997) Recombination and gene flux caused by gene conversion and crossing over in inversion heterokaryotypes. Genetics 146:695–709.

Nei M and Tajima F (1981) DNA polymorphism detectable by restriction endonucleases. Genetics 97:145–163.

Nevado B, Ramos–Onsins SE and Perez–Enciso M (2014) Resequencing studies of nonmodel organisms using closely related reference genomes: optimal experimental designs and bioinformatics approaches for population genomics. Mol Ecol 23:1764–1779.

Nichols KM, Wheeler PA and Thorgaard GH (2004) Quantitative trait loci analyses for meristic traits in *Oncorhynchus mykiss* Environ Biol Fish 69:317–331.

Niehuis O, Gibson JD, Rosenberg MS et al. (2010) Recombination and its impact on the genome of the haplodiploid parasitoid wasp *Nasonia.* PLOS ONE, 5:e8597.

Nielsen R (2005) Molecular signatures of natural selection. Annu Rev Genet 39:197–218.

Nijhout HF (2003) The control of body size in insects. Dev Biol 261:1–9.

Noor MAF, Cunningham AL and Larkin JC (2001) Consequences of recombination rate variation on quantitative trait locus mapping studies: simulations based on the *Drosophila melanogaster* genome. Genetics 159:581–588.

Nordborg M, Charlesworth B and Charlesworth D (1996) The effect of recombination on background selection. Genet Res 67:159–174.

Northwest Carbon Pty Ltd (2011) Management of large feral herbivores (camels) in the Australian rangelands draft methodology. Reference 2011FA001 Published under the framework of the Carbon Farming Initiative on the homepage of the Australian Government, Department of Environment. Available: http://www.climatechange.gov.au.

Nosil P, Vines TH and Funk DJ (2005) Reproductive isolation caused by natural selection against immigrants from divergent habitats. Evolution

59:705–719.

Nosil P (2007) Divergent host plant adaptation and reproductive isolation between ecotypes of *Timema cristinae* walking sticks. Am Nat 169:151–162.

Nosil P, Funk DJ and Ortiz–Barrientos D (2009) Divergent selection and heterogeneous genomic divergence. Mol Ecol 18:375–402.

Nosil P (2012) *Ecological Speciation.* Oxford Series in Ecology and Evolution.

O'Brown NM, Summers BR, Jones FC et al. (2015) A recurrent regulatory change underlying altered expression and *Wnt* response of the stickleback armor plates gene *EDA*. eLife, 4:e05290.

Ogden R and Thorpe RS (2002) Molecular evidence for ecological speciation in tropical habitats. Proc Natl Acad Sci USA 99:13612–13615.

Oleksyk TK, Smith MW and O'Brien SJ (2010) Genome–wide scans for footprints of natural selection. Philos Trans R Soc Lond B 365:185–205.

Orme D, Freckleton R, Thomas G et al. (2012) The *caper* package: comparative analysis of phylogeny and evolution in R. http://CRAN.R-project.org/

Orr HA (1998) The population genetics of adaptation: the distribution of factors fixed during adaptive evolution. Evolution 52:935–949.

Östlund–Nilsson et al. (2006) *Biology of the three–spined stickleback.* Boca Raton, FL, CRC Press.

Otto SP and Barton NH (1997) The evolution of recombination: removing the limits to natural selection. Genetics 147:879–906.

Otto SP and Lenormand T (2002) Resolving the paradox of sex and recombination. Nat Rev Genet 3:252–261.

Pagel M (1999) inferring the historical patterns of biological evolution. Nature 401:877–884.

Paradis E, Claude J and Strimmer K (2004) Analyses of phylogenetics and evolution in R language. Bioinformatics 20:289–290.

Parker GA and Begon M (1986) Optimal egg size and clutch size: effects of environment and maternal phenotype. Am Nat 128:573–592.

Payne RB, Payne LL, Woods JL et al. (2000) Imprinting and the origin of parasite–host species associations in brood–parasitic indigobirds, *Vidua chalybeata.* Anim Behav 59:69–81.

Pearks Wilkerson AJ, Raudsepp T, Graves T et al. (2008) Gene discovery and comparative analysis of X–degenerate genes from the domestic cat Y chromosome. Genomics 92:329–338.

Pearse DE, Miller MR, Abadia–Cardoso A et al. (2014) Rapid parallel evolution of standing variation in a single, complex, genomic region is

associated with life history in steelhead/rainbow trout. Proc R Soc B 281:20140012.

Peichel CL, Nereng KS, Oghi KA et al. (2001) The genetic architecture of divergence between threespine stickleback species. Nature 414:901–905.

Peichel CL, Ross JA, Matson CK et al. (2004) The master sex–determination locus in threespine sticklebacks is on a nascent Y chromosome. Cur Biol 14:1416–1424.

Pfaender J, Miesen FW, Hadiaty RK et al. (2011) Adaptive speciation and sexual dimorphism contribute to diversity in form and function in the adaptive radiation of Lake Matano's sympatric roundfin sailfin silversides. J Evol Biol 24:2329–2345.

Phillips PC (2005) Testing hypotheses regarding the genetics of adaptation. Genetica 123:15–24.

Pinares–Patiño CS, Ulyatt MJ, Waghorn GC, Lassey KR, Barry TN et al. (2003) Methane emission by alpaca and sheep fed on lucerne hay or grazed on pastures of perennial ryegrass/white clover or birdsfoot trefoil. J Agric Sci 140: 215–226.

Pinares–Patiño CS, Franco FE, Battistotti M et al. (2013) Methane emissions from alpaca and sheep fed lucerne hay as either chaff or pellets. Adv Anim Biosci 4:584 (Abstr.).

Pinheiro J, Bates D, DebRoy S et al. (2015). *nlme*: Linear and Nonlinear Mixed Effects Models. R package version 3.1-122, http://CRAN.R-project.org/package=nlme.

Posada D (2008) jModelTest: Phylogenetic model averaging. Mol Biol Evol 25:1253–1256.

Present TMC and Conover DO (1992). Physiological basis of latitudinal growth differences in *Menidia menidia*: Variation in consumption or efficiency? Funct Ecol 6:23–31.

Price T and Schluter D (1991) On the low heritability of life–history traits. Evolution 45:853–861.

Pritchard JK, Stephens M and Donnelly P (2000) Inference of population structure using multilocus genotype data. Genetics 155: 945–959.

Pritchard J and Wen W (2004) Documentation for structure software: version 2. Available: http://pritch.bsd.uchicago.edu/software/readme-2-1/readme. html.

Purcell S, Neale B, Todd–Brown K et al. (2007) PLINK: a toolset for whole–genome association and population–based linkage analysis. Am J Hum Genet 81:559–575.

R Development Core Team. (2012–2014). R: A language and environment for statistical computing. Vienna: R Foundation for Statistical Computing.

Raeymaekers JAM, Van Houdt JKJ, Larmuseau MHD et al. (2007) Divergent selection as revealed by P_{ST} and QTL–based F_{ST} in three–spined stickleback (*Gasterosteus aculeatus*) populations along a coastal–inland gradient. Mol Ecol 16:891–905.

Raeymaekers JAM, Boisjoly M, Delaire L et al. (2010) Testing for mating isolation between ecotypes: laboratory experiments with lake, stream and hybrid stickleback. J Evol Biol 23:2694–2708.

Ramsey J, Bradshaw HD and Schemske DW (2003) Components of reproductive isolation between the monkeyflowers *Mimulus lewisii* and *M. cardinalis* (Phrymaceae). Evolution 57:1520–1534.

Ravinet M, Prodoehl PA and Harrod C (2013) Parallel and nonparallel ecological, morphological and genetic divergence in lake–stream stickleback from a single catchment. J Evol Biol 26:186–204.

Rego C, Santos M and Matos M (2007) Quantitative genetics of speciation: Additive and non–additive genetic differentiation between *Drosophila madeirensis* and *Drosophila subobscura*. Genetica 131:167–174.

Reimchen TE, Stinson EM and Nelson JS (1985) Multivariate differentiation of parapatric and allopatric populations of threespine stickleback in the Sangan River watershed, Queen Charlotte Islands. Can J Zool 63:2944–2951.

Reimchen TE (1992) Extended longevity in a large–bodied stickleback, *Gasterosteus*, population. Can Field Nat 106:122–125.

Reimchen TE (1994) Predators and morphological evolution in threespine stickleback. In: Bell MA, Foster SA, editors. The evolutionary biology of the threespine stickleback. Oxford: Oxford University. pp 240–273.

Reist JD (1985) An empirical evaluation of several univariate methods that adjust for size variation in morphometric data. Can J Zool 63:1429–1439.

Ren DR, Ren J, Ruan GF et al. (2012) Mapping and fine mapping of quantitative trait loci for the number of vertebrae in a White Duroc × Chinese Erhualian intercross resource population. Anim Genet 43:545–551.

Renaut S, Grassa CJ, Yeaman S et al. (2013) Genomic islands of divergence are not affected by geography of speciation in sunflowers. Nat Commun 4.

Reusch TBH, Wegner KM and Kalbe M (2001) Rapid genetic divergence in postglacial populations of threespine stickleback (*Gasterosteus aculeatus*): the role of habitat type, drainage and geographical proximity. Mol Ecol 10:2435–2445.

Revell LJ (2010) Phylogenetic signal and linear regression on species data. Methods Ecol Evol 1:319–329.

Rice WR (1987) Speciation via habitat specialization: The evolution of reproductive isolation as a correlated character. Evol Ecol 1:301–314.

Rice WR and Hostert EE (1993) Laboratory experiments on speciation: what have we learned in 40 years? Evolution 47:1637–1653.

Rieseberg LH (2011) Chromosomal rearrangements and speciation. Trends Ecol Evol 16:351–358.

Ritchie MG (2007) Sexual selection and speciation. Annu Rev Ecol Evol Syst 38:79–102.

Robbins CT (1993) Wildlife feeding and nutrition. San Diego, CA, USA: Academic Press.

Roberts S, Narisawa D, Harmey D et al. (2007) Functional involvement of *PHOSPHO1* in matrix vesicle–mediated skeletal mineralization. J Bone Miner Res 22:617–627.

Robinson BW and Wilson DS (1994) Character release and displacement in fishes – a neglected literature. Am Nat 144:596–627.

Rockman MV and Kruglyak L (2009) Recombinational landscape and population genomics of *Caenorhabditis elegans*. PLOS Genet, 5:e1000419.

Rockman MV (2011) The QTN program and the alleles that matter for evolution: all that's gold does not glitter. Evolution 66:1–17.

Roeder GS (1997) Meiotic chromosomes: it takes two to tango. Genes & Development 11:2600–2621.

Roesti M, Hendry AP, Salzburger W et al. (2012a) Genome divergence during evolutionary diversification as revealed in replicate lake–stream stickleback population pairs. Mol Ecol 21:2852–2862.

Roesti M, Salzburger W and Berner D (2012b) Uninformative polymorphisms bias genome scans for signatures of selection. BMC Evol Biol 12:94.

Roesti M, Gavrilets S, Hendry AP et al. (2014) The genomic signature of parallel adaptation from shared genetic variation. Mol Ecol 23:3944–3956.

Roff DA (2002) Life history evolution. Sunderland: Sinauer.

Rogers SM and Bernatchez L (2006). The genetic basis of intrinsic and extrinsic post–zygotic reproductive isolation jointly promoting speciation in the lake whitefish complex (*Coregonus clupeaformis*). J Evol Biol 19:1979–1994.

Rohlf FJ (2001) tpsDig, tpsRelw, tpsRegr. Distributed by the author. Department of Ecology and Evolution, State University of New York, Stony Brook, NY.

Roselius K, Stephan W and Stadler T (2005) The relationship of nucleotide polymorphism, recombination rate and selection in wild tomato species. Genetics 171:753–763.

Rosenblum EB and Harmon LJ (2011) 'Same same but different': replicated ecological speciation at White Sands. Evolution 65:946–960.

Ross JA and Peichel CL (2008) Molecular cytogenetic evidence of rearrangements on the Y chromosome of the threespine stickleback fish. Genetics 179:2173–2182.

Rundle HD and Nosil P (2005) Ecological speciation. Ecol Lett 8:336–352.

Saalfeld WK and Edwards GP (2010) Distribution and abundance of the feral camel (*Camelus dromedaries*) in Australia. Rangeland J 32:1–9.

Sabeti PC, Reich DE, Higgins JM et al. (2002) Detecting recent positive selection in the human genome from haplotype structure. Nature 419:832–837.

Sabeti PC, Schaffner SF, Fry B et al. (2006) Positive natural selection in the human lineage. Science 312:1614–1620.

Salomé PA, Bomblies K, Fitz J et al. (2012) The recombination landscape in *Arabidopsis thaliana* F_2 populations. Heredity 108:447–455.

Salzburger W, Ewing GB and von Haeseler A (2011) The performance of phylogenetic algorithms in estimating haplotype genealogies with migration. Mol Ecol 20:1952–1963.

Sanderson SL, Cheer AY, Goodrich JS et al. (2001) Crossflow filtration in suspension–feeding fishes. Nature 412:439–441.

Sandor C, Li W, Coppieters W et al. (2012) Genetic variants in *REC8*, *RNF212*, and *PRDM9* influence male recombination in cattle. PLOS Genet, 8:e1002854.

Sandstedt SA and Tucker PK (2004) Evolutionary strata on the mouse X chromosome correspond to strata on the human X chromosome. Genome Res 14:267–272.

Santos H, Burban C, Rousselet J et al. (2011) Incipient allochronic speciation in the pine processionary moth (*Thaumetopoea pityocampa, Lepidoptera, Notodontidae*). J Evol Biol 24:146–158.

Sauer FD, Fellner V, Kinsman R et al. (1998) Methane output and lactation response in Holstein cattle with monensin or unsaturated fat added to the diet. J Anim Sci 76:906–914.

Schaeffer SW and Anderson WW (2005) Mechanisms of genetic exchange with the chromosomal inversions of *Drosophila pseudoobscura*. Genetics 171:1729–1739.

Scheet P and Stephens M (2006) A fast and flexible statistical model for large–scale population genotype data: applications to inferring missing genotypes and haplotypic phase. Am J Hum Genet 78:629–644.

Scherthan H, Weich S, Schwegler H et al. (1996) Centromere and telomere movements during early meiotic prophase of mouse and man are associated with the onset of chromosome pairing. J Cell Biol 134:1109–1125.

Schliep KP (2011) *Phangorn*: Phylogenetic analysis in R. Bioinformatics 27:592–593.

Schluter D and McPhail JD (1992) Ecological character displacement and speciation in sticklebacks. Am Nat 140:85–108.

Schluter D (1995) Adaptive radiation in sticklebacks: trade–offs in feeding performance and growth. Ecology 76:82–90.

Schluter D (2000) *The ecology of adaptive radiation.* Oxford: Oxford University.

Schulze E, Lohmeyer S and Giese W (1997) Determination of 13C/12C – ratios in rumen produced methane and CO_2 of cows, sheep and camels. Isotopes Environ Health Stud 33:75–79.

Schwarm A, Ortmann S, Wolf C et al. (2008) Excretion patterns of fluids and particle passage markers of different size in banteng (*Bos javanicus*) and pygmy hippopotamus (*Hexaprotodon liberiensis*): two functionally different foregut fermenters. Comp Biochem Physiol A 150:32–39.

Schwarm A, Ortmann S, Wolf C et al. (2009a) More efficient mastication allows increasing intake without compromising digestibility or necessitating a larger gut: comparative feeding trials in banteng (*Bos javanicus*) and pygmy hippopotamus (*Hexaprotodon liberiensis*). Comp Biochem Physiol A 152:504–512.

Schwarm A, Ortmann S, Wolf C et al. (2009b) Passage marker excretion in red kangaroo (*Macropus rufus*), collared peccary (*Pecari tajacu*) and colobine monkeys (*Colobus angolensis*, *C. polykomos*, *Trachypithecus johnii*). J Exp Zool A 311:647–661.

Schwarm A, Ortmann S, Wolf C et al. (2009c) No distinct difference in the excretion of large particles of varying size in a wild ruminant, the banteng (*Bos javanicus*). Eur J Wildl Res 55:531–533.

Schwarm A, Ortmann S, Fritz J et al. (2013) No distinct stratification of ingesta particles and no distinct moisture gradient in the forestomach of nonruminants: the wallaby, peccary, hippopotamus, and sloth. Mamm Biol 78:412–421.

Seehausen O, Terai Y, Magalhaes IS et al. (2008) Speciation through sensory drive in cichlid fish. Nature 455:620–623.

Sharpe DMT, Räsänen K, Berner D et al. (2008) Genetic and environmental contributions to the morphology of lake and stream stickleback: implications for gene flow and reproductive isolation. Evol Ecol Res 10:849–866.

Shikano T, Natri HM, Shimada Y et al. (2011) High degree of sex chromosome differentiation in stickleback fishes. BMC Genomics 12:474.

Shimada Y, Shikano T, Kuparinen A et al. (2011) Quantitative genetics of body size and timing of maturation in two nine–spined stickleback

222

(*Pungitius pungitius*) populations. PLOS ONE 6.

Shin J–H, Blay S, McNeney B et al. (2006) LDheatmap: an R function for graphical display of pairwise linkage disequilibrium between single nucelotide frequencies. J Stat Softw 16:1–8.

Silanikove N (1994) The struggle to maintain hydration and osmoregulation in animals experiencing severe dehydration and rapid rehydration: the story of ruminants. Exp Physiol 79:281–300.

Silverstein JT, Wolters WR and Holland M (1999) Evidence of differences in growth and food intake regulation in different genetic strains of channel catfish. J Fish Biol 54:607–615.

Slatkin M (1987) Gene flow and the geographic structure of natural populations. Science 15:787-792.

Smith KN and Nicolas A (1998) Recombination at work for meiosis. Curr Opin Genet Dev 8:200–211.

Smith TB, Wayne RK, Girman DJ et al. (1997) A role for ecotones in generating rainforest biodiversity. Science 276:1855–1857.

Smith G, Fang Y, Liu X et al. (2013) Transcriptome–wide expression variation associated with environmental plasticity and mating success in cactophilic *Drosophila mojavensis*. Evolution 67:1950–1963.

Smukowski CS and Noor MAF (2011) Recombination rate variation in closely related species. Heredity 107:496–508.

Snyder RJ (1991) Quantitative genetis analysis of life histories in two freshwater populations of the threespine stickleback. Copeia 2:526–529.

Sobel JM, Chen GF, Watt LR et al. (2010) The biology of speciation. Evolution 64:295–315.

Sobel JM and Chen GF (2014) Unification of methods for estimating the strength of reproductive isolation. Evolution 68:1511–1522.

Sommer U (1985) Seasonal succession of phytoplankton in Lake Constance. BioScience 35:351–357.

Song Y–Q, Cheung KMC, Ho DWH et al. (2008) Association of the asporin D14 allele with lumbar–disc degeneration in Asians. Am J Hum Genet 82:744–747.

Soria–Carrasco V, Gompert Z, Comeault AA et al. 2014 Stick insect genomes reveal natural selection's role in parallel speciation. Science 344:738–742.

Spencer CCA, Deloukas P, Hunt S et al. (2006) The influence of recombination on human genetic diversity. PLOS Genet 2:1375–1385.

Sponheimer M, Robinson T, Roeder B et al. (2003) Digestion and passage rates of grass hays by llamas, alpacas, goats, rabbits, and horses. Small Rumin Res 48:149–154.

St–Pierre B and Wright A–DG (2012) Molecular analysis of methanogenic archaea in the forestomach of the alpaca (*Vicugna pacos*). BMC Microbiol 12:1–10.

Stamatakis A (2014) RAxML version 8: a tool for phylogenetic analysis and post–analysis of large phylogenies. Bioinformatics 30:1312–1313.

Stearns SC (1992) *The evolution of life histories*. Oxford: Oxford University Press.

Stephens M, Smith NJ and Donnelly P (2001) A new statistical method for haplotype reconstruction from population data. Am J Hum Genet 68:978–989.

Stern DL and Orgogozo V (2008) The loci of evolution: how predictable is genetic evolution? Evolution 62:2155–2177.

Steuer P, Südekum K–H, Müller DWH et al. (2013) Fibre digestibility in large herbivores as related to digestion type and body mass – an in vitro approach. Comp Biochem Physiol A 164:319–326.

Stevens CE and Hume ID (1998) Contributions of microbes in vertebrate gastrointestinal tract to production and conservation of nutrients. Physiol Rev 78:393–427.

Stevison LS and Noor MAF (2010) Genetic and evolutionary correlates of fine–scale recombination rate variation in *Drosophila persimilis*. J Mol Evol 71:332–345.

Stinchcombe JR and Hoekstra HE (2008) Combining population genomics and quantitative genetics: finding the genes underlying ecologically important traits. Heredity 100:158–170.

Stoelting KN, Nipper R, Lindtke D et al. (2013) Genomic scan for single nucleotide polymorphisms reveals patterns of divergence and gene flow between ecologically divergent species. Mol Ecol 22:842–855.

Storz JF (2005) Using genome scans of DNA polymorphism to infer adaptive population divergence. Mol Ecol 14:671–688.

Storz JF and Wheat CW (2010) Integrating evolutionary and functional approaches to infer adaptation at specific loci. Evolution 64:2489–2509.

Streisfeld MA, Young WN and Sobel JM (2013). Divergent selection drives genetic differentiation in an R2R3–MYB transcription factor that contributes to incipient speciation in *Mimulus aurantiacus*. PLOS Genet doi:10.1371/journal. pgen.1003385.

Stump AD Pombi M, Goeddel L et al. (2007) Genetic exchange in *2La* inversion heterokaryotypes of *Anopheles gambiae*. Insect Mol Biol 16:703–709.

Sturtevant AH and Beadle GW (1936) The relations of inversions in the X chromosome of *Drosophila melanogaster* to crossing over and disjunction. Genetics 21:554–604.

Sutherland TM (1988) Particle separation in the forestomach of sheep. In: Dobson A, Dobson MJ (eds) Aspects of digestive physiology in ruminants. Cornell University Press, Ithaca, pp 43–73.

Swain DP (1992) The functional basis of natural selection for vertebral traits of larvae in the stickleback *Gasterosteus aculeatus*. Evolution 46:987–997.

Swofford DL (2003) *PAUP*: Phylogenetic analysis using parsimony (* and other methods)*. Sunderland: Sinauer Associates.

Takahashi A, Liu YH and Saitou N (2004) Genetic variation versus recombination rate in a structured population of mice. Mol Biol Evol 21:404–409.

Tang K, Thornton KR and Stoneking M (2007) A new approach for using genome scans to detect recent positive selection in the human genome. PLOS Biol, 5:e171.

Taylor EB, Gerlinsky C, Farrell N et al. (2012) A test of hybrid growth disadvantage in wild, free–ranging species pairs of threespine sticklebacks (*Gasterosteus aculeatus*) and its implications for ecological speciation. Evolution 66:240–251.

Tenaillon MI, Sawkins MC, Long AD et al. (2001) Patterns of DNA sequence polymorphism along chromosome 1 of maize (*Zea mays ssp. Mays* L.). P Natl Acad Sci USA 98:9161–9166.

Tennessen JA and Akey JM (2011) Parallel adaptive divergence among geographically diverse human populations. PLOS Genet, 7:e1002127.

Terai Y, Seehausen O, Sasaki T et al. (2006) Divergent selection on opsins drives incipient speciation in Lake Victoria cichlids. PLOS Biol, doi:10.1371/journal.pbio.0040433.

The UniProt Consortium (2013) Update on activities at the Universal Protein Resource (UniProt) in 2013. Nucleic Acids Res. 41:D43–D47.

Thibert–Plante X and Hendry AP (2009) Five questions on ecological speciation addressed with individual–based simulations. J Evol Biol 22:109–123.

Thibert–Plante X and Hendry AP (2010) When can ecological speciation be detected with neutral loci? Mol Ecol 19:2301–2314.

Thibert–Plante X and Hendry AP (2011) The consequences of phenotypic plasticity for ecological speciation. J Evol Biol 24:326–342.

Thibert–Plante X and Gavrilets S (2013). Evolution of mate choice and the so–called magic traits in ecological speciation. Ecol Lett 16:1004–1013.

Thielemans MF, Francois E, Bodart C et al. (1978) Mesure du transit gastrointestinal chez le porc a l'aide des radiolanthanides. Comparaison avec le mouton. Ann Biol Anim Biochim Biophys 18:237–247.

Thompson CE, Taylor EB and McPhail JD (1997) Parallel evolution of lake–stream pairs of threespine sticklebacks (*Gasterosteus*) inferred from mitochondrial DNA variation. Evolution 51:1955–1965.

Thouverey C, Strzelecka–Kiliszek A, Balcerzak M et al. (2009) Matrix vesicles originate from apical membrane microvilli of mineralizing osteoblast–like saos–2 cells. J Cell Biochem 106:127–138.

Tompson SW, Bacino CA, Safina NP et al. (2010) Fibrochondrogenesis results from mutations in the *COL11A1* type XI collagen gene. Am J Hum Genet 87:708–712.

Tortereau F, Servin B, Frantz L et al. (2012) A high density recombination map of the pig reveals a correlation between sex–specific recombination and GC content. BMC Genomics 13.

Trudel M, Tremblay A, Schetagne R et al. (2001) Why are dwarf fish so small? An energetic analysis of polymorphism in lake whitefish (*Coregonus clupeaformis*). Can J Fish Aquat Sci 58:394–405.

Tulgat R and Schaller GB (1992) Status and distribution of wild Bactrian camels *Camelus bactrianus ferus*. Biol Conserv 62:11–19.

Turesson G (1922) The species and the variety as ecological units. Hereditas 3:100–113.

Udén P, Colucci PE and Van Soest PJ (1980) Investigation of chromium, cerium and cobalt as markers in digesta. Rate of passage studies. J Sci Food Agric 31:625–632.

Urton JR, McCann SM and Peichel CL (2011) Karyotype differentiation between two stickleback species (*Gasterosteidae*). Cytogenet Genome Res 135:150–159.

Vallenas A, Cummings JF and Munnell JF (1971) A gross study of the compartmentalized stomach of two new–world camelids, the llama and guanaco. J Morphol 134:399–423.

Van Soest PJ, Robertson JB and Lewis BA (1991) Methods for dietary fiber, neutral detergent fiber, and nonstarch polysaccharides in relation to animal nutrition. J Dairy Sci 74:3583–3597.

Van Wesenbeeck L, Odgren PR, Coxon FP et al. 2007. Involvement of *PLEKHM1* in osteoclastic vesicular transport and osteopetrosis in incisors absent rats and humans. J Clin Invest 117:919–930.

Van Weyenberg S, Sales J and Janssens GPJ (2006) Passage rate of digesta through the equine gastrointestinal tract: a review. Live–stock Sci 99:3–12.

Veit G, Zwolanek D, Eckes B et al. (2011) Collagen XXIII, novel ligand for Integrin a2b1 in the epidermis. J Biol Chem 286:27804–27813.

Vernet J, Vermorel M and Jouany JP (1997) Digestibility and energy utilisation of three diets by llamas and sheep. Ann Zootech 46:127–137.

226

Voight BF, Kudaravalli S, Wen X et al. (2006) A map of recent positive selection in the human genome. PLOS Biol 4:e72.

von Engelhardt W and Schneider W (1977) Energy and nitrogen metabolism in the llama. Anim Res Dev 5:68–72.

von Engelhardt W, Haarmeyer P, Kaske M et al. (2006a) Chewing activities and oesophageal motility during feed intake, rumination and eructation in camels. J Comp Physiol B 176:117–124.

von Engelhardt W, Haarmeyer P and Lechner–Doll M (2006b) Feed intake, forestomach fluid volume, dilution rate and mean retention of fluid in the forestomach during water deprivation and rehydration in camels (*Camelus sp.*). Comp Biochem Physiol A 143:504–507.

Wade MJ and Kalisz S (1990) The causes of natural selection. Evolution 44:1947–1955.

Wake DB, Wake MH and Specht CD (2011) Homoplasy: from detecting pattern to determining process and mechanism of evolution. Science 331:1032–1035.

Wang J–L, Lan G, Wang G–X et al. (2000) Anatomical subdivisions of the stomach of the Bactrian camel (*Camelus bactrianus*). J Morphol 245:161–167.

Wang J, Naa J–K, Yu Q et al. (2012) Sequencing papaya X and Yh chromosomes reveals molecular basis of incipient sex chromosome evolution. P Natl Acad Sci USA 109:13710–13715.

Wang W and Kirsch T (2002) Retinoic acid stimulates annexin–mediated growth plate chondrocyte mineralization. J Cell Biol 157:1061–1069.

Ward AB and Brainerd EL (2007) Evolution of axial patterning in elongate fishes. Biol J Linn Soc 90:97–116.

Warner ACI (1981) Rate of passage through the gut of mammals and birds. Nutr Abstr Rev B 51:789–820.

Webster MT and Hurst LD (2012) Direct and indirect consequences of meiotic recombination: implications for genome evolution. Trends Genet 28:101–109.

Webster SE, Galindo J, Grahame JW et al. (2012) Habitat choice and speciation. Int J Ecol, Article ID 154686.

Weir BS and Cockerham CC (1984) Estimating F–statistics for the analysis of population–structure. Evolution 38:1358–1370.

Weiss MJ, Cole DEC, Ray K et al. (1988) A missense mutation in the human liver/bone/kidney alkaline–phosphatase gene causing a lethal form of hypophosphatasia. Proc Natl Acad Sci USA 85:7666–7669.

West–Eberhard MJ (2003) *Developmental plasticity and evolution.* Oxford: Oxford University.

Westram AM, Galindo J, Alm M et al. (2014) Do the same genes underlie parallel phenotypic divergence in different *Littorina saxatilis* populations? Mol Ecol 23:4603–4616.

Wheeler JC (1995) Evolution and present situation of the South American *Camelidae*. Biol J Linn Soc 54: 271–295.

Wickham H (2009) *ggplot2*: Elegant graphics for data analysis. New York: Springer.

Wilson MA and Makova KD (2009) Genomic analyses of sex chromosome evolution. Annu Rev Genomics Hum Genet 10:333–354.

Wong AK, Ruhe AL, Dumont BL et al. (2010) A comprehensive linkage map of the dog genome. Genetics 184:595–605.

Wray GA (2007) The evolutionary significance of cis–regulatory mutations. Nat Rev Genet 8:206–216.

Wu CI (2001) The genic view of the process of speciation. J Evol Biol 14:851–865.

Wund, MA, Baker JA, Clancy B et al (2008) A test of the 'Flexible stem' model of evolution: ancestral plasticity, genetic accommodation, and morphological divergence in the threespine stickleback radiation. Am Nat 172:449–462.

Xu SZ (2003) Theoretical basis of the Beavis effect. Genetics 165:2259–2268.

Yeaman S and Whitlock MC (2011) The genetic architecture of adaptation under migration–selection balance. Evolution 65:1897–1911.

Yeaman S (2013) Genomic rearrangements and the evolution of clusters of locally adaptive loci. Proc Nat Acad Sci USA 110:1743–1751.

Zaykin DV, Pudovkin A and Weir BS (2008) Correlation–based inference for linkage disequilibrium with multiple alleles. Genetics 180:533–545.

Zeng B and McGregor M (2008) *Review of commercial options for management of feral camels. Managing the impacts of feral camels in Australia: a new way of doing business*. Desert Knowledge Cooperative Research Centre, Alice Springs, Australia. pp. 221–282.

Supplementary Material
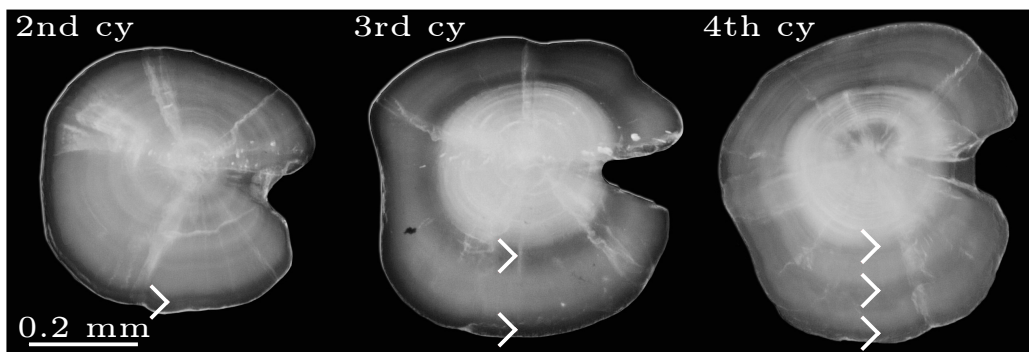
Figure S 1: Representative sagittal otoliths of stickleback from Lake Constance in their second, third, and fourth calendar year (cy), photographed at 50x magnification. The dark (transparent) ring zones, accreted in spring (Jones and Hynes 1950) and used for age determination, are indicated by white arrows.

Table S 1: Geographic situation of the three field sites chosen for the transplant experiment ('transplant sites'). The 'sampling sites' are the localities where we sampled the parental fish from which the fish for the transplant experiment were derived. The distance to lake is the water distance between each transplant site and Lake Constance.

Transplant site (country)	Associated sampling site	Distance from sampling site (km)	Distance to lake (km)	Latitude (Noth)	Longitude (East)
Singen (D)	BOH	11.2	21.6	47°46'54"	8°50'36"
Erlen (CH)	NID	6.3	14.9	47°32'52"	9°12'33"
Lauterach (AT)	HOH	21	4.7	47°28'21"	9°42'18"

Table S 2: Mean body mass (and standard deviation) of male and female stickleback from the lake and the NID population used for the maturation size threshold experiment. The data represent the measurements taken in the beginning of the experiment, and are given separately for each of the three experimental rounds.

	Lake		NID	
Experimental round	Females	Males	Females	Males
1	0.8±0.24	0.63±0.12	0.78±0.16	0.73±0.13
2	0.83±0.24	0.76±0.12	0.73±0.24	0.67±0.19
3	1.28±0.24	1.18±0.13	1.16±0.33	0.94±0.19

Table S 3: Stomach content of stickleback sampled during winter (December 15, 2014) at the NID stream site. For methodological detail see Berner et al. (2008) and chapter 1

	Lake		NID				
Specimen ID	Vemiform insect larvae*	Copepoda**	Chydorid cladocera	Isopoda	Ephemeroptera	Trichoptera	Collembola
Ga3149	7	9	0	3	0	0	0
Ga3150	19	4	0	0	1	2	1
Ga3151	24	3	3	0	1	0	0
Ga3152	11	5	2	1	1	0	0
Ga3153	12	7	2	0	0	0	0
total	73	28	7	4	3	2	1

* mainly chironomidae and ceratopogonidae
** non–calanoid

Figure S 2: epresentative male stickleback from COW lake (bottom) and COW stream (top). Photo credit: Daniel Berner.
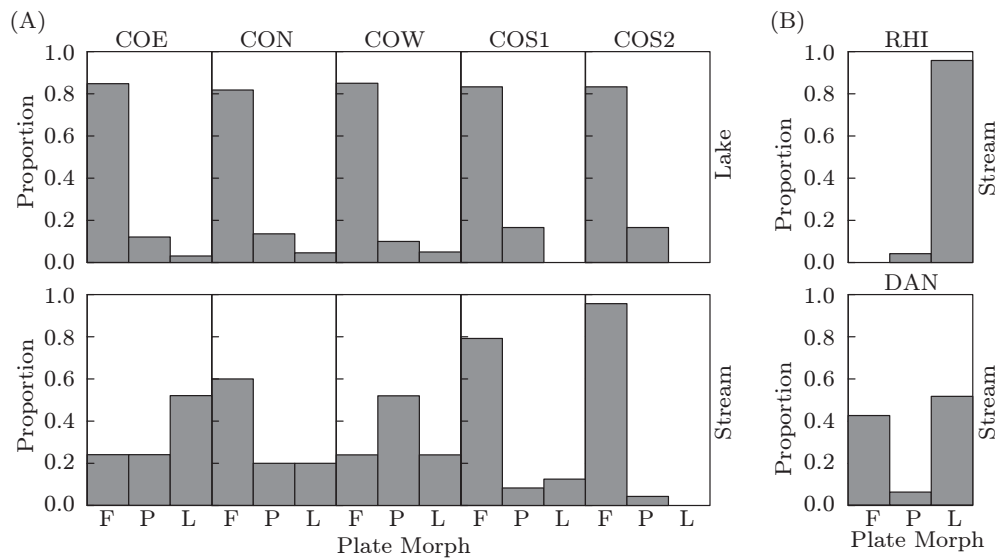
Figure S 3: Proportion of fully (F), partially (P), and low–plated (L) stickleback morphs in the five lake-stream pairs (A; lake samples on top, stream samples on the bottom), and in the two solitary stream–resident populations (B). Sample site codes are given in Table 1. P-values are from permutation tests for lake–stream shifts in plate morph frequency within each system. Note the general trend toward plate reduction in the stream samples as compared to the lake samples. P–values and plate morph frequencies for the COW and COS2 system already investigated previously (Berner et al. 2010a) are slightly different from those reported in that study because of random permutation, and because the present study analyzed subsamples of the previous study.

Figure S 4: Photographs of the field transplant enclosures used at the three experimental sites. The transplant sites are labeled according to their associated field sampling sites, see Table S1.
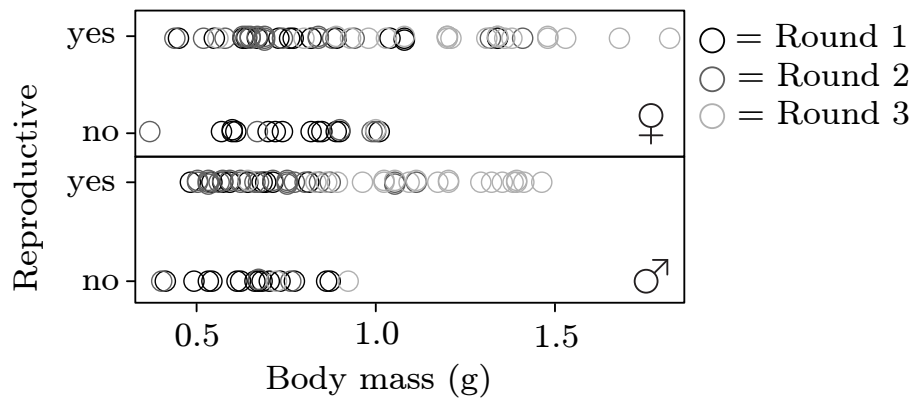
Figure S 5: Distribution of female and male stickleback body mass in relation to whether an individual reached maturity during the maturation size threshold experiment. Across all experimental rounds, individuals heavier than approximately 1 g always started to reproduce.

Figure S 6: Photographs of field transplant enclosures used at the three experimental sites. The transplant sites are labeled according to their associated field sampling sites (see Fig. 3.1 in the paper).
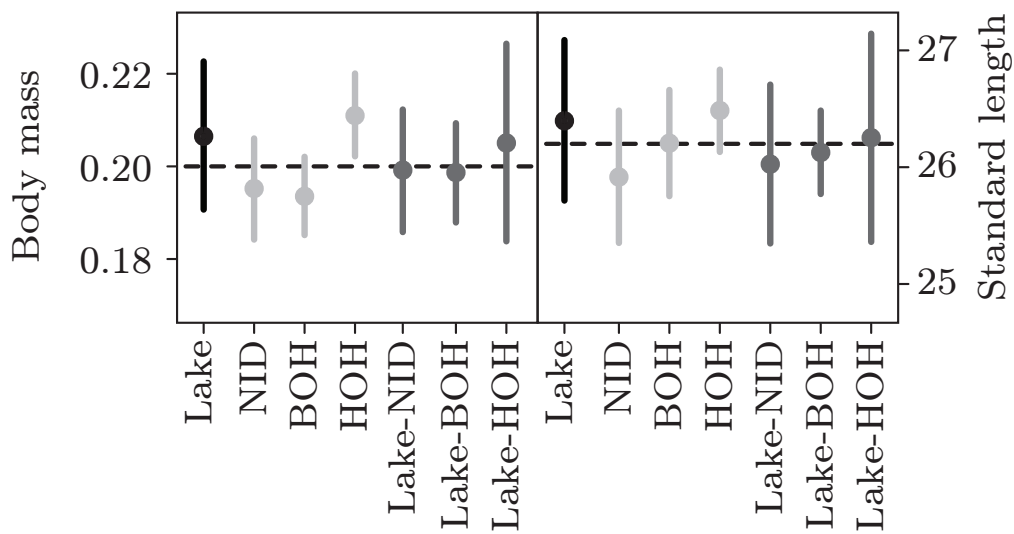
Figure S 7: Body mass (left) and standard length (right) of 20 haphazardly chosen individuals per cross type one day before the release into the experimental enclosures. Means and parametric 95% confidence intervals for the lake population are drawn in black, for the stream populations in light grey, and for the F_1 hybrids in dark gray. The dashed lines represent the grand means across all 140 fish (body mass: 0.2 g; standard length: 26.2 mm). To test for size differences among the cross types, we performed non-parametric permutation tests by randomizing the response (body mass and standard length) over the predictor (cross type) 9999 times and using the distribution of the F–statistic to derive P–values. Both tests indicated no body size difference among the cross types (P = 0.352 for body mass and P = 0.499 for standard length)..
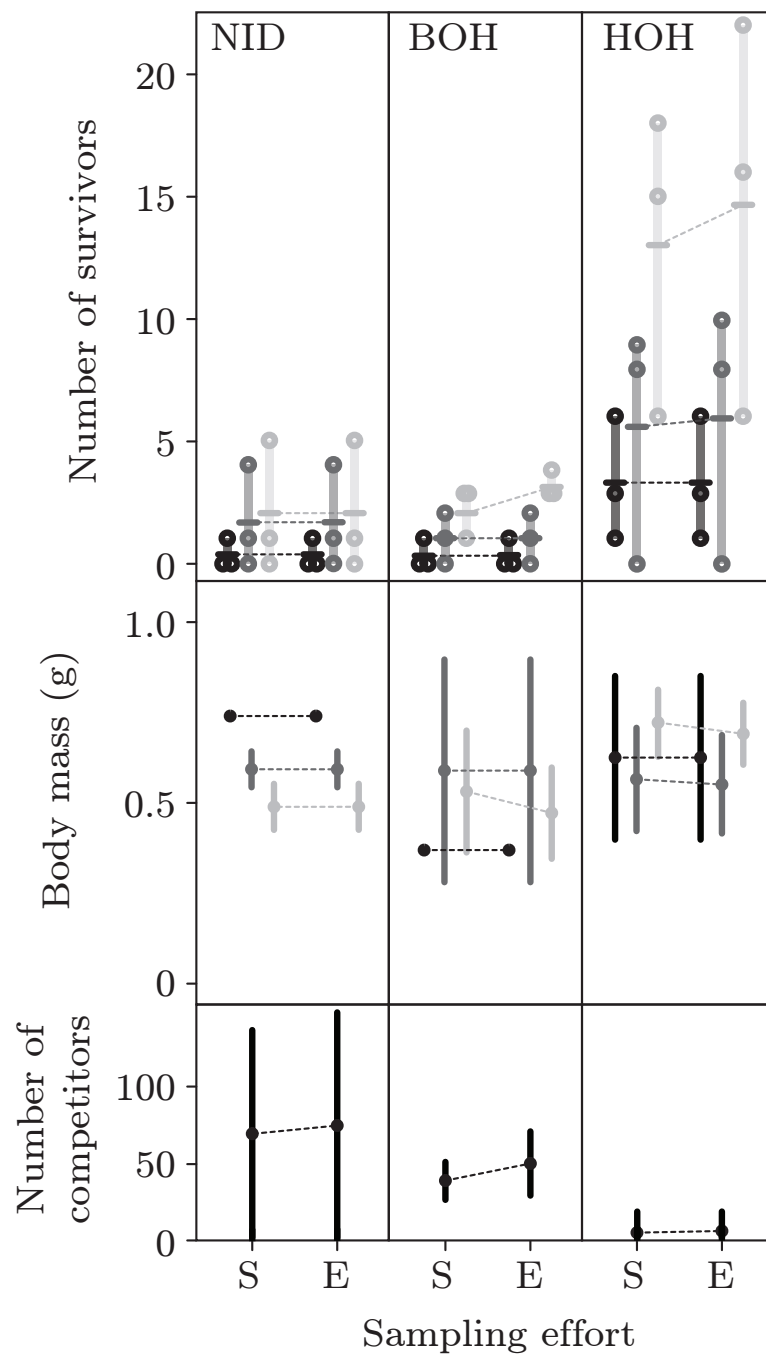
Figure S 8: Number of survivors (upper row), body mass (middle row), and number of competitors (lower row) in the enclosures at the end of the field experiment (29 weeks post–release), based on the standard sampling effort ('S'; see Materials and Methods) and extended sampling ('E'). The latter involved two additional rounds of minnow trapping with the standard sampling scheme in each enclosure. Data for lake, stream, and F_1 hybrid fish are shown in black, light gray, and dark gray. Following the conventions in Fig. 3.2, the survival data are presented as raw individual counts (minima and maxima connected by vertical bars) along with their means across the replicate enclosures (horizontal bars). For body mass and the number of competitors, the dots and error bars represent means and parametric 95% confidence intervals across the enclosures. Results from standard and extended sampling are connected by dashed lines. The first round of extended sampling yielded seven additional experimental stickleback (three at BOH and four at HOH), all of which were stream fish. The second round of extended sampling recovered one additional experimental stream fish and one F_1 hybrid at the HOH site. Overall, extended sampling thus added eight stream fish, one hybrid, and zero lake fish to the 89 total individuals captured with the standard scheme (stream: 52; F_1 hybrids: 25; lake: 12). Similarly, extended sampling added 53 total competitors (NID: 17; BOH: 33; HOH: 3) to the grand total of 352 captured with the standard scheme. Although no conclusion in our study changes qualitatively when adding the data from extended sampling to the analyses, we emphasize that considering the additional (almost exclusively stream) individuals only reinforces our inference of strong viability selection against immigrants and hybrids.
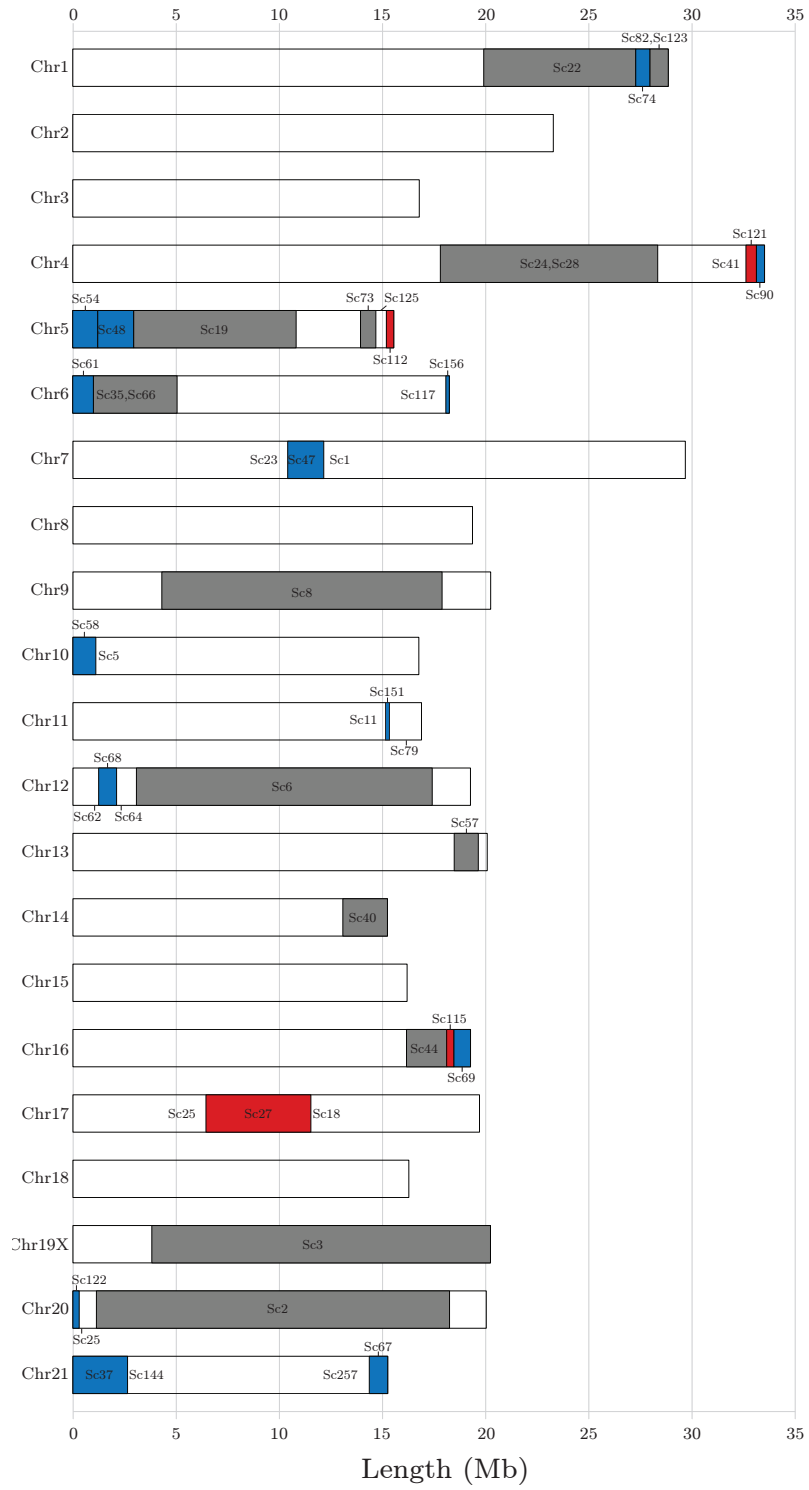
237

Figure S 9: Reassembly of the Broad S1 threespine stickleback reference genome according to a de novo linkage map based on 282 F_2 individuals and 2'165 genome–wide single nucleotide polymorphisms (SNPs). Each bar represents a chrrmosome (1–21); the length of the bar gives the total chromosome span (in megabase). Correctly assembled chromosome regions are shown in white. Scaffolds originally placed in the correct chromosome but in incorrect sense are shown in gray. Previously unanchored scaffolds that were integrated into the chromosomes are shown in blue (if incorporated in normal sense) and red (if incorporated in reverse sense). Each scaffold that was reversed and/or relocated is named (e.g. Sc22). For relocated scaffolds, we also provide the name of the flanking scaffold on each side. Note that scaffolds shorter than 140 kb were ignored. These scaffolds were generally represented by 1–3 SNPs only and typically mapped to chromosome ends.

Table S 4: Characterization of additional, suggestive ($0.05 \leq P < 0.1$) QTL for skeletal divergence between lake and stream stickleback. The presentation follows Table 5.5. Plate number was mapped using only individuals unambiguously heterozygous at the Ectodysplasin (*EDA*) locus.

Trait	Marker	Chr.	Position (bp)	LOD	P	PVE	HSE	Dir.	Cand. gene
GRL	chrIII-13014992	3	13'014'992	4.06	0.07	4.4	0.14(0.52)	L*	
HL	chrXIII-18688122	13	19'444'640	4.05	0.086	4.6	0.40(0.60)	S*	
VNo	chrII-5665753	2	5'665'753	4.05	0.076	3.6	0.31(0.57)	L*	
	chrV-6319659	5	4'509'573	3.96	0.089	3.6	0.11(0.21)	L*	
PNo	chrXIII-18503873	13	19'628'889	4.4	0.091	9.7	2.97(0.75)	S	
P11H	chrXVII-2292374	17	2'292'374	4.12	0.098	5.8	0.36(0.53)	L	*ALPL*(31)
P13H	chrV-3764951	5	7'064'281	4.15	0.069	5.6	0.33(0.54)	L	*PLEKHM1*(12)

The first column lists traits with the following abbreviations: Gill raker length = GRL; Head length = HL; Vertebral number = VNo; Plate number = PNo; Plate 11 height = P11H; Plate 13 height = P13H.

Table S 5: Genetic diversity within each of the four study populations. Diversity is calculated based exclusively on 'loner SNPs' (i.e. SNP occurring alone on their RAD locus, see Material and methods). The first two data columns indicate the number and corresponding proportion of the total loner SNPs (N = 62'332) actually being polymorphic within each population (in parentheses the proportions are scaled such that the lake is 100%). This proportion is lowest in the lake population. Analogously, the third and fourth data columns report the number and porportion of the total triallelic loner SNPs (N = 368) actually being tri–allelic within each population (in parentheses the proportions are scaled as above). This latter diversity index is again lowest in the lake population.

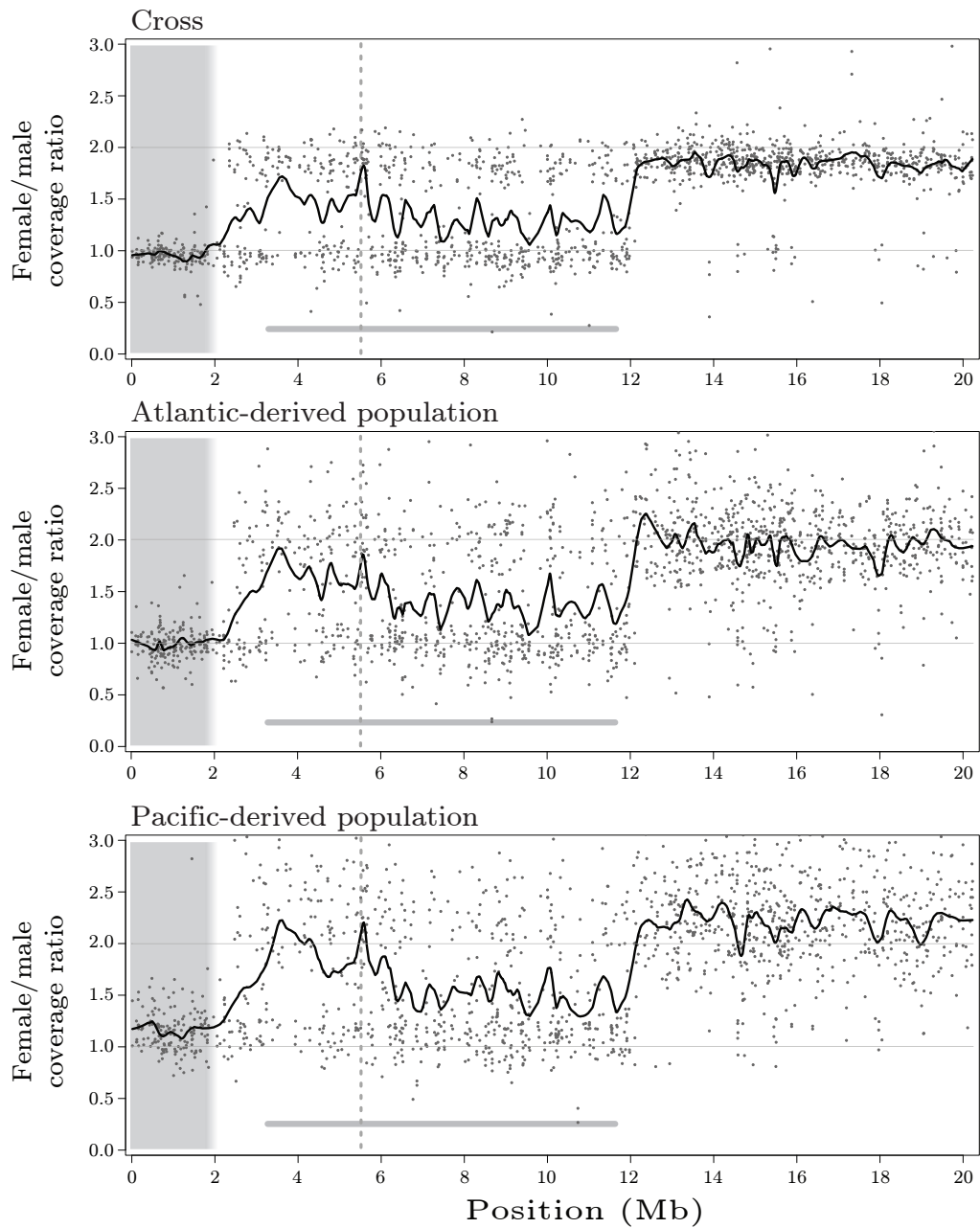| Population	Number of loner SNPs polymorphic in focal population	Proportion of loner SNPs polymorphic in focal population	Number of tri–allelic loner SNPs polymorphic in focal population	Proportion of tri–allelic loner SNPs polymorphic in focal population
Lake	44'070	0.707 (100.0%)	103	0.280 (100.0%)
BOH	45'838	0.735 (104.0%)	97	0.264 (94.2%)
NID	46'632	0.748 (105.8%)	126	0.342 (122.3%)
GRA	56'280	0.903 (127.7%)	188	0.511 (182.5%)

Figure S 10: Degeneration of the threespine stickleback Y chromosome revealed by female versus male RAD sequence coverage, compared across analyses based on different populations. The top panel is a copy of the graphic shown in Fig. 4.3, drawn based on data from our F_2 population (100 individuals per sex). The middle and bottom panels were drawn by following the same plotting conventions, but are based on samples from two natural populations independently evolved in geographic isolation and from different marine ancestors (Atlantic, CHE; Pacific, Boot Lake). Sample size in these latter analyses was 13–14 per sex and population. Note the striking consistency in female to male coverage across the different analyses
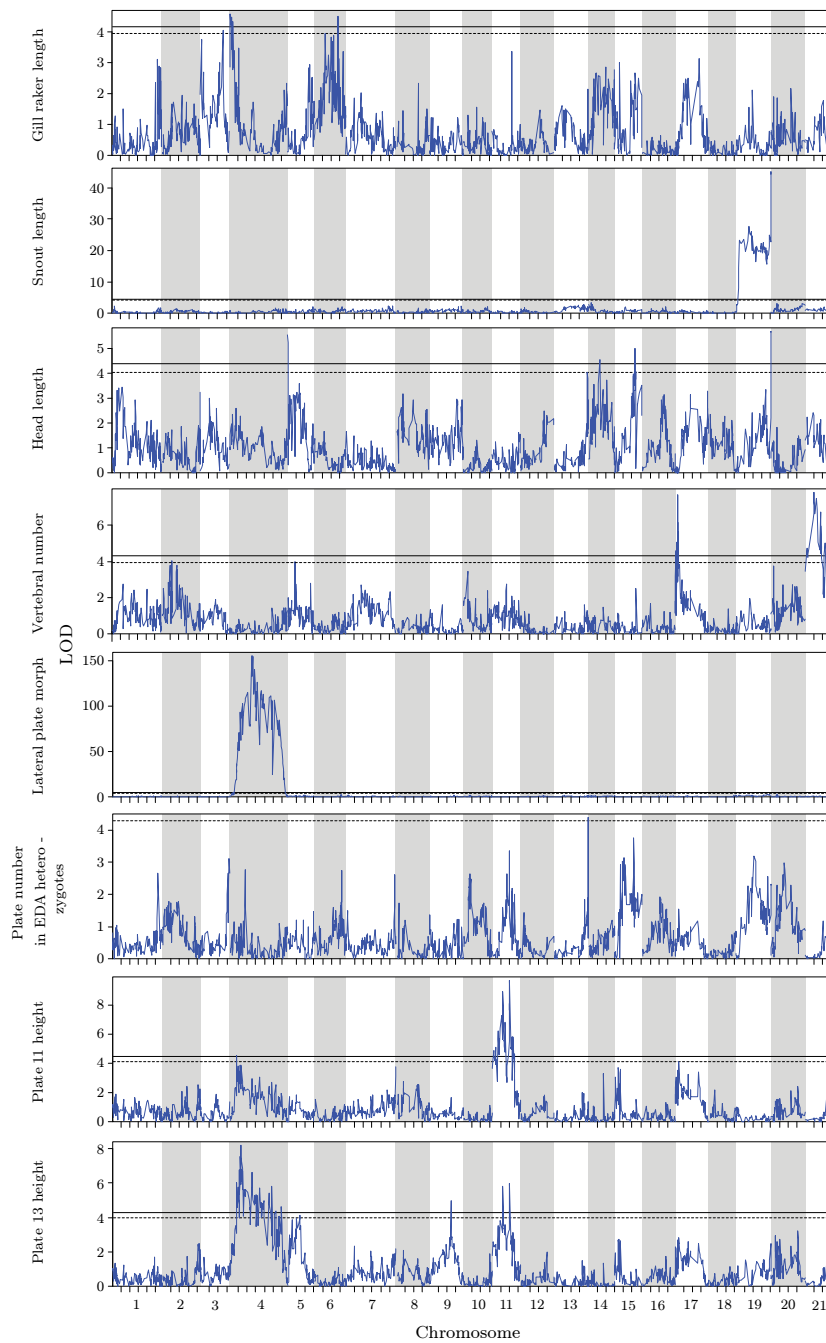
Figure S 11: Genome-wide LOD profiles for all eight traits. The chromosomes are separated by white and gray background shading. Tick marks along the X–axis indicate 5 Mb intervals, drawn separately for each chromosome. Horizontal lines represent genome–wide 0.05 (solid) and 0.1 (dashed) LOD significance thresholds based on 1'000 random permutations. Note that the Y–axes are scaled differently among the traits.

241
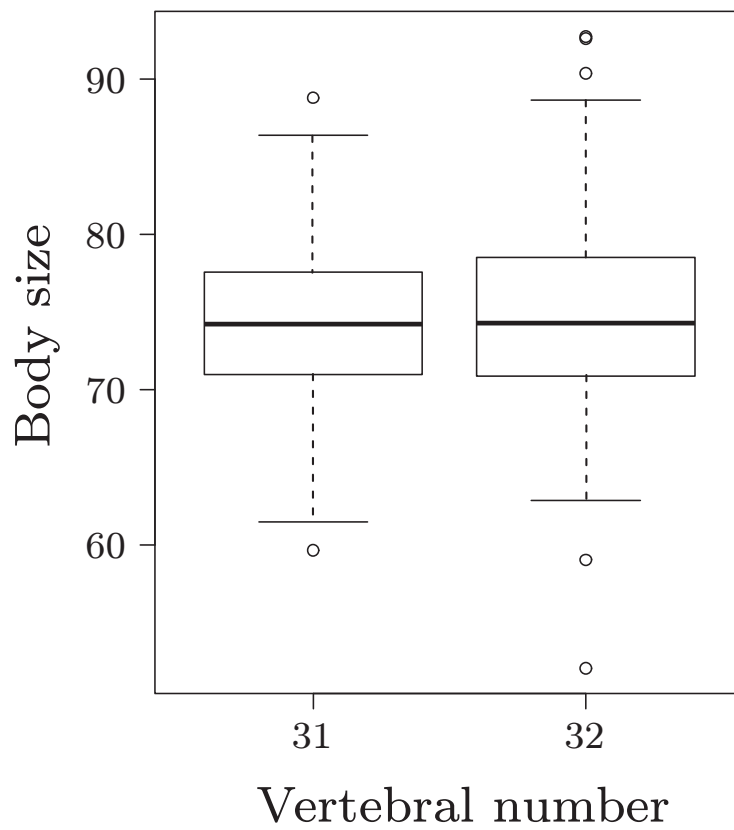
Figure S 12: Body size (quantified as geometric morphometric centroid size, in mm) in relation to vertebral number. Shown are only individuals with 31 (N = 197) and 32 (N = 258) vertebrae. The graph type is a boxplot with the whiskers representing 1.5 times the interquartile range.
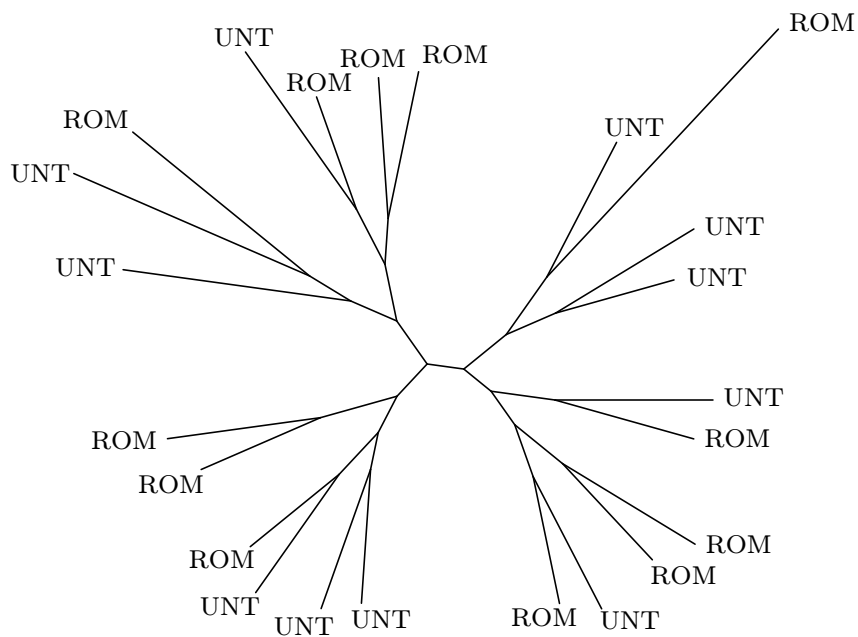
Figure S 13: Phylogenetic analysis restricted to the two stickleback samples from Lake Constance. The unrooted maximum likelihood tree is based on 55'561 genome–wide SNPs in fish sampled from two lake sites approximately 20 km apart. The sites are Romanshorn (ROM), Switzerland, western lake shore, and Unteruhldingen (UNT), Germany, eastern shore). Consistent with a genome-wide median FST of zero between ROM and UNT, the phylogeny reveals the absence of genetic structure between the two sites, indicating that Lake Constance is inhabited by a single panmictic stickleback population. The same conclusion was drawn earlier based on microsatellite markers and stickleback samples from four different lake sites.
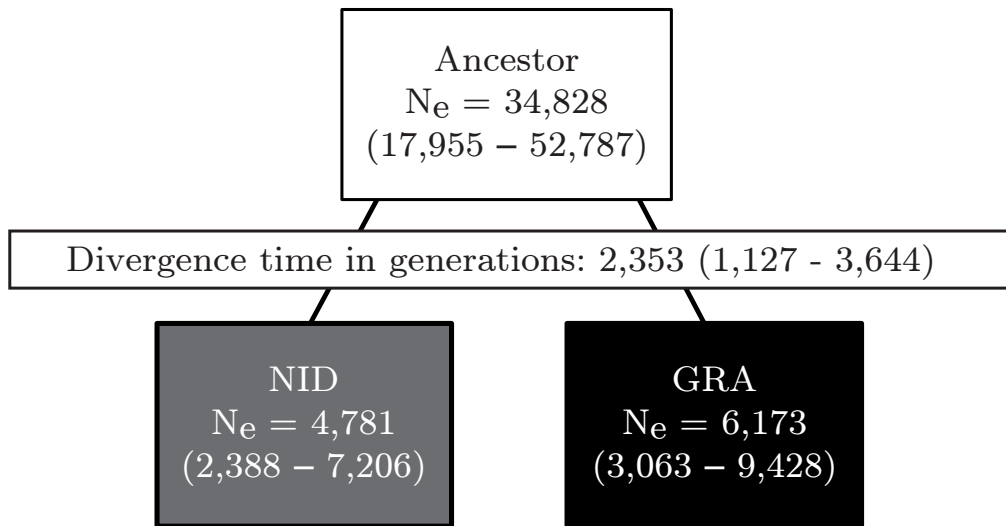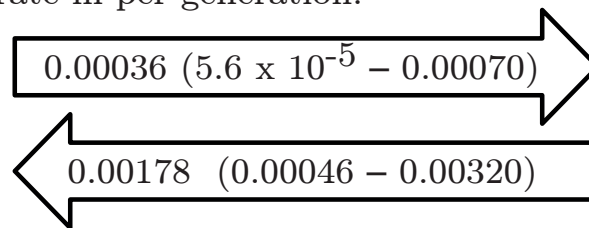
Figure S 14: Demographic analysis based on a reduced model including the GRA and NID stream populations only. Plotting conventions are as in the full model including all study populations (Fig. 6.1b). The GRA and NID populations are the genetically most variable of our study populations (see main text). In the reduced model, the split between GRA and NID from a common ancestor is estimated to have occurred more recently compared to the full model, although the confidence intervals overlap widely between the models. A potential reason for the deeper splitting time in the full model is upward bias due to extensive genome-wide selective sweeps experienced by the lake population. We thus consider the splitting time estimate from the reduced model a better approximation of the true time since stickleback colonized the Lake Constance basin. However, both models support qualitatively similar conclusions about the colonization history of the Lake Constance basin.
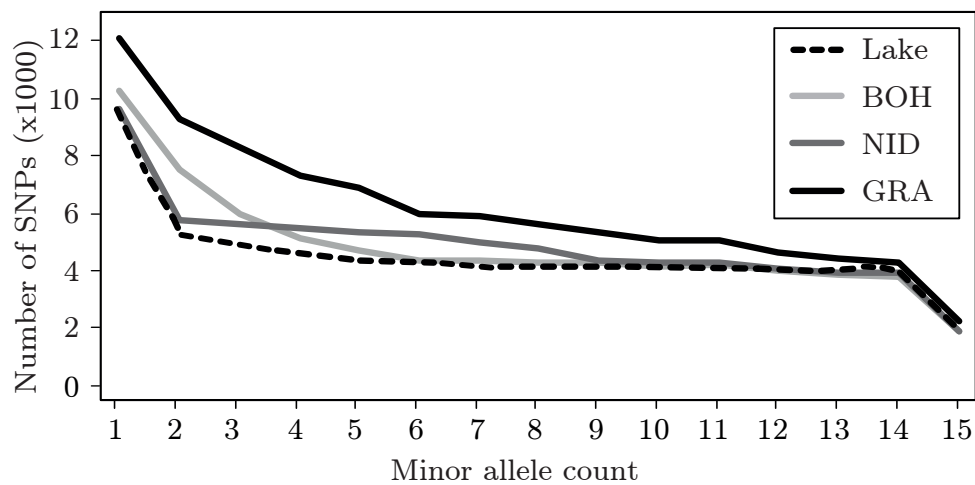
Figure S 15: Observed site frequency spectra (SFS) of the four study populations. The X–axis indicates the occurrence of the minor allele among 30 randomly sampled nucleotides at a given genome position (the minor allele frequency (MAF) would thus be obtained by dividing the counts by 30). The Y–axis gives the number of sites falling into each minor allele count class in each population. Like the joint SFS used for demographic inference, these population-specific SFS are based on 14.8 million nucleotide positions, although for the ease of presentation, only the polymorphic sites (i.e. minor allele count >0) are shown. Note the low number of polymorphisms across most minor allele count classes in the lake population relative to the stream populations (especially GRA). Accordingly, the lake population exhibited the highest proportion of monomorphic sites (minor allele count $=$ 0); in millions, lake: 14.770; BOH: 14.765; NID: 14.764; GRA: 14.745.
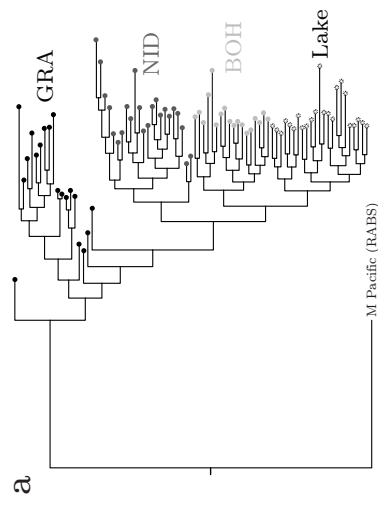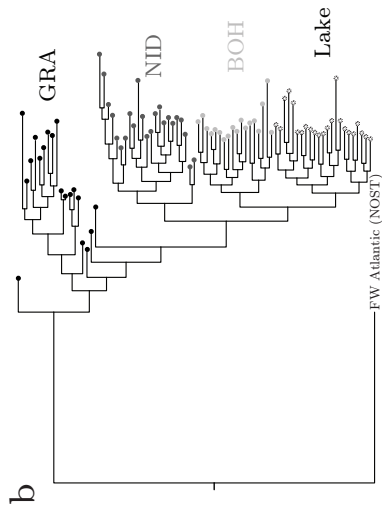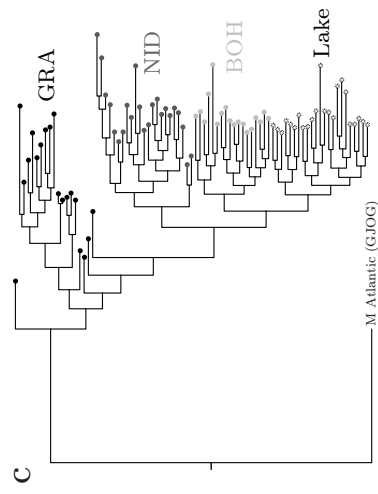
Figure S 16: Phylogenetic relationships among the Lake Constance study populations rooted using different outgroups. To verify the robustness of the rooted ML phylogeny by using the reference genome individual (a freshwater individual from the Pacific, see Fig. 6.1c) as an outgroup, we generated additional trees using several other outgroups, including (a) a marine Pacific (sampling population: 'Rabbit Slough', Alaska), (b) an freshwater Atlantic (sampling population: 'Norway Stream', Norway), and (c) a marine Atlantic (sampling population: 'Gjögur', Iceland) stickleback individual. Genotypes for these individuals were retrieved from the 'Stickleback Genome Browser'. These analyses consistently resulted in very similar tree topologies supporting identical conclusions.
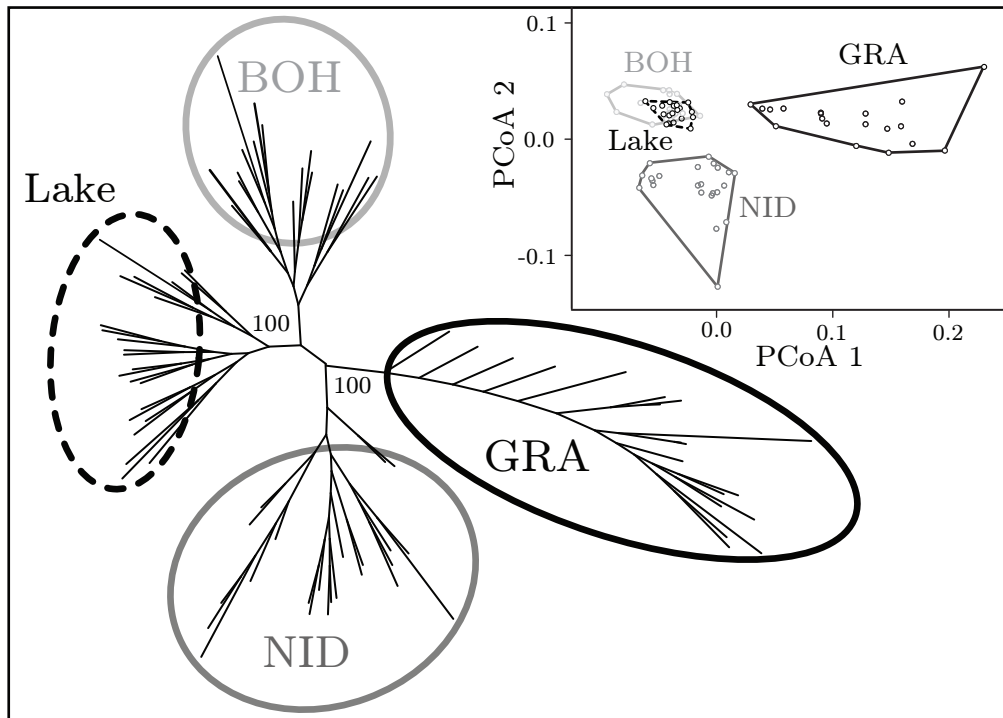

Figure S 17: Phylogenetic and principal coordinate analysis of the four stickleback populations from the Lake Constance basin. The unrooted maximum likelihood tree (based on 51'188 SNPs; bootstrap support in percent is given for the key nodes) reveals reciprocal monophyly of the four populations. Both the tree and the principal coordinate ordination (insert) further show the close relatedness of the lake and the BOH population, and that genetic diversity increases from the lake population to the BOH, NID, and GRA stream populations.
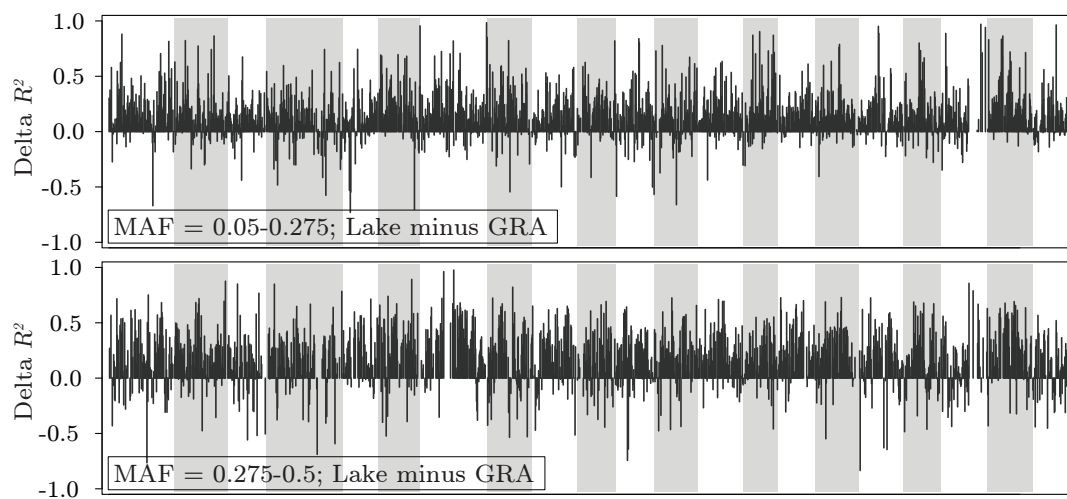
Figure S 18: Influence of using SNPs from different MAF classes on the difference in LD between the lake and the GRA population. Shown is Delta R^2 (see Fig. 6.2b) based on low–MAF (top) and high–MAF (bottom) SNPs. The MAF classes are separated using the same thresholds as used in the insert of Fig. 6.2a. Irrespective of the MAF class, LD is higher in the lake than in GRA along most of the genome.
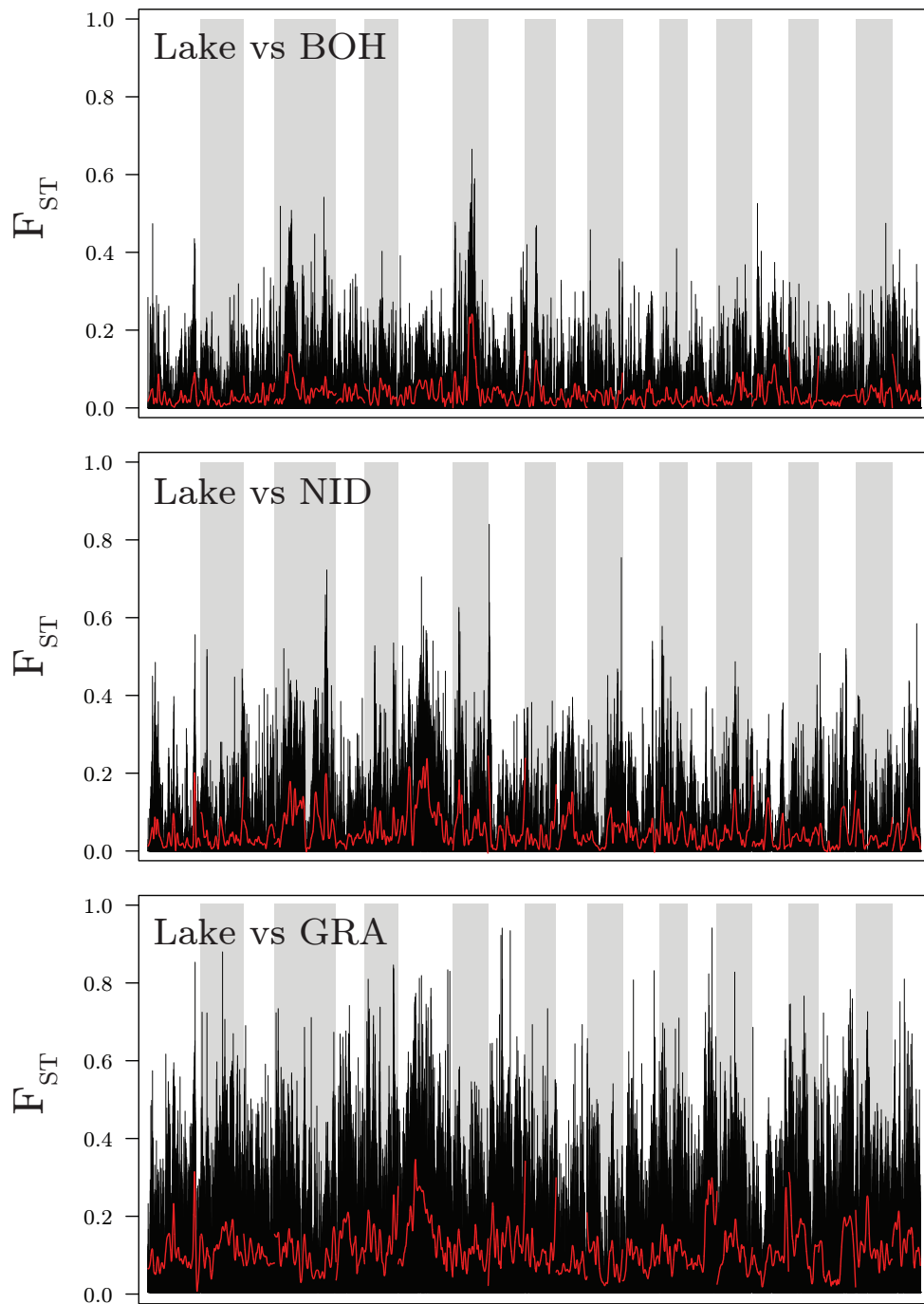
Figure S 19: Genome–wide divergence (F_{ST}) for all lake-stream comparisons. The black vertical lines represent the raw F_{ST} values, the red profiles show these values smoothed by LOESS, and the background shading separates the 21 chromosomes. Note the increase in baseline differentiation from BOH (median F_{ST} = 0.005; 55'476 SNPs) to NID (0.013; 57'119 SNPs) and GRA (0.061; 60'052 SNPs).
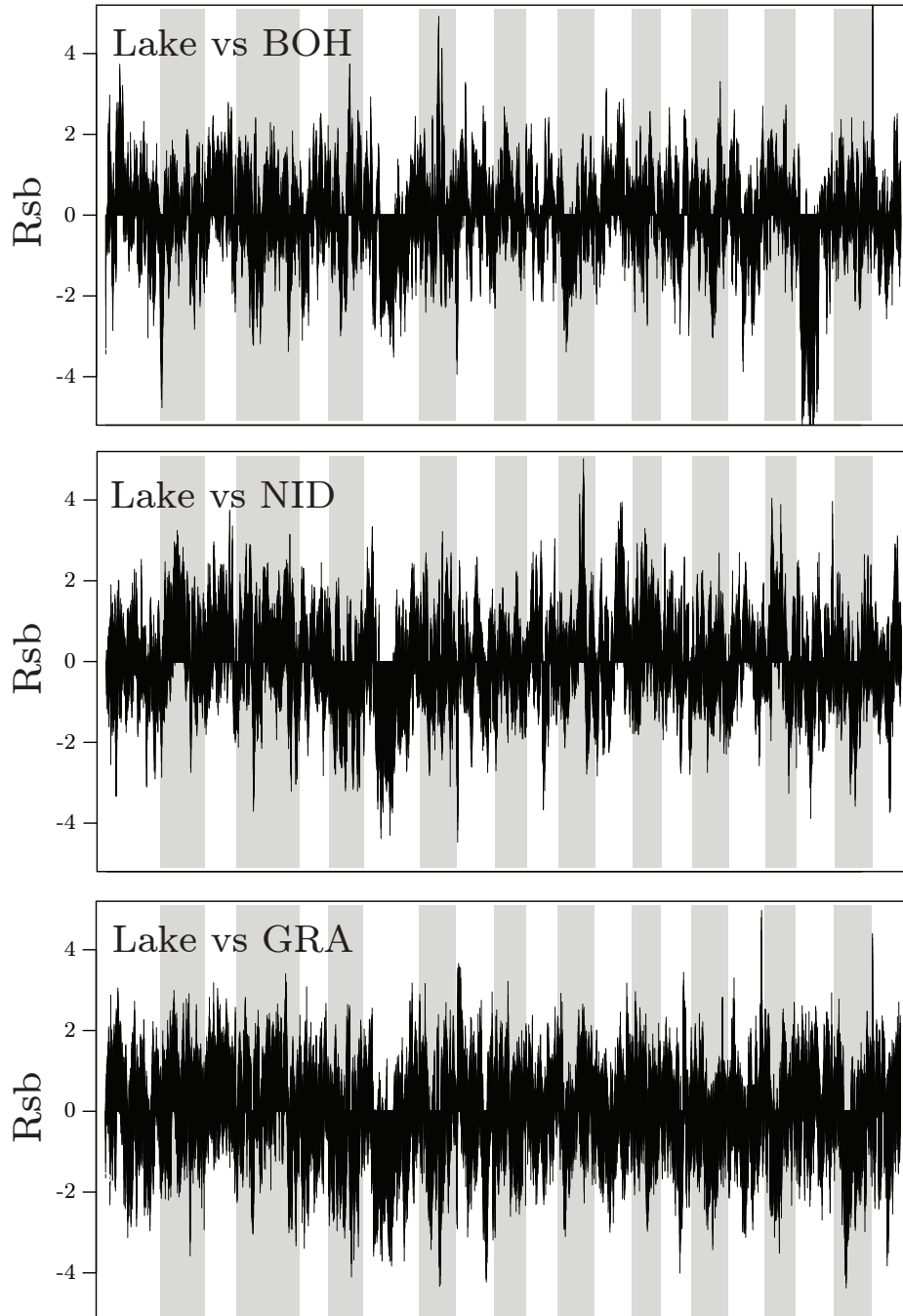
Figure S 20: Difference in haplotype decay around genome–wide SNPs, as captured by Rsb, for each lake–stream population pairing. The background shading separates the 21 chromosomes. A total of 87'738 SNPs were used in all lake–stream comparisons.
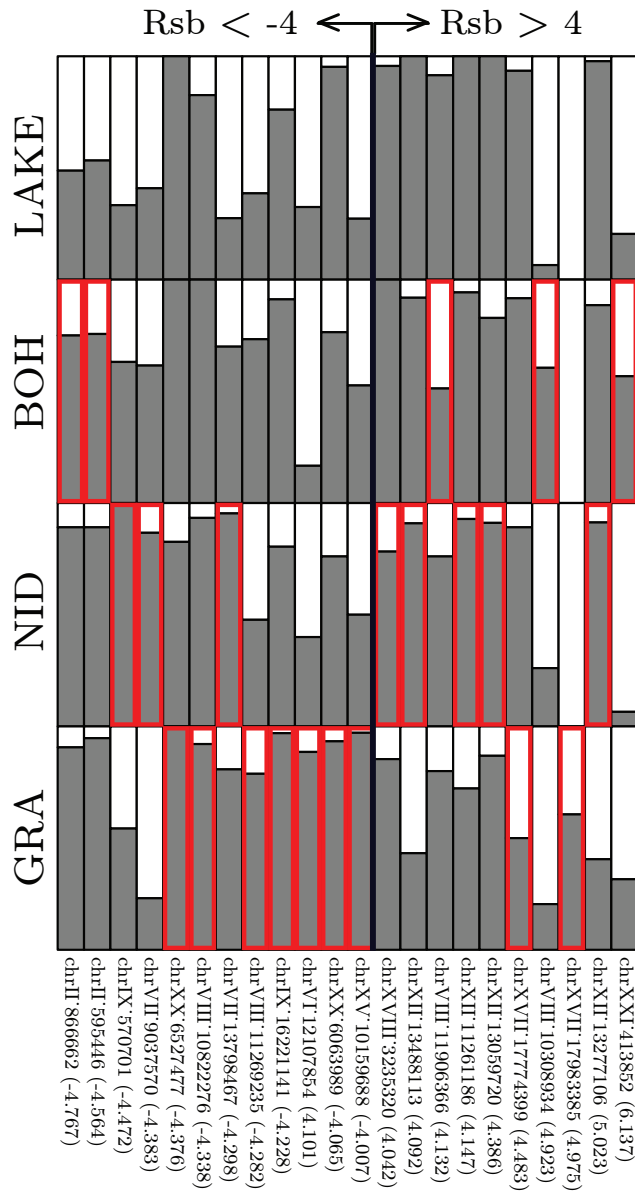
Figure S 21: Allele frequencies within each population at the top 22 lake–stream Rsb extremes. At each Rsb extreme (columns), the stream population producing an absolute Rsb > 4 in comparison to the lake is framed in red. On the bottom, the genomic position and the highest Rsb value observed across all lake–stream comparisons are given for each Rsb extreme. Negative Rsb extremes generally display relatively balanced polymorphism in the lake, but strong bias toward a specific allele in the stream(s), hence suggesting stream–specific selective sweeps. By contrast, positive Rsb extremes tend to exhibit relatively balanced polymorphism in the streams but are near fixation for a specific allele in the lake, thus indicating lake–specific selective sweeps.
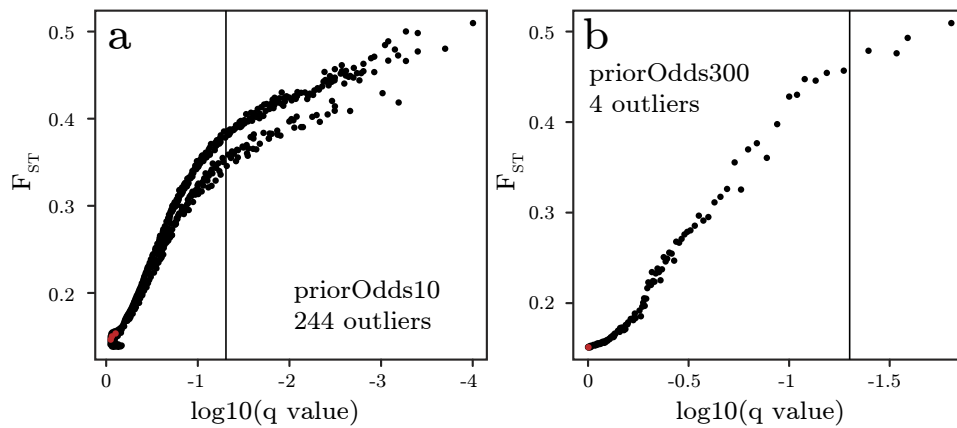
Figure S 22: BayeScan divergence outlier analysis in the Lake Constance and GRA stream population pair. Analysis to explore if markers near the Ectodysplasin (*Eda*) gene, known to be under divergent selection between these populations, are recognized as selection outliers by a popular outlier detection program not requiring a reference genome. The analysis used 60'052 SNPs, and was run both with default settings (a), and with the prior odds for neutrality increased to 300 (b) (default is 10). According to the software manual, the latter setting should be more appropriate for our large marker data set, while the default is perhaps too liberal. The graphics display the results of these two outlier scans, with the five markers near *Eda* exhibiting the highest F_{ST} in our differentiation scan printed in red (see top panel in Fig. 6.5c; positions on ChrIV: 12'815'791; 12'818'350; 12'818'237; 12'820'744; 12'822'878). SNPs on the right of the vertical line (244 and 4 in the two scans) qualify as differentiation outliers at a false discovery rate of 0.05. None of the markers near *Eda* are identified as outliers by BayeScan.
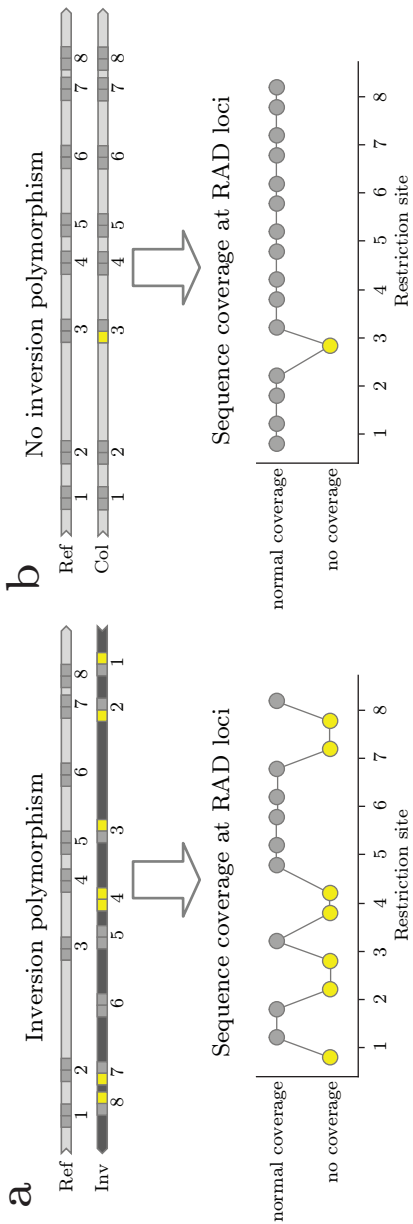
Figure S 23: Strategy for the detection of inversion polymorphisms using RAD locus coverage. (a) An individual harboring the inverted inversion type ('Inv'; dark gray background shading) relative to the reference sequence ('Ref'; light gray background) (for simplicity, individuals are haploid in this figure). The small squares represent the two RAD loci flanking restriction enzyme cutting sites to either side (sister RAD loci). If the 'Inv' inversion type shows substantial divergence from the reference, individuals carrying this type will lack sequence coverage at many RAD loci when aligned to the reference (RAD loci too strongly differentiated to align to the reference are shown as yellow squares). The bottom panel shows the resulting pattern of sequence coverage across RAD loci for this inversion type. (b) An individual carrying the inversion type collinear ('Col') to the reference (top), and the resulting sequence coverage along this chromosomal segment (bottom). If the different inversion types segregate at different frequencies within two populations, mean sequence coverage across chromosome windows within the inversion will be biased toward the population in which the 'Inv' type is less common, relative to chromosome segments outside the inversion. An analogous signature emerges when comparing the variance in sequence coverage across chromosome windows within and outside inversions between populations. Both signals, i.e. bias in the ratio of mean sequence coverage and coverage variance between populations along the genome, were exploited in our study and both consistently detected the three inversions, although only the former is presented (Fig. 6.6a). (Note that distortions in mean coverage and coverage variance along chromosomes can also be used to detect inversions in a single population, although the comparison of populations provides additional information on shifts in inversion frequencies.) The prerequisites for the above inversion detection approaches are that the inverted and collinear segments display substantial sequence divergence (recent inversions cannot be detected), and that the density of restriction sites is high enough to allow calculating the bias in the ratio of mean sequence coverage or the coverage variance between populations in relatively small chromosome windows while still integrating coverage data from a reasonably large number of RAD loci (a low–frequency restriction enzyme digest will allow detecting large inversions only). Moreover, comparing coverage statistics between populations will detect inversion only when these populations have diverged sufficiently in the frequency of the inversion types.

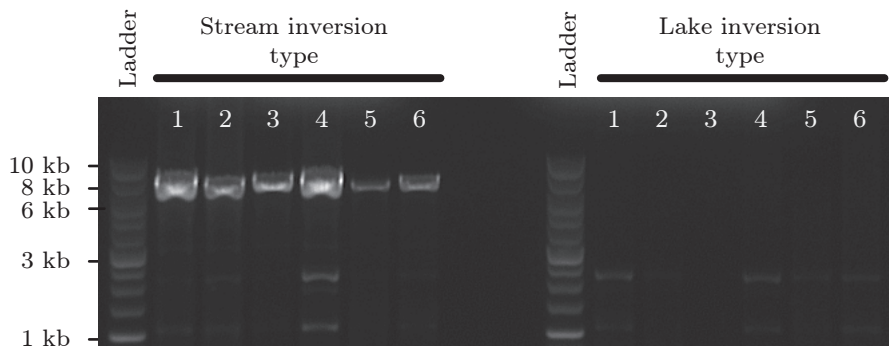## ChrI inversion
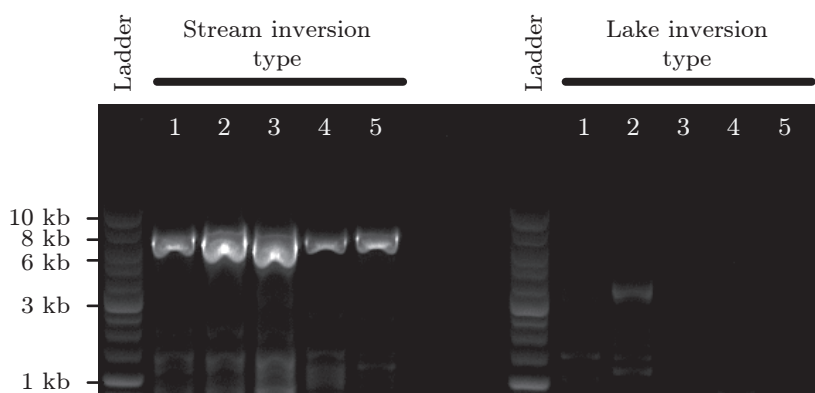
ChrXI inversion

Figure S 24: Confirming inversions by inversion type–specific PCR across expected breakpoints. For the putative ChrI and ChrXI inversions detected based on RAD sequence coverage, we used RAD loci flanking one inversion breakpoint to design PCR primer pairs expected to yield a PCR product for the inversion type specific to the streams, but no product for the inversion type fixed in the lake (see Fig. 6.7c). The underlying RAD loci were required to display robust alignment to the reference genome in all populations, thus ensuring that any absence of PCR amplification was due to the physical relocation of a primer site, and not to the degeneration of a primer site. For the ChrI inversion, we assessed 13 individuals homozygous for the stream type, of which nine (70%) amplified successfully, and ten individuals homozygous for the lake type, of which none amplified (five individuals of each group are shown on the gel image). For the ChrXI inversion, we assessed five individuals homozygous for the stream type and seven heterozygous individuals, all of which amplified successfully. By contrast, none of the ten individuals homozygous for the lake type amplified (six individuals of each group are visualized; the individuals 5 and 6 in the stream inversion group are heterozygous). These analyses thus confirm that the candidate regions are truly inversions. Note that the ChrI (and also the ChrXXI) inversion has been confirmed independently through PCR, using different primer pairs than in the present study2. The ChrXI inversion, however, has not previously been verified by PCR. As representatives of both inversion types, our PCRs considered primarily individuals from the stream populations in the Lake Constance basin (these populations are polymorphic for the inversions; Fig. 6.7). A few individuals from the Lake Geneva basin (Fig. 6.7c), however, were included in all reactions, which showed that geographic origin did not influence amplification success. The primer combinations used for this analysis were 5'–GCTGGTCAATATGTCCACTC–'3 (forward) and 5'–GTTACAATATGCCAATTACATGTC–'3 (reverse) for ChrI (approximate expected product size: 6.2 kb), and 5'–GGAGAAGCCTCAACCTATACG–'3 (forward) and 5'–GGTGAGCAACTTGAACCAAG–'3 (reverse) for ChrXI (6.8 kb). Long–range PCRs were performed with 37 cycles using Phusion High–Fidelity PCR chemistry (New England BioLabs), following the manufacturer's protocol.

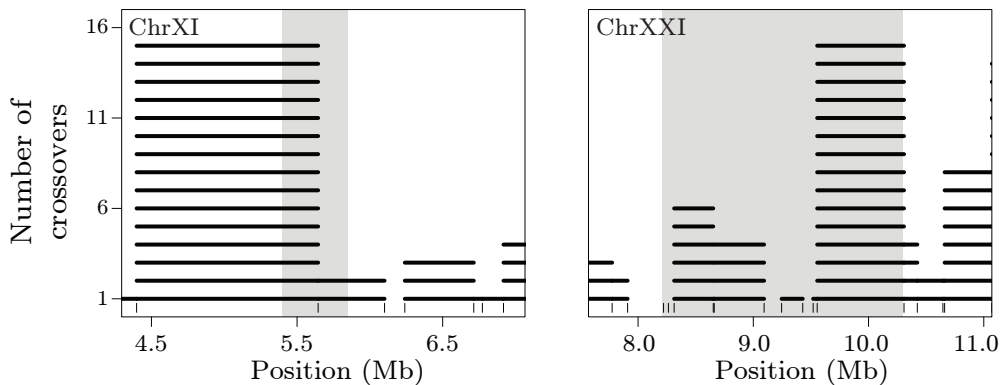**Figure S 25:** Recombination rate around the ChrXI and ChrXXI inversions in a laboratory cross population. Plotting conventions are as in Fig. 6.6f. For the ChrXI and ChrXXI inversion, the cross population underlying the recombination analysis reported in Fig. 6.6f is monomorphic. We here show that, as expected, recombination in these regions is not suppressed, thus providing a negative control for the analysis presented in Fig. 6.6f.
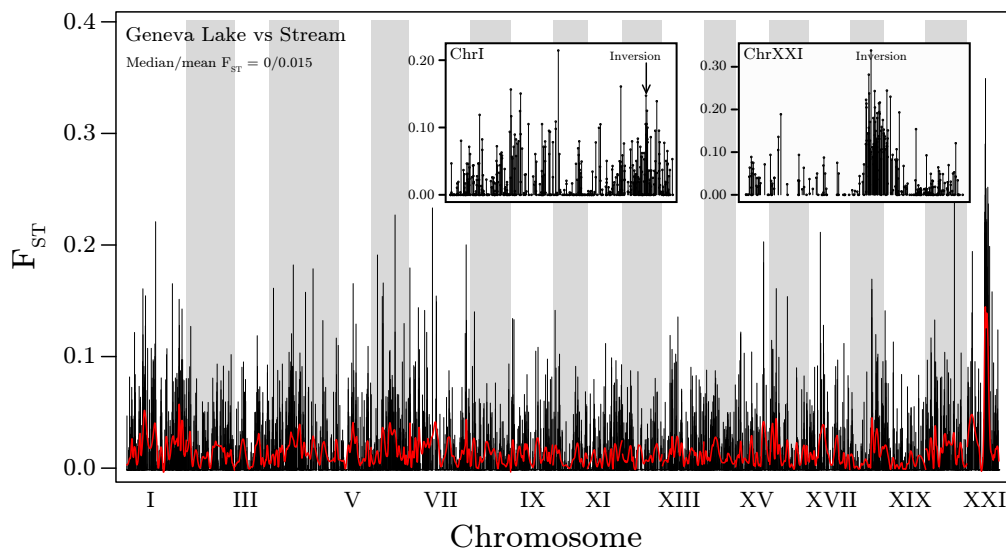
Figure S 26: Genetic differentiation (F_{ST}) between the Lake Geneva population, and a stream population from a tributary of this lake. The black vertical lines represent the raw lake–stream F_{ST} values, the red profiles show these values smoothed by LOESS, and the background shading separates the 21 chromosomes. The genome region displaying the strongest differentiation is located on ChrXXI and coincides with the large inversion on that chromosome (right insert; average F_{ST} across this inversion: 0.160). Relative to the low genome–wide baseline differentiation (given in top–left corner), the ChrI inversion also exhibits strong lake–stream divergence (left insert; average F_{ST} across this inversion: 0.084).
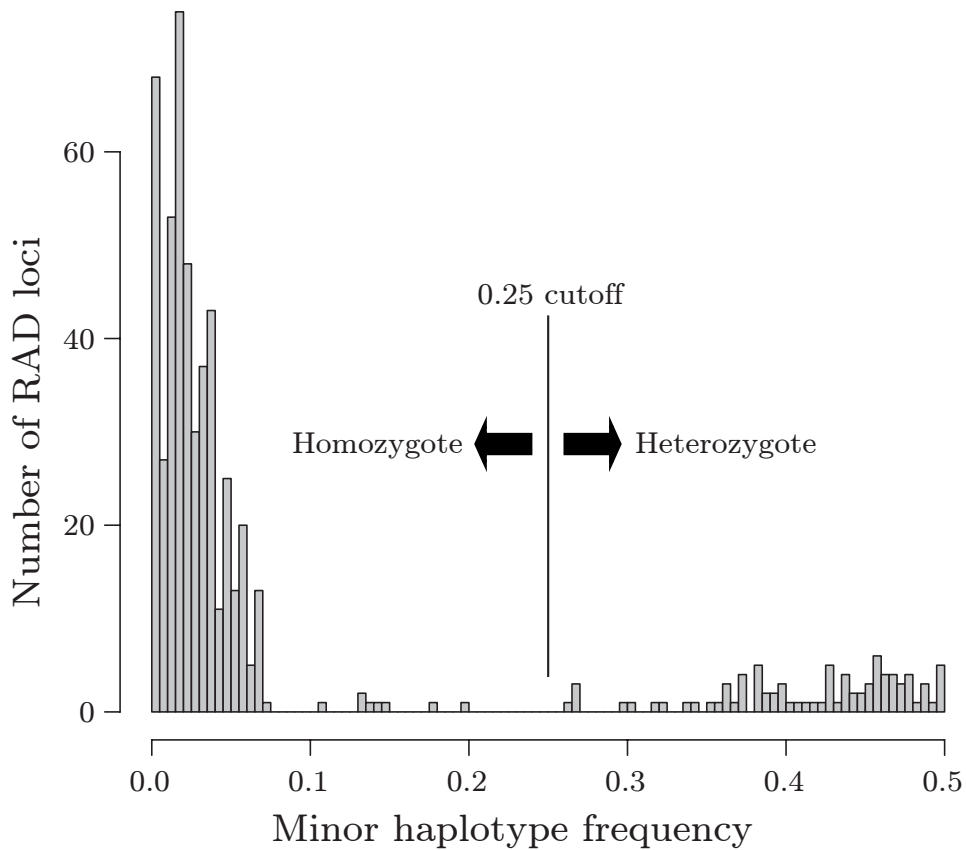
Figure S 27: Determining an appropriate threshold for distinguishing homozygote and heterozygote RAD loci during consensus genotyping. To identify this threshold, we determined the frequency of all haplotypes occurring at 250 haphazardly chosen RAD loci in each of three individuals displaying low, medium, and high raw Illumina sequence coverage. Among these 750 total RAD loci, we discarded those in which the two most frequent haplotypes together failed to account for >70% of all haplotypes and/or to reach a sum of 15 (see Material and methods). Across the remaining 562 RAD loci, we then calculated the minor haplotype frequency, defined as the count of the second most frequent haplotype divided by the sum of the two most frequent haplotypes. The distribution of this statistic indicated that a cutoff around 0.25 effectively separated truly heterozygous RAD loci from those appearing variable because of a technical artifact.

Table S 6: Dataset including the literature data used for statistical comparison of camelids and ruminants.

Species	Source	BM	CH_4			
		kg	L d^{-1}	L kg^{-1} DMI	L kg^{-1} dNDF	% DEI
Camelids						
Vicugna pacos	(Johnson and Johnson 1995)*	42.0	2.5	4.2	20.2	1.6
Vicugna pacos	(Martin et al. 2010)*	48.0	2.9	5.7	24.6	
Vicugna pacos	(Beauchemin et al. 2008)*	63.3	20.8	24.7	130.9	
Vicugna pacos	(Hacksten and van Alen 1996)	64.0	22.4	22.4		
Lama glama	(Sevens and Hume 1998)*	64.0	51.6	32.1	77.1	
Lama glama	(Franz et al. 2010)	100.8	33.7	28.5	81.1	12.6
C. dromedarius	(Wang et al. 2000)*	330.0	69.7	15.9		
Ruminants						
Capra hircus	(Vallenas et al. 1971)	32.5	17.2	19.0		8.9
Capra hircus	(Lechner-Doll and von Engelhardt 1989)	33.3	22.9	23.1		8.6
Capra hircus	(von Engelhardt et al. 2006)	33.5	26.2	40.4		13.3
Capra hircus	(Lerner et al. 1988)	37.3	16.3	21.4		7.9
Capra hircus	(IPCC 2006)	40.0	14.8	22.1		
Capra hircus	(Meyer er al. 2010)	60.0	40.0			13.2
Capra hircus	(Meyer er al. 2010)	100.0	67.0			13.2
Ovis aries	(NRC 2007)	26.2	19.5	31.1	82.8	13.8
Ovis aries	(Meyer er al. 2010)	27.0	23.0			11.0
Ovis aries	(Heller et al. 1986)	32.4	21.6	27.3		
Ovis aries	(Hintz et al. 1973)	33.7	25.1	26.1	77.3	7.5
Ovis aries	(Meyer et al. 2010)	37.0	34.0			12.0
Ovis aries	(Kayouli et al. 1993)	38.6	25.7	29.8		
Ovis aries	(Dulphy et al. 1997)	39.9	21.5			
Ovis aries	(Dulphy et al. 1997)	40.0	15.1			
Ovis aries	(Sponheimer et al. 2003)	40.3	24.4	31.8		
Ovis aries	(Dulphy et al. 1997)	42.2	14.5			
Ovis aries	(Ghali et al. 2004)	43.0	18.0	18.8		
Ovis aries	(Ghali et al. 2011)	43.6	22.3	24.3		
Ovis aries	(Dulphy et al. 1997)	44.0	23.6			
Ovis aries	(St–Pierre and Wright 2012)	45.3	34.2	31.1		
Ovis aries	(Sponheimer et al. 2003)	46.9	27.1	29.3		
Ovis aries	(Dulphy et al. 1997)	47.2	27.5			
Ovis aries	(Sponheimer et al. 2003)	48.2	23.9	22.5		
Ovis aries	(Dulphy et al. 1997)	58.1	32.5			
Ovis aries	(Dulphy et al. 1997)	58.7	12.4			
Ovis aries	(Schulze et al. 1997)	58.8	50.6	31.6		11.9
Ovis aries	(Sponheimer et al. 200)	59.2	29.0	23.1		
Ovis aries	(Ghali et al. 2011)	59.7	24.2	27.1		
Ovis aries	(Meyer et al. 2010)	60.0	36.0			13.2
Ovis aries	(Franz et al. 2010)	65.1	33.4	28.9	84.8	13.4
Ovis aries	(Ghali et al. 2011)	67.4	27.2	25.2		
Ovis aries	(Ghali et al. 2011)	72.6	28.9	22.4		
Ovis aries	(Guerouali and Laabouri 2013)	90.6	28.1	34.4	106.8	15.8
Ovis aries	(Guerouali and Laabouri 2013)	92.7	33.7	24.8	76.3	10.0
Ovis aries	(Guerouali and Laabouri 2013)	98.7	29.1	21.6	93.0	11.0
Ovis aries	(Meyer et al. 2010)	110.0	57.0			13.2
Bos indicus	(Carmean et al. 1992)	358.5	258.4	48.5	103.3	20.0
Bos taurus	(Vernet et al. 1997)	272.0	155.4	32.0		11.2
Bos taurus	(Vernet et al. 1997)	302.0	166.6	30.5		10.6
Bos taurus	(Pinares–Patiño et al. 2003)	545.5	415.0	27.6	56.2	7.7
Bos taurus	(Liu et al. 2009)	606.0	354.2	24.8		
Bos taurus	(Liu et al. 2009)	606.0	385.5	27.1		
Bos taurus	(Liu et al. 2009)	606.0	435.8	29.1		
Bos taurus	(Liu et al. 2009)	606.0	469.2	31.7		
Bos taurus	(Dulphy et al. 1997)	610.0	279.3			
Bos taurus	(Pinares–Patiño et al. 2013)	611.0	451.2	33.4	59.2	10.6
Bos taurus	(Liu et al. 2009)	649.0	472.1	35.0	65.6	12.1

Values are ordered by species and body mass. Empty cells indicate that the corresponding data were not available from that source. Note that in many cases not all available data were taken from the respective publication, but only those measurements that were obtained with roughage–only diets. Values indicated with asterisks were not included in the analysis as animals were not kept on a roughage–only diet or methane measurements were not carried out by respirometry. *BM* body mass; *DMI* dry matter intake; *dNDF* digestible neutral detergent fiber; *DEI* digestible energy intake.

Curriculum vitae

Dario Moser

Personal details

Postal address:	Helvetiaplatz 28
	4055 Basel
	Switzerland
Phone:	0041 79 777 19 89
E–mail:	dario.moser@unibas.ch
Date of birth:	February 25, 1986
Place of birth:	Basel, Switzerland
Nationality:	Swiss

Education

2013–ongoing PhD student at the Department of Environmental Sciences, University of Basel, Switzerland.

2010–2012 Master of Science in Animal Biology at the Department of Environmental Sciences in the W. Salzburger group, University of Basel, Switzerland.

2007–2010 Bachelor of Science in Biology, University of Basel, Switzerland.

Talks, posters and other academic activities

2015 Oral presentation during the *Eighth international conference on stickleback behavior and evolution*, Stony Brook University, New York,

USA: 'Local adaptation in threespine stickleback revealed by a long term field transplant experiment'.

2014 *Research seminar* at the Zoological Institute, University of Basel, Basel, Switzerland: 'Strong lake–stream divergence in stickleback life history is a plastic response to trophic niche shift'.

2013 Poster presentation during the *XIV congress of the European society for evolutionary biology*, University of Lisbon, Lisbon, Portugal: 'Repeated lake–stream divergence in Stickleback life history within a central European lake basin'.

2013 Member of the organizing committee of the *biology13* conference, University of Basel, Basel, Switzerland.

2012 Poster presentation during the *biology12* conference, University of Fribourg, Fribourg, Switzerland: 'Rapid and repeated life history divergence between lake and stream sickleback fish within the Lake Constance drainage'.

2011 Student representative in the habilitation commission of Lukas Schärer.

Lab skills

General molecular techniques (e.g., DNA extraction, PCR, gel electrophoresis, sequencing), microscopy, RAD library preparation, fish husbandry, fish crossing and lab experiments with live fish (common garden experiments).

Fieldwork experiences

2010–2016 Intense fieldwork in the Lake Constance basin: fish sampling in rivers and the lake, enclosure construction and maintenance, conduction of long term field experiments (field work in winter time) and negotiation with the fisheries authorities from Austria, Germany and Switzerland.

2011 Lake Tanganyika, Zambia (2.5 weeks): Fish sampling in rivers, transect diving and fishing with gill nets.

Publications

Moser D, Frey A and Berner D (2016) Fitness differences between parapatric lake and stream stickleback revealed by a field transplant. **Journal of Evolutionary Biology** doi:10.1111/jeb.12817.

Roesti M, Kueng B, **Moser D** and Berner D (2015) the genomics of ecological vicariance in threespine stickleback fish. **Nature Communications** 6:8767.

Moser D, Kueng B and Berner D (2015) Lake-Stream Divergence in Stickleback Life History: A Plastic Response to Trophic Niche Differentiation? **Evolutionary Biology** 42:328–338.

Dittmann M, Runge U, Ortmann S, Lang R, **Moser D**, Galeffi C, Schwarm A, Kreuzer M, Clauss M (2015) Digesta retention patterns of solute and different-sized particles in camelids compared with ruminants and other foregut fermenters **Journal of Comparative Physiology B** 185:559–573.

Dittmann M, Runge U, Lang R, **Moser D**, Galeffi C, Kreuzer M and Clauss M (2014). Methane emission by camelids **PLOS ONE** 9:e94363.

Berner D, **Moser D**, Roesti M, Buescher H and Salzburger W (2014) Genetic architecture of skeletal evolution in European lake and stream stickleback. **Evolution** 68:1792–1805.

Roesti M, **Moser D** and Berner D (2013) Recombination in the threespine stickleback genome – patterns and consequences. **Molecular Ecology** 22:3014–3027.

Moser D, Roesti M and Berner D (2012) Repeated lake–stream divergence in stickleback life history within a Central European lake basin. **PLOS ONE** 7:e50620.

Review activities

Evolutionary Ecology Research, Molecular Ecology, PLOS ONE and Royal Society Open Science.